CLOSELY-COUPLED INTEGRATION OF LOCATA AND GPS FOR ENGINEERING APPLICATIONS

Lukasz Kosma Bonenberg

12th January 2014

Nottingham Geospatial Institute

A thesis submitted to the University of Nottingham
for the degree of Doctor of Philosophy
in the Faculty of Engineering

Abstract

GPS has become an almost indispensable part of our infrastructure and modern life. Yet because its accuracy, reliability, and integrity depend on the number and geometric distribution of the visible satellites, it is not reliable enough for the safety of life, environmental or economically critical applications.

Traditionally, this has been addressed by augmentation from dedicated support systems, or integration with other sensors. However, from an engineering perspective only expensive inertial systems or pseudolites offer the accuracy required. In the case of pseudolites, the equivalent of ground based satellites, geometry constraints, fading multipath, imprecise clocks, the near-far effect, tropospheric delay and legislative obstructions make them difficult to implement.

This thesis takes a step forward, by proposing a loosely coupled integration with Locata, a novel, terrestrial positioning technology, based on the pseudolite concept. It avoids the above pitfalls by utilising frequency and spatially separated antennas and a license-free frequency band, though this comes at the cost of in-bound interference. Its ability to provide stand-alone position and network synchronisation at nanosecond level is used commercially in open-cast mining and in military aviation. Discussion of Locata and GPS technology has identified their shortcomings and main limiting factors as well as the advantages of the proposed integration. During the course of this research, tropospheric delay, planar solution and known point initialisation ambiguity resolution methods have been identified as the main limiting factors for Locata. These are analysed in various static and kinematic scenarios. Discussion also includes ambiguity resolution, noise and interference detection and system performance in indoor and outdoor scenarios.

The proposed navigation engine uses a closely coupled integration at the measurement level and LAMBDA as the ambiguity resolution method for Locata and GPS. A combined solution is demonstrated to offer a geometrical improvement, especially in the respect of height determination, with centimetre to decimetre accuracy and a minimum requirement of two signals from any component. This study identifies that proper separation and de-correlation of Locata and GPS ambiguities and better tropospheric models are essential to reach centimetre level accuracy.

The thesis concludes with examples of system implementation including: seamless navigation, city-wide network deployment, urban canyons, a long term-monitoring scenario and indoor positioning. This demonstrates how the proposed navigation engine can be an advantage in areas such as: civil engineering, GIS, mobile mapping, deformation, machine navigation and control.

♣ ♢ ♣

Acknowledgements

I have been very fortunate to receive much help and support during the development of this thesis. My academic supervisors, Prof. Gethin Roberts, and Dr. Craig Hancock offered mentoring and encouragement. Dr Marcus Andreotti, currently with Novatel, provided support in area of digital signal processing and hardware design and Dr Chris Hide advised on Kalman Filters and POINT.

Huib De Light offered support with Python and Linux. Nonie Politi designed the initial C version of Locata LBF converter. Without David Luff it would have been difficult to develop my understanding of the C++ receiver front end. Sergiusz Pawlowicz and Peter Kieft supported my Latex learning curve. Jihye Park has greatly improved my understanding of atmospheric modelling for GNSS, while Gbamis Olukayode Peter was a great help during the long-term monitoring trials.

Discussions with Benoît Bidaine, and Matthieu Lonchay from the University of Liège about clear communication, presentation and Matlab plots translated into, I hope, the pleasing results that can be seen inside this work. Dr. Joel Barnes, Ian Sainsbery, David Smart, and Nunzio Gambale, from Locata Corporation have provided me with great support.

Georgina Philips, Steve Fuller and Dan MacSweeney were kind enough to proof read this work.

Last, but definitely not least, I would like to thank people from my personal life – family and friends who supported me directly and indirectly during the work on this PhD thesis. There are too many to name, and I can't thank you enough. A beautiful copy of Sun Tzu's "Art of War" was a great mental help to me during the final stages of this work.

Thank you.

The research itself is supported by the Engineering and Physical Sciences Research Council. My visit to Australia was sponsored by the Royal Academy of Engineers Travel Grant, and the University of Nottingham's BEST award.

Nani gigantium humeris insidentes.

♣ ♢ ♣

Novelty and aims of the work

Civil Engineering demands the availability of centimetre-level positioning in all locations. In the case of GPS, or any other GNSS, this level of accuracy can only be achieved by using integrated carrier phase (ICP) observations, requiring ambiguity resolution (AR) (estimation of the unknown number of full cycles counted between the transmitting satellite and the receiver).

Locata is a novel, terrestrial positioning technology which provides a GNSS-like positioning concept. Both GPS and Locata face geometry-based accuracy limitations, affecting mostly the height component[1]. But, as demonstrated on pseudolites (Locata precursors), even a single terrestrial signal can improve the vertical accuracy of the tightly-integrated system (Lee, Soon, Barnes, Wang and Rizos, 2008; Meng et al., 2004; Yang, He and Chen, 2010). This approach would also address the Locata AR float solution via Known Point Initialisation (KPI)[2].

Currently, only a loosely-coupled integration between Locata and GPS exists, the Leica Geosystems Jigsaw360 used in open-cast mining[3]. Furthermore, academic research in this area is either limited to the simulated LAMBDA implementation for Locata (Bertsch, 2009), or does not include the ambiguity resolution (Lee et al., 2008; Lee, Wang, Rizos and Grejner-Brzezinska, 2004; Rizos, Grejner-Brzezinska et al., 2010).

A novel, tightly coupled integration of GPS and Locata presented in this thesis, solves and improves on a number of existing problems, offering:

- combined ambiguity resolution (AR) for both systems,
- kinematic based ambiguity resolution,
- mitigation, at least in part, of the open sky requirement,
- geometry improvement allowing 3D position for the Locata component,
- utilisation of all existing signals[4],
- time synchronisation,
- use of Locata binary format (LBF), instead of ASCII output.

During the course of the work, a dedicated navigation engine was designed and tested, using both simulated, and real data. This software, see figure 6.10, page 94, combines Matlab and C++ code, to produce a fully functioning workflow. LBF is developing rapidly, and while frequent changes makes writing software complex; the benefit of additional data, including the navigation message (NAV) overlay, is a major advantage over the previously used ASCII output. A Locata front end for the

[1] GPS vertical accuracy is 1.2 – 2.0 times worse than the planar one. For Locata, the co-planarity of the transceivers limits vertical position and requires careful planning to avoid planar only positioning.

[2] Ambiguities and clock offset are estimated using known point. This approach will only produce a float solution, due to model imperfections and system biases.

[3] This system is actively deployed in the De Beers "flagship" Venetia diamond mine in South Africa where a Locata-only solution (after GNSS RTK initialisation) is used to provide at the 95% level 10 centimetre in the horizontal and 20 centimetre vertical (Barnes, LaMance et al., 2007).

[4] Currently a loosely-coupled GPS/Locata can only utilise signals from one device at the time (see figure 4.1, page 46).

POINT Software Suite was also written (see section 6.1, page 89). In addition, this research led to the establishment of the first European Locata test bed (as discussed in appendix F).

♣ ♢ ♣

Contents

♣ ♢ ♣

List of Figures

♣ ♢ ♣

List of Tables

List of Acronyms

A GPS	Assisted GPS, improving TTFF with additional information received via Internet or mobile network.
A/D	Analog to digital (converter).
A/S	Anti Spoofing, encryption of P code using Y code.
AA	Acquisition Assist Word, third word in each Locata NAV sub frame.
AFM	Ambiguity Function Method.
AGC	Automatic Gain Control.
AIAA	American Institute of Aeronautics and Astronautics.
APC	Antenna Phase Centre.
APL	Johns Hopkins University Applied Physics Laboratory.
AR	Ambiguity Resolution, required for carrier phase solution.
BeiDou	Ursa Major, Chinese Navigation Satellite System (CNSS).
bps	Bits per second.
BPSK	Binary Phase Shift Keying (modulation technique).
C/A code	Coarse/Acquisition code (1.023 MHz).
CDGPS	Carrier phase Differential GPS navigation.
CDMA	Code Division Multiple Access.
CNAV	New GPS civilian navigation message.
CNSS	Chinese Navigation Satellite System (CNSS), also known as BeiDou.
COMPASS	First stage of CNSS development (regional).
CORS	Continually Operating Reference Stations.
CTP	Conventional Terrestrial Pole.
dB	Decibels, logarithmic measurement of power or gain ratios.
dBic	Decibels relative to the gain of an ideal, isotropic, circularly polarised antenna.
dBm	Decibels relative to one milliwatt.
dBW	Decibels relative to one Watt.
DGPS	Differential (code phase) GPS and name of NASA SBAS networks.
DOP	Dilution of Precision.
DSP	Digital Signal Processing.
DSRC	Dedicated Short Range Communication, vehicular communication medium.
EGNOS	European Geostationary Navigation Overlay Service, SBAS system.
EIRP	Effective Isotropic Radiated Power.
EKF	Extended Kalman Filter.
ERNP	European Radio Navigation Plan.
ESA	European Space Agency, responsible for GALILEO.
FAA	Federal Aviation Administration.
FCC	Federal Communications Commission.
FDMA	Frequency Division Multiple Access.
FHSS	Frequency Hopping Spread Spectrum.
FKP	Rover based N RTK correction.
FOC	Full Operational Capacity.
GDOP	Geometric Dilution of Precision.
GEO	Geostationary Earth Orbit satellites.
GGTO	GPS to Galileo time offset.
GHz	Gigahertz (billion of cycles per second).
GIC	Geosynchronous Integrity Channel (part of WAAS).
GLONASS	Global'naya Navigatsionnaya Sputnikovaya Sistema, Russian satellite navigation system.
GNSS	Global Navigation Satellite Systems, common name for all space borne systems.
GPS	Global Positioning System, American satellite navigation system.
GSM	Groupe Speciale Mobile, European standard for digital cellular phones.

GTRF	Galileo terrestrial reference frame, related to ITRF.
HDOP	Horizontal Dilution of Precision.
HMI	Hazardous Misleading Information.
HOW	Hand over Word, part of a GPS navigation message.
HRMS	Horizontal accuracy of long GPS baselines.
IAT	International Atomic Time, related to UTC but continuous.
IBLS	Integrity Beacon Landing System.
ICAO	International Civil Aviation Organisation.
ICD	Interface Control Document.
ICP	Integrated Carrier Phase, mm level observables for GNSS and Locata.
IEEE	Institute of Electrical and Electronics Engineers.
IERS	International Earth Rotation and Reference System Service.
IGSO	Inclined Geosynchronous Satellite Orbit.
iMAX	Network based N RTK correction.
INS	Inertial Navigation System.
IOC	Initial Operational Capacity.
ISM	Industrial Scientific Medical Frequency Bands, not requiring licence to transmit signals, most popular are 2.4GHz and 5.75GHz.
ITA	International Atomic Time.
ITRF	International Terrestrial Reference Frame, maintained by IERS, current version is ITRF2008.
IVHS	Intelligent Vehicle Highway System.
JPL	NASA Jet Propulsion Laboratory.
KPI	Known Point Initialisation, AR technique.
L band	All frequencies between 1 and 2 GHz.
L1	First L band GPS frequency: 1575.42 MHz (154 x 10.23 MHz).
L2	Second L band GPS frequency: 1227.60 MHz (120 x 10.23 MHz).
L3	Third L band GPS frequency: 1381.05 MHz (135 x 10.23 MHz).
LAAS	Local area augmentation system.
LAMBDA	Least squares Ambiguity De correlation Adjustment, AR method.
LBF	Locata Binary Format.
LCOE	Low Correlator Output Event, Locata noise indicator.
LHCP	Left Hand Circular Polarisation.
LINE	Locata In line Navigation Engine, Locata proprietary post processing software.
LL	LocataLite transmitter.
LORAN	Long Range Navigation system.
LOS	Line of Sight.
LP	Linear Polarisation of transmitted signal.
LSA	Least Square Adjustment.
LSSI	Locata Signal Strength Indicator, an estimation of received signal power, as observed by the rover.
LTC	Locata Transmission Cycle.
MAX	Rover based N RTK correction.
MCS	Master Control Station (for the GPS constellation).
MDB	Internal and external reliability along with its accuracy characteristics.
MDB	Minimal Detectable Bias.
MEMS	Micro electro mechanical systems, low cos INS.
MEO	Medium Earth Orbit Satellite, most GNSS SV fall into this category.
MET	Meteorological.
MHz	Megahertz (millions of cycles per second).
MNAV	New GPS military navigation message.
MSAS	Multi functional Satellite Augmentation System, predecessor to QZSS.
MSS	Mobile Satellite Service.
mW	Milliwatt.
N RTK	Network Real Time Kinematic.

NASA	National Aeronautics and Space Administration.
NAV	Navigation Message, transmitted on the GNSS (GPS) and Locata carrier phase.
nLOS	Non line of sign, usually refereed to multipath signal.
NNSS	Navy Navigation Satellite System, also known as TRANSIT.
NTF	Numarela Test Facility, dedicated, 30 acre large, outdoor test facility located in Australia, owned and maintained by the Locata Corporation.
OTF	On The Fly, usually referring to data processed during observation campaign, with results being available in real or almost in real time.
OWI	Open Word Interface, Leica's proprietary communication interface, introduced with 600 series.
P code	Precise code (10.23 MHz).
PCO	Antenna phase centre offset, a difference between physical centre of antenna and its electrical centre, to where ranges are measured to.
PDOP	Position Dilution of Precision.
PGA	Programmable Gate Array (type of hardware boards).
ppm	Parts per million.
PPP	Precise Point Positioning.
PPS	Pulse per second, frequency standard provided by GNSS receivers, providing a sharp rising/falling signal repeating every second.
PRN	Pseudo Random Noise, a digital code with noise like properties.
PRS	Network based N RTK correction.
QC	Quality Control.
QPSK	Quadrature Phase Shift Keying (modulation technique).
QZSS	Quasi Zenith Satellite System, Japanese Satellite Augmentation System.
RAIM	Receiver Autonomous Integrity Monitoring, a position quality confidence metric used in the aviation.
RCPI	Receiver Channel Power Indicator, Locata signal characteristic.
RF	Radio Frequency.
RHCP	Right Hand Circularly Polarised.
RIN	Royal Institute of Navigation.
RMS	Root Mean Square.
RNP	Required Navigation Performance (for aircraft landing systems).
ROC	Receiver Operating Characteristic.
RSS	Root Sum Square.
RTCM	Radio Technical Commission for Maritime Service.
RTK	Real Time Kinematic.
Rx	Receiver.
S/A	Selected Availability (currently not in use).
S1	Locata first S band frequency: 2.41228GHz (236 x 10.23 MHz).
S2	Locata second S band frequency: 2.46543GHz (~241 x 10.23 MHz).
SBAS	Satellite Based Augmentation System.
SDCM	System for Differential Correction and Monitoring, Russian SBAS system.
SDMA	Spatial Division Multiple Access.
SLR	Satellite Laser Ranging.
SNR	Signal to Noise Ratio.
SoOP	Signals of Opportunity, navigation method.
SPS	Standard Positioning Service.
SSS	SPACE Software Suite.
T/R	Transmit/Receive (switch).
TACAN	Tactical Air Navigation.
TAI	International atomic time, continuous time scale based on the atomic clock.
TANS	Trimble Advanced Navigation Sensor (a GPS receiver).
TCXO	Temperature Controlled Crystal Oscillator, usually deployed with GNSS receivers.
TDMA	Time Division Multiple Access.
TDOP	Time Dilution of Precision.

TH/DS CDMA	Time hopped DS CDMA.
TL	TimeLock, Locata time synchronisation method.
TLM	Telemetry Word, first word in each Locata NAV sub frame.
TM	Time Word, second word in each Locata NAV sub frame.
TMBOC	Time Multiplexed Binary Offset Carrier, a type of GNSS signal modulation.
TMF	Tropospheric Mapping Function.
TOW	GPS time of the week.
TS	Total Station.
TTFF	Time to First Fix, indication how quickly GNSS unit can become operational.
Tx	Transmitter.
UAV	Unmanned Aerial Vehicle.
UHF	Ultra High Frequency (all frequencies between 300 MHz and 3 GHz).
UNSW	University of New South Wales.
UoN	University of Nottingham.
US	User Segment.
UT1	Mean Universal Time, defined as two conservative transits of the sun over the meridian of the mean earth (Greenwich). Non continuous time which we observe.
UTC	Coordinated Universal Time, coordinated (agreed) implementation of UT1, also not continuous.
UWB	Ultra Wide Band, band dopping system offering good multipath mitigation indoors but of limited range.
VCO	Voltage Controlled Oscillator.
VDOP	Vertical Dilution of Precision.
VLBI	Very Long Baseline Interferometry.
VRMS	Vertical accuracy of long GPS baselines.
VRS	Virtual reference station, network based NRTK correction.
WAAS	Wide Area Augmentation System, American SBAS system.
WBI	Wide Band Interference.
WGS84	Word Geodetic System 1984 ellipsoid.
Y code	Precise code (P code) after encryption.

♣ ♢ ♣

Mathematical Notations

General Symbols

c The speed of light, 299 792 458 $^{\mathrm{m}}/_{\mathrm{s}}$.

CP_k^i Correlator performance (in logarithmic scale), see equation 5.3 on page 74.

I_k^i In-phase correlator output for channel i at epoch k, see equation 5.3 on page 74.

QI_k^i Locata signal quality indicator for channel i at epoch k, see equation 5.4 on page 75.

Q_k^i Quadraphase correlator output for channel i at epoch k, see equation 5.3 on page 74.

ρ_{MP} Multipath delay, see equation 4.9 on page 59.

R Radius of Earth, see equation 4.4 on page 52.

ϵ_A^S Signal propagation error – all unmodelled errors, including the random noise, see equation A.2 on page 133.

$RCIP_k^i$ Receiver Channel Power Indicator for channel i at epoch k, see equation 5.4 on page 75.

SNR_k^i Quater-phase correlator output, see equation 5.4 on page 75.

f_i Carrier frequency i, where $f_i = \frac{c}{\lambda}$.

G_{ant} Antenna performance, with 1 equal the theoretically perfect (lossless) antenna, see equation 4.3 on page 52.

L_{231} Okumura-Hata COST231 urban range model, including multipath, modified to suit the European cities, see equation 4.12 on page 60.

L_{ECC-33} ECC-33 urban range model, including multipath for the wireless communication, see equation 4.13 on page 60.

$\triangle\rho_{MP}$ Multipath delay, see equation 4.10 on page 60.

L_{FM} Path loss caused by the fading multipath, see equation 4.11 on page 60.

L_{FS} Free space path loss, see equation 4.3 on page 52.

λ_i The wavelength of the carrier frequency f_i where $\lambda_i = c \cdot f_i$.

$\triangle_\rho$ Ray path curvature (Earth curvature), see equation 4.5 on page 54.

σ_{base} The double difference rover positional accuracy, see equation 4.6 on page 54.

$TL_i^M(t_k)$ Final carrier phase TimeLoc correction between master (M) and slave (i) at epoch t_k, see equation 3.2 on page 28.

Navigation Solution Symbols

ρ Distance between transmitter and the rover, see equation 4.9 on page 59.

$\rho_A^i(t_k)$ Geometric range between receiver A and SVi at epoch t_k, see equation A.2 on page 133.

N_A^i The carrier-cycle integer ambiguity between the receiver A and the SVi, see equation A.5 on page 134.

$\phi_A^i(t_k)$ The carrier-phase measurement (in cycles) between the receiver A and the SV_i at epoch t_k, see equation A.5 on page 134.

ϕ_k^{Tx} the carrier-phase measurement between the receiver and the transmitter at epoch k using Tx frequency, with i$\in \mathbb{Z}$ and j$\in$A-D, see equation 5.5 on page 78.

$P_A^i(t_k)$ The code (pseudo-range) measurement (in meters) between the receiver A and the SVi at epoch t_k, see equation A.3 on page 134.

ϱ Geometric distance (range) between SV and receiver, see equation A.5 on page 134.

σ_i GPS observation weight, based on the elevation angle, see equation 4.7 on page 57.

$\triangle_{trop}$ Locata Tropospheric delay, see equation 4.8 on page 57.

$\varphi_r^s(t)$ Beat phase, see equation A.5 on page 134.

ρ_S Distance to the apparent horizon, see equation 4.4 on page 52.

Least Square Adjustment and LAMBDA Symbols

A Observation matrix, see equation C.19, page 149.

D Double difference Operator Matrix, see equation C.2 on page 142.

$\rho_{AB}^{ij}(t_k)$ Double Difference of geometric range difference between receivers A&B and SV i&j, at epoch t_k, simplified to ρ_{AB}^{ij} in the subsequent equationssee equation C.8, page 147 .

L Residual matrix L (calculated - observed), see equation C.15 on page 143.

a LAMBDA ambiguity related parameters, see equation C.27 on page 147.

b LAMBDA remaining non-ambiguity related parameters, including position, see equation C.27 on page 147.

L_Φ Carrier Phase (ICP) part of residual matrix L (calculated - observed) see equation C.14, page 147 .

L_P Pseudo-range part of residual matrix L (calculated - observed) see equation C.13, page 147 .

O_{DD} Vector of double differenced observations, see equation C.3 on page 142.

Q Symmetric covariance-variance matrix, see equation C.26 on page 146.

W Weight matrix, see equation C.6 on page 142.

$\hat{x}$ Vector of unknowns (best estimation of), see equation C.23 on page 146.

1 Introduction

"We penetrated deeper and deeper into the heart of darkness."
Joseph Conrad (Nalecz coat-of-arms), Heart of Darkness

THE history of GNSS started in the late '50s, almost as a by-product of the heated space race between the USA and USSR. This created a theoretical and practical basis for the deployment of first of the NAVSTAR satellites, now known as GPS, in 1978. As the accuracy of the system exceeded expectations, a safety measure was introduced - Selected Availability (S/A), which reduced system accuracy for non-military users[1].

The reduction of S/A to zero level, on the 2nd of May 2000, opened a new chapter for GNSS navigation, starting a mass market revolution using GPS Standard Positioning Service (SPS), whose accuracy was within a few metres. This had a profound effect, expanding the GPS user-base from geodetic and military, into such industries as: aviation, marine, logistics, engineering, and other mass-market applications. Today, GPS is ubiquitous, and its uses include such sensitive industries as: banking, energy and communication.

The common perception of GPS as an ultimate positioning tool, offering position anywhere on the globe, is simply not true. Its accuracy depends on the satellite geometry and open sky visibility. For centimetre-level accuracy carrier phase measurements, ambiguity resolution (AR), and a differential approach, requiring at least two receivers working simultaneously are essential. GPS denied areas are very common, and progress into them is becoming logarithmically more difficult. This thesis pushes this boundary forward by discussing a novel Locata and GPS integration. It not only partly mitigates lack of sky visibility, but also offers provision of precise time synchronisation and RTK level positioning.

Contents

[1] S/A introduced the unknown corrections to the ephemerides and dithering of the satellite clocks. Those values where known only to military users.

MODERN societies need increasingly accurate, reliable, and predictable methods of navigation to meet the ever increasing demands of communication and transportation. Due to its global reach, ease of use, deployment and maintenance costs, Global Navigation Satellites Systems (GNSS) are seen as the perfect solution. The current "black box" approach however creates a large risk, as even specialised users tend to have an almost blind trust in this invisible utility (The Royal Academy of Engineering, 2011).

1.1 Current state-of-the-art

To calculate a position, GPS requires a line of sight to at least four satellites, with accuracy dependent on the number, and geometric distribution of the satellites. The removal of S/A, improvements in hardware, signal, atmospheric and navigation engineering have brought us instant positioning capacity[2], Assisted GPS (A-GPS) for mobile users, but there have been no corresponding improvements to carrier-phase accuracy, which remains at centimetre-level.

Navigation Mode	Planar Accuracy (1σ)[a]
Standard Positioning Service (SPS) [b]	5 – 10 m
DGPS[bc]	0.5 – 1 m
Precise Positioning Service (PPS)[bd]	0.1 – 0.3 m
RTK-GPS[ce]	0.01 m
NRTK-GPS[ce]	0.01 – 0.03 m
Long term observations[f]	0.000 3 – 0.001 m
Precise Point positioning (PPP)[g]	0.2 – 0.3 m

Table 1.1 – GPS techniques accuracy overview

[a] GPS vertical accuracy is 1.2 – 2.0 times worse than the planar one.
[b] This method uses only pseudo-range observations.
[c] Double differencing is used to produce the solution.
[d] Restricted to military users.
[e] Further information can be found in section 2.5 on page 21.
[f] Can be stand alone, but requires long observation times with precise orbits and clock products.
[g] Stand alone option, taking advantage of precise clock, orbit and atmospheric models with a convergence time of up to 20 min.

Most mass-market applications use the Standard Positioning Service (SPS), accurate to the level of a few metres, using pseudo-range (code). For sub-metre accuracy other methods are required (see table 1.1, page 3). An instantaneous fix can be provided using differential techniques, such as Real Time Kinematic (RTK), and Network-RTK (N-RTK)[3], which require at least two receivers collecting data simultaneously. With precise orbits and clock models it is possible to provide position at the

[2] Compare with Cobb (1997) for example.
[3] Both RTK and N-RTK provide instantaneous centimetre positioning, with the latter using a number of base stations, known as CORS networks, to create a virtual base station (VBS) from which differential observations are made. More details can be found in section 2.5 on page 21.

decimetre level using Precise Point positioning (PPP) with a single receiver, but convergence times of up to 20 min limit its usage.

Civil engineering works, such as mapping utilities, setting out or monitoring, are restricted by satellite geometry[4], open sky visibility, and multipath, especially in a urban environments (G. W. Roberts, Meng, Brown and Dallard, 2006). The satellite signal is also easy to block; privacy-oriented devices with complete circuit designs are available online (Fried, 2005, 2011). These can create a serious hazard in the hands of less civic-minded members of society[5]. Even more dangerous, is intentional and malicious spoofing of position and/or time, potentially immobilising transportation, money flow and communication (Humphreys, 2012b; Shepard, Bhatti and Humphreys, 2012). Any GNSS ground and space infrastructure is also extremely expensive to maintain, and concerns were raised during the recent American financial crisis (The Royal Academy of Engineering, 2011).

Suggested remedies, including the modernisation of receiver design, utilisation of extra SBAS/GBAS signals, algorithm changes, or the utilisation of multi-constellation GNSS (Hancock, Roberts and Taha, 2009; Humphreys, 2012a; Massatt, Fritzen, Scuro and O'Neill, 2006; Scott, 2012; Wesson, Rothlisberger and Humphreys, 2012), can only partly mitigate the problems. The recent case of Lightsquared, who attempted to utilise the nearby radio band for high speed terrestrial 4G LTE wireless broadband[6], presented a serious threat to GNSS, and demonstrated that extra protection, including dedicated legislation, is necessary to prevent such situations.

An independent back-up system, capable of truth-proofing user position could be another solution. Pseudolites (ground based satellites, usually transmitting on the GPS L1 frequency) have been discussed for aviation based GBAS augmentation very much from the beginning of GPS (Cobb, 1997; Parkinson, Spilker, Axelrad and Enge, 1996). Lee et al. (2008); Meng et al. (2004); J. J. Wang, Wang, David, Leo and Kyu (2004); Yang et al. (2010) concluded that using pseudolites to augment GPS geometry, improves horizontal and vertical accuracy – the latter being an Achilles heel of the system. The terrestrial signal offers both an integrity check, and a much more stable accuracy, compared with GPS alone (see figure 1.1, page 5).

A change in legislation, limiting use of the L1 frequency to space-born signals, has severely limited any further research. Locata, operating in the 2.4 GHz licence-free ISM band, does not share these restrictions. Created by the Locata Corporation, it allows network synchronisation to the nanosecond level, using a novel procedure known as TimeLoc. As with GPS, a centimetre-level position requires visibility to at least four LocataLites (Barnes et al., 2004; Montillet, 2008; Montillet et al., 2009).

Not many terrestrial systems can offer such accuracy; eLORAN, WiFi fingerprinting, signals of opportunity (SoOP) or mobile network triangulation can only achieve 10 – 100 m accuracy. Ultra wide band (UWB) and the Inertial Navigation System (INS) offer centimetre-level accuracy, but are either limited in range or time, as positional drift is very hard to control.

[4] North-south direction movements have been found to be of lesser accuracy, due to the gap in GNSS constellation in the northern quadrant, roughly 315 – 45° for the UK.

[5] It is also due to its low manufacture quality, and lack of power control, as could be seen with Newark Airport LASS interference (Davis, Enge and Gao, 2012).

[6] Detailed description of the Lightsquared problem can be found at `http://www.gps.gov/spectrum/lightsquared/`.

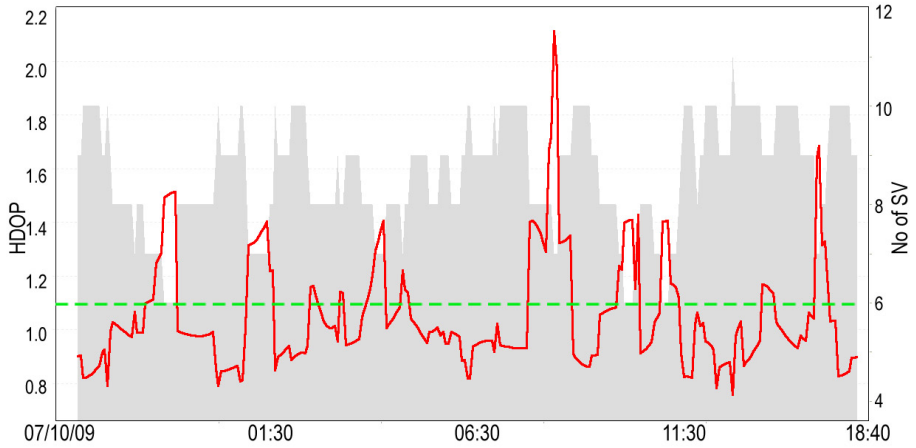

Figure 1.1 – GPS (red) and Locata (green) DOP comparison

Comparison of 24 h static Locata observations and simulation of equivalent GPS observations.

1.2 Thesis outline

This thesis is divided into eight chapters, which discuss both the theoretical and the practical aspects of the integration of Locata and GPS. A list of acronyms, mathematical notations, and detailed appendices, discussing the algorithms, Locata and GPS observables and software workflow, are provided. Non essential aspects, such as indoor positioning, have only been mentioned briefly.

Chapter 2 discusses the origins and nature of modern navigation technology, starting from terrestrial radio navigation, right through to modern day Global Navigation Satellite Systems (GNSS). All four systems will be introduced and compared. Discussion also includes Space and Ground Based Augmentation Systems with relevant pseudolite implementations. This chapter concludes with a discussion of the current state-of-the-art in navigation, indicating the problems that GNSS currently faces and highlighting the importance of pseudolite systems.

Chapter 3 describes Locata and GPS, focusing particularly on the aspects important from an integration perspective. This is important, as the successful integration of different systems requires a thoughtful understanding of the components involved.

Chapter 4 discusses the proposed integration between Locata and GPS. It describes the existing loosely-coupled integration, as implemented in the Leica Jigsaw 360, and proposes a tightly-coupled one. The feasibility of the new approach is discussed by comparing the main limiting factors – time, range, orbit determination, PCO, atmospheric effects, multipath and the near far-effect.

Chapter 5 demonstrates the limitations of current KPI in static and kinematic scenarios. It is followed by KPI analysis, demonstrating the effect of the initial estimation bias and Locata position bias. Finally, signal quality indicators, in-bound interference, noise, multipath and cycle slip detection methods will be discussed.

Chapter 6 focuses on the novelty of this thesis - practical Locata and GPS integration. This includes a detailed description of the workflow, calculation details and Ambiguity Resolution (AR). The chapter finishes with discussion of the results and recommendations for future work

Chapter 7 discusses the applications of the integrated system, taking into account its commercial feasibility. Starting with a general discussion about seamless navigation in a city-wide network deployment, this chapter will then focus on practical applications in urban canyons, a long term-monitoring scenario and indoor positioning. The urban canyon application demonstrates a dedicated tool for planning deployment in these areas, while long-term monitoring and indoor applications demonstrate the stability and accuracy of a Locata only solution.

Chapter 8 summarises the findings and discusses the possibilities for the future research in this area.

1.3 House keeping notes

This document has been created using open source software. Excelled **Lyx** TEX/LATEX fronted (The LyX Team, 2009) was used for typing and layout, references were organised using **JabRef** (JabRef Development Team, 2008). Graphics have been prepared using **GIMP** (GIMP Development Team, 1996) for raster graphics, and **Inkscape** (Inkscape Development Team, 2006) or **TikZ** LATEX package were used for the vector graphics. Most of the block diagrams were created using Microsoft Office Visio 2003.

In the course of this work I have used: **Notepad++** (Ho, 2003), GPS Toolkit (Tolman et al., 2004), TEQC (Estey and Meertens, 1999), GNUTools, and GnuPlot, among others. All transformations to OSGB grid have been made using the free **Grid InQuest** from Ordinance Survey[7]. The Matlab routine or Leica Geo Office have been used for data collected outside of Great Britain. This transformation does not apply scale factor and utilises Constell Inc. (2012) routines.

The majority of the navigation engine was written in **Matlab** (MathWorks, 1984) using the University of Delft LAMBDA library[8] (de Jonge and Tiberius, 1996). I used **Code::Blocks** (The Code::Blocks Team, 2005) for any C++ code, mostly front-end and binary converters . A number of supporting routines have been written in **Python** (Python Software Foundation, 1991), due to its flexibility and quick deployment. Optimised Matlab code can match C++ or Python speed (Getreuer, 2009), but its I/Q always remains a factor, with differences up to a factor of 60.

[7] http://www.ordnancesurvey.co.uk/oswebsite/gps/osnetfreeservices/furtherinfo/questsoftware.html

[8] http://www.citg.tudelft.nl/over-faculteit/afdelingen/geoscience-and-remote-sensing/research-themes/gps/lambda-method/

2 Research Background

"If I have seen further, it is by standing on the shoulders of giants"
Isaac Newton

This chapter discusses modern navigation technologies; starting from terrestrial radio navigation, right through to modern-day Global Navigation Satellite Systems (GNSS). There are currently four GNSS systems, either in operation, or undergoing deployment, which will be introduced, compared and contrasted. Space and Ground Based Augmentation Systems, and relevant pseudolite implementation are also discussed. This chapter concludes with a discussion of the current state-of-the-art in navigation, indicating the problems that GNSS currently faces, and highlighting the importance of pseudolite systems.

Contents

NAVIGATION is the technology and practice of getting from point A to B[1]. It tends to be based on bearings and azimuths (dead reckoning to the sun or other natural objects, or, as in Homer's Odyssey, using stars or a compass to determine north). Even the revolutionary metre[2] had to be determined by triangulation and star measurements, with distance measurements limited to a single baseline[3]. This changed in 1734 with Harrison's precise time piece, which in time led to distance accuracy far exceeding angular measurements, as a result, "when" and "where" became closely related questions[4].

2.1 Terrestrial positioning

The navigation revolution took some time to get underway. J.C. Maxwell's theory, A. G. Bell's phone and the first instance of wireless communication only happened towards the end of the following century[5]. Radio only gained widespread recognition with Marconi's Trans-Atlantic wireless transmission in 1901, and Reginald Fessenden's first public broadcast on Christmas Day 1906 (Kendal, 2011). This soon moved to military applications such as radio positioning systems, using the principles of hyperbolic navigation, where position is calculated by the intersection of hyperbolic curves, created by differencing signals from two or more radio sources (Laurila, 1976). Time bias and distance reliance were reduced by grouping transmitters in chains, with one master and a number of slave transmitters, but only planar positioning was possible.

The first radio navigation system was GEE, with a waveband of 20 – 70 MHz and a range of 300 mi, which was initially deployed as a blind landing system at the start of World War II. With Decca[6], it created the base for the civilian-based LORAN system (1943), Chayka – its Russian counterpart, and Omega (1968). Omega was the first truly global navigation system, and through sacrificing accuracy for global coverage (see figure 2.1, page 10), it was also able to provide signals deep underwater – very important for submarines in the Cold War era. This system pulsed four carrier wave signals, within the 10 – 14 kHz band, in an accurately defined pattern (Willigen, 2012).

Each of these systems suffered from the use of non-direct sky wave observations and unstable time, reducing positional accuracy. Currently only LORAN is active, although this was shut down in the US in 2008. Its modern incarnation, eLORAN, is being mooted as a possible backup system for GNSS.

2.2 Pseudolites

The NAVSTAR Global Positioning System (GPS) was the first of the space-born navigation systems. Approved in 1973, it was based on Timation time transfer satellites, and Project 621B, which was

[1] As per definition by Royal Institute of Navigation (RIN).

[2] As "natural" and "scientific" value it was supposed to equal one ten-millionth of the distance from the North Pole to the Equator, the quadrant of the Earth's circumference, as measured along the Paris meridian from Dunkerque to Barcelona.

[3] Work was carried out from 1792-1798 by Pierre Méchain and Jean-Baptiste Delambre.

[4] Indeed, a metre is defined as a distance the light will travel in vacuum within $1/299\,792\,458$ s.

[5] In 1873, 1876 and 1866 respectively.

[6] Decca used 70 – 1 290 MHz band with 400 mi range.

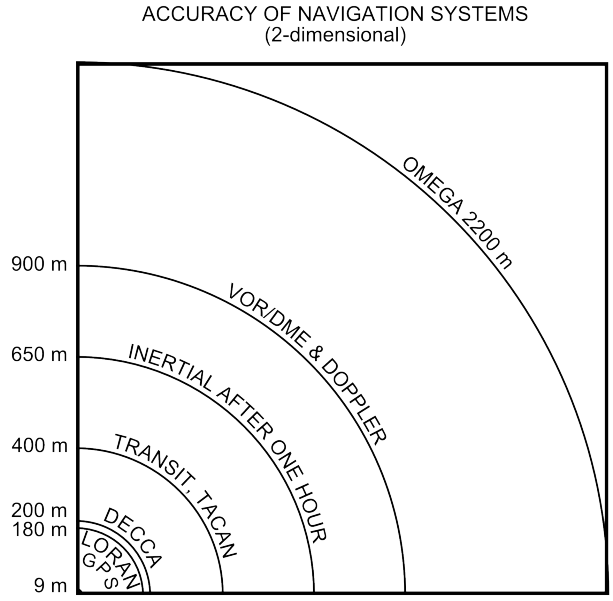

Figure 2.1 – Overview of terrestrial navigation systems accuracy

Work found at http://en.wikipedia.org/wiki/File:Accuracy_of_Navigation_Systems.svg / CC BY-SA 3.0

researching pseudo-random noise (PRN) for satellite ranging. The concept was tested at Yuma Proving Ground using terrestrial transmitters and a rover aboard an aircraft, which led to the creation of pseudolites. Early research on static terrestrial transmitters emitting GPS-like signals, focused on the increased availability and usability of GPS, mostly for aviation (Cobb, 1997; Parkinson et al., 1996). At this time a dual role for pseudolites was assumed:

- Signal augmentation, through an increase in the number and improved geometry of available signals, which also lead to a marked improvement in the vertical fix;
- An enhanced data link able to provide the corrections in a fashion similar to SBAS, (see section 2.5, page 20), especially for approach, landing (aviation) and port entry (marine).

A pseudolite needs careful planning and hardware design as it is subject to a number of limiting factors including:

Multipath a non-direct signal, which manifests itself as a severe signal power and phase shift. This can produce a severe reduction in signal quality, and in certain circumstances prevent the rover from receiving any signal.

Imprecise clocks inexpensive, temperature compensated crystal oscillators (TCXO) are used, which require differencing or other means of keeping time synchronisation.

Near-far effect due to the relatively short distance from transmitters to the rover, the received signal at the rover can be so strong that it suppresses any other transmission. Solutions to this problem include: exclusion zones, antenna beam forming, pulsing signals, time, frequency, and code separation. Historically, due to low hardware intrusion, pulsing signals with code separation were preferred (Cobb, 1997; Parkinson et al., 1996).

Tropospheric delay caused by the signal refracting in the atmosphere leading to signal delay and diffraction.

Legality of transmitting on the L1 frequency in the USA and other countries.

Short signal range of around 10 km due to the power input used and the nature of local terrain (Cobb, 1997; Locata Corporation Pty Ltd, 2011a).

The use of additional signals, arriving from lower elevation angles offers a large improvement in height determination, assuming precise clock integration. A large geometry change[7] improves the quality and speed of ambiguity resolution (Cobb, 1997; Hofmann-Wellenhof, Lichtenegger and Wasle, 2008; Kaplan and Hegarty, 2006; Meng et al., 2004; Yang et al., 2010). RAIM[8] can also benefit from constant, predictable and strong signals making it ideal for the SBAS[9] reliability requirement (Lee et al., 2008; Soon et al., 2003; J. J. Wang et al., 2004).

The GPS PRN 33-37 bands have been reserved for terrestrial use (Global Positioning System Wing, 2010), but with the increase in satellite availability, the focus has shifted from availability and accuracy to integrity. Further research on terrestrial applications (Barnes, Wang, Rizos and Tsujii, 2002; Meng et al., 2004) came to a halt as, due to the concerns of the aviation industry, US and Australian legislation has protected the GPS L1 frequency, 1 559 – 1 610 MHz. Across rest of the world, especially in Asia and Europe, pseudolite technology is still actively being developed, with the latter focusing on the Galileo frequency (Dietz et al., 2007; Gottifredi et al., 2008; Schlötzer, Martin and v. Voithenberg, 2007). New European Union dedicated pseudolite legislation allows controlled use of pseudolites (Electronic Communications Committee, 2012, 2013).

2.3 Locata

The Locata Corporation have been developing positioning technology since 1995. The first prototype was based on the Marconi Corp. Allstar GPS receiver (Mitel GP2000 chipset) (Barnes et al., 2003a). This proof of concept, still transmitting on the GPS L1 frequency, has been used to demonstrate a number of applications, including indoor positioning and bridge monitoring (Barnes et al., 2004, 2002).

This research work was carried with the University of New South Wales (UNSW) using IntegriNautics IN200, Spirent and dedicated Marconi Corp. Allstar GPS receivers (Barnes et al., 2002; Meng et al., 2004; Soon et al., 2003). With legislation restricting the use of GNSS frequencies in the US and Australia, this work has stopped, and the subsequent Locata hardware, based on flexible Xilinx Field Programmable Gate Array (FPGA) board, has moved to the 2.4 GHz licence-free ISM band.

The University of New South Wales Satellite Navigation and Positioning Group Lab (UNSW SNAP Lab) is a centre of excellence for this technology. Until recently it operated a fully functioning LocataNet test-bed able to conduct research into areas such as: LAMBDA ambiguity resolution, hardware and the GNSS/INS/Locata multi-sensor navigation package for aviation (WEB)[10] (Bertsch, 2009; Cheong, 2012;

[7] Pseudolite can offer almost instant line-of-sight change of more than 90°.

[8] Receiver Autonomous Integrity Monitoring (RAIM), a position quality confidence metric used in the aviation. See appendix D on page 155.

[9] This augmentation system will be discussed in section 2.5 on page 19.

[10] `http://www.gmat.unsw.edu.au/snap/work/theme4.htm`

Khan, Rizos and Dempster, 2010). The University of Nottingham, the first non-Australian university to gain access to this technology, has been actively involved in Locata research since 2007, starting with the single frequency firmware version v.2.4 . This research, apart from confirming the centimetre-level positioning capability of the system, highlighted a susceptibility to devices utilising wireless communication protocol IEEE 802.11 (commonly known as WiFi) in-bound interference (Montillet, 2008). Locata research is also carried out at the University of Ohio, focusing on sensor integration (Rizos, Grejner-Brzezinska et al., 2010).

Leica Geosystems and the US Army are active commercial partners to Locata, in the areas of mining and aviation respectively (Barnes, LaMance et al., 2007; Carr, 2012; Craig and Locata Corporation, 2012; Gakstatter, Murfin and Shears, 2011). After initial interest, Trimble and Caterpillar invested in their own pseudolite technology Terralites. Locata was also deployed in the Sydney Bay area, testing maritime applications of the system (Harcombe, 2012).

A LocataNet consists of a Terrestrial Segment (TS), which provides the positioning signal, and a navigation User Segment (US), a roving unit (rover) providing position (Locata Corporation Pty Ltd, 2011a). The system uses the precise network time provided by TimeLoc (see section 3.1, page 30), to calculate position in a GNSS-like fashion using code and carrier phase. Since firmware version v.3.0 the system utilises two frequencies:

S1 2 412.28 MHz,

S6 2 465.43 MHz,

these provide a cluster of four signals per transceiver. The main difference between Locata and the standard pseudolite concept are:

- Utilization of the 2.4 GHz licence-free ISM band;
- TimeLoc precisely synchronising whole network to a dedicated time source, with either local or GPS Time;
- A pulsing, digital signal utilising Time and Code Division Multiple Access (TH/DS-CDMA) using a spatially separated dual frequency antenna array;
- The ability to provide a stand alone solution without need for a base station (double differencing).

Ambiguity Resolution

For centimetre-level fix, an integrated carrier phase (ICP) needs to be observed and an unknown number of full cycles counted between the transmitter and the receiver, accounted for in a process known as ambiguity resolution (AR). Traditionally, GPS uses a code-based solution as an initial approximation, it then uses either combined observations (SPS, PPP), or double differencing against the known base station (RTK, N-RTK) to produce float estimates. AR such as LAMBDA will be used to estimate integer ambiguities. The utilisation of pseudolites to aid the AR was proposed in Cobb (1997), with further suggestions about the multi-frequency approach in Zimmerman et al. (2000).

Locata pseudo-range (code) solution is not sufficiently precise, so Known Point Initialisation (KPI) is used instead. This requires either a known point or a GPS feed to provide an initial fix (see figure 4.1, page 46). Bertsch (2009) has researched the LAMBDA approach, but using only simulated data.

2.4 Global Navigation Satellite Systems

The acquisition of German rocket technology by the Russians and the German experts recruited by the Americans after WWII, formed the starting point of space exploration and the Space Race. The starting pistol sounded on the 4th of October 1957 with the signal transmitted by the Russian Sputnik 1. Unmodulated signal observations led to Doppler-based navigation systems and the development of dedicated mathematical tools, including the Kalman Filter, the full potential of which could only be realised by the computers of the eighties. Simultaneously, the development of very long baseline interferometry (VLBI) allowed for the precise measurement and modelling of satellite orbits in relation to ever changing earth coordinate systems (Hofmann-Wellenhof et al., 2008). Pseudolites and GNSS technologies are thus very closely related, having similar navigation principles and methodology.

In the following section, four space systems, referred to collectively as GNSS, will be discussed, each one presents a unique solution to the problems of navigation. Due to the nature of this thesis, certain aspects have been touched upon only briefly. For detailed information about each system see Davis et al. (2012); Hofmann-Wellenhof et al. (2008); Leick (2004); Parkinson et al. (1996) and the relevant Interface Control Documents (ICD) (China Satellite Navigation Office, 2011; Global Positioning System Wing, 2010; GSW, 2010a, 2010b; Russian Institute of Space Device Engineering, 2008), as well as the next chapter.

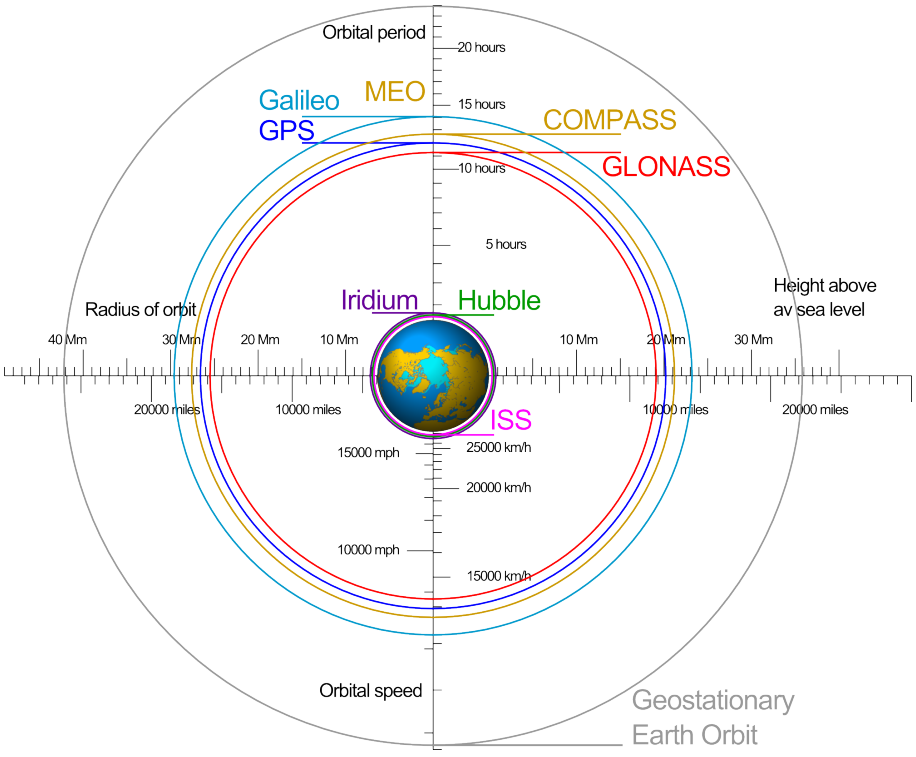

Figure 2.2 – GNSS constellations and selected satellites

Adapted from http://commons.wikimedia.org/wiki/File:Comparison_satellite_navigation_orbits.svg / CC BY-SA 3.0

Any GNSS is extremely expensive to deploy and maintain, hence the activity in pseudolite system research, despite their limitations (see section 2.2, page 9). Space systems are divided into three

segments:

Space Space-borne equipment, predominantly signal bearing satellites. Thus it is extremely expensive to deploy, and requires onstant monitoring and control to maintain system accuracy.

Control Responsible for the determination, monitoring and prediction of orbits, clocks, signal stability and other vital calculations. In the case of GPS this is the master control station at Shriever Air Force Base in Colorado Springs. In conjunction with monitoring stations in: Hawaii, Colorado Springs, Ascension Island, Diego Garcia, Kwajalein; and ground control stations in Ascension, Diego Garcia and Kwajalein. The system is augmented by 14 sites operated by the National Geospatial Intelligence Agency to compute the precise ephemerides.

The user The end beneficiary of the system and stream of revenue (though no GNSS is capable of maintaining itself without governmental funding).

NAVSTAR Global Positioning System

The military TRANSIT[11] system, launched in 1964, was the first space-born navigation system. Its satellites orbited in a polar plane at an altitude of 1 100 km (Leick, 2004). This solved one of the major problems of early terrestrial systems - the non-direct sky wave. An accuracy of 100 m was achievable by using two carrier waves at 150 MHz and 400 MHz, Doppler shift measurements and corrections for ionospheric group delay. Intermittent signal availability[12], user velocity sensitivity and a planar-only position made it of only limited use for aviation. However, it was much used in marine navigation, both commercial and military, including use by submarines.

The direct predecessor of NAVSTAR, Timation, was first launched in 1972. It was equipped with very stable clocks, facilitating precise time transfer and navigation capacity[13] (Parkinson et al., 1996). This system used the same simple receiver as its predecessors, a far cry from the capacity and complexity of modern GNSS receivers[14]. Timation demonstrated what a major breakthrough the US Air Force Project 621B was – a successful test of satellite-ranging based on the pseudo random noise (PRN) over a communication channel[15]. The NAVSTAR Global Positioning System (GPS) was approved in 1973, using existing Timation satellites, with the first dedicated satellite being launched in 1978 (Hofmann-Wellenhof et al., 2008; Parkinson et al., 1996). Following the initial operation period using pseudolites, GPS reached full operational status (FOC) in 1995.

Following a decision by the US military establishment in 1990, the clocks and ephemeris data for civilian users were deliberately degraded by introduction of Selective Availability (SA). This was

[11] Also known as Navy Navigation Satellite System NNSS, developed by the Johns Hopkins University Applied Physics Laboratory.

[12] As mutual interference limited the number of usable satellites to five, the signal was available with 35 – 100 min gaps, depending on the observer's longitude (Parkinson et al., 1996).

[13] Navigation was to be carried out using side-tone ranging - solving ambiguity using a variety of synchronised tones.

[14] System bandwidth was 15 kHz. In comparison LORAN required 20 kHz bandwidth, while the modern GNSS receivers require in excess of 60 MHz (Willigen, 2012).

[15] the communication channel would also allow transmission of ephemeris and clock information to the user at 50 $^{\text{bit}}/_{\text{s}}$.

followed in 1994 by the encryption of military P (with P(Y)), which prevented civilian users from using L2 frequency signals. Dual frequency use was important for the reduction of any atmosphere related effects, see section 4.7, page 57, hence it severely reduced the system navigation capacity for civilian users. The needs of civilian users were made painfully clear by the 1983 Korean civilian airliner incident (International Civil Aviation Organization, 1993) which prompted President Ronald Reagan to guarantee free use of GPS for civilians. On 2nd May 2000 SA was reduced to zero (but not turned off), opening up GPS to mass market interest (Leick, 2004).

Currently, GPS utilises two frequencies:

L1 1 575.42 MHz: modulated with civilian C/A code,

L2 1 227.6 MHz: modulated with military P(Y) code.

It is intended to introduce civilian and military signals on existing frequencies, with an additional frequency, L5, common to all GNSS systems, see table B.1, page 139. Multiple frequencies allow, among other things, better mitigation of atmospheric effects. This split between a precise military signal and a less-precise civilian one is common to all GNSS systems.

GLONASS

The Russian military system Tsiklon (Cyclone) from 1967[16], and its civilian counterpart Tsikada (Cycad), from 1979, worked on the same principle as the TRANSIT system, using 150 MHz and 400 MHz frequencies. The constellations, of six, and four satellites respectively, were augmented, by Parus (Sail)[17] in 1976. Parus was intended for military submarine navigation - the equivalent of America's Timation. Collectively they formed the base for the Russian global navigation system - GLONASS (Global'naya Navigatsionnaya Sputnikovaya Sistema), whose first satellites were launched in 1982[18] (Hofmann-Wellenhof et al., 2008; Kunegin, 2000). The system became fully operational in September 1993 with a nominal constellation of 24 satellites completed in 1996. A subsequent lack of funding led to its quick decline, with satellite numbers reaching the working minimum of between six to eight, in 2001. GLONASS has recently received a major increase in governmental funding, with full constellation restored in 2013. Due to its military background GLONASS offers two levels of service, in the same fashion as GPS:

- a standard precision service, open to civilians, also referred to as O - open signal,
- a high precision military service, S - using an obfuscated signal, which is not encrypted in the manner of GPS(Y), but instead, its Pseudo-Random Noise (PRN) is unknown.

GLONASS is currently supported by a control network of six stations (Moscow, St. Petersburg, Yeniseisk, Komsomolsk, Balkhash and Brazilia), with another six planned, one outside of Russian territory and one in the North Pole (Revnivykh, 2012). Its coordinate system, *Parametry Zemli 1990* (PZ90) is known and so is its relation to ITRF2008, with metre level accuracy. The time system used is

[16] Launch date of the first satellite. The system is reported to have been under development since as early as 1958.

[17] Also known as Tsiklon B.

[18] In October 12, 1982 one operational and two test satellites were to have been launched but due to technical problems, the first operation satellite was launched in January 1984.

closely related to UTC, with an offset of 3 hours (Standard Moscow Time), but inserts the leap seconds so that GLONASS time is not continuous.

Unlike GPS, all GLONASS satellites use the same code, transmitted on a range of different frequencies in order to identify satellites (see table B.2, page 140), and to prevent cross-correlation between them[19]. The antenna's beam patterns were designed to serve space receivers as well (Hofmann-Wellenhof et al., 2008; Parkinson et al., 1996). With a limited number of frequencies (12+2) each pair of satellites in antipodal positions use the same frequency, as it is impossible for non-space receivers to track both of them at the same time. Broadcast ephemerides, unlike GPS, are given by the position and velocity of satellites.

Modernisation plans include, moving to the CDMA signal to a new G3 frequency, upgrade of the navigation messages including time offsets between GPS and GLONASS (to within $30{\cdot}10^{-9}$ s), leap second corrections, pseudo-range accuracy estimations and hardware delay between G1 & G2 frequencies (Hofmann-Wellenhof et al., 2008). Details are not yet finalised, hence the indicative values in table B.2 on page 140. One of the most important modernisations is the implementation of CDMA. The GLONASS FDMA approach, while mathematically superior to CDMA and more resistant to narrowband interference, requires a more complex front end and, more importantly, does not allow interoperability with other GNSS.

The CDMA signal is currently being tested on the only operating GLONASS-K satellite[20] using the temporary G3 frequency[21]. The author is not aware of any pseudolite systems utilising GLONASS frequencies, especially as the FDMA and lack of dedicated terrestrial PRNs makes such a pseudolite system very difficult to implement.

Galileo

In the early 1990's, the EU aspired to produce a GNSS in close cooperation, and to be interoperable with GLONASS. This was later dropped in favour of an independent system (Cojocaru, Birsan, Batrinca and Arsenie, 2009; Kaplan and Hegarty, 2006). The rationale for an independent system was the fear of European dependency on the military GPS, which could be interrupted should any armed conflict break out. Named after Galileo Galilei, it is a civilian system under civilian control. This programme is further justified by current uncertainties over the GPS budget, and the age of its over-performing satellites (The Royal Academy of Engineering, 2011).

Starting in 2000, initial efforts concentrated on the EGNOS SBAS system (see section 2.5, page 19). The first Galileo test satellite, GIOVE-A was launched in December 2005, in order to secure bandwidth allocation. Due to its civilian nature, Galileo has a large, globally distributed ground segment, with nearly the same coverage as GPS, and exceeding both GLONASS and Beidou. The two main control stations are in Germany and in Italy, with ten ground tracking stations and 40 sensor stations.

Galileo is based on a service-oriented approach, offering:

[19] The FDMA frequency separation provides excellent −60 dBm cross-correlation, despite the PRN being shorter than the GPS one. This design makes GLONASS the most narrow-band and interference resistant GNSS.

[20] Also known as Urugan-K, launched in 2011 (European Space Agency, 2011; Zak, 1997). In 2013 three GLONASS-K satellites were destroyed during a failed launch attempt.

[21] The G3 frequency is supposed to change from current 1 202.025 MHz to 1 207.14 MHz with the launch of GLONASS-K2, currently expected in 2015 (Zak, 1997).

OS open service, free for all users;

CS an encrypted premium commercial service, offering improved accuracy and guarantee of service - a unique selling point;

PRS the public regulated service, offering a critical encrypted service in time of crisis with OS accuracy for both selected EU and non-EU government agencies;

IMS integrity monitoring service, providing integrity information for life-critical applications. This used to be known as the safety of life service (SOL) ;

SAR a two-way search and rescue service, co-designed by the EU, the USA, Russia and Canada, operating on the 150 MHz frequency and able to detect 150 signals at the time.

There are currently only four active satellites in space[22] but there are a number of pseudolite-based sites including, GATE and SEA GATE, which offer the possibility of testing Galileo-ready equipment[23]. The Galileo terrestrial reference frame (GTRF) is directly related to the International Terrestrial Reference Frame (ITRF), it is intended to differ from ITRF2008 by no more than 3 cm (2σ). Galileo's time is continuous, with a nominal offset to International Atomic Time (ITA), hence its atomic clock is steered towards ITA, with an accuracy of $30{\cdot}10^{-9}$ s (at 2σ).

Galileo embodies a number of unique features. The signals are designed to prevent spoofing, reject multipath[24], and improve signal quality in weak signal environments, such as indoors (E5a). Common GNSS signals will be present on the E1 and E5a frequencies, (see table B.3, page 141). The navigation message provides GPS to Galileo time offset (GGTO) to $5{\cdot}10^{-9}$ s accuracy and with I/NAV and G/NAV real-time integrity monitoring (Hofmann-Wellenhof et al., 2008).

Beidou – Chinese Navigation Satellite System (CNSS)

Chinese interest in satellite navigation is known to have started in early '80s, but no details are available. The initial concept, nicknamed Double Star, was based on geostationary communication satellites; it only reached the demonstration stage, before being abandoned in 1989[25]. A new concept of a regional augmentation system, Compass, was then developed. Compass was intended to be developed firstly as a regional augmentation system, and subsequently to be upgraded, by adding satellites, to provide global coverage.

At the initial regional stage, coverage was to include the whole of China, and neighbouring countries. Information about the constellation design is inconsistent, and various versions have been presented. Recent publications suggest that the system will be a combination of GNSS and an SBAS, providing:

- Five GEO satellites positioned at 58.75°E, 80°E, 110.5°E, 140°E and 160°E.
- Three Inclined Geosynchronous Satellite Orbit (IGSO) satellites at an altitude of 35 786 km and an inclination of 55° to the equatorial plane.

[22] This number excludes two test satellites, which are currently not active.

[23] Transmitters are placed on mountain tops with receiver equipment based inside the track. This is different to the GPS Yuma test bed, with the receiver on planes and transmitters on the ground (Hofmann-Wellenhof et al., 2008).

[24] Multipath occurs when a signal arrives at the antenna from more than one path or direction, thus causing the antenna to receive a combination of direct and non-direct signals, see section 4.8, page 61.

[25] Only two geostationary communication satellites have been launched in this system.

- 27 Medium Earth Orbit (MEO) satellites at an altitude of 21 528 km and an inclination of 55° to the equatorial plane (China Satellite Navigation Office, 2012; Liu, 2009).

The official name of the system is Beidou[26], or the Chinese Navigation Satellite System (CNSS) (China Satellite Navigation Office, 2011; Liu, 2009). The first successful satellite launch was in 2000, and as of the end of 2012 there are 14 satellites in the constellation[27]; the regional system was declared operational in December 2011 (Hofmann-Wellenhof et al., 2008; Kaplan and Hegarty, 2006).

The China Geodetic Coordinate System 2000 (CGCS2000), is related to the International Terrestrial Reference Frame (ITRF2008) and is very similar to the reference frame implemented by Galileo (China Satellite Navigation Office, 2011; Davis et al., 2012). BeiDou Time (BDT) is continuous, with a nominal offset to International Atomic Time (ITA). The starting point was 00:00 Jan 1st, 2006 (UTC). Like GPS, COMPASS presents two levels of service:

Open the standard accuracy civilian service, with two-way communication within China[28];

Precise the authorised military service, with improved accuracy, integrity of information and dedicated communication (Liu, 2009).

CNSS has the lowest monitoring capacity of all systems, as all of its five tracking stations are located within China[29], providing only 35° of full arc visibility. Planned interoperability with other GNSS systems includes common frequency and modulation – TMBOC in the L1 and L5 frequency band, planned by 2020 (Davis et al., 2012). Both planned, and existing signals, are presented in table B.6 on page 143. No information about BeiDou pseudolite systems is currently available.

2.5 Augmentation systems

Accuracy, reliability and integrity of GNSS is heavily dependent on the number and geometric distribution of the available satellites. This can lead to local shortcomings, which are serious, as even seemingly uncoupled devices, installations and services are over-reliant on GNSS (The Royal Academy of Engineering, 2011). Implementation of an augmentation system can mitigate this.

Designed to improve Time to First Fix (TTFF), accuracy, and positional integrity; its accuracy and coverage need to be balanced against physical, mechanical and electronic restrictions. Space and Ground Based Augmentation Systems, known as SBAS and GBAS respectively, and discussed below, trade accuracy for simplicity and the provision of the real time warning levels. The Continually Operating Reference Station (CORS) networks (see section 2.5, page 21), are limited in coverage but offer centimetre-level accuracy.

There has been much research into pseudolite-based GBAS for airports, harbours and similar facilities. It is quite rare for pseudolites to address the same market segment as CORS; however, Locata is an exception.

[26] Chinese for Ursa Major.
[27] Five GEO, four MEO and five IGSO (China Satellite Navigation Office, 2012).
[28] Provision of 160 byte long messages.
[29] Those are Changchun, Kunming, Lintong, Shanghai and Urumqi.

Space Based Augmentation System (SBAS)

A Space Based Augmentation System (SBAS), comprising both ground and space segment, is primarily intended for use in aviation for take-off and landing. It is a network of terrestrial monitoring stations compute code based satellite orbits, clock and ionospheric corrections as well as an integrity message[30]. Calculated corrections are uploaded using the C-band, to Geostationary Earth Orbit (GEO) satellites which transmit corrections to the user on the L band[31], with a dedicated SBAS data message[32]. The aim is to provide the Standard Positioning Service (SPS) with metre level positional, and $10{\cdot}10^{-9}$ s level time accuracy. GEO satellites, lying low on the horizon, are not ideal for urban users and this service is predominantly aimed at aviation and maritime users, who are interested in integrity monitoring (Hofmann-Wellenhof et al., 2008; Kaplan and Hegarty, 2006).

Civilian Service

The first SBAS was the American Wide Area Augmentation System (WAAS), implemented in 2000, it reached initial operational capacity (IOC) in 2003. This system includes 38 reference stations and four GEO satellites, with communication provided via three master control stations.

The European Geostationary Navigation Overlay Service (EGNOS) became fully operational in 2011. It is designed to address the needs of marine and land users, with corrections also sent via the internet[33]. Currently the system consists of 40 monitoring stations, four master control stations (one active, one hot backup and two cold backups), and three GEO satellites. It is still being actively developed and is expected to cover Africa and be deployed on the L1 and L5 frequencies.

The Japanese Quasi-Zenith Satellite System's (QZSS) design aims to provide a positional service in urban canyons and mountainous environments, across East Asia and Oceania (Hofmann-Wellenhof et al., 2008). It has grown from the Japanese Satellite Augmentation System (MSAS) and offers unique figure-of-eight orbits providing signals from elevation angles exceeding 70°, using GPS-like signals on the L1, L2, and L5 frequencies and the experimental LEX on E6 (see table B.5, page 142). The first satellite was successfully launched in early 2011 and while recent earthquake activity delayed the deployment of the remaining three, it has been confirmed that the system's full operation is a priority.

Russia is also developing its own System for Differential Correction and Monitoring (SDCM) utilising the GLONASS G1 frequency. The first satellite was launched in December 2011. Apart from the stations in Russian territory, plans are in place to locate ground stations in Australia, Indonesia, Brazil, and Nicaragua.

India is following others by planning a GPS and GEO Augmented Navigation (GAGAN) service, with the first satellite launch in 2013.

[30] This does not include any local phenomena, such as solar flare, tropospheric delay, receiver specific corrections and multipath.

[31] Usually the GPS L1 frequency is used, being the only fully protected frequency.

[32] Its ranging code is the same as GPS, but the data rate is higher.

[33] EGNOS Data Access Service at `http://egnos-portal.gsa.europa.eu/developer-platform/developer-toolkit/egnos-data-access-service-edas`

Commercial Service

SBAS-like services are also provided by commercial companies including: John Deere and Company, Trimble, and Fugro. Fugro offers the marine based StarFix, SeaStar and MarineStar services alongside the land based OmniStar service, which is now owned by Trimble. Each of these systems operates in a similar fashion providing:

- Sub-metre accuracy DGPS using differential L1 corrections;
- A Precise Point Positioning (PPP) service, with a decimetre accuracy, using dual frequency GPS (XP) which can also be combined with GLONASS (G2);
- A dual frequency phase-based, sub-decimetre positioning service (HP).

Corrections, computed at over 100 reference stations around the globe, are sent via GEO satellites to user receivers using the Radio Technical Commission for Maritime Service (RTCM) format. These corrections are used to calculate Virtual Base Stations (VBS) by the user's receiver (see section 2.5, page 21). The most precise HP services utilise the Global Differential GPS (DGPS) network operated by NASA's Jet Propulsion Laboratory (JPL). This network was primarily designed as a support for NASA missions, providing position for spacecraft using GPS, in addition it offers real-time satellite monitoring (Fugro, nd; Hofmann-Wellenhof et al., 2008). This approach, combined with utilisation of Inmarsat communication satellites, has lower information overheads than public SBAS services.

Ground Based Augmentation Systems (GBAS)

Ground Based Augmentation Systems (GBAS) provide augmentation for a specific local area and are limited to the terrestrial component only. A Local Area Augmentation System (LAAS), as defined by Civil Aviation Organisation (ICAO)[34], provides L1 code-based, metre level position, and real-time integrity checks within a 45 km radius area. Pseudolites were originally considered as a part of this structure, and a number of such systems have been developed. They are usually based on existing L1 GPS receivers, such as the IntegriNautics IN200 pseudolite or the Spirent pseudolite, which were able to receive both GPS and pseudolite signals simultaneously (Cobb, 1997; Lee et al., 2008; Soon et al., 2003; J. J. Wang et al., 2004). Legislation protecting the L1 broadcast band has stalled future work in this area. In 2011 Locata was designated by ICAO as a backup candidate for GBAS (Gakstatter et al., 2011).

EADS Astrium GmbH, has designed a dedicated pseudolite system for augmentation using Galileo signals in maritime environments. These signals can be tracked by an off-the-shelf Serpentio GeneRx Receiver (Dixon and Morrison, 2008). Pseudolites are also used at Galileo's GATE and SEAGATE testing grounds, sporting a modified pulsing scheme (Abt, Soualle and Martin, 2007; Dietz et al., 2007; DLR, 2012; Schlötzer et al., 2007). A number of smaller, GBAS-like systems for the precision agriculture market exist, actively competing with StarFire (see section 2.5, page 19), and sending corrections over the internet or by DBM radio.

[34] The U.N. body charged with regulating global aircraft navigation and safety.

Low Frequency Augmentation Systems – LORAN

One of the major weaknesses of any pseudolite augmentation system, in common with GNSS, is a reliance on radio, satellite or cellphone-based communication, which makes it vulnerable to accidental or deliberate jamming. Relatively small-sized devices with a low power output can block signals over a large area. Low-frequency systems, such as LORAN, make such attempts much more difficult and have been discussed as GNSS augmentation or a backup systems (Helwig, Offermans, Stout and Schue, 2012; Hofmann-Wellenhof et al., 2008; Kaplan and Hegarty, 2006; Pelgrum, 2006).

LORAN was designed at the Massachusetts Institute of Technology (MIT) in 1943, based on prior terrestrial navigation systems (see section 2.1, page 9). Only the planar position can be determined, and successful triangulation requires at least three transmitters, as clock-offset needs to be estimated. For this reason LORAN stations have usually been grouped in chains of 3-6 offering a range of 1 200 M. The initial design was replaced in 1957 by LORAN-C with an initial accuracy of only 460 m (see figure 2.1, page 10). This low level of accuracy is a function of the unpredictable nature of the ground wave.

The Volpe study in 2001, and the proposed ERNP (European Radio Navigation Plan) in 2004, lead to the development of the eLORAN (EuroFix in Europe) which offers a realistic augmentation capacity and a precise time and frequency source with $50{\cdot}10^{-9}$ s time accuracy. eLORAN could be used to re-open American stations, shut down in 2010[35] (Helwig et al., 2012). This differential LORAN, with precise clocks and ground wave modelling, offers an accuracy of 22 m (95%). Chayka (Sea Gulf) a Russian counterpart, transmits a similar signal, but it is not time-synchronised with LORAN, so any attempts to combine the two systems would degrade positional accuracy (Pelgrum, 2006).

Property	GNSS	Loran-C / Chayka
Frequency	Ultra High Frequency (1-2 GHz range)	Low Frequency (90-110 kHz)
Transmitters	Space based	Terrestrial
Transmitter power	Low (50-200W)	High (250 kW – 1 MW)
Signal structure	CDMA	Pulsed TDMA/CDMA
Signal Propagation	Line-of-sight	Ground wave / sky wave

Table 2.1 – GNSS and LORAN comparison from Pelgrum (2006)

Continually Operating Reference Station (CORS) and Network RTK

Continually Operating Reference Station (CORS) is the backbone of Network Real Time Kinematic (N-RTK) positioning, using the double differencing approach to mitigate GNSS system biases. CORS extends the RTK baseline limits of 10 km to 60 – 100 km. This system is very prone to local atmospheric anomalies, scintillation, and receiver-based biases, such as multipath (Hofmann-Wellenhof et al., 2008). With a number of base stations used, VBS can be calculated, by the interpolation of known corrections in the vicinity of the user, creating a virtual, short baseline (see table 4.5, page 53), using the following methods:

[35] http://www.uscg.mil/ANNOUNCEMENTS/alcoast/675-09_alcoast.txt

network-based which requires a bi-linear connection with the rover providing its approximate position (using SPS), and receiving calculated corrections. This can be implemented by iMAX, PRS and VRS methods;

rover-based where both raw observations and correction coefficients are sent to the rover, which then calculates the corrections. This is implemented by MAX and FKP corrections, it is similar to DGPS and OmniStar in approach.

Each of these methods requires a large bandwidth, although this can be reduced if mono directional mode is used (Wübbena, Bagge and Schmitz, 2001). CORS is designed as a regional system, with the information supplied by commercial companies, usually with government support to share the cost. CORS is the only augmentation system offering centimetre-level positioning in real-time[36].

2.6 Current state-of-the-art

This chapter has outlined the history and the current state of modern navigation technologies, both terrestrial (with focus on pseudolites), and Locata, and space-born systems. The pseudolite concept faces many challenges, but there are a number of commercial products already on the market.

Naviva (Naviva, 2012) is able to both self-synchronise, and with a GNSS time source, produce stand-alone solutions similar to Locata. It has been promoted for open-cast mining. Other frequencies have also been experimented with by the Australian Centre for Remote Sensing (CRS), which produces pseudolite technology transmitting in GPS L1 or alternatively in 915 MHz (Brekke, Wilson and Brown, 2008). Novariant (formerly IntegriNautics) Terralites use XPS 10 GHz frequency band and are able to receive both GPS and XPS signals[37].

Astrium, part of EADS, developed a number of Galileo signal generators as well as pseudolite systems. Dixon and Morrison (2008) discusses maritime usage of a Galileo-based pseudolite system, allowing stand-alone and GNSS augmentation mode. Another Astrium system, SekaN uses a combination of L1 pseudo-range and phase for self-calibration, providing metre level planar positioning (Schlötzer et al., 2007).

The European Insiteo, offers a range of indoor positioning services, with accuracy down to a few metres for smart-phone applications, along with assisted GPS and WiFi fingerprinting (Insiteo, nd).

IIS Fraunhofer Red Fir, known as Witracksystem, was designed for football sport events (Adel, Thielecke, Grun and Wansch, 2006). Although it failed as a commercial venture, it is now an academic research project, with clock synchronisation archived by fibre optic connections.

Repeaters, capable of re-transmitting GPS signals indoors with a known delay for mobile, code-based, navigation, are the only type of pseudolites officially recognised by the EU and Great Britain (Electronic Communications Committee, 2012, 2013).

NSL Skyclone[38] is a simulation tool that allows testing of signal obstructions “on the fly”.

[36] Recently, CORS real-time atmospheric models have been used to enhance the accuracy of GBAS/SBAS systems. It is also not uncommon for those systems to share the same facilities.

[37] This technology was purchased by Trimble in 2010, who have hopes for sales in for the open-cast mining and precise agriculture markets (Montillet, 2008; Trimble, nd). System accuracy statistics are yet to be published.

[38] `http://www.nsl.eu.com/datasheets/Skyclone_flyer.pdf`

European research into pseudolite applications covers: locating munitions and explosives, asset management, robotics, automated highway systems, machine control or structural deformation (Barnes et al., 2002; Lee et al., 2008; LeMaster, Matsuoka and Rock, 2002; Meng et al., 2004; Montillet et al., 2009; Politi et al., 2007). There is also academic interest in Asian universities, fuelled by rapidly growing markets. Their current efforts are behind European research, and the author is not aware of any commercially valid development from this part of the world, yet with the size and activity of this market, this is likely to change in the future.

Locata is currently commercially deployed in open-cast mining, aviation and as a maritime test network in the Sydney Bay area (Barnes, LaMance et al., 2007; Carr, 2012; Craig and Locata Corporation, 2012; Gakstatter et al., 2011; Harcombe, 2012). Research has also addressed deformation monitoring, indoor navigation, asset management, aviation, unmanned aerial vehicles (UAV) and machine control (Amt and Raquet, 2007; Barnes, LaMance et al., 2007; Barnes, Rizos, Pahwa, Politi and van Cranenbroeck, 2007; Bonenberg, Hancock and Roberts, 2010; Bonenberg, Roberts and Hancock, 2010a; Gakstatter et al., 2011; LaMance and Small, 2011; Rizos, Roberts, Barnes, and Gambale, 2010).

Compatibility and Interoperability are the two most important buzz words for GNSS. Currently right hand circular polarization, Code Division Multiple Access (CDMA) modulation, 1 176.45 MHz and 1 575.42 MHz carrier frequencies seem set to be adopted as standard by all (Davis et al., 2012). Schönemann, Becker and Springer (2011) speculate that more frequencies and open signals may even lead us away from differencing techniques. But from a hardware point of view, large bandwidths and multiple signals are complex and expensive to deal with. This could be addressed by the utilisation of simple, perhaps single frequency receivers, aided by precise corrections estimated from local CORS networks (C. Roberts, 2011). However, even with multiple constellations, the same geometry-based challenges remain (Hancock et al., 2009; G. W. Roberts et al., 2006).

Due to atmospheric characteristics all space-born navigation signals lie in the optimal sky window of 1 – 2 GHz (Huang and Boyle, 2008), which physically limits the available spectrum, and, while some see that interoperability could be a solution (Gibbons and Pratt, 2011), other research indicates that exceeding the "sweet spot" of three to four constellations might degrade overall accuracy (Hein, 2010). Space-borne signals are weak and can be affected by a number of physical phenomena, as they penetrate the atmosphere. For instance, recent solar activity has lead to an increase in signal scintillation, produced by ionospheric irregularities especially in equatorial regions, limiting GNSS performance.

Human interference, in the form of accidental and deliberate spoofing is creating further problems. LAAS at Newark airport in USA, has experienced a number of downtime incidents, due to passing truck drivers using personal privacy devices on the nearby freeway (Davis et al., 2012). Shepard et al. (2012) have demonstrated how easy it is to inject hazardous misleading information (HMI) into modern receivers or even hijack military drones. This creates problems for system security and user safety, degrading GPS reliability, so that it is not reliable enough to be the sole means of safety for environmental or economically critical applications (Humphreys, 2012b; Scott, 2012; Shepard et al., 2012; The Royal Academy of Engineering, 2011).

New methods to combat these threats are currently being researched. A resilience network which tracks and identifies spoofers exists both in the USA and in Great Britain (The Royal Academy of

Engineering, 2011). Civilian authentication of GPS signals has also been suggested (Humphreys, 2012a; Scott, 2012). Research into implementation of atomic clocks for GPS receivers, and dual (left and right) polarised front ends, push the accuracy boundary further, as both time and multipath-related biases could soon be mitigated (Kale, Adane, Ucar, Bardak and Yavuz, 2012).

For safety's sake, over-dependency on a single technology must lead to renewed interest into other positional technologies, either as a backup, or as augmentation of GNSS. LORAN anti-spoofing capacities have been discussed, but its 22 m accuracy makes it unsuitable for engineering applications. Similar levels of accuracy are offered by other modern navigation solutions such as Signals of Opportunity (SoOP). The only real alternative to pseudolites is the inertial navigation system (INS). However, price, initialisation mechanisms, and drift remain an issue here. Locata augmentation can fill the missing gap here, with deployment costs lower than CORS or high-end INS, and it is capable of providing similar accuracy with integrity checks. Additional signals in urban canyons, deep valleys, or other areas of restricted visibility, are vital for any engineering application using GNSS.

♣ ♢ ♣

3 Description of the Locata and GPS

"Man is the measure of all things: of things that are, that they are; of things that are not, that they are not."
Protagoras

THE successful integration of different systems requires a thoughtful understanding of the components involved. This chapter will discuss both the Locata and GPS systems, focusing on those aspects that are important to a successful integration of the two. This is especially important in regard to Locata, as only a limited amount of information has been published on the subject (Khan, 2011; Locata Corporation Pty Ltd, 2011a; Montillet, 2008).

Contents

3.1 Locata

Locata is an innovative positioning technology developed in Australia. A network of ground-based transmitters, known as LocataLites, transmit four GPS-like code and phase signals in the 2.4 GHz licence-free ISM band, which provide a centimetre-level positioning fix. Unlike pseudolites, a Locata network is precisely synchronised using TimeLoc technology (Barnes et al., 2003b). This allows single-point positioning, meaning that a centimetre-level positional fix can be obtained without a reference (base) station.

The Locata Corporation has developed both the concept and the hardware, as an answer to the problems arising from the need of GNSS for direct sky visibility. Commercial deployments of the system include:

- The open-cast Boddington gold mine in Western Australia[1] in combination with the Leica Jigsaw360 (Barnes, LaMance et al., 2007; Carr, 2012; Gakstatter et al., 2011).
- The US Air Force White Sand Testing Grounds (Craig and Locata Corporation, 2012; Trunzo, Benshoof and Amt, 2011).
- The Sydney Bay maritime test bed (Harcombe, 2012).

A network of Locata transceivers known as a LocataNet is made up of two types of device: a single master, and a series of slaves. Slaves are able to maintain constant time by synchronising with the master receiver. Should this not be possible, a slave can synchronise with other slaves through cascade synchronization. The system achieves positional fix in a GNSS-like fashion, using code and an integrated carrier phase (ICP). Successful 3D trilateration requires inter-visibility of least four LocataLites, to solve for position, height and receiver clock offset. Due to the static and terrestrial nature of the transmitters, signal acquisition can be simplified, although ambiguity estimation becomes more difficult, as only the rover can introduce geometry changes (Cobb, 1997). The current generation of Locata hardware is only capable of float ambiguities estimation using Known Point Initialisation (KPI)[2].

Each LocataLite broadcasts its position as a part of its navigation data[3], allowing the system to be independently scaled[4]. Locata transceivers, are often nearly co-planar, due to environmental restrictions, so the accuracy of vertical coordinates can be limited. As with any terrestrial positioning system, Locata is highly susceptible to fading multipath effects. Another problem is bandwidth crowding, due to the large number of other devices are using the 2.4 GHz licence-free ISM band. This introduces not only noise, but also "legal spoofing", quite unlike the GNSS signal band (Montillet, 2008).

Signal structure

In order to counter multipath and noise problems, Locata uses frequency and a spatially separated cluster of four signals, Tx_{A-D}. The transmitter antenna array consists of two transmitting (Tx1 and Tx2) and one receiving (Rx) antenna (see figure 3.1, page 28). Starting from firmware version v.5.0,

[1] Following a successful proof-of-concept installation at a diamond mine in South Africa.

[2] New hardware (see section 3.1, page 35), is capable of AR using geometry change and an EKF. This approach, originally designed for the Timetenna, differs from the one proposed in this thesis, as discussed in chapter 6 (page 82).

[3] The data channel overlay was introduced with Locata firmware version v.4.0.

[4] Up to firmware version v.6.0 DS-CDMA & TDMA limited the number of units in the network to ten. The updated TDMA scheme allows for up to 50 units (see section 7.1, page 107).

these signals are identified as xA-D, x being Locata transceiver ID (see figure 3.1, page 28). For the sake of clarity this nomenclature will be applied to all firmware versions of Locata. Due to TimeLoc coupling, the receiver needs to be much closer to Tx1 than Tx2 and separation between Tx1 and Tx2 is directly related to the expected distance between transceiver and rover[5]. Up to release of firmware version v.7.0 Locata transmitted on two nominal carrier frequencies:

S1 $2.412\,28\,\text{GHz} = 236 \cdot 10.23MHz$,

S6 $2.465\,43\,\text{GHz} =\sim 241 \cdot 10.23MHz$

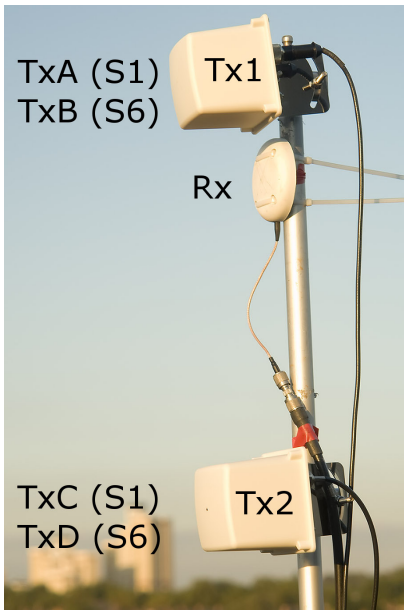

Figure 3.1 – A Locata transceiver antenna array unit

Both frequencies lie within the 2.4 GHz licence-free ISM band and are bi-phase shift key (BPSK) modulated by the modulo-2 sum of the C/A-code and the NAV data (bit train). All transmitted signal elements, carrier, code and data, are commonly derived from the temperature-compensated crystal oscillator (TCXO), currently an industry standard in geodetic receivers (Locata Corporation Pty Ltd, 2011a; Montillet, 2008).

The ISM band is heavily populated by a plethora of other multiple transmitting devices - including remote controllers, cordless phones, fluorescent lights, remote communication, bluetooth devices, microwave ovens, not to mention devices utilising wireless communication protocol IEEE 802.11 (commonly known as WiFi) (Khan et al., 2010). In order to comply with FCC 15.247 Locata uses a nominal transmission power of 23 dBm. In-band interference, noise and the near-far effect, led to the adoption of Time-Hopping/Direct Sequence Code Division Multiple Access (TH/DS-CDMA) – a pulsing scheme where each device is identified by its time of transmission and a unique PRN (Cheong, 2012; Cheong, Dempster and Rizos, 2009; Locata Corporation Pty Ltd, 2011a).

[5] The recommended separation between Tx1 and Tx2 for distances up to 1.0 km is 1 m and 1.5 m for distances exceeding 1.6 km (Barnes, Rizos, Kanli and Pahwa, 2006).

Apart from this the Locata signal is almost identical to the GPS L1 C/A structure, though it is vertically polarised, due to multipath resistance, which led to investigations into right-hand circular polarisation for future aviation applications (Locata Corporation Pty Ltd, 2011a) . Each LocataLite transmits within its assigned 100 µs long N-slots in each TDMA frame. Prior to firmware version v.6.0 a sliding sequence was used, with the same N-slot assignment in each TDMA frame, which limited the number of units transmitting synchronously to ten.

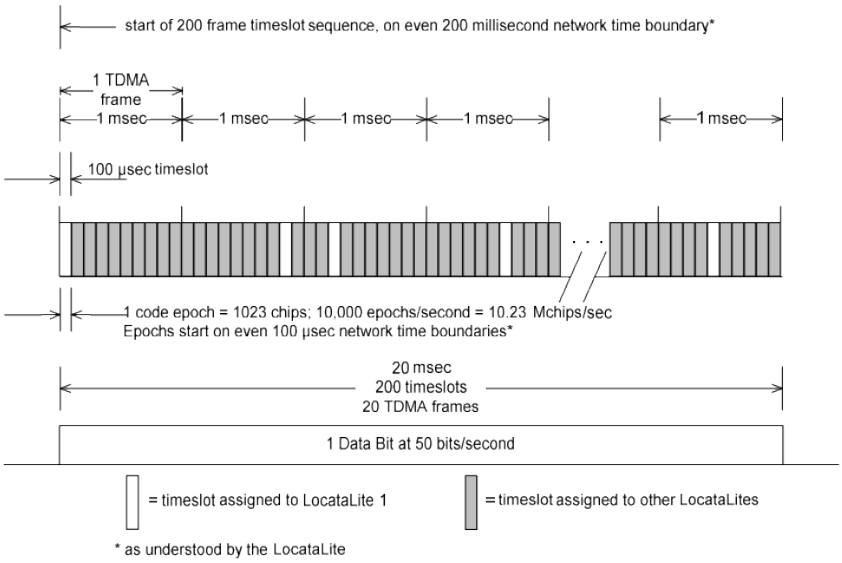

Figure 3.2 – The relationship between data, code and modified TH/DS-CDMA scheme timeslot timing, from Locata Corporation Pty Ltd (2011a)

Since the introduction of firmware version v.6.0, the time allocation has varied between TDMA frames creating a sequence that repeats only once every 200 TDMA frames, creating a 0.2 s long Super Frame,[6] as shown in figure 3.2. Each 5th Super Frame is synchronous with a Locata second (boundary to boundary) and allows for synchronisation of up to 50 units (see section 7.1, page 107).

Pseudo-range code and the navigation message

Locata Corporation Pty Ltd (2011a) defines 200 Gold Sequence PRN codes, each 1023 chips long, with the first 36 codes matching the equivalent GPS C/A codes. Each PRN is complete within its assigned N-slot, which is an advantage over prior GPS based pseudolite designs, due to the tenfold increase in the chipping rate (see table 3.6, page 42).

The codes are a modulo-2 sum of two 1 023 bit linear patterns: G1 and delayed $G2_i$[7]with odd codes by convention being assigned to the S1 frequency ($Tx_{A,C}$), and even some to the S6 frequency ($Tx_{B,D}$)[8] (Kaplan and Hegarty, 2006; Locata Corporation Pty Ltd, 2011a). The carrier phase is additionally

[6] This adds signal orthogonality and adequate signal discrimination to overcome the significant "near-far" problem, as Locata signals can vary as much as 80dB, due to the TimeLoc procedure (Locata Corporation Pty Ltd, 2011a).

[7] The GPS approach is to delay both G1&G2 to create the final code.

[8] Prior to firmware version v.5.0, signals had been designated Tx_{1-4} and identified by their PRN codes. The convention was to assign 1-20 sequentially to S1 and 21-40 to S6. The equivalent of Tx_{A-D} should be then PRN 1,21,2,22. For ease of use this was changed in firmware version v.4.0 to PRN 1,2,3,4.

modulated by the navigation data (NAV) at either 50 bit/s or 100 bit/s[9]. This message is contained within 1 200 bit Frames, each consisting of two equal length subframes (see figure 3.6, page 43), the first containing information about specific transmitters in the network and overall network characteristics[10], while the second contains almanac data on two pages:

- **Subframe 1** TLM, TM, AA[10], characteristics and coordinates of the transmitter Tx_{A-D}, Tropospheric Scale Factor, MET.
- **Subframe 2**

  Page 1 ($SF2_{1i}$) TLM, TM, AA[10], MET, self-positioning status, hardware status (battery and temperature).

  Page 2 ($SF2_{2i}$) PPS status, group delay bias[11], TimeLoc status, TCXO status, firmware.

Each Locata transmitter (LL) uses four signals, so it is possible to provide a single almanac for a number of units and thus reduce the theoretical initialisation time from 96 to 24 s[12]. Signal acquisition is supported by the Acquisition Assist Word (AA), network size and the ID of the eight nearest LL, one per message[13]. Information includes LocataLite ephemerides, system time, network status, correction factors, and Group Delay Bias Corrections for Rx_{B-D} (Locata Corporation Pty Ltd, 2011a). Currently, within firmware version v.5.0 those components are either in the test stage, or only valid as a post-processing option for Locata in-line navigation engine (LINE).

TimeLoc

TimeLoc is the backbone of the Locata system, providing consistent time within the LocataNet. One transmitter acts as the network master with the remainder, known as slaves, synchronised to the Master TxA signal using TimeLoc. This is done either directly, or indirectly by hopping, in a two-stage process. The initial, pseudo-range estimate for slave i in epoch t_k is calculated from:

$$TL_i^M(t_k) = (P^M(t_k) - P_i(t_k)) - (\rho_i^M(t_k) + \rho_{Rx}^{TxA}(t_k)) \tag{3.1}$$

where the first segment is the measured clock offset and the second is the combination of the master-slave spatial separation $\rho_i^M(t_k)$ and slave's coupling distance $\rho_{Rx}^{TxA}(t_k)$, both are known from their navigation message. To obtain the precise time carrier phase difference, the following is used:

$$TL_i^M(t_k) = \frac{t\Phi^M(t_k) - \Phi_i(t_k)}{c} - (\rho_i^M(t_k) + \rho_{Rx}^{TxA}(t_k)) \tag{3.2}$$

Equation 3.2 requires an ambiguity search, where the accuracy is dependant on the initial estimate from equation 3.1. Pseudo-range is sensitive to multipath, residual troposphere-induced link delays

[9] May be configured to achieve either better tolerance to interference or faster NAV data decoding. Cycle duty does not affect the data, as bit change occurs once per 20 or 10 TDMA frames.

[10] The main information sets are repeated within the first three words of each Subframe. Telimetry Word (TLM) contain LL, signal (A-D), network ID and the Tropospheric Scale Factor; Time Word (TM), time (as understood by this transmitter), synchronisation status and LL health; Acquisition Assist Word (AA) network size and neighbour LL ID.

[11] See section 3.2 and table 3.1 on page 32 for details.

[12] To start positioning four independent signal origins, as opposed to four different PRNs, are required.

[13] Subframe 1 transmits information for the first four transceivers, and subframe 2 for next four transceivers. It will be always the shortest list, being based on proximity, so the message will be repeated every 48 s or less.

and signal cross correlations, which make the verification of TimeLoc accuracy during the network establishment essential (Barnes et al., 2003a; Locata Corporation Pty Ltd, 2011a; Montillet, 2008). For the same reason, a good inter-visibility between master and slave is required. But, should this be obstructed, synchronisation can be obtained via another TimeLoc'ed slave via the TimeLoc hopping scheme. The whole procedure for TimeLoc (direct or hopped) is described in following steps:

Step 1. The master, set up on known point, synchronises to the external time source by coupling its transceiver A (TxA) with its receiver (Rx),[14] using equations 3.1 to 3.2 on the facing page . If Locata proprietary time is used this step is ignored;

Step 2. The master unit starts transmitting the reference signal via Tx_A with normal transmission power;

Step 3. The slave, set up on a known point, acquires the reference signal from the master, decodes the co-ordinates of reference signal antenna TxA, and starts broadcasting TxA using low transmission power;

Step 4. The slave acquires its own signal, and by coupling its TxA with its Rx, adjusts the pseudo-range offset between itself and the reference signal, using equation 3.1;

Step 5. The slave can then solve for AR, and adjust the carrier phase offset between itself and the reference signal using equation 3.2[15];

Step 6. TimeLoc is obtained.

TimeLoc is continuously monitored. When link accuracy exceeds the threshold (see table 3.1, page 32), its signal will be flagged as unhealthy and transmission power lowered until TimeLoc is re-gained. TimeLoc synchronizes the signal between antenna phase centres (APC) of the Master's TxA and the slave's TxA and Rx antenna, which leads to is a group delay between Rx_A and Rx_{B-D} in each individual emitter. In future releases, the navigation message (NAV) will include an estimation of the master clock drift and ageing coefficients with an uncertainty of $10{\cdot}10^{-11}$ s (Locata Corporation Pty Ltd, 2011a).

Slave units use the same TDMA pulsing scheme at all times, but prior to obtaining TimeLoc (see Step 5), it is unable to determine the millisecond boundaries; therefore, it broadcasts its own pulsing signal out of slot (with respect to the master). This is not a problem as:

- Interference caused by its own signals will only occur 10% of the time, by virtue of the new TDMA scheme. Locata tracking is able to tolerate such interference;
- Interference caused by the master signal is insignificant, as the slave signal is 30 dBm stronger than the received master signal due to the free space path loss.

Unlike the transceivers, the rover is unable to estimate the carrier phase difference with the Master, due to it having neither a Tx antenna nor precise coordinates. Furthermore, its TimeLoc procedure is based

[14] The coupling is achieved through signal attenuation, matching TxA signal with Rx. With this approach, hardware delays are taken into account.

[15] Locata uses a pulse signal, and the slave is unable to determine its millisecond boundaries before this step. Up to that step, the signal has to be accumulated over an entire millisecond, to ensure signal decoding.

on pseudo-range observations and it requires signals from at least two other transceivers to obtain network time synchronisation. Residual clock offset is estimated as part of the navigation solution, in a manner similar to GNSS. The rover maintains network time by aligning second boundaries with the pseudo-range, which can generate small discrepancies, as discussed in section (6.1 on page 89). Once time is synchronised, a slave transmits a PPS-like message, see figure 4.4, page 50[16] (Bonenberg, Roberts and Hancock, 2010b).

TimeLoc accuracy is summarised in table 3.1 (and section 4.3 on page 48), which discusses the practical verification of values stated. Since firmware version v.4.0, TimeLoc can be synchronised with GPS time using an external GPS receiver (Locata Corporation Pty Ltd, 2010b)[17]. Otherwise, Locata's proprietary time is used, it is continuous, physically defined by the master clock, and identified by a combination of week number, and time of the week[18].

	Characteristics	Value[a]
TimeLoc	Maximum phase noise	0.03 cycle = $11{\cdot}10^{-12}$s rms
	Typical cycle ambiguity	6 cycles = $2{\cdot}10^{-9}$s
	Mean slave synchronisation offset	$3{\cdot}10^{-11}$s
	Power Cut Threshold[b]	0.3 cycle = $1{\cdot}10^{-10}$s
	Group Delay uncertainty	$1{\cdot}10^{-11}$s
	Synchronisation uncertainty to external source	$1{\cdot}10^{-7}$s
LocataNet	Short term stability	ppm ($1{\cdot}10^{-6}$)
	Long Term stability	$1^{\text{ppm}}/_{\text{yr}}$[c]
	Thermal stability	< 1 ppm [d]
	PPS Tracking noise	$10{\cdot}10^{-9}$ s
	PPS Tracking bias	$1{\cdot}10^{-9}$ s[e]

Table 3.1 – TimeLoc accuracy parameters, based on (Locata Corporation Pty Ltd, 2011a)

[a] Based on current hardware performance.
[b] Based on firmware version v.3.0 parameters.
[c] Up to maximum of 10.
[d] Operating within the temperature range of $-30-85\,^{\circ}$C.
[e] Compensated during configuration.

[16] This is not a strict PPS message as it is defined by a measurement epoch (typically 2 Hz, 5 Hz and 10 Hz). The pulse is also narrower than the GPS one ~$13{\cdot}10^{-9}$ s (Locata Corporation Pty Ltd, 2010a).

[17] This synchronisation technique differs from other pseudolite systems. Astrium pseudolites for example, first synchronise internally, then synchronise to the external time source (Dixon and Morrison, 2008).

[18] Locata ASCII and LBF output had time limited to 403 199 s – a whole week. With the introduction of Locata Binary Messaging Protocol (LBMP) in firmware version v.5.0 time is denominated as {week, time_of_week}.

The coordinate system

As long as all transmitters share the same coordinate system, its definition is very flexible, which is advantageous indoors or for Locata-only networks. No projection or scale corrections would be required for networks smaller than 10 km (Bonenberg, 2003). Any longer baselines would require careful planning (Hofmann-Wellenhof et al., 2008; Kaplan and Hegarty, 2006; Leick, 2004). Locata suggest using WGS-84 coordinates[19], so that implementation accuracy rests solely on the Tx antenna's coordination. Given the short baselines, this should be at centimetre-level for phase measurements (Locata Corporation Pty Ltd, 2011a). This is normally conducted using a total station, but there is also self-survey option, using a top mounted GPS receiver, implemented in firmware version v.4.2.

Locata hardware

The Locata proof of concept was based on the Marconi Corp. Allstar GPS receiver, transmitting on the L1 frequency only (Barnes et al., 2003a). Subsequent commercially released versions are all based on the Xilinx Field Programmable Gate Array (FPGA), which allows alterations of the electronic properties by means of the firmware. Locata transceivers share common components with rovers, but they have additional components for signal transmission, and current flow. Therefore, their dimensions and weight are greater (see table E.1, page 159). The author has been successfully operating the Locata system, for extended periods of time, in the -5 to $30\,^{\circ}\mathrm{C}$ temperature range.

Successive firmware releases have applied changes not only to the algorithms, but also to hardware behaviour; it is therefore important to know which version is being used. Each release is marked as ***v.version.release.patch*** where:

version represents interoperability within a LocataNet, all units need to use the same version to operate with each other,

release represents feature additions or improvements, which do not affect interoperability,

patch represents bug fixes, mostly in the beta testing, before the public release.

These firmware changes have been summarised in table 3.2 on page 37. Further information can be found in the official release notes accompanying every new release since firmware version v.4.0, or in research papers (Cheong et al., 2009; Khan et al., 2010; Montillet, 2008).

The dual frequency signal was introduced in firmware version v.3.0. Synchronisation with GPS time[20] was introduced in firmware version v.4.0 (Locata Corporation Pty Ltd, 2010a) along with a number of algorithm changes leading to an overall improvement in stability and quality of fix. The introduction of a fixed cycle duty removed the possibility of "rogue" transmissions from Locata networks[21]. Self-surveying was introduced with firmware version v.4.2 and remote operation in firmware version v.5.0. The next release, used in the White Sand tests (Craig and Locata Corporation, 2012) was not publicly released, while firmware version v.7.0 has yet to appear.

[19] Any local (ENU) or national (ENH) grid coordinates presented in this thesis have been transformed after data collection. Grid InQuest was used for the UK, Leica Geo Office arbitrary transformation for Australia. GPS data is processed in the same fashion.

[20] Using a SigNav uTevo GPS time receiver with $15{\cdot}10^{-9}$ s outdoor accuracy (SigNav, 2008).

[21] This would spoof all communication on ISM frequency within the range of the rogue transceiver.

Locata can use any of the following 2.4 GHz passive antennas:

- AeroAntenna AT2400-2, 5dBi patch antenna (70/70 3dBi beam);
- LCom HG2412P, 12dBi directional antenna (70/70 3dBi beam);
- LCom HG2403U, 3dBi omnidirectional antenna;
- LCom HG2403MGURW(B), 3dBi omnidirectional, used from firmware version v.2.4, with null in radiation pattern to the zenith and inferior negative elevation signal rejection, see figure 3.4, page 35;
- Pacsat 24dBi dish (GA2424);
- Aircraft certified Rx Coopers 3dBi hemispherical antenna (21-40-60);
- The proprietary beam forming Timetenna for indoor measurements.

Apart from the Coopers and Pacsat antennas, the remaining antennas are commonly available, with a weak phase centre offset (PCO) determination. Locata transceivers tend to use AT2400-2 as Rx while Locata rovers tend to use an omnidirectional antenna, with weak reception for negative vertical angle signals. Locata front-end uses these characteristics to detect multipath (see section 4.8, page 61). The down side is the limit on high and low antenna combinations in a network, which reduces VDOP and vertical accuracy (see section 4.4, page 50). While initially the rover supported 40 channels, this was reduced to 36 channels from firmware version v.4.0, due to FPGA processing restrictions.

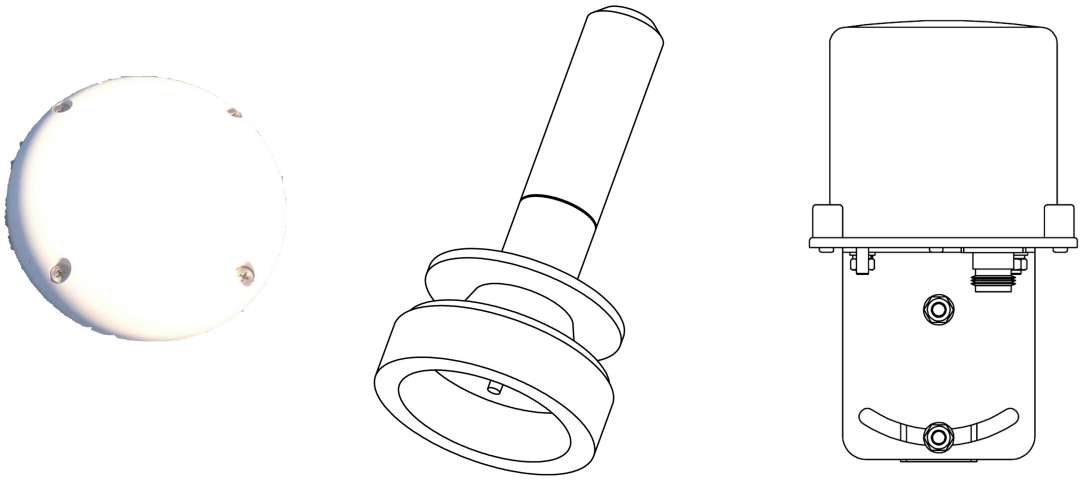

Figure 3.3 – Locata Antennas, left to right, AT2400-2, HG240U and HG2412

Timetenna is a dedicated antenna for indoor use, using null-steering and TimeLoc to provide a centimetre-level indoor fix by the removal of multipath. It also allows on-the-fly (OTF) initialisation, instead of KPI, as the initial position can be determined with enough precision (Gakstatter et al., 2011; LaMance and Small, 2011; Rizos, Roberts et al., 2010). Currently, there are two antennas capable of receiving both Locata and GPS signals:

- The AntCom GPS/Locata hemispherical antenna 3dBi (G5Ant-52ATT1-Lo1-C1.0), capable of Locata and GPS (L1+L2) signal as used at the Boddington Gold Mine;

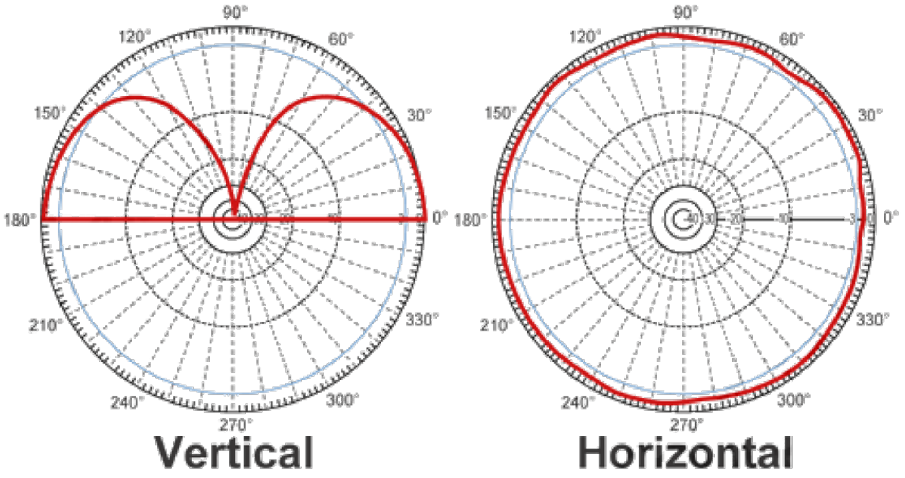

Figure 3.4 – Radiation pattern of the LCom HG2403MGURW omni-directional antenna of the rover

- Locata's bespoke combination of LCom HG2403U and Leica AX1202GG antennas, see figure 6.9, page 93.

New hardware and firmware version v.7.0

Locata is currently working on a new generation of hardware, using a modernised (FPGA) board, a different operating system and improved processing capacity. The latest firmware version v.7.0, was tested in the Boddington Gold Mine, before general release in 2013. It provides:

- Ability to track up to 64 signals at one time, with further improvement possible,
- higher front-end measurement rates, and positional updates,
- improvement in the Timetenna beam-forming capability (more look directions, finer resolution, more simultaneous beams);
- Ethernet connectivity providing:
  - remote firmware upgrades,
  - remote monitoring of equipment, for long-term set-ups.

This hardware is intended to support the new pseudo-random TDMA sequence which has increased the maximum number of units in the network from 10 to 50. This is possible as N-slot allocation varies between each TDMA frame (see figure 3.2, page 29). At worst 20 % of slots will be shared in one Super Frame. The following frequencies have also been introduced, following the principle of $S_i = 2.409165 \times 10^9 + i \times 1.023 \times 10^6$Hz:

S02 2.411 211 GHz,

S05 aka S1 2.414 280 GHz,

S52 2.462 361 GHz,

S55 aka S6 2.465 430 GHz,

S62 2.472 591 GHz,

This release also introduces changes in the navigation engine with the Least Squares Adjustment (LSA) being replaced by an Extended Kalman Filter (EKF), where new hardware is used, the provision of geometry based AR OTF. This is discussed in chapter 6 on page 82.

The Locata In-line Navigation Engine (LINE)

LINE is the Locata Corporation's proprietary navigation software, which acts as an on-line navigation engine for the rover. LINE firmware version v.3.0 was described in Montillet (2008) and, despite subsequent substantial changes in the navigation engine and processing, the end user experience is very much the same. The engine uses a Least Squares Adjustment (LSA) which is expected to be replaced by an Extended Kalman Filter (EKF) in future versions of LINE.

The user can configure LINE through command line parameters, or through modification of processing parameters in the ASCII configuration set-up file. This includes:

- code or phase solution output with or without pseudo-range smoothing using the Hatch Filter,
- modification of the output rate (Hz),
- removal of particular signals or whole clusters,
- alternative measurement combiner types:

  h0 all available signals used,

  h1 uses a single signal - based on best signal-to-noise ratio (SNR),

  h2 one measurement is formed by averaging 4 signal clusters,

  h3 one measurement is formed by averaging 4 signal clusters, weighted according to their SNR.

3.2 GPS

Apart from being a component in the proposed integration, GPS is a founding element for both pseudolite and Locata. The Marconi Corp. Allstar GPS receiver formed the basis for Locata's proof of concept. Therefore, a thorough understanding of GPS is essential for a complete understanding of concepts involved. The following sections provide only a brief description of the GPS system, discussing concepts directly related to this thesis. For further reading see Hofmann-Wellenhof et al. (2008); Kaplan and Hegarty (2006); Leick (2004).

Signal characteristics and navigation message

Modern GPS receivers can decode code messages with 10^{-3} chip length resolution, which equates to $0.3-0.5$ m in the range and the phase beat 10^{-2} cycle, the equivalent of $1.9-2.7$ mm. To obtain centimetre accuracy full cycles have to be accounted for in the Ambiguity Resolution (AR) process.

The received signal contains pseudo-range and a navigation message, with information about satellite health, ephemerides, an almanac and various corrections. Time offsets between GPS and other GNSS systems are expected in the future (Hofmann-Wellenhof et al., 2008). An overview of the GPS current and planned signal can be found in table B.1 on page 139 and B.6 on page 143. L2 frequency requires

	Known Locata Firmware Version						
	v.1.x	**v2.4**	**v.3.0, v3.2, v3.4**	**v.4.0**	**v4.2**	**v.5.0**	**v.7.0**
Release Date	~2003	2007	2008	2010	2010	2011	2013
Carrier Freq	L1 (1 575.42 MHz)	S1	S1(2.412 28 GHz) S2(2.465 43 GHz)				multiple
PRN Code	C/A (DS-CDMA)	Proprietary TH/DS-CDMA, based on C/A					
Chipping Rate[a]	1.023MHz	10.23MHz					
Transmitter output[b]	unknown	20dBm	23dBm				
Hardware	Mitel GP2000 chipset[c]	Xilinx FPGA board hardware					FPGA
Positioning rate	1Hz	$\leqslant$ 25Hz[d]	$\leqslant$ 50Hz[d]				10Hz
Channels	unknown	40	36				64
Notes	Limited range prototype.	First commercial release.	Dual frequency, improved noise and multipath reduction.	GPS time synch with PPS pulse and MET support. NAV message includes ephemeris and MET. LBF and configuration change.[e]	LBF change. Self-survey, TTFF and long term stability improved. New output format.[f]	LBF changed, provision for remote network control and monitoring capacity. Multiple networks possible. Changes to NAV. Improved multipath rejection.	Remote upgrade, new TDMA scheme and support for large networks (20+ LocataLites, 100 km, airborne rover)

Table 3.2 – Locata hardware and firmware development

[a] In the case of Locata Bandwidth, the Chipping Rate is doubled (Khan, 2011).
[b] This is directly related to the system range (see 4.5 on page 54).
[c] Using modified Marconi Corp Allstar GPS receiver.
[d] This speed only refers to the TimeLoc and the allowed setting range. The actual value is unknown.
[e] Changes include a single device configuration file, continuous PRN allocation and fixed duty cycle. RCPI has been introduced.
[f] Interleaved TPV and GSA, GSV and RMC NMEA messages.

Link	Frequency [MHz]	Description
L1	1 575.42	Coarse-acquisition (C/A) and precision P(Y) codes. In the future additional civilian (L1C) and military (M) codes will be available.
L2	1 227.60	P(Y) code. L2C and military codes on the Block IIR-M and newer satellites.
L3	1 381.05	Military systems of nuclear detonation detection (NDS) and NDS analysis package. L4 has been studied for additional ionospheric correction.
L4	1 379.913	
L5	1 176.45	The proposed Integrity Monitoring Service (IMS), originally proposed as a civilian safety-of-life (SoL) signal.

Table 3.3 – GPS frequencies usage, after Hofmann-Wellenhof et al. (2008)

additional P(Y) decoding, for which a number of techniques exist, with the resulting signal accuracy dropping to a C/A level (Hofmann-Wellenhof et al., 2008; Kaplan and Hegarty, 2006; Leick, 2004).

The navigation message is composed of a 37 500 bit master-frame, subdivided into 25, 1 500 bit long frames. Each frame is divided into five subframes with 10 words in each. It takes 0.6 s to transmit the word and 12.5 min to transmit a complete master-frame. Each sub-frame starts with the telemetry word (TLM) consisting of the synchronisation pattern (10 001 011) and the hand-over word (HOW). This contains the time of week (TOW)[22] of the next subframe leading edge. The subframe contains:

Subframe 1 time, user range accuracy, satellite health, signal group delay, three coefficient for a quadratic polynomial modelling satellite clock correction.

Subframe 2-3 broadcast ephemerides.

Subframe 4 ionospheric and UTC data and almanac for PRN beyond the first 24 satellites.

Subframe 5 almanac and health status of the first 24 satellites.

Subframes 1-3 repeats in each frame, while subframes 4-5 are frame specific. The introduction of two new data-types are expected: civilian navigation (CNAV) and military navigation (MNAV) messages, providing more accurate data in a flexible data format[23]. These navigation messages, with small differences, are expected to be transmitted on the new L5I and L1CD bands (GSW, 2010a, 2010b; Hofmann-Wellenhof et al., 2008).

GPS time

Before we discuss GPS time, it is useful to explain the difference between the two most popular time definitions: atomic and mean sidereal time.

Mean sidereal time, also known as Universal Time (UT), is correlated with the Earth's rotation - which is affected by: seasonal variations and zonal tides and while it was logical when it was first introduced

[22] TOW is also known as the Z-count and as multiple of 1.5s allows synchronisation with the P code.

[23] The new structure will compose of header, data fields and cyclic redundancy check-word (CRC), in a manner similar to Locata messages.

in the nineteenth century, it is not a continuous time scale. Solar Mean Universal Time (UT1)[24] is used in reference to atomic time.

Time as used on a day-to-day basis is known as Coordinated Universal Time (UTC). This is an atomic implementation of UT, maintained by International Atomic Time (TAI) and based on Ephemeris Time (ET), which relates to the orbital position of Earth around the Sun as a state from 1st January 1977. This time is continuous and in order to maintain the relation to UT, "leap seconds" are introduced when $\triangle UT1 = UT1 - UTC \approx 0^s.9$. This is announced by International Earth Rotation and Reference System Service (IERS) six months in advance, on either, 30th June or 31st December (Leick, 2004). There is a growing consensus in favour of abolition of the "leap second", especially in view of server problems after the last leap second was introduced. A final debate is expected in 2015.

UTC	0
IAT	+35"
GPS	+16"

Table 3.4 – Relation between GPS, UTC and IAT times, as of July 2012

GPS time began at midnight of Sunday January 6, 1980 and it is recorded by a GPS week number[25] and seconds in a week[26]. This is physically maintained by atomic clocks at the GPS ground control stations and satellites, nominally within 1 µs ($1{\cdot}10^{-6}$ s) from TAI [27] (Kaplan and Hegarty, 2006). It is a continuous time scale and "leap seconds" are not applied. Table 3.4 compares three atomic times: GPS, UTC and IAT time. A difference between atomic times and sidereal UT is apparent from GPS satellite positions repeating $+^{24^h}/_{365} \approx +4^{'}$ earlier each day.

Definition of coordinate systems

Traditionally, the Earth's global frame is defined mathematically by an ellipsoid in an attempt to best match its shape, orientation and scale at its centre of mass. Matters are complicated when we measure to objects orbiting our planet, due to the constant motion of the Earth's surface, which is affected by:

- Tectonic plate movement, $0-50\,^{\mathrm{mm}}/_{\mathrm{yr}}$;
- Solid Earth Tides caused by the gravitational attraction of the sun and the moon and introducing landmass movement up to 300 mm vertical and 50 mm in plan. These can be precisely estimated from relatively simple models;
- Ocean loading - deformation of seabed and coastal land due to water mass redistribution, which does not exceed 50 mm in the vertical component, and 20 mm in the planar. This can be precisely estimated from coastal outline data and tide models;

[24] Mean Universal Time is defined as two consecutive transits of the sun over the meridian of the mean Earth (Greenwich), and is an observable, physical time.

[25] $1023 + 1 \equiv 0$ (modulo 1024), with roll over ~ every 19.6 years, with the first one on 21-22 Aug 1999, next ones on 6 April 2019 and 20 November 2038 (Langley, 1998).

[26] $604799 + 1 \equiv 0$ (modulo 604800).

[27] Currently around 50 ns ($50{\cdot}10^{-9}$ s).

- Polar motion (wander) - semi-periodic, with a period of 434 days, and a varying amplitude not exceeding 10 m. This problem is mitigated through the definition of the conventional terrestrial pole (CTP), which provides coordinate system orientation, as an average position over time. Precise fix position is impossible (Leick, 2004).

Due to these constant motions, particularly polar wander, the Earth frame needs constant updating; the current frame is ITRF2008 (International Earth Rotation and Reference Systems Service, 1987). Each instance of the ITRF is related, and requires "back in time" conversion between each of them. In comparison, the GPS coordinate system is "frozen in time", and is calculated with respect to the World Geodetic System 1984 (WGS-84) ellipsoid, calculated from Transit measurements of about 1 500 terrestrial sites[28]. A major update, WGS-84(G730)[29], on 29 June 1994, corrected the imprecise Earth gravitation constant, vital for satellite orbit calculation, see table B.6, page 143. Following updates, G873 of 29 January 1997 and G1150 of 20 January 2002, WGS-84 was brought very close to the ITRF, see table 3.5, page 40[30]. An established relationship between WGS-84 and the ITRF permits transformations between the coordinate systems, provided that not only the coordinates, but also the time of observation is known.

Maintenance of orbits between the GNSS systems is even more complex, mostly due to military secrecy obscuring those parameters, and unpublished changes to orbit determinants. To this end, IGNSS independent orbit calculations are vital, as they maintain the relationship between different GNSS satellite orbits[31] (International GNSS Service, nd; Ziebart and Bahrami, 2012).

Semi major Axis of the ellipsoid **a**	6 378 137.0m
Flattening of the ellipsoid **f**	$298.257\,223\,563^{-1}$
Angular velocity of the Earth ω_e	$7\,292\,115{\cdot}10^{-11}\,\mathrm{rad/s}$
Earth's gravitational constant μ	$3\,986\,004.418{\cdot}10^{8}\,\mathrm{m^3/s^2}$

Table 3.5 – Parameters of WGS-84(G1150) ellipsoid, after Hofmann-Wellenhof et al. (2008)

The least certain component of any GNSS fix is height, mostly due to satellite geometry, but also by the ellipsoid being only an approximation of the Earth's datum. A plumb line is a line perpendicular to the equipotential surfaces, related to the gravitational force, and the mass distribution of Earth, which does not have a simple analytical expression. To account for this, a discrete geoid model[32], obtained by satellite altimetry and gravity measurements, is used. Knowledge of precise geoid undulations (differences between ellipsoid and geoid height), is required to properly match terrestrial and GNSS observations (Brockmann, 2012; Hofmann-Wellenhof et al., 2008).

[28] With 1 – 2 m accuracy.

[29] 730 indicates the GPS week on which definition started.

[30] These updates are essential for any datum-critical work. For example, the original WGS-84 was coincidental with American Datum (NAD83) while the current is 2.2m lower (Hofmann-Wellenhof et al., 2008; Kaplan and Hegarty, 2006).

[31] To this end, the International Terrestrial Reference Frame (ITRF) is determined and maintained by the International Earth Rotation and Reference System Service (IERS), using centimetre-level Very Long Baseline Interferometry (VLBI) observations to distant pulsars, and Satellite Laser Ranging (SLR).

[32] "*Equipotential surface which would coincide with the mean ocean surface of the Earth, if the oceans and atmosphere were in equilibrium, at rest relative to the rotating Earth, and extended through the continents and is very affected by Earth's mass distribution such as major mountain ranges.*" (Leick, 2004)

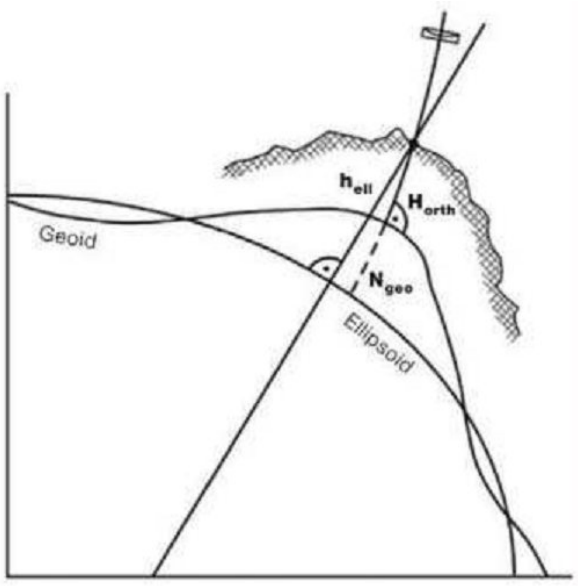

Figure 3.5 – Relation between different height systems, from Brockmann (2012)

3.3 Problems and challenges

Any terrestrial positioning technology faces multipath, imprecise clocks, the near-far effect and the tropospheric delay among others. Locata deals with those problems through a combination of hardware and signal based solutions. Time-Hopping/Direct Sequence Code Division Multiple Access (TH/DS-CDMA) and a 10% pulsing scheme, use an extended bandwidth and spreading waveforms with 20 dB processing gain to maintain signal quality (Cheong et al., 2009; Locata Corporation Pty Ltd, 2011a; Stansell, 1986). The four spatially, and frequency separated signals from each Locata are very effective multipath and noise mitigation methods (see section 7.3, page 113).

Locata operates in the 2.4 GHz licence-free ISM band, so any licensing regime is avoided at a cost of **in-bound interference**, due to the large number of devices operating within this band. Research into channel overlap, with devices utilising wireless communication protocol IEEE 802.11 (commonly known as WiFi)[33], transmitting at between 16 to 19 dBm, has focused on laboratory testing and early single frequency release (Abello, Dempster and Politi, 2007; Khan et al., 2010; Montillet et al., 2009). The author has shown the system's capacity to operate indoors alongside an active WiFi network (Bonenberg, Hancock and Roberts, 2010). However, careful location planning, and initial monitoring is recommended. To this end, the author has created a simple mission planning tool that provides estimates of the optimal location of the Locata transmitter for set up in known areas (Bonenberg, Roberts and Hancock, 2012), (discussed in chapter 7 on page 106). For indoor environments, beam steering Timetenna is reported to have outstanding mitigation characteristics (Gakstatter et al., 2011; Rizos, Roberts et al., 2010). It is also possible to improve the characteristics of other antennas (Bonenberg, Hancock and Roberts, 2010).

The most important GPS shortcomings, as discussed in this chapter, are:

[33] As shown on figure 5.6 on page 78.

- The requirement of open sky visibility;
- The fact that accuracy is based on the geometrical position of the satellites at the given epoch, as shown in figure 1.1 on page 5;
- It is prone to multipath and noise interference as well as deliberate and accidental jamming. Successful spoofing has also been conducted (Humphreys, 2012a, 2012b; Scott, 2012; Shepard et al., 2012; Wesson et al., 2012);
- It is of limited integrity unless a specialised service, such as SBAS or GBAS is used;
- It is prone to scintillation or other atmospheric phenomena;
- It is perceived as a "black box", with the user having unfounded trust in its absolute accuracy.

It is in the alleviation of most of these shortcomings that Locata can make a unique contribution, which will be discussed in next chapter.

	GNSS	**GPS**	**Locata**
Transmitter Location	MEO+GEO	MEO	Terrestrial
Signal Separation	CDMA[a]+FDMA[b]	CDMA[a]+TDMA[c]	CDMA + TDMA
Data Speed	25 – 1 000 $^{\text{bit}}/_{\text{s}}$	50 $^{\text{bit}}/_{\text{s}}$	100 $^{\text{bit}}/_{\text{s}}$[d]
Pulsing scheme	n/a	n/a	10x100 µs slots[e]
Frequency used	1.1 – 1.6 GHz	1.1 – 1.6 GHz	S band (2.4 GHz)
Code rate [Mcps]	1.023 – 10.23	1.023 – 10.23	10.23
Time to send NAV	150 – 1 200 s[f]	750 s	24 – 96 s
NAV Data structure	varied[g]	5 Subframes SF1-3: 1 page SF4-5: 25 pages	2 Subframes SF1: 1 page SF2: $Px2^h$ pages
Atmospheric delay	Ionosphere and Troposphere		Troposphere
Allowed number of transmitters [i]	24-36	36	50[j]
Transmitter output	$\leqslant 50W$	$\leqslant 50W$	$\leqslant 1W$[k]
RF[l]	−128.5 dBm	−128.5 dBm	−100.0 dBm

Table 3.6 – GNSS and Locata comparison

[a] Signal is transmitted both in-phase and quadraphase (I&Q).
[b] GLONASS only
[c] L2C uses a combination of CDMA and TDMA.
[d] Optional 50 bps.
[e] Equivalent of 10% duty cycle.
[f] GLONASS (C/A) 150 s per super frame; GLONASS (P) 720 s ; GALILEO < 1 200 s per frame.
[g] GLONASS: 5 frames with 15 strings; GALILEO: 12 subframes with 5 pages.
[h] Where P is the number of LL in the network. Currently only two out of eight pages available are used.
[i] Based on ICD or system specifications, not the actual number of transmitters/satellites.
[j] Locata Corporation Pty Ltd (2011a) provides 200 PRNs but firmware version v.5.0 only supports two subnets.
[k] A hardware limitation due to compliance with FCC 15.247. With amplifiers 10 W was reported (Craig and Locata Corporation, 2012).
[l] Minimal signal strength required to decode the message.

♣ ♢ ♣

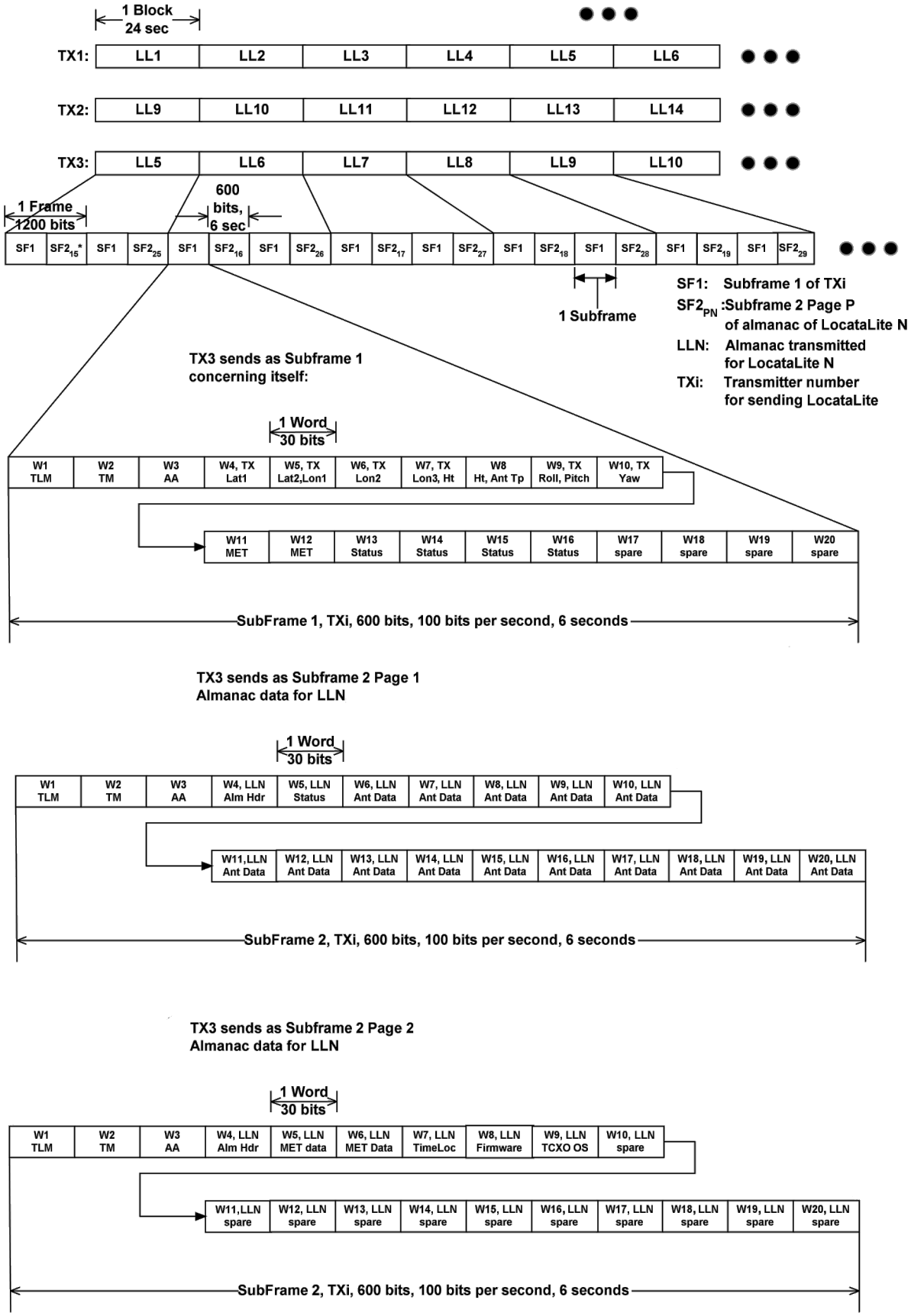

Figure 3.6 – Locata navigation message frames, from Locata Corporation Pty Ltd (2011a)

4 The feasibility of integration

"So it is said that if you know your enemies and know yourself, you can win a hundred battles without a single loss"
Sun Tzu, The Art of War

THIS chapter will discuss the proposed integration between Locata and GPS, starting with a description of the existing loosely-coupled integration, the Leica Jigsaw 360 system, and then moving on to a proposed tightly-coupled integration. The following feasibility study discusses the main limiting factors of the system: time, range, orbit determination, PCO, atmospheric effects, multipath and the near-far effect.

Some of the work presented here has been previously published in (Bonenberg, Hancock and Roberts, 2010; Bonenberg, Hancock, Roberts, Ogundipe and Lee, 2009; Bonenberg, Roberts and Hancock, 2010a; Bonenberg et al., 2012).

Contents

PREVIOUS discussion has outlined a number of problems that GPS faces including: multipath, scintillation, accuracy, reliability and an integrity depending on satellite geometry. Shepard et al. (2012), have also demonstrated the possibility of injecting Hazardous Misleading Information (HMI) into military drones. Combined with the rise of personal privacy devices, this has created a large security threat, especially for safety and environmental and economically critical applications (Davis et al., 2012; Humphreys, 2012b; Scott, 2012). These problems can also affect augmentation systems such as SBAS, GBAS or centimetre-level CORS.

The promise of multiple constellations only partly addresses these issues (Hancock et al., 2009; Hegarty and Gibbons, 2012), while introducing problems of inter-constellation compatibility and interoperability. Proposed signal verification (Humphreys, 2012a; Scott, 2012; Wesson et al., 2012), would require significant alterations to existing hardware.

The provision of additional signals would be an ideal solution, solving both visibility and security issues vital for a number of applications including: open cast mines, motorways (at complex junctions), tight construction sites, airports or other areas where nearby obstructions limit visibility of the sky (Lee et al., 2004). Pseudolites, the predecessors of Locata, were originally proposed as an augmentation system (Cobb, 1997; Davis et al., 2012; Hofmann-Wellenhof et al., 2008; Kaplan and Hegarty, 2006; Parkinson et al., 1996), but due to hardware and legislation challenges, pseudolites have not been fully embraced. Locata re-addresses the issue by utilising the 2.4 GHz licence-free ISM band and TimeLoc to maintain precise time. The similarities with GPS (see table 4.1, page 45), not only make integration easier, but also address the issue of HMI injection and unintentional spoofing. While a similar solution is possible with other sensors, especially INS or eLORAN, they are limited either in accuracy or duration (see section 3.3, page 41).

Locata	**GPS**
Locata position	Satellite orbits estimation
Antenna phase centre offset	Antenna phase centre offset
TimeLoc bias	Receiver and Satellite Clock bias
Tropospheric delay	Ionospheric and tropospheric delay
Multipath, noise and interference	Multipath, noise, interference and spoofing
LocataNet Geometry	Satellite Geometry
Ambiguity Resolution	Ambiguity Resolution

Table 4.1 – Accuracy limiting factors for Locata and GPS

4.1 Existing loosely-coupled Integration

Currently, the only known and working integration between Locata and GPS, is provided as part of Leica Geosystems Jigsaw 360 – Leica Mining Solution, as operated at Newmont's Boddington Gold Mine in Queensland, Australia. This loosely-coupled integration is maintained via the open Word Interface, Leica's proprietary multi-sensor communication interface (Leica Geosystems, 2002), which allows for

coordinate, and Quality Control (QC) indicators exchange. Each system provides an independent fix[1], and if the GPS QC drops below the threshold, usually due to limited sky visibility, a Locata fix is used, as shown in figure 4.1.

Published results, both from the trials in De Beers Venetia diamond mine in South Africa[2], and Newmont's Boddington Gold Mine in Australia, show centimetre-level planar accuracy from both systems, and inferior height determinant when Locata is used (Barnes, LaMance et al., 2007; Carr, 2012). While easy to perform and maintain, with both systems completely independent, observations from other system are always ignored. This leads to:

- a predominantly 2D position of the Locata based solution,
- Locata ambiguity resolved using KPI from GPS positional feed,
- a requirement of at least four signals (for Locata and GPS) to calculate a valid fix,
- the observations from other systems (apart from QC) being ignored.

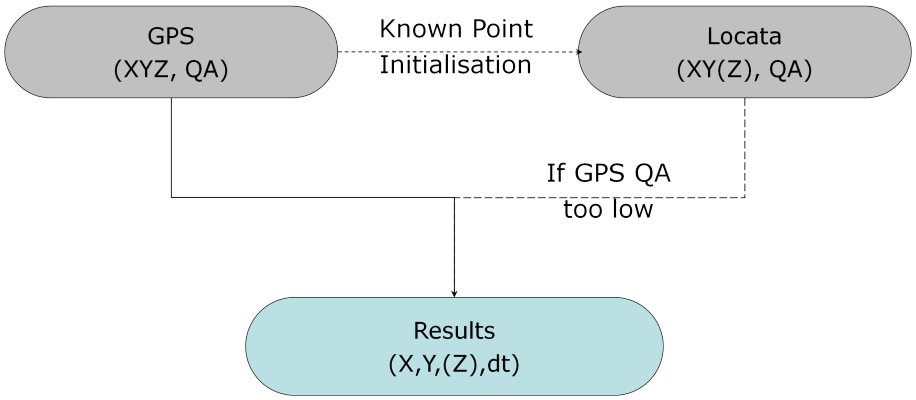

Figure 4.1 – Existing integration used in Leica Geosystems Jigsaw 360

4.2 The proposed closely-coupled Integration

Grewal, Weill and Andrews (2006) describe five levels of integration between independent systems:

Separate: each component is used separately, with the secondary system usually operating as a backup in case of a main system failure.

Loosely: both systems output positional data, which is then combined into one solution. This approach is currently used for the Leica Geosystems Jigsaw 360.

Closely: integration at the measurement stage, coalesced in a common adjustment/filter process to produce a single positional solution. This approach combines the strengths of each system, and does not require hardware modifications.

Tightly: a combined positional solution is used to aid the measurement process (for example predicting Doppler shift in the GNSS module). A feedback loop between the navigation segment and front end hardware is required.

[1] Locata KPI need to be initialised from the GPS feed.

[2] This mine covers the area of 1.2 km×0.8 km and is 0.25 km deep, with vertical walls limiting GPS visibility.

Deeply: observations of the navigation system are used to calculate the position, and aid other components in the measurements process (i.e. tracking loops). This will usually require common hardware throughout the integrated system.

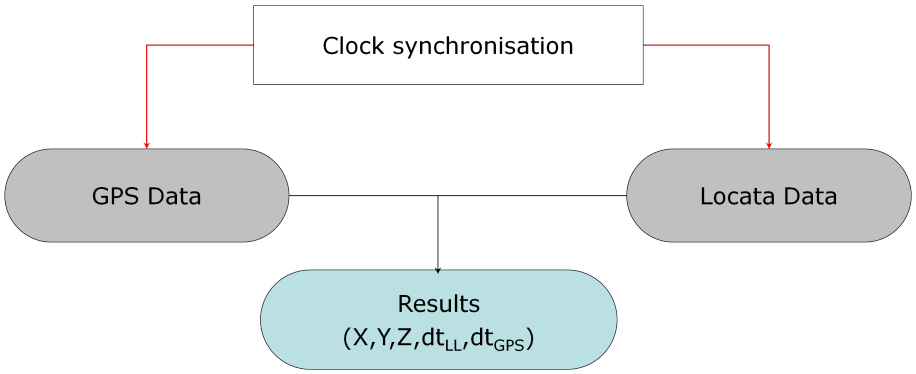

Figure 4.2 – Proposed integration

The proposed **closely-coupled** integration is a natural progression from the existing loosely-coupled integrated system, as it does not require hardware modification. Existing research into aviation and deformation monitoring (Cobb, 1997; Lee, Wang and Rizos, 2005; Meng et al., 2004; Soon et al., 2003; J. J. Wang et al., 2004) shows that closely-coupled integration can improve the accuracy, integrity, availability and ambiguity resolution (AR), which should also be easier to solve.

Locata based research has yet to address this issue, though prerequisites such as LAMBDA and post-AR EKF integration have been discussed (Bertsch, 2009; Rizos, Grejner-Brzezinska et al., 2010). The proposed novel navigation engine collects observations from both systems, and performs combined AR for both systems using LAMBDA (as discussed in chapter 6 (page 82)). A minimum of two signals per component and five in total are required as both Locata and GPS time offsets need to be solved[3]. This approach has no less flexibility than the previous approach, as an independent solution can be still calculated (see figure 4.3, page 49), offering:

- For an integrated solution (green track in figure 4.3 on page 49):
  - geometry improvement,
  - the ability of Locata to initialise on-the-fly,
  - improved ambiguity resolution, offering a faster and less error-prone approach (Cobb, 1997; Hofmann-Wellenhof et al., 2008; Lee et al., 2005),
  - a minimum of five signals, which are required to calculate fix, with a minimum of two signals per component to solve for the two time offsets,
  - up to three independent solutions (each component independently and an integrated solution), which can be calculated with both components working. This offers independent quality control leading to error mitigation, integrity and spoofing protection[4].
- Where only one system is capable of working (red track in figure 4.3 on page 49):

[3] While it is theoretically possible to estimate $dt_{\nabla} = dt_{LL} - dt_{GPS}$, in practice this approach is not precise enough.

[4] Unlike LORAN, Locata can be jammed by reasonably small size devices; but does on other hand offer superior fix accuracy (Helwig et al., 2012; Pelgrum, 2006).

- ability to maintain ambiguity resolution during the "outages", and providing accurate and instant re-initialisation of the off-line component,
- an extended range of the system, in common with the current approach,
- a requirement of four signals per component.

An overview of this process can be seen in figure 4.3 on the facing page. Similarity of limiting factors between Locata and GPS can be used to create a "seamless" system following the "black box" principle, preferred by users, and offering improved QC. As the navigation system operates on the observation level, calculating combined fix using a Least Squares Adjustment (LSA), a number of prerequisites need to be fulfilled:

- a common time, or the ability to relate to a common time system;
- matching accuracy of both systems;
- a common coordinate system or ability to relate to one, discussed in section (as 3.1 on page 33);
- a range capable of providing a solution in the requested area;
- the stability of the solution of both systems as discussed in section (7.3 on page 113).

This approach is different from the GPS and INS integration as each component can maintain its own accuracy for prolonged periods of time[5], but similar in the accuracy improvement when both systems are present. The following section will discuss and assess the feasibility of those factors.

4.3 Time

At the observation level, time synchronisation translates directly into positioning accuracy. Bao-yen (2005); Kaplan and Hegarty (2006), estimate maximum satellite velocity at $800-930\,\mathrm{m/s}$, or a millimetre per $1{\cdot}10^{-5}\,\mathrm{s}$. This requirement is delivered by both systems, as pseudo-range measurements require nanosecond level clocks (1 ns). Both Locata and GPS use inexpensive Temperature Compensated Crystal Oscillators (TCXO). Clock steering (Allan, Ashby and Hodge, 1997) is able to estimate pseudo-ranges to the nearest nanosecond, necessary for an accurate fix on the surface of the earth.

The accuracy of a clock is defined by its frequency accuracy, frequency stability, time accuracy and time stability (Allan et al., 1997). Frequency and time stability describe the instantaneous behaviour of the clock between epochs, and can be steered if a more accurate source of time is available, or the characteristics of a clock are known. Frequency and time accuracy relate to the long-term performance of the clock, and its agreement with UTC. GPS, with its dedicated control network of atomic clocks, maintains its time within $1{\cdot}10^{-8}\,\mathrm{s}$ of the UTC[6]. GPS is the *de facto* time system for almost every application, and information about its performance can be found in Hofmann-Wellenhof et al. (2008); Kaplan and Hegarty (2006). Locata however, has not been researched so intensively, and the following sections will discuss its short and long-term clock characteristics in more detail.

[5] INS accuracy is subject to drift, accelerating with time. A tactical grade IMU can provide stability for a day, whereas a low cost micro electro mechanical system (MEMS) sensor can only maintain it for a few seconds, as presented in figure (2.1 on page 10).

[6] See section 3.2 on page 38 and table B.6 on page 143.

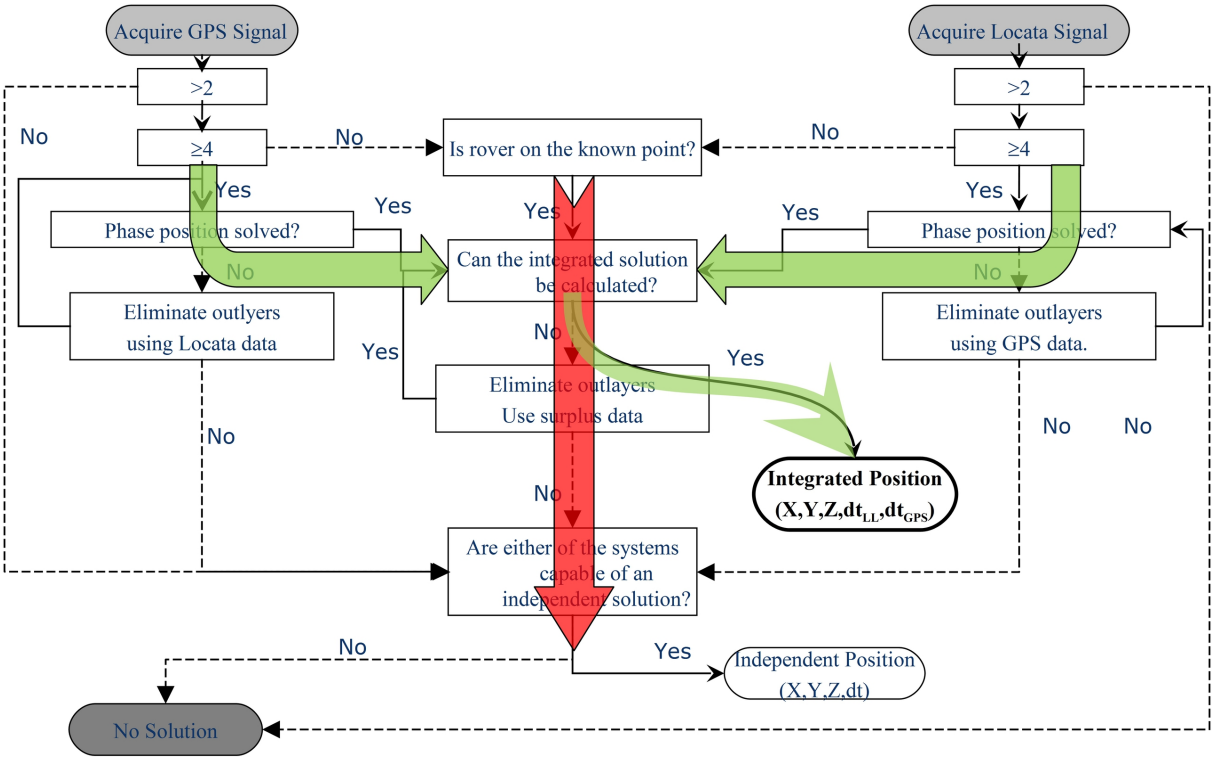

Figure 4.3 – The Integrated system (Locata/GPS) positioning algorithm

The green route indicates the combined system, while the red route indicates a single system fix.

TimeLoc accuracy

TimeLoc, the equivalent of the GPS atomic clock control, provides TCXO nanosecond steering[7] (see section 3.1, page 30). The effectiveness of this method can be verified by comparing the GPS and Locata rovers' pulse per second (PPS) output (Bonenberg, Roberts and Hancock, 2010b). PPS is used as the frequency and time standard, visualised as sharp rising/falling signal edge, repeating every second. Figure 4.4 on the following page shows PPS from GNSS and Locata rovers, synchronised to GPS feed, within 20 ns from each other.

TimeLoc stability

TimeLoc long term stability was tested in laboratory conditions, by connecting the Locata Master unit's, operating in Locata proprietary time, and outputting data every second with $1{\cdot}10^{-2}$ s tag resolution, to a PTDL1 data logger. Incoming data was time tagged with a resolution of $(1\,000{\pm}1){\cdot}10^{-7}$ s (Geospatial Research Centre, 2008). Two separate trials were conducted:

- A test of four Locata transceivers, using firmware version v.3.0-3.4, with 3-4 days long scenarios;
- A test of unit with the most stable clock over seven days.

The accuracy of time tagging prevented any estimation of short-term clock accuracy estimation, which is of less importance in long term clock stability. As TCXO requires approximately 68 s warm-up before

[7] Accuracy is on a microsecond level, between 0.5 and 2 µs.

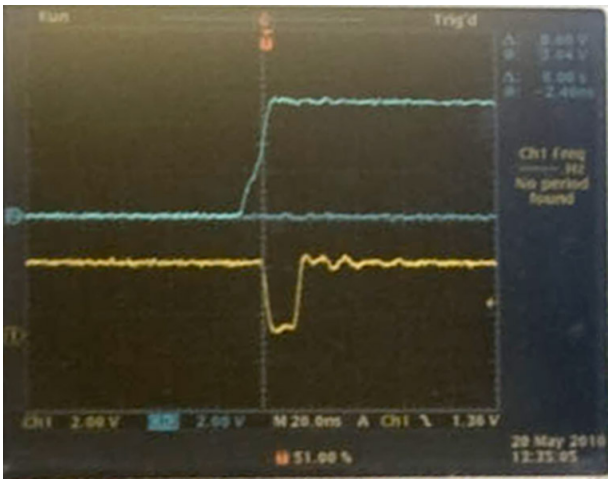

Figure 4.4 – Comparison of Locata and GPS PPS signal (yellow and blue) with 20 ns step

obtaining maximum efficiency, therefore the starting section was excluded from the first trial analysis, presented in. table 4.2 and in demonstrating good clock performance .

Frequency Accuracy	No of samples	Sample duration
$(13\pm5)\cdot10^{-3}$ s/d	12	(82 ± 11) h

Table 4.2 – TimeLoc frequency accuracy

The most stable unit was used for a seven day trial, with matching results. The clock stability was estimated at $18\cdot10^{-3}$ s/d agreeing with theoretical values (see table 3.1, page 32). The jumping pattern and the step-like drift, visible in figure 4.5, are caused by differences between PTDL1 and Locata output tagging and communication port delay: data was transmitted on the full second.

4.4 Positioning accuracy

While their time keeping methods are different (with GPS time maintained by control and space segment atomic clocks[8] and Locata by use of TimeLoc), both systems estimate distance by measuring the travel time[9]. Pseudo-ranges can only provide only metre level accuracy, therefore, a centimetre-level fix requires an integrated carrier phase (ICP) observations, and estimation of the ambiguity (the number of full cycles between satellite and receiver), in the process known as ambiguity resolution (AR).

The geometrical weakness of GPS is most evident in the height component and open sky requirement. On the other hand, with Locata, the planarity of transmitters leads to a 2D only fix. Amt and Raquet (2006), suggested height fixing, with height estimated from a digital terrain model (DTM), or other sensor. LINE will output the last known height in this case.

[8] Current analysis demonstrates that falling prices and miniaturisation of atomic clocks will make them feasible for GNSS rover implementation in the near future.

[9] This is about $70\cdot10^{-3}$ s for GPS.

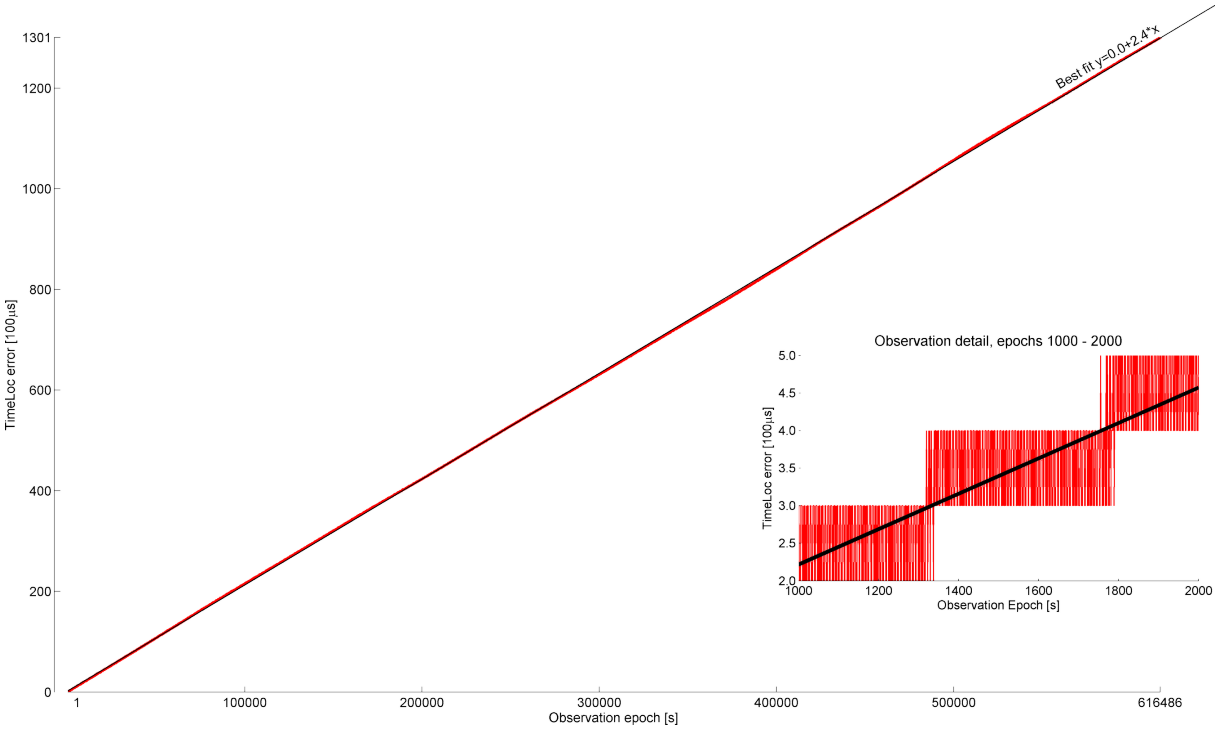

Figure 4.5 – TimeLoc frequency stability

GPS double-differenced AR is affected by the baseline length, clocks, and noise measurements. Locata uses single-differencing, but, as its pseudo-ranges contain a bias[10], a Known Point Initialisation (KPI)[11] method is used to estimate float ambiguities. Bertsch (2009), suggested fixing them using LAMBDA, but without the practical verification.

Differencing conventions for Locata and GPS

Differencing - a linear combination calculated between receivers, satellites or observation time (epochs), is used to remove system errors, thus achieving a centimetre-level fix[12] (Hofmann-Wellenhof et al., 2008). Naming conventions for Locata and GPS vary, due to TimeLoc based network synchronisation (see table 4.3, page 52). This highlights a main difference: Locata uses single-differencing for positioning, while RTK-GPS uses double-differencing (Barnes et al., 2006; Barnes, Rizos et al., 2007; Montillet, 2008). In theory, Locata ICP should offer higher levels of accuracy than that offered by GPS, as with each differencing observation, noise increases by $\sqrt{2}$.

Difference	GNSS (GPS)	LL
Single (△)	receiver	transceivers[a]
Double(△▽)	satellite	time[b]
Triple (△▽△)	time[c]	N/A

Table 4.3 – GNSS and Locata differencing name standardisation

[a] To reduce the clock error, it is a good practice to differentiate against the Master transceiver.
[b] Used for cycle slip detection (as per equation 5.5 on page 80).
[c] Used as AR method or for cycle slip detection.

Method	Total Station[a]		Locata	GPS
Distance[km]	**Angular accuracy**[m]	**Distance Accuracy**[m]	**Distance Accuracy**[m]	
0.1	0.0003	0.001	0.01	0.01
1.0	0.003	0.002	0.01	0.01
10.0	0.029	0.011	0.01	0.01
100.0	0.291	0.101	0.01	0.01
$22{\cdot}10^3$	63.995	22.001		0.01

[a] Leica TS30 total station with angle accuracy of $0.6''$ and distance accuracy of 0.6 mm+1 ppm.

Table 4.4 – Comparison between terrestrial distance and angular measurements and radio methods, adapted from Bonenberg (2003)

DOP – Dilution of Precision

DOP (Dilution of Precision) is defined as the squared sum of the symmetric covariance-variance matrix Q diagonal[13], and can be visualised as a volume of the polyhedron circumscribed by a unit sphere. In such a shape the vertical determinant will always be weaker then the planar one[14]. This approach does not take into account a scale factor (the clock offset or TimeLoc) and Earth gravitation constant for GPS.

Table 4.4 compares the error propagation of a terrestrial total station, using both Locata and GNSS. These results not only demonstrate that with increased separation, the distances become the most efficient measurements, but also that GNSS-type observations do not suffer visibly from accuracy degradation. Yet, due to atmospheric effects, Hofmann-Wellenhof et al. (2008) demonstrate the simple

[10] This bias is due to delays in the hardware and rover TimeLoc clock offset and can be removed in post processing, see figure 6.11, page 96.
[11] KPI requires either a known points or a GPS feed to provide initial estimation for AR, see figure 4.1, page 46, which can lead to a wrong solution, see section 5.2, page 70.
[12] A very promising PPP approach is not discussed in that thesis.
[13] Values are calculated in geodetic coordinates (XYZ). To estimate the planar and height a transformation to grid (ENH) or geographic coordinates (LLH) is used (Hofmann-Wellenhof et al., 2008).
[14] Pseudolites augmentation should mitigate that (Lee et al., 2008, 2004; Meng et al., 2004; J. J. Wang et al., 2004).

relation between the accuracy of RTK-GPS measurements and baseline length (see table 4.5, page 53). This becomes more complex as we consider longer baselines, as per Soycan and Ocalan (2011), we can use the following equations to estimate the horizontal and vertical accuracy (HRMS and VRMS)[15]:

$$\begin{aligned} HRMS &= 27.117 + 0.163 \times BL - 1.897 \times OD - 1.604 \times SVs + 0.972 \times PDOP \\ VRMS &= 60.993 + 0.304 \times BL - 3.742 \times OD - 2.288 \times SVs + 1.377 \times PDOP \end{aligned} \quad (4.1)$$

Observation Type	**Planar accuracy**[a]	**suggested observation time**[b]
Static	5 mm + 0.5 ppm	10 min + 1 min/km[c]
Kinematic	50 mm + 0.5 ppm	–

[a] GPS vertical accuracy is 1.2 – 2.0 times worse than the planar one.

[b] Distance refers to the baseline length, which should not exceed 10 km. This method can only provide very crude results for N-RTK, as VBS is utilised.

[c] In case of single frequency receivers, increase observation time twofold.

Table 4.5 – Expected accuracies of the RTK technique, in relation to baseline length (Hofmann-Wellenhof et al., 2008)

Accuracy implications of the TimeLoc procedure

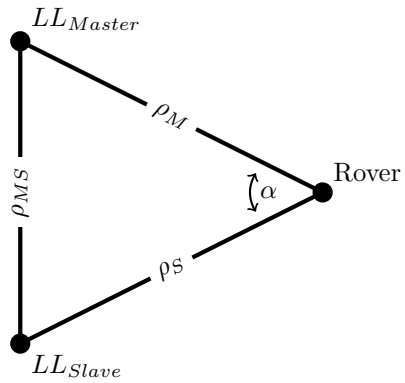

Figure 4.6 – TimeLoc effect on single differencing (△)

As a ground-based system, Locata signals are only affected by tropospheric delay, which can be precisely modelled, if external information is available, giving higher levels of precision than GPS. On the other hand, any residual bias in TimeLoc will affect fix accuracy. Without the loss of generality, let us assume single differencing (△) between the Master and Slave (see figure 4.11, page 61). Simplifying to planar the TimeLoc influence can be described as:

$$\triangle_{\triangle TL} = \rho_M - \rho_S - \rho_{MS} \quad (4.2)$$

where $\rho_\bullet$ represents TimeLoc bias (see equation 4.8, page 61). Knowing that $\rho_{SM} = \sqrt{\rho_M^2 + \rho_S^2 - 2\rho_M\rho_S\cos\alpha}$ three geometrical scenarios can be considered :

[15] Both HRMS and VRMS are estimated in mm. The observation duration (OD) is in min, baseline length (BL) in km. Number of satellites (SVs) and positional dilution of precision (PDOP) are taken as a mean value through the observation period.

1. $\alpha \to 0$ $\rho_{SM} = \sqrt{\rho_M^2 + \rho_S^2 - 2\rho_M\rho_S} \Rightarrow \triangle_{\triangle TL} \to 0$
2. $\rho_M >> \rho_S$ $\rho_{SM} = \sqrt{\rho_M^2 + \rho_S^2} \Rightarrow \triangle_{\triangle TL} =\sim -\rho_S$
3. $\rho_M = \rho_S$ $\rho_{SM} = \rho_M \Rightarrow \triangle_{\triangle TL} = -\rho_M$

TimeLoc bias will reach zero, only with long and similarly sized baselines, a most unlikely circumstance. Therefore, in order to keep the TimeLoc bias small, all observation distances should be similar. It is very important to closely monitor any problems in inter-visibility between Locata transceivers, as they will directly affect the fix accuracy.

4.5 System range

Though single differencing Locata does not require a base station, its range is limited by transmitter power, and the Line-Of-Sight (LOS), between the transmitters and the rover. The 2.4 GHz licence-free ISM band signal, used by Locata, can only propagate in three ways: directly, as a ground reflected wave or by scattering (Burnside, 1991). Any non-direct signal, is regarded as multipath (see section 4.8, page 61), and combined with environmental factors, such as rain or fog, multipath will reduce the system range and introduce noise and observation biases. Environmental effects introduce attenuation not exceeding $0.5\,^{\mathrm{dB}}/_{\mathrm{km}}$ for signals using sub 10 GHz frequency. The system range of Locata can be therefore approximated using the free space path loss[16] (Huang and Boyle, 2008):

$$L_{FS} = 20\log_{10}(\frac{4\pi\rho}{\lambda}G_{ant}) \tag{4.3}$$

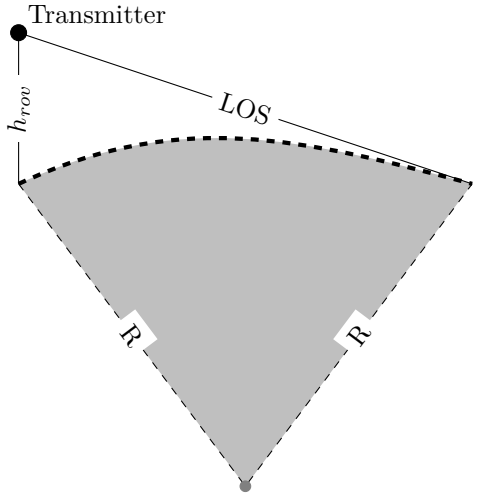

Figure 4.7 – Apparent horizon calculations

This maximum range will be reduced by obstructions, noise, and multipath, and will not in any case exceed inter-visibility between the transceivers and the rover. The distance to the apparent horizon,

[16] Where λ indicates signal wavelength, ρ geometric separation of transmitter and antenna and G_{ant} antenna performance, assuming for simplicity that transmitter and receiver antenna share the same characteristics.

(see figure 4.7, page 54), can be estimated from Cousins' theorem,[17] using equation 4.4

$$\rho_S = R \arccos(\frac{R}{R+h}) \tag{4.4}$$

or, for field purposes, directly from figure 4.7 on the preceding page using Pythagoras' equation $\rho_S = \sqrt{h^2 + 2hR}$. Ranges up to 10 km require an antenna located 8 m above the surrounding area (see figure 4.8, page 56). This is easily obtainable during normal deployment, using roofs or high raised and secured areas. Yet the reverse approach, for bridges or other high raised structures, is problematic, as the current LCom HG2403U omni-directional antenna of the rover has very low sensitivity to the negative angle signals (see section 3.1, page 33).

The Locata signal, as a ground-wave follows the curvature of the Earth, and is affected by a tropospheric delay of up to 350 ppm, which can be mitigated by mathematical models to 5 – 20 ppm. Earth curvature can be safely ignored, as it reaches only millimetre level within the Locata range. It can be estimated from equation 4.5 (Laurila, 1976)

$$\triangle_\rho = \frac{\rho^3}{43R^2} \tag{4.5}$$

4.6 Orbit determination, phase centre offset and geometry

To properly determine the distance, in addition to time and range, the knowledge of the position and orientation of the transmitter at the measurement epoch is vital. Depending on the level of accuracy required, this will include the antenna characteristics of both the transmitter and the receiver and their phase centre offsets, which will vary according to the angle of reception. GPS uncertainty in antenna position (orbit determination) can be related to rover positional accuracy using equation 4.6[18] (J. J. Wang et al., 2004)

$$\sigma_{base} = \sigma_\rho \frac{\rho_{base}}{\rho_{SV}} \tag{4.6}$$

The phase centre offset (PCO) is absolute, and at centimetre-level. To mitigate this, satellite antennas are calibrated and constantly monitored by ground control stations. Furthermore, the receivers, particularly geodetic ones, use antenna with known PCO[19] .

The Locata transceiver self-survey feature, introduced in firmware version v.4.2 (Locata Corporation Pty Ltd, 2010b), can also be used to verify the stability of its antennas,[20] but it does not address the PCO (Abello, Dempster and Milford, 2007). Starting from firmware version v.5.0, the antenna type, and its 3D orientation can be provided, which, although not fully implemented, is expected to reduce this bias and provide better multipath mitigation (Locata Corporation Pty Ltd, 2011a, 2011b).

[17] Where h indicates transmitter height above the surrounding area and R refers to the radius of the Earth (see section 2.4, page 13).

[18] with $\rho_\bullet$ indicating distance (between rover and consequently base and satellites) and $\sigma_\bullet$ distance accuracy.

[19] One of the early mitigation techniques was to orientate all antennas in the same direction - north by convention (Leick, 2004). Using the differential technique, and assuming that all antennas are the same, the offset would be significantly reduced.

[20] This requires an external GPS RTK receiver utilising OWI interface and assumes that all Locata transceiver's antennas are located in the same plumb line, with known vertical offsets.

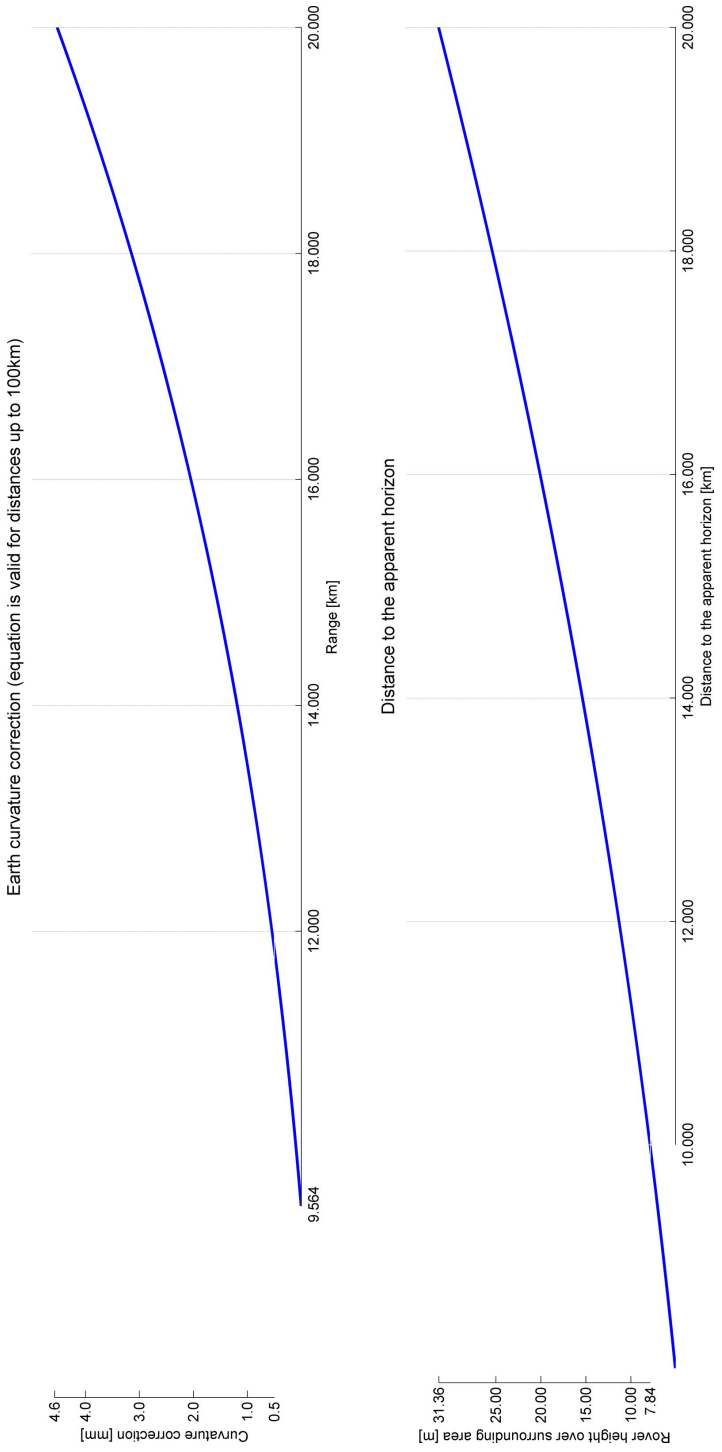

Figure 4.8 – Terrestrial system range and Earth curvature correction

GPS Satellite Ephemeris	Accuracy [m]	Satellite Clocks[ps][a]	Latency
Broadcast	1.000	5 000±2 500	real time
Ultra Rapid (predicted half)[b]	0.050	3 000±1 500	real time
Ultra Rapid (observed half)[b]	0.030	150±50	3-9 hrs
Rapid[b]	0.025	75±25	17-41 hrs
Final[b]	0.025	75±20	12-18 days

[a] Each $10{\cdot}10^{-12}$ s is equivalent of 3 mm.
[b] IGS orbit products.

Table 4.6 – Accuracy of IGS orbit products

4.7 Tropospheric and ionospheric effects

The Earth's atmosphere consist of layers of gases which surround the planet and are retained by the planet's gravity. It protects life on Earth by absorbing ultraviolet solar radiation, warming the Earth's surface through heat retention (greenhouse effect), and reducing temperature extremes between day and night (the diurnal temperature variation). From a GPS point of view, the two most important parts of the atmosphere are the troposphere and the ionosphere (see figure 4.9, page 58):

The Ionosphere is the upper part of atmosphere, and consists of a shell of electrons and electrically charged atoms and molecules at between 80 – 650 km altitude. The Kármán line at 100 km is regarded as the boundary between the atmosphere and outer space. Ionospheric free electrons advance phase velocity (phase observations), and delay the group velocity (code observations). This effect is frequency dependant[21], and can be estimated using multi-frequency observations, or eliminated altogether in an ionosphere free combination, if the baseline does not exceed 400 km under normal scintillation conditions (Verhagen, 2004). Ionospheric scintillation is characterised by a rapid fading in signal power levels, resulting from electron activity and directly correlated with the solar maximums, which can lead to signal tracking loss.

The troposphere is the lowest portion of the Earth's atmosphere, and therefore it is in contact with Earth's surface. Its depth varies from 7 km at the poles, to up to 20 km in tropical regions, with an average of 13 km. It contains approximately 80% of the atmosphere's mass and 99% of its water vapour and aerosols, and is characterised by a temperature decrease with altitude of $6.5\,^{\circ}\mathrm{C}/\mathrm{km}$. It consists of dry and wet components; the dry component is up to ten times larger but much more predictable, with variation below 1% in a few hours in comparison with 10 - 20% for the wet one. Tropospheric group velocity and phase velocity are the same, with a wet part delay 0 – 0.4 m in the zenith direction, determined with an accuracy of 0.02 – 0.05 m, based on semi-empirical models. Dry delay is 2.2 – 2.4 m in the zenith direction, but can be almost fully discounted if surface pressure observations are available (Hofmann-Wellenhof et al., 2008).

[21] Inversely proportional to the square of the frequency of the signal.

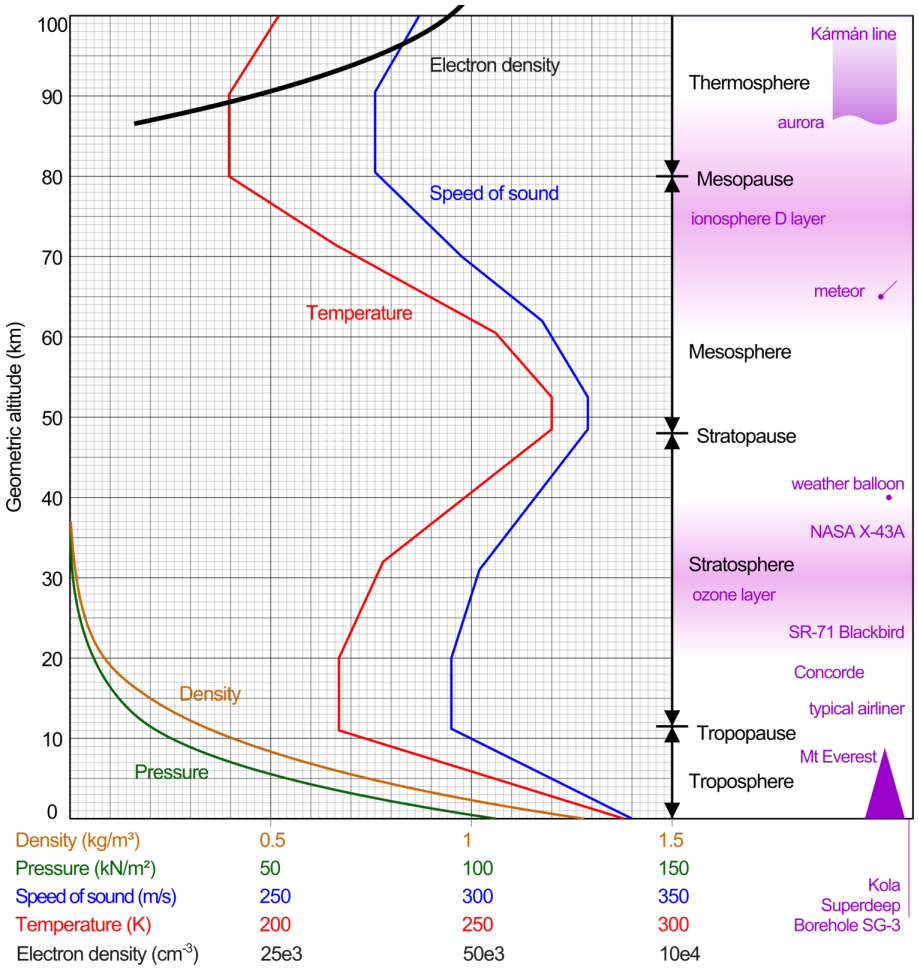

Figure 4.9 – Atmosphere overview

Adapted from http://en.wikipedia.org/wiki/File:Comparison_US_standard_atmosphere_1962.svg / CC BY-SA 3.0

The average atmospheric pressure at sea-level is 1 013.2 mbar (1 009 mbar for UK). The lowest pressure (892.3 mbar) was recorded on 2 September 1935 at Florida Keys, USA[22]. The highest recorded pressure was 1 083.8 mbar in Siberia. The highest atmospheric temperature recorded was 58 °C, at El Azizia in Africa, on September 13, 1922. UK records were 38.5 °C in Brogdale, Kent, on 10 August 2003 and −27.2 °C at Braemar in the Grampians, on 10 January 1982 (Burnside, 1991; Lavergnat and Sylvain, 2000; Parkinson et al., 1996).

Ionospheric and tropospheric models

Any signal travelling through the atmosphere will be subject to signal absorption, which reduces its range, strength, and delay, through signal bending and propagation of speed deviations. There are a number of models that can calculate ionospheric and tropospheric corrections separately. Models described in Kleusberg and Teunissen (1998); Klobuchar (1991); Saastamoinen (1972); Seeber (1993)

[22] Even lower readings have been recorded at the centre of hurricanes, producing even lower pressure, with 870 mbar recorded in 1979 in the eye of Typhoon Tip.

estimate for zenith angle, with other elevation angles estimated via mapping functions.

The ionosphere is notoriously difficult to model, especially at low elevation angles, one approach is to calculate the residuals directly using larger data samples. As wet delay is the most prominent factor, and its estimation using CORS networks is possible, it is this factor that determines the selection criteria for the GPS double difference reference satellite (the satellite with the highest elevation), signals from lower lying satellites need to penetrate a much thicker layer of the ionosphere. Accuracy can be roughly estimated, following Pinchin (2011), from equation 4.7[23]:

$$\sigma_i = \frac{\sigma_{obs}}{\sin(EL_i)} \tag{4.7}$$

The troposphere is easier to model, and, while delay can reach 300 ppm, dedicated L1 frequency models are capable of removing nearly all of this delay. Due to the low elevation angles a new model had to be implemented for pseudolites using the L1 frequency, as described in Soon et al. (2003); J. J. Wang et al. (2004); J. J. Wang, Wang, Sinclair, Watts and Lee (2005). As Locata utilises the S band (2.4 GHz) we should assess whether these models can be reused for these frequencies. Millimetre-Wave Propagation Model (MPM) (Rueger, 2002) allows the comparison of the characteristics of the Locata S and the GPS L band (1.1 – 1.6 GHz) using typical weather for Europe:

Clear Day 0.0 $^{g}/_{m^3}$ of suspended water droplets , 0.0 $^{mm}/_{hr}$ rain rate;

Foggy Evening 4.0 $^{g}/_{m^3}$ of suspended water droplets , 0.1 $^{mm}/_{hr}$ rain rate;

Heavy Rain 0.8 $^{g}/_{m^3}$ of suspended water droplets , 50.0 $^{mm}/_{hr}$ rain rate.

Results, presented in figure 4.10 on the following page, show a similar tropospheric delay throughout the frequencies in question, suggesting that the existing L1 pseudolite models can be used for Locata. As mentioned above, these models are not perfect, mostly due to the assumption of a homogeneous troposphere along the path of the signal. The difference between the models is minimal (Choudhury, 2012), mostly due to mathematical limitations; this is one of the reasons why Locata AR is solved as a float.

The tropospheric effect also influences TimeLoc, and equation 4.2 on page 53 can be used to quantify this effect. Assuming single difference between the master and slave Locata unit, and a planar only solution, (see figure 4.11, page 61) we can simplify the problem into three geometrical scenarios:

1. $\alpha \to 0$ $\rho_{SM} = \sqrt{\rho_M^2 + \rho_S^2 - 2\rho_M\rho_S} \Rightarrow \triangle_{\triangle trop} \to 0$
2. $\rho_M >> \rho_S$ $\rho_{SM} = \sqrt{\rho_M^2 + \rho_S^2} \Rightarrow \triangle_{\triangle trop} = \sim -\rho_S$
3. $\rho_M = \rho_S$ $\rho_{SM} = \rho_M \Rightarrow \triangle_{\triangle trop} = -\rho_M$

[23] EL is elevation – vertical angle between rover and satellites; σ_{obs} the standard measurement uncertainty. It is customary to disregard any observations lower then 10° unless a choke ring antenna is used.

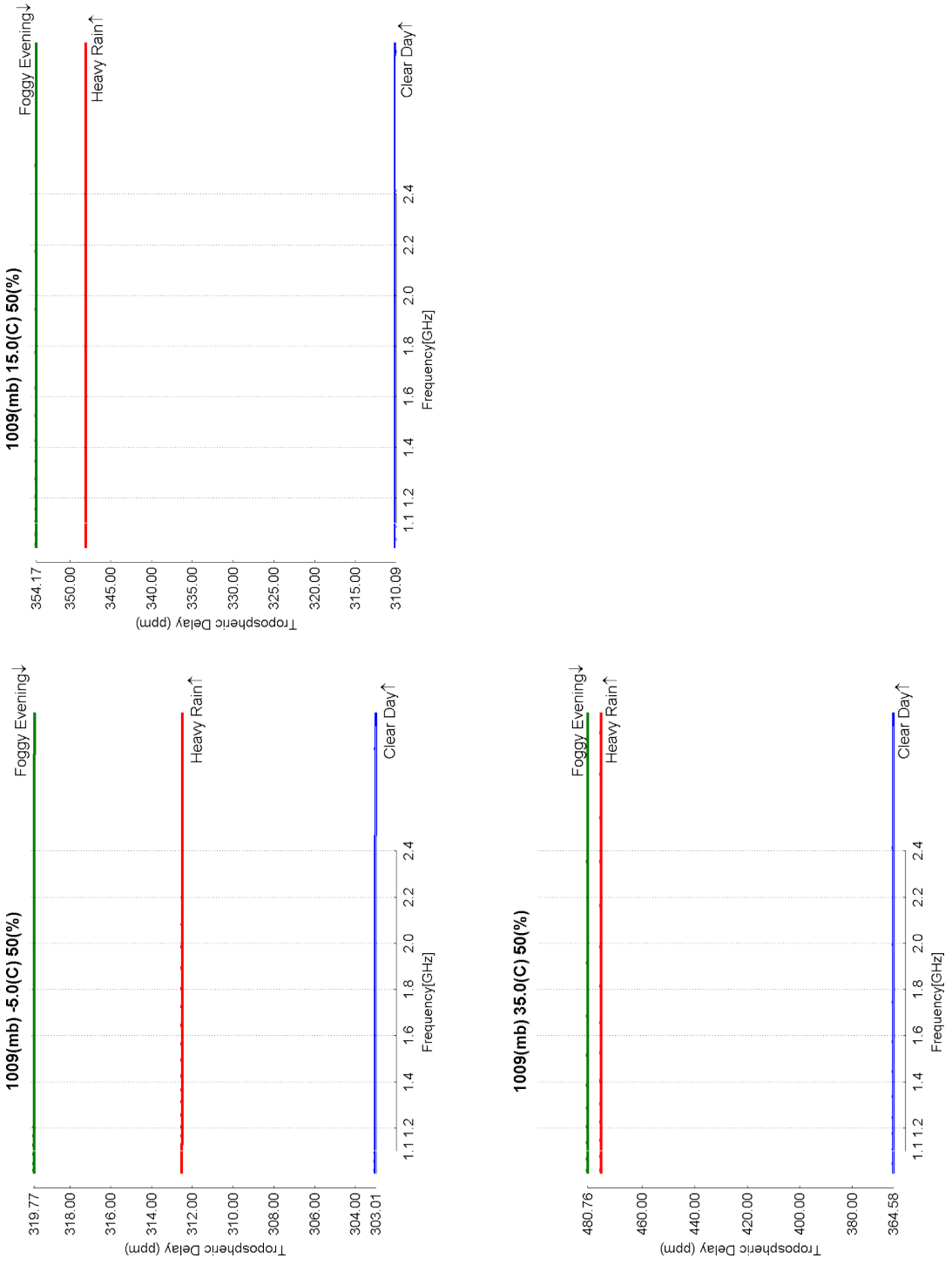

Figure 4.10 – MPM Tropospheric delay for L and S frequencies

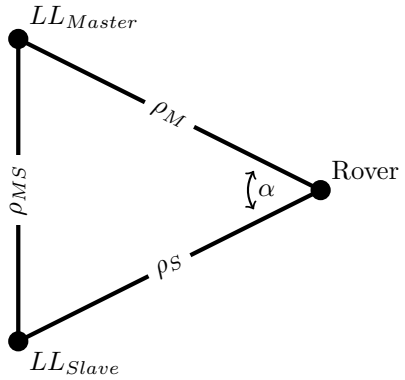

Figure 4.11 – Single differencing and the TimeLoc effect on the tropospheric model

The difference will reach zero, only with similarly sized baselines, and homogeneous atmospheric conditions throughout the network. Otherwise, the remaining effect has to be corrected by the model. Until recently Locata has utilised an L1 based tropospheric model[24](J. J. Wang et al., 2005):

$$\begin{aligned} \triangle_{trop} &= \triangle_{trop}^{dry} + \triangle_{trop}^{wet} \\ \triangle_{trop}^{\bullet} &= \rho N_{trop}^{\bullet}(1 - \frac{dh}{H_0^{\bullet}}) \\ N_{trop}^{dry} &= 77.6\frac{P}{T} \\ N_{trop}^{wet} &= 22770\frac{f}{T^2}10^{\frac{7.4475(T-273)}{t-38.3}} \end{aligned} \tag{4.8}$$

Trials carried out at White Sands Air Force Base (Craig and Locata Corporation, 2012), demonstrated tropospheric modelling based on multiple MET sampling through the network, in very similar fashion to the CORS network model for the ionosphere. This approach is to be implemented in firmware version v.7.0.

4.8 Multipath

Multipath occurs when the signal arrives at the antenna from more than one path or direction, thus causing the antenna to receive a combination of direct and non-direct signals. The latter will be delayed in phase and code, with varying amplitude, reduced power and a shift of phase[25]. It is likely to interfere with the direct (LOS) signal. It can, in extreme cases, lead to complete loss of signal (Barnes et al., 2006). It is also possible that only the non-direct signal will be received, in this case most mitigation techniques will fail (Groves, Wang and Ziembart, 2012; Hofmann-Wellenhof et al., 2008; Kaplan and

[24] where P is atmospheric pressure in *mbar*, T temperature in *Kelvin*, f relative humidity, $dh = h_{rov} - h_{LL}$ is the height difference between rover and transmitter, ρ is the slope distance between them, both in *metres*. $H_0^{\bullet}$ is the fixed scale height for the dry and wet component, respectively 42 700 m and 12 000 m.

[25] Less known shadowing effects, due to foliage or light obstruction attenuation, can increase signal power.

Hegarty, 2006). Multipath ρ_{MP} is dependent on a number of factors and its quantification is very difficult, but the simplified equation 4.9[26] can be used to assess its impact:

$$\begin{aligned} P_{MP} &= P + \partial_{MP} + \epsilon \\ \phi_{MP} &= (\rho + \rho_{MP})\lambda + N + \epsilon \end{aligned} \tag{4.9}$$

Great effort has been made in attempts to mitigate multipath, including correlator design, wider signal bandwidths, wider pre-correlation bandwidths and narrower early-late spacing. Galileo signals are intended to offer increased multipath resistance, once they have been correctly tracked. Improvements to antenna design and coatings can also limit multipath, and Kaplan and Hegarty (2006) discusses signal calibration using GPS sidereal day orbits repetition[27]. The utilisation of ray-tracing modelling to remove any multipath effect has also been suggested (Andreotti, 2006; Lau and Cross, 2007). Therefore, for practical calculations, it can be reliably assumed that multipath will not exceed 0.25 cycle[28] (Kaplan and Hegarty, 2006; Yang et al., 2010), or 3 cm for Locata.

With pseudolites, signal calibration has been suggested for the removal of multipath residuals (Dixon and Morrison, 2008; Yang et al., 2010). Locata utilises a unique signal clustering technique as each transmitter emits four signals, which are separated both in frequency, and spatially (Barnes et al., 2006). Additionally, Timetenna, the dedicated indoor antenna, uses beam steering to mitigate multipath (Gakstatter et al., 2011; Rizos, Roberts et al., 2010). A standard choke ring antenna or base plate has also been demonstrated to reduce this effect (Bonenberg, Hancock and Roberts, 2010).

Implications for system range

The effect of multipath effect on signal range can be estimated from a singular reflection model, using equation 4.10[29](Holmes, 2007; Huang and Boyle, 2008).

$$\triangle\rho_{MP} = \frac{2h_{trans}h_{receiver}}{\rho} \tag{4.10}$$

An extreme case arises when the phase is reversed, with $\rho = \lambda/2$[30]:

$$L_{FM} = 20\log_{10}(\frac{2\pi\rho^3}{\lambda h_{trans}h_{receiver}}G_{ant}) \tag{4.11}$$

Due to mathematical simplification, equation 4.11 is only valid if $\sum h \ll \rho$, and related to extreme conditions, which are in any case highly likely to prevent any communication, as observed by (Barnes

[26] Where P_{MP} indicates pseudo-range (code) and Φ_{MP} carrier phase affected by the multipath bias (ρ_{MP}).

[27] Sidereal day is equivalent to 23.934 47 h as earth total rotation takes 366 days.

[28] This is also a reason why the close reflections effect is more prominent.

[29] Delay $\triangle\rho_{MP}$ is estimated in metres. $h_\bullet$ is height of the transmitter and the rover respectively, while ρ is their spatial separation.

[30] Phase difference of 180° or 0.5 cycle.

et al., 2006). The typical urban range for **L1 pseudolite**s can be estimated using the Okumura-Hata COST231 fading channels model from equation 4.12 (Holmes, 2007)

$$L_{231} = 46.3 + 33.9 \log f - 13.82 \log h_{trans} + \log d(44.9 - 6.55 \log h_{trans}) + 3.2(11.75 h_{rov})^2 - 1.97 \quad (4.12)$$

For **Locata** we can use the model ECC-33 for wireless systems, as per equation 4.13

$$\begin{aligned} L_{ECC-33} = {} & 20.41 + 100.294 \log f + 29.83 \log \rho + 95.6(\log f)^2 - 13.958 \log(\frac{h_{trans}}{200}) \\ & - 5.8(\log \rho)^2 - (42.57 + 13.7 \log f)(\log h_{rov} - 0.585) \end{aligned} \quad (4.13)$$

A comparison of all discussed scenarios, fading multipath, COST231, ECC-33, and free space loss (see equation 4.3, page 54) is presented in figure 4.12 on the following page. The extended range of 30 km achieved at White Sands (Craig and Locata Corporation, 2012), has been shown for comparison. It can be observed that the urban range of Locata is greater than its L1 one, with a difference of 44 dBm due to shorter wavelength, but this will fall off in the presence of severe fading multipath

4.9 Near-far effect

Large power differences between space and ground-born signals can also lead to strong cross-correlation between C/A codes, leading to losses of up to −21 dB, which could easily push any space-born system under the noise floor. Alleviation of this effect is paramount for GPS and pseudolite cooperation, and a number of solutions have been researched (Cobb, 1997; Parkinson et al., 1996) including:

- The utilisation of pseudolites on a non-constant basis, purely for AR optimisation, with pseudolite location preventing users from entering the “near” area;
- Tuning antenna patterns or the utilisation of antenna array to form Controlled Reception Pattern Antenna (CRPA): predetermination of pseudolite position allows a reduction in transmitting power for other directions;
- Frequency hopping, which is again limited by the front-end capacity (limited dynamic range and “hard-limiting”), as, despite its excellent cross-correlation properties, the receiver will see a decrease in the satellite signal strengths;
- Code Division Multiple Access (CDMA), as utilised by GPS, with different Gold codes or other, longer code sequences in order to limit cross-correlation;
- Frequency Division Multiple Access (FDMA), as utilised by GLONASS. The signal is transmitted on a frequency offset from L1, within the same frequency band as GPS. With proper offset (over 1.023 MHz), cross-correlation is eliminated and cross band interference reduced;
- Utilisation of another radio frequency, as with Locata;
- Time Division Multiple Access (TDMA) a concept utilised by Locata.

Cobb (1997); Parkinson et al. (1996) recommended a TDMA approach, mostly due to the hardware compliance of existing devices, suggesting a 5 to 7 % pulsing scheme for the C/A code[31] leading to a

[31] Both the sensitivity of the front-end A2D, and chipping rate are important here. Simple, single-bit receivers can maintain 10%-12%, while P-code tracking requirements are as low as 1% (Cobb, 1997).

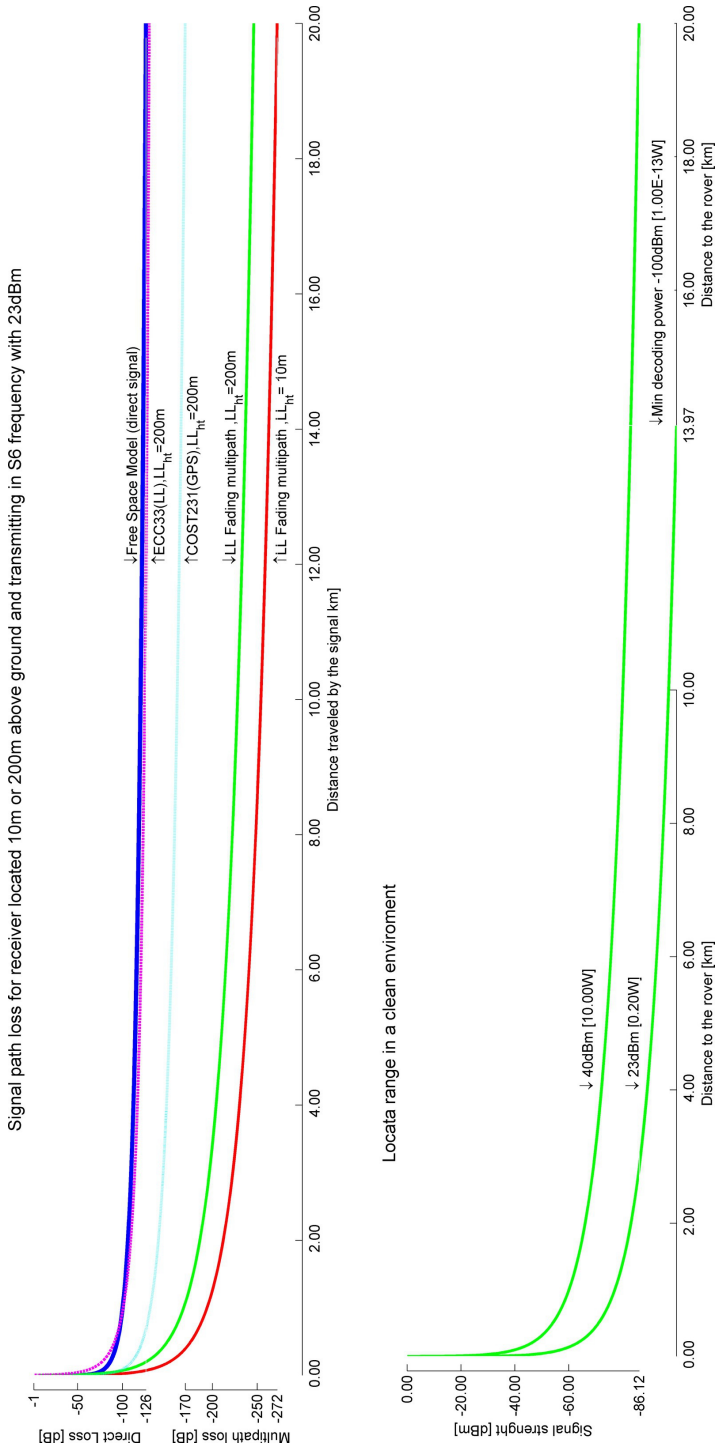

Figure 4.12 – Multipath effects on signal propagation

signal loss of 1.5 dB in the "near" zone. The worst-case cross-correlation for L1 based pseudolites is estimated at 21.6 dB (Cobb, 1997), and 250 dB for Locata, due to TimeLoc procedure. To prevent saturation, Locata uses:

- a digital signal with a 10 % duty cycle[32], with changing time bin allocations, (see section 2.4, page 14);
- Time-Hopping/Direct Sequence Code Division Multiple Access (TH/DS-CDMA), which utilises both code and time separation between receivers (Cheong et al., 2009; Locata Corporation Pty Ltd, 2011a; Stansell, 1986) (see section 3.1, page 27).

4.10 Summary

This chapter has discussed the prerequisites of integration, analysing its feasibility based on number of factors common to Locata and GPS. Both systems are on the centimetre order of accuracy and while this feasibility study highlighted geometry-related issues, an integrated system is expected to mitigate those. Most importantly, both systems are of similar range, if RTK-GPS is used. Discussion about orbit determinations, atmospheric effects, co-planarity, and multipath highlighted the areas of concern but also showed how the integrated system is addressing these directly.

♣ ♢ ♣

[32] Since firmware version v.4.0 this has been fixed at 10%. In the previous releases this value was set by the user creating the possibility of ISM frequency spoofer if duty cycle was to be set to 100% using *SlotMask[0x3fffffff]*.

5 Locata positional fix accuracy

"Repeat old incantations of humanity fables and legends because this is how you will attain the good you will not attain, repeat great words repeat them stubbornly like those crossing the desert who perished in the sand."
Zbigniew Herbert, The Envoy of Mr Cogito

THIS chapter will provide a practical verification of Locata system accuracy. It will demonstrate the limitations of current KPI in static and kinematic scenarios, varying in type and size, from a large outdoor network to much smaller indoor one. It is followed by a KPI analysis, demonstrating the effect of the initial estimation bias and Locata position bias. Finally, signal quality indicators, in-bound interference, noise and multipath and cycle slip detection methods will be discussed.

Some of the results in this chapter have been published before in (Bonenberg, Hancock and Roberts, 2010; Bonenberg et al., 2009; Bonenberg, Roberts and Hancock, 2010a).

Contents

5.1 The accuracy of the system solution

PREVIOUS studies have demonstrated Locata's centimetre-level fix, comparable with RTK-GPS, in both indoor (Barnes et al., 2003c) and outdoor kinematic tests (Barnes, Rizos et al., 2007; Montillet et al., 2009). To achieve this accuracy, integrated carrier phase measurements (ICP) and ambiguity resolution (AR) are required. In the case of Locata, only the Known Point Initialisation (KPI) method can be used, due to the system's weak pseudo-range solution. Impact of this has not been discussed before, therefore the following sections will cover this gap, outlining both the limitations of KPI and demonstrating the advantages of a new combined AR for engineering applications.

The static tests

Locata system accuracy is geometry based, and is susceptible to the effects of noise and multipath. To examine these vulnerabilities, four scenarios have been selected, varied by network size, and environmental noise (as shown in figure 5.1). The four test scenarios were:

A The Numarela Test Facility (NTF), which is a dedicated, 30 acre, outdoor test facility in Australia, in the proximity of the Snow Mountains, the Kosciuszko Peak and Cooma airport. The facility is owned and maintained by the Locata Corporation. This contains a network of ten LocataLites, with separation between transmitters in excess of 2 km and height differences of up to 150 m.

B The open courtyard of the University of New South Wales (UNSW), which is surrounded by tall academic buildings, with visible multipath to the west, and good VDOP. The network consists of four LocataLite transceivers.

C The roof of the Sir Clive Granger Building on University Park, at the University of Nottingham. A small network, due to environmental restrictions - the roof has two discrete levels, the transceivers (shown by blue dots), are almost co-planar. Small obstructions, such as vegetation and protruding building elements are also present.

D An indoor scenario in the atrium of the Nottingham Geospatial Building on the Jubilee Campus of the University of Nottingham, a three-storey building with exposed internal architectural steelwork.

All tests used Locata firmware version v.3.2. GPS results for scenarios B&C were conducted using Leica System1200 and post-processing was carried out using Leica Geo Office 7.5. The base station for the tests was within 100 m. The Locata position was calculated using the carrier solution in the proprietary LINE software with the *h2* setting[1].

The results (see table 5.1, page 69), are similar for each network, although the smaller networks (C&D) produced only planar positions. While confirming the results of previous research in some respects (Abello, Dempster and Politi, 2007; Khan et al., 2010; Montillet et al., 2009)[2], those results might not be able to provide a reliable estimation of system accuracy. Locata's KPI requires either a known point, or a GPS feed to provide an initial estimate for AR. This might lead to over-optimistic results,

[1] This is similar to the rover (on-line) solution, as one measurement will be formed by averaging four signals from the cluster.

[2] Prior research was conducted using single frequency Locata firmware version v.2.4.

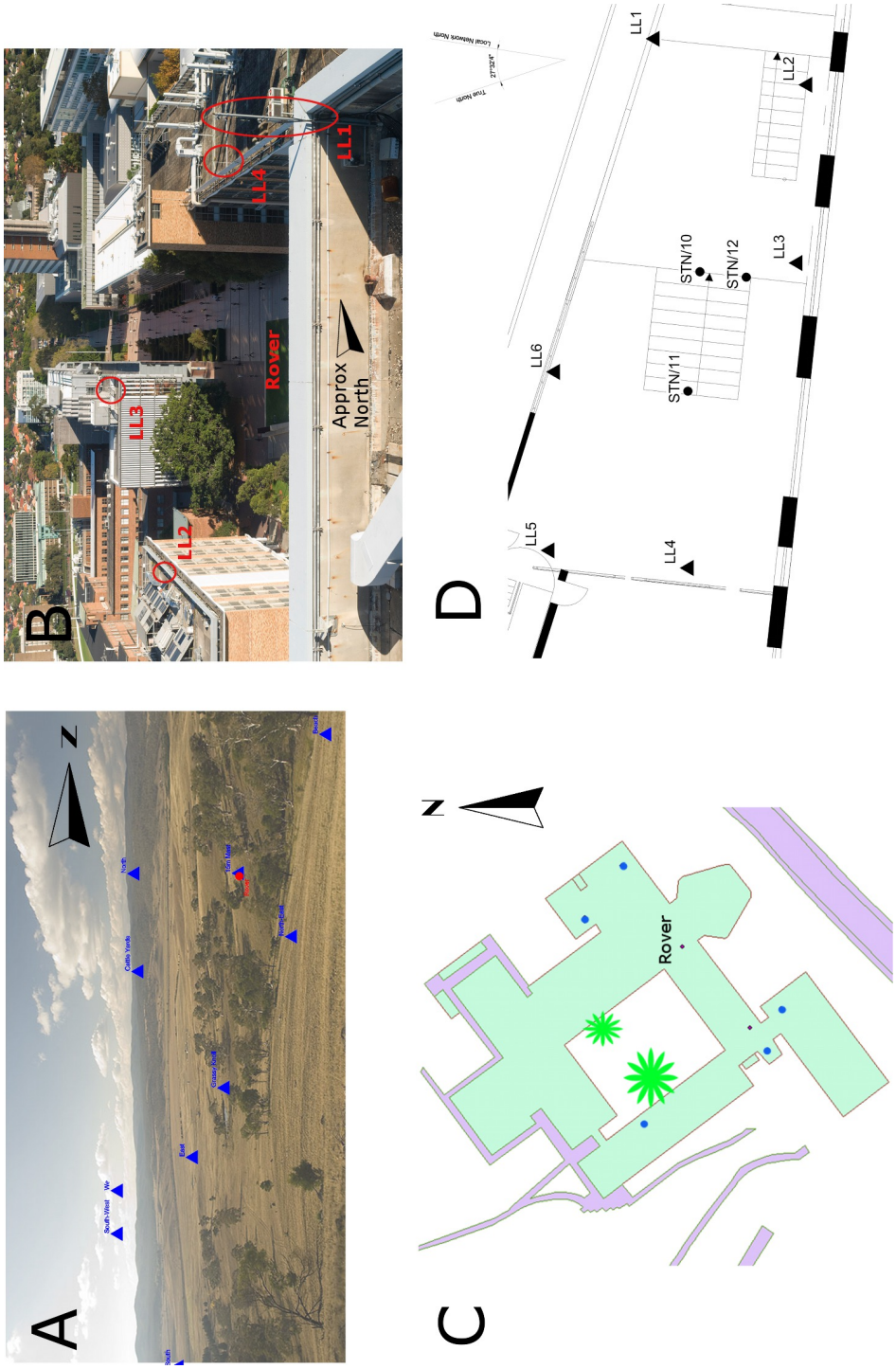

Figure 5.1 – Overview of scenarios A-D

Scenario	Locata			RTK GPS		
[m]	**dE**[a]	**dN**[a]	**dH**[a]	**dE**	**dN**	**dH**
A	0.002	0.001	0.005			
B	0.004	0.004	0.009	0.005	0.010	0.010
C	0.006	0.004	N/A[b]	0.008	0.011	0.009
D[c]	0.007	0.005	N/A[b]			

Table 5.1 – Comparison of Locata and GPS accuracy

[a] The absolute difference from truth (known point coordinates) in a planar gird (ENH).

[b] Height fixed by LINE.

[c] Accuracy depends on the mitigation method used, with the best result presented here. For more details see section 7.4 on page 119.

as constant biases, such as noise and multipath would be absorbed as well. Should this be the case, as similarities in B-D suggest, the results do not show the positional bias but rather its change[3]. This hypothesis can only be verified with kinematic data.

The dynamic (kinematic) test

The previous section demonstrated that even in environments with different levels of noise and types of obstruction, Locata produces a very similar results, which, in the opinion of the author, are caused by KPI producing over-optimistic results. To verify if KPI is capable of producing unreliable results, kinematic trials have been conducted at the Nottingham Geospatial Institute Open Sky Roof Laboratory. The size of the network and the environment makes it similar to network C, and can be taken as being representative of an urban environment[4].

The network size exaggerates any change in the geometry, but at the cost of increased noise, due to roof structures that include: observation pillars, parapet walls and cooling units[5]. Experiments in this environment can be indicative of Locata performance in urban areas. Where transmitter location possibilities are limited, networks tend to be smaller, and the rover will have to pass very close to the transmitters. Apart from the known tract alignment, seven points (L1–7) were coordinated. During the circumnavigation, the rover, which was mounted on a train, occupied each for 20 to 70 s.

The first trial, marked as OTF (on-the-fly) in the figure 5.2, demonstrates a drift in the south-east part of the track, identifiable as undetected cycle slip[6]. Assuming an over-aggressive KPI, a less stringent navigation engine would improve the resulting fixes. Data post-processed in LINE, with increased

[3] Locata transmitters are static, as will multipath effect; noise and in-bound interference, mostly by devices utilising wireless communication protocol IEEE 802.11 (commonly known as WiFi), will introduce dynamic patterns (Abello, Dempster and Politi, 2007; Khan et al., 2010; Montillet et al., 2009).

[4] See appendix F on page 161.

[5] More details about the Nottingham Geospatial Institute Open Sky Roof Laboratory can be found in appendix F on page 161.

[6] Cycle-slip occurs when observation of the beat phase (the difference between the satellite-transmitted carrier and receiver-generated replica) is interrupted and the phase ambiguity count has to be reinitialised. This will visualise as a jump in position, roughly equivalent to integer number of cycles (Hofmann-Wellenhof et al., 2008). Further discussion can be found in section 5.4 on page 80.

rejection rate, float reinitialisation and planar only solution[7], is marked as PP. Table 5.2 demonstrates fix improvement, with the exception of the clean environment (L1–3). Both results are comparable with those from an open-cast mine environment (Barnes, LaMance et al., 2007) but are weaker than results from clear environments (Barnes et al., 2006; Barnes, Rizos et al., 2007). This suggests that environmental impact cannot be assessed by static observations. It also demonstrates that Locata navigation solutions can be fine-tuned during deployment.

	OTF[a]		**PP**[b]	
Point	$\mathbf{d_{Planar}}$[m][c]	$\mathbf{d_H}$[m]	$\mathbf{d_{Planar}}$[m][c]	$\mathbf{d_H}$[m]
L1	0.01		0.01	
L2	0.07		0.14	
L3	0.20		0.25	
L4	0.26		0.16	Height fixed
L5	0.15		0.10	
L6	0.68		0.10	
L7	0.53		0.15	
TM[d]	1.04	0.61	0.28	

Table 5.2 – Kinematic test, comparison of known points and internal closure

[a] Standard LINE post-processing options, matching OTF rover results.
[b] Modified LINE post-processing options.
[c] $\sqrt{(d_E^2 + d_N^2)}$
[d] Internal misclosure, measured between the first and last point on the track.

5.2 KPI on an inaccurately coordinated point

Hofmann-Wellenhof et al. (2008) estimated that a 20 m bias in the initial position estimation will translate into a 1 ppm error in the double-differenced baseline between the rover and the base. This is due to the constant motion of the satellites, although, with long observation periods, static positioning accuracy visibly improves. However, for Locata this approach is impossible, as:

- static, and usually almost co-planar transceivers are used,
- the single differencing method is used to determine position,
- pseudo-ranges are affected by the TimeLoc bias,
- the KPI technique produces float ambiguities.

The previous section highlighted concerns with KPI results, indicating that prolonged static observations are impractical. Future proof will be presented in following sections with known offsets applied to

[7] The following settings where used: *NavSolver_MaxPDOP = 20.0; NavSolver_Max3DVDOP = 1.0; SignalQuality_MaxRcpiDiff = 150; SignalQuality_MaxPrDiff = 50.0; AmbiguityReinitialization_Method = float;*

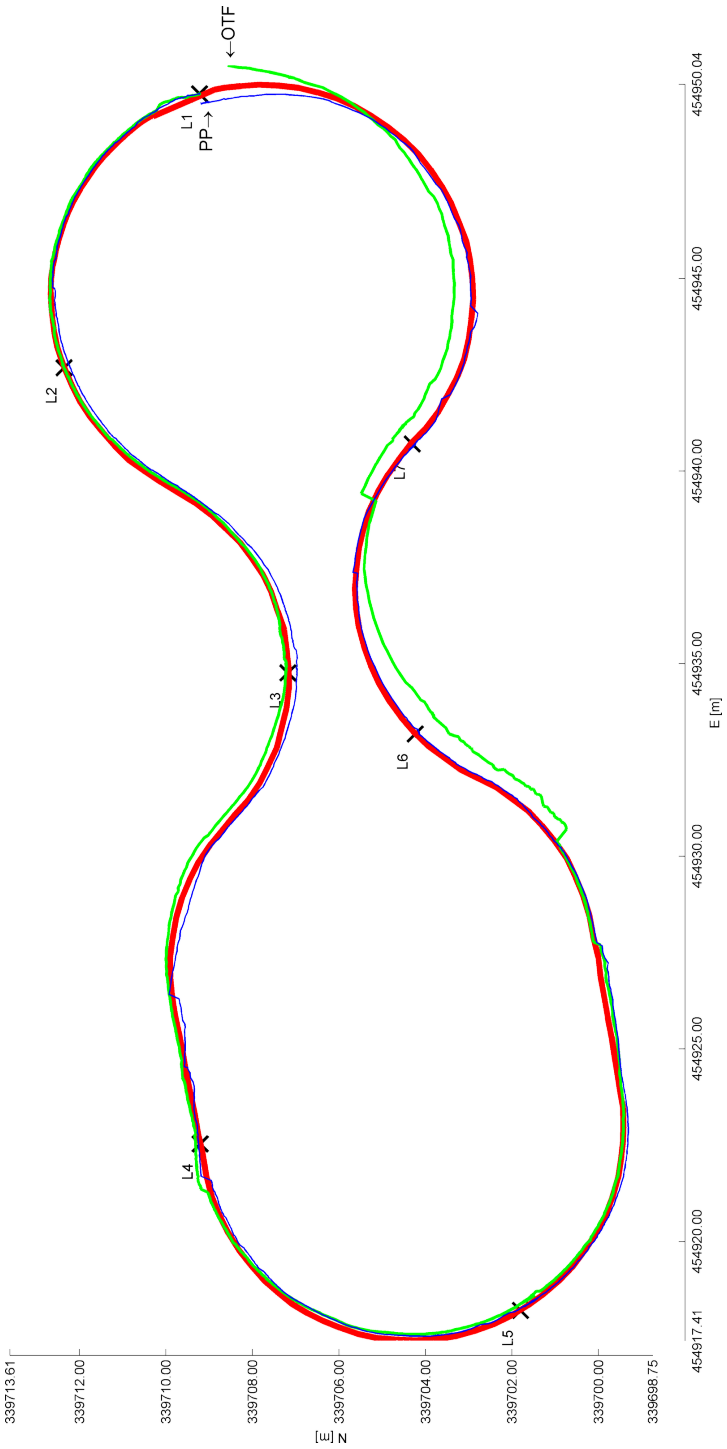

Figure 5.2 – Kinematic test results comparison

All coordinates are in the OSGB grid (ENH), with a scale factor applied.

Figure 5.3 – Mounting of Locata antenna on a train during the kinematic trials

the rover's starting position through kinematic and static data from NTF (Scenario A). To obtain a complete perspective, the last section will discuss offsets applied to Locata transceiver antennas.

The static scenario

For this scenario, 1 098 static epochs from scenario A were re-processed in LINE, with an initial erroneous offset applied to the rover by 0.03 – 1 000 m[8] in either the planar, or height position only. It was expected that LINE would detect any offset smaller than 0.5 cycle, that is 0.06 m. But, the results (see table 5.3 on page 74) show that any offset translates directly into a positional shift. Only unambiguous pseudo-range results are not affected, but cannot be utilised as a check due to their metre level accuracy. Erroneous results will only fail when the offset size creates a faulty, and therefore unsolvable, geometry[9].

The kinematic scenario

As a comparison, the same initial position estimate bias (offset) was applied to kinematic scenario A. Figure 5.4 on the facing page, shows that in the case of the integrated carrier phase (ICP), the whole track is affected, with the relative positions between the epochs remaining similar. The pseudo-range solution is not affected, and its accuracy matches the static results.

A transceiver coordinates error

Scenario A data was reprocessed in LINE and a 20 m offset was applied to transmitted position of a single Locata transceiver, LL1, LL3 or LL6[10]. Results in figure 5.5 on page 75, show that the ICP solutions are only minimally affected by the applied offset, even with LL6 located in the middle of the

[8] Offsets of 0.03 m, 0.06 m, 0.12 m, 0.18 m, 0.50 m, 1.00 m, 2.00 m, 50.00 m, 100.00 m, 400.00 m and 1 000.00 m were used.

[9] On this occasion: 400 m planar or 100 m in height.

[10] These transceivers were 1 760 m, 370 m and 20 m respectively from the rover's starting point.

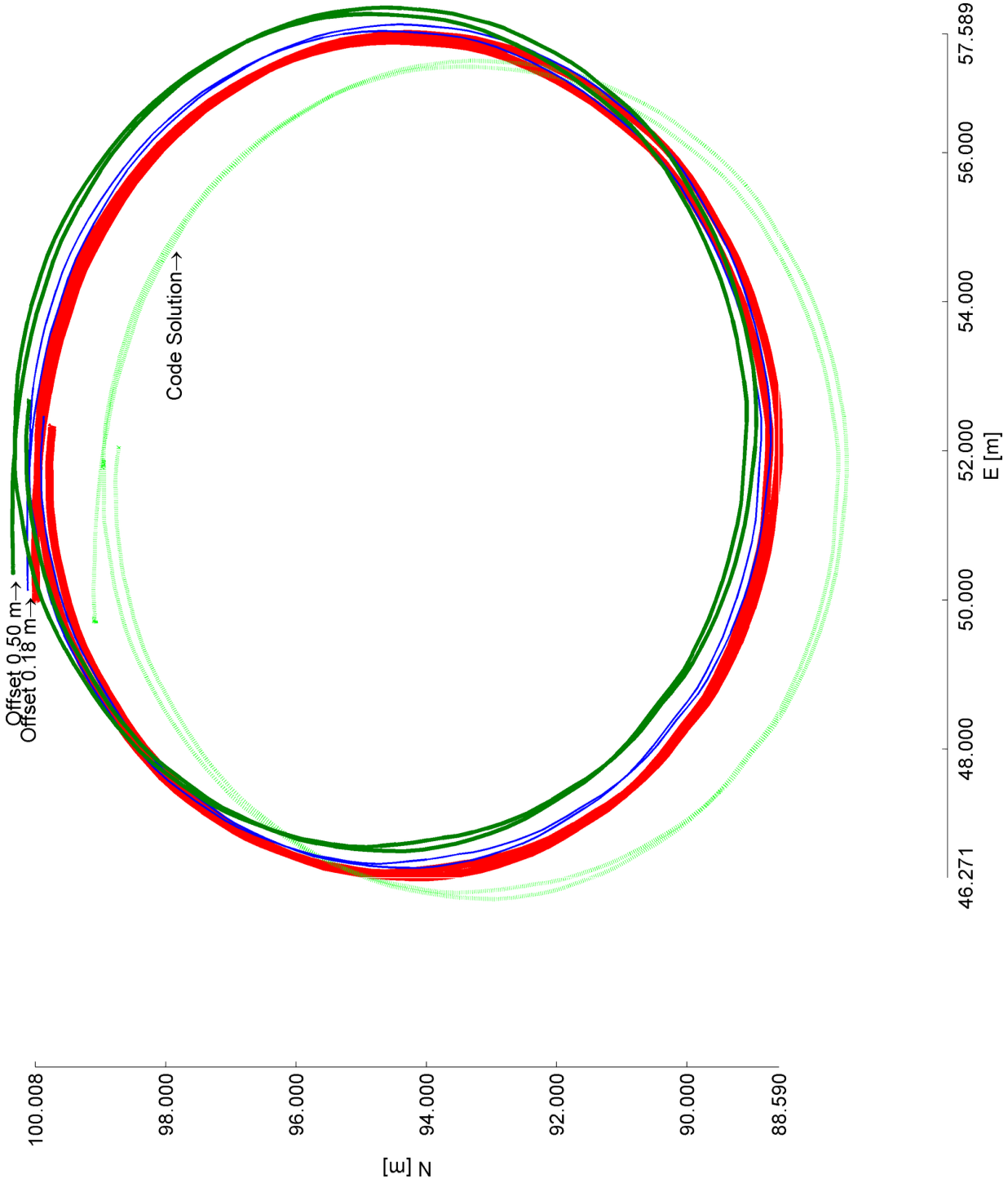

Figure 5.4 – KPI kinematic scenario results

The coordinates are on the local grid (ENH) using arbitrary conversion and without application of a scale factor. True trajectory marked in the thick red. For readability only two offsets and the code solution are shown.

Applied Offset	Precision			Accuracy	
[m][a]	$\mathbf{SD_E}$[m]	$\mathbf{SD_N}$[m]	$\mathbf{SD_H}$[m]	$\mathbf{d_{Planar}}$[m][b]	$\mathbf{d_H}$[m]
0.000	0.001	0.030	0.001	0.004	0.028
0.03[c]	0.001	0.001	0.004	0.028	0.005
0.18[c]	0.001	0.001	0.004	0.178	0.005
0.18[d]	0.002	0.001	0.004	0.002	0.184
0.50[c]	0.001	0.001	0.004	0.498	0.005
Code[e]	0.018	0.017	0.020	0.934	0.583
100.00[c]	0.002	0.001	0.000	99.998	0.001
400.00[c]	0.003	0.001	0.000	399.998	0.000

Table 5.3 – KPI static results

[a] For clarity only selected results are presented in the table.
[b] $\sqrt{(d_E^2 + d_N^2)}$
[c] Planar offset: $d_E = d_E + \sqrt{2}$ offset and $d_N = d_N + \sqrt{2}$ offset.
[d] Height offset: $d_H = d_E + offset$.
[e] These results are consistent for all applied offsets.

vehicle's path. The code solution is visibly shifted with epoch-to-epoch positioning noisy at all times. Resulting position offset does not include TimeLoc errors, as the transmitters were synchronised with the correct coordinates[11].

The simulations presented in above section demonstrated that KPI accuracy metrics are unreliable and another method has to be present to provide the accuracy estimation. On other hand, in the kinematic scenario, KPI provides accurate relative, epoch-to-epoch, positioning. This method can also absorb a transmitter's positional errors, which is an advantage, should the positional accuracy of the Locata antennas be lower than expected. This can find a direct application in bridge monitoring, or similar applications where relative positioning is more important than the absolute positioning. Yet, for the integrated system such an approach is not acceptable and would lead to unexpected biases.

5.3 Observational noise

Noise can be generated either by the system itself (hardware delay, heat) or other systems (interference) and environmental effects (atmosphere effects, heat, scattering, multipath[12]). The sum of these effects is described as thermal or observational noise respectively. This noise should be detected, and if possible quantified, due to its effect on positional fix.

[11] This is especially relevant for the master (LL1), as this offset would affect all units in the network.
[12] Multipath has been covered in detail in section 4.8 on page 61.

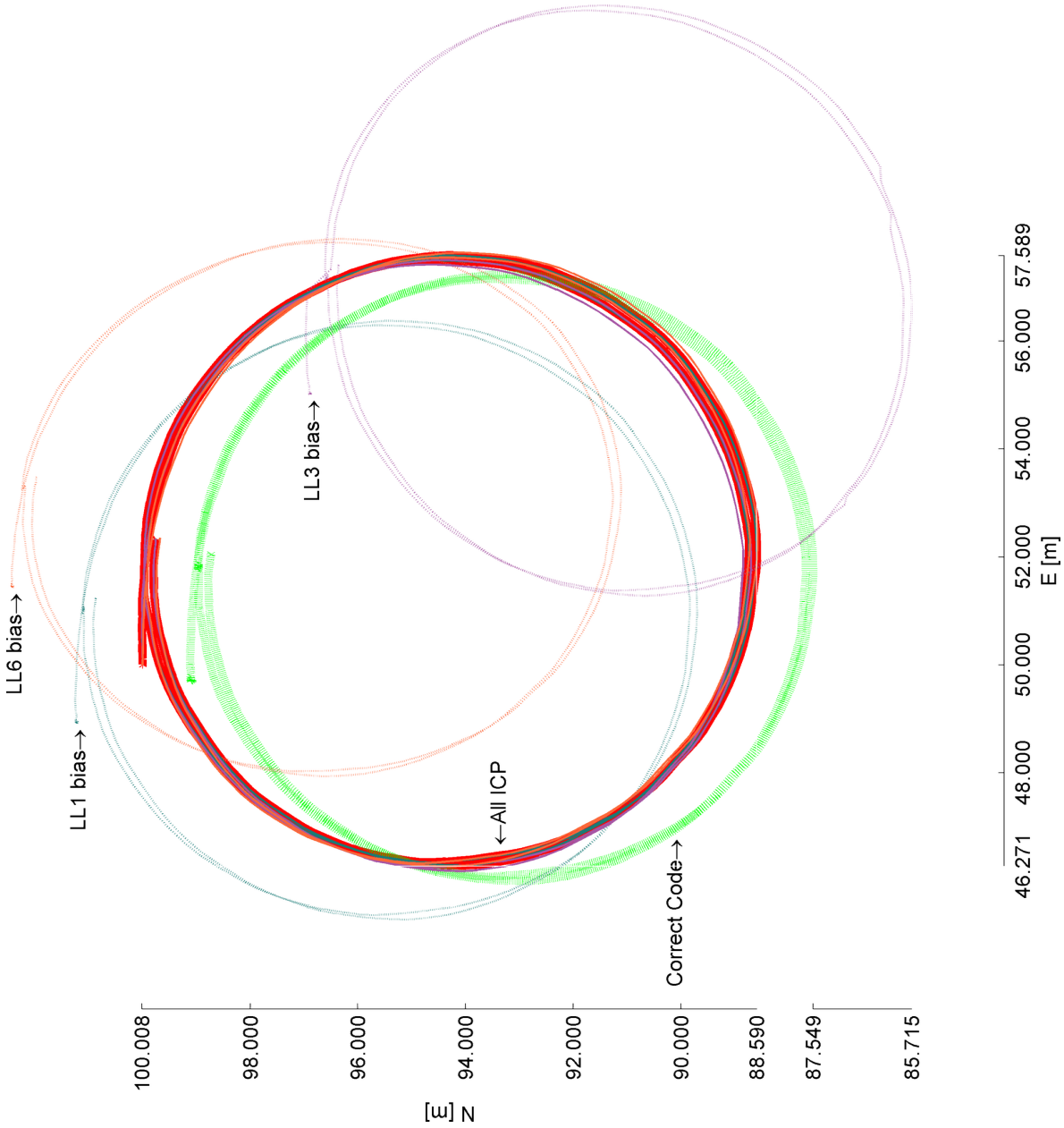

Figure 5.5 – Transceiver coordinates error, true position marked in the thick red

Offset of 20 m was applied to the Tx_{A-B} antennas of either LL1, LL3 or LL6. True trajectory is marked in the thick red, unbiased code solution in green. KPI integrated carrier phase solutions are indicated as ICP.The coordinates are on the local grid (ENH) using arbitrary conversion and without application of a scale factor.

Detection using geometry characteristics

Locata geometry is known, or easy to estimate, and so it can be used to identify the source of the noise by calculating difference between **a-priori**[13] and **a-posteriori**[14] results (Bonenberg, Hancock and Roberts, 2010; Bonenberg et al., 2009). As the height determinant of Locata fix is clearly weaker than the planar determinant, this problem can be reduced to the solution of 2D error ellipses. These are defined by the semi-major and minor axes (a, b) and azimuth (α), and calculated from the symmetric covariance-variance matrix Q using equation 5.2 below:

$$Q = \begin{bmatrix} \partial_E^2 & \partial_{EN} \\ & \partial_N^2 \end{bmatrix} \tag{5.1}$$

$$\begin{aligned} a = \quad \sqrt{\lambda_{max}} &= \sqrt{1/2(\partial_E^2 + \partial_N^2 + \sqrt{\partial_E^2 - \partial_N^2 + 4\partial_{EN}^2}} \\ b = \quad \sqrt{\lambda_{min}} &= \sqrt{1/2(\partial_E^2 + \partial_N^2 - \sqrt{\partial_E^2 - \partial_N^2 + 4\partial_{EN}^2}} \\ \tan\alpha \quad &= \frac{\partial_{EN}}{a - \partial_E^2} \end{aligned} \tag{5.2}$$

Not all deviations from the **a priori** are indicative of a bias, due to the inherent accuracy of the method. It is important to compare not only the ellipse's orientation α; but also its shape, as defined by its eccentricity e. Consequently, we can assume that the bias should affect the Eastings and Northings equally, hence **a posteriori** results should present smaller values for e and similar values for α. Differences in both indicate the likely presence of noise. This method is not suitable for GPS, as the satellites are in constant motion, but could be a part of the integrated system, to avoid undetected bias.

Locata signal quality indicators

Apart from observables, Locata records an number of signal quality related datasets, which can be used to assess the presence of noise on the channel, as well as for detecting interference. The data falls into two types:

- The quality of the received signal, estimated by the Signal-to-Noise-Ratio (SNR) and the Receiver Channel Power Indicator (RCPI)[15];
- Correlator by-products, which are capable of detecting nose, In-phase and Quadraphase components (I&Q)[16] and Low-Correlator-Output Events (LCOE)[17] as identified by Khan et al. (2010).

I&Q indicate the signal lock and if the phase lock loop is successful, I signal will be at maximum (signal plus noise) and the Q signal will be at minimum (containing only noise). Therefore, a simple Costa

[13] **A-priori** is based on known geometry, and calculated using minimally constrained LSA (holding one point and the azimuth fixed). A free version of COLUMBUS software (Best-Fit Computing, nd) was used, with Locata observations treated as single, centimetre-level, distance measurements.

[14] **A-posteriori** is estimated from the recorded data, by calculating the standard deviations.

[15] Provides an estimation of received signal power, as observed by the rover. Some authors refer to it as the Locata Signal Strength Indicator (LSSI). It has been introduced with firmware version v.4.0.

[16] In-phase and quadraphase components of the carrier stripped received signal (Kaplan and Hegarty, 2006).

[17] A count of all correlator lock problems within the epoch.

Loop discriminator can be used, as per equation 5.3

$$CP_k^i = 10 \log_{10} \sqrt{(I_k^i)^2 + (Q_k^i)^2} \tag{5.3}$$

Analysis suggests that I & Q values are not accumulated throughout the epoch, but provided as snapshots of particular state, making it less useful for analysis. LCOE is one of two flags used to identify interference on a particular channel, it provides a running count in the particular epoch. A logarithmic scale is most useful for analysis of LCOE. In the author's experience, SNR values are unreliable for heavy noise, but bearing this in mind, they can still be used for overall scenario analysis. Correlator-based information is not described in official documentation. In combination with RCPI it can be used to estimate quality of received signal i at epoch k using equation 5.4

$$QI_k^i = \frac{RCIP_k^i}{SNR_k^i} \tag{5.4}$$

Interference and indoor noise

The above methods were used to analyse A-D (see section 5.1, page 67). Although they are not of equal duration, this is not a factor with highly correlated observations. Based on the environments described, noise should be more prominent in scenarios C&D.

	a priori				**a posteriori**				**HDOP**	**LL**	$\triangle_{\boldsymbol{\alpha}}{}^a$	$\triangle_{\mathbf{e}}$
	$\mathbf{a}$[m]^b	$\mathbf{b}$[m]	$\boldsymbol{\alpha}$[°]	$\mathbf{e}^c$	$\mathbf{a}$[m]$^{5.2}$	$\mathbf{b}$[m]	$\boldsymbol{\alpha}$[°]	$\mathbf{e}^c$				
A	0.020	0.009	108	0.89	0.006	0.005	117	0.55	0.8	10	-9	0.34
B	0.021	0.015	173	0.70	0.025	0.022	142	0.47	1.3	4	31	0.22
C	0.024	0.012	134	0.87	0.031	0.006	127	0.98	1.6	5	7	-0.12
D^d	0.022	0.013	27	0.81	0.049	0.015	180	0.95	1.2	6	27^e	-0.15

Table 5.4 – Comparison of **a priori** and **a posteriori** Locata error ellipses at 95% (2σ) confidence level

[a] Estimated minus observed.
[b] As per equation 5.2.
[c] Eccentricity $e = \sqrt{\frac{a^2-b^2}{a^2}}$ $e \in (0,1)$ for an ellipsoid and $e = 0$ for circle.
[d] Best results presented. For more details see section 5.3.
[e] $\pm\pi$ as it is impossible to recognise an exactly reversed ellipsoid.

Table 5.4 demonstrates that neither orientation nor Horizontal Dilution of Precision (HDOP) will identify noise by itself. Changes to α and a reduction in e correctly identify noise in multipath environments C&D. Unfortunately, is it not possible to directly quantify the amount of noise using these methods.

Khan (2011); Montillet (2008) demonstrated that with firmware version v.2.4, or in a laboratory environment, devices utilising wireless communication protocol IEEE 802.11 (commonly known as

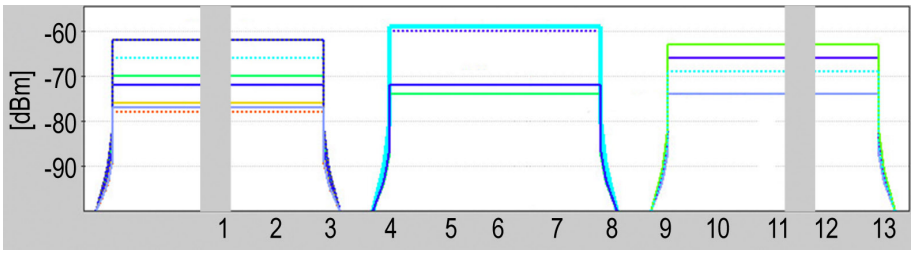

Figure 5.6 – NGB inSSIDer (MetaGeek, 2005) WiFi scan showing channel use, Locata S1 & S6 frequencies marked in grey

WiFi) are the greatest source of interference to the Locata signal. This is due to a direct frequency overlap (see figure 5.6, page 78), which is more prominent for the S6 frequency, where two channels are overlapped. These findings can be confirmed by an analysis of the data collected in the indoor scenario D, where a number of WiFi hotspots were present[18].

To quantify the effect of this interference, the Case I study from section (5.1 on page 67), has been divided into two datasets, based on wireless network activity[19]. Day data (08:00-18:00) has been identified as a period of active usage while Night (21:00-07:00) is a period of very intermittent and low usage. A buffer time was introduced to remove any bias.

Figure 5.7 on the facing page, compares the SNR, CP and LCOE values for the two scenarios over two frequencies. Both CP and LCOE are presented in logarithmic scale (dBm). For clarity, only the average SNR and LCOE for each epoch is presented. In the case of CP a maximum value is used.

The S1 and S6 SNR for both scenarios are similar, with visibly weaker S6, probably due to the two WiFi channel overlap. CP values look similar in scale and frequency. For clarity, the LCOE graph presents only Day dataset absolute values for S1 &S6, showing only the difference between the night and day scenarios for each frequency. Results agree with the SNR results.

A comparison of positional accuracy for both scenarios[20] (presented in table 5.5 on page 80), shows negligible accuracy ($\mathbf{d}_\bullet$) and precision ($\mathbf{SD}_\bullet$) difference, which confirms the previous findings.

These results are not conclusive, as a number of factors, such as people movement, KPI, and multipath could not be quantified. However, it does indicate that WiFi interference is tenable - the actual effect on the fix seems negligible. It also provides evidence of Locata's ability to detect and identify problems, thus making the system capable of self-monitoring, vital to an integrated system set-up.

Spoofing

The weak transmission power of GNSS signals makes them more vulnerable to any accidental or deliberate interference (Davis et al., 2012; Shepard et al., 2012). Utilisation of known terrestrial signals, with much higher transmission power levels[21], can be used to provide an additional layer of information, thus making spoofing attacks much more difficult (Scott, 2012). This is not to say that Locata cannot

[18] Identified WiFi signal power was below −60 dBm.
[19] This estimation, based on overall use of the network, has been provided by the University of Nottingham IT team.
[20] Introduced in Montillet (2008).
[21] Locata transmits at 23 dBm. In comparison the GPS signal does not exceed −130 dBm.

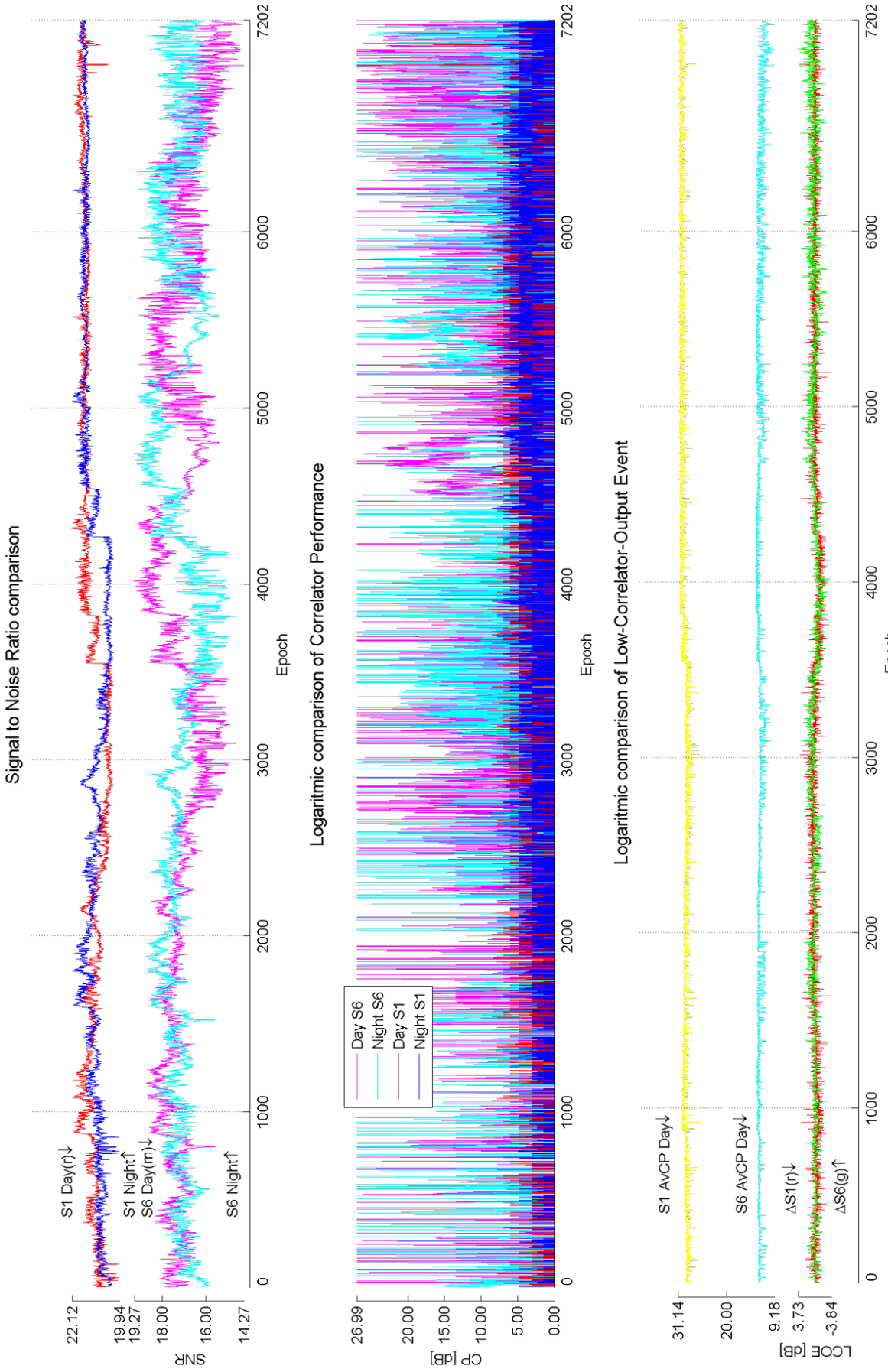

Figure 5.7 – Parametric quantification of indoor noise (scenario D)

Scenario		SD_E	SD_N	d_E	d_N	[m]
Day	**h0**[a]	0.007	0.006	0.010	-0.003	
	h3[b]	0.005	0.004	0.006	-0.005	$\triangle \mathbf{d_p}$[c]
Night	**h0**[a]	0.007	0.006	0.008	-0.009	-0.002
	h3[b]	0.006	0.004	0.008	-0.004	-0.001

Table 5.5 – Comparison of day and night positional results

[a] LINE no signal selection post-processing option. (See section 3.1 on page 36 for more details).
[b] LINE signal selection based on SNR post processing option. (See section 3.1 on page 36 for more details).
[c] Difference in accuracy, $\sqrt{(d_E^2 + d_N^2)}_{night} - \sqrt{(d_E^2 + d_N^2)}_{day}$.

be spoofed, as its PRN characteristics are publicly available (Locata Corporation Pty Ltd, 2011a). Yet the static nature of transmitters allows better detection of such attempts, using the methods described above.

5.4 Cycle-slip detection

Cycle-slips are caused by observation noise, and occur when the beat phase (the difference between the satellite-transmitted carrier and the receiver-generated replica) is interrupted, and the phase ambiguity count has to be reinitialised. This will cause as a jump in the estimated position of the rover, roughly equivalent in magnitude to an integer number of cycles (Hofmann-Wellenhof et al., 2008). Cycle-slip detection uses analysis of ICP measurements. Locata transceivers, with their cluster of four signals each, use two methods of identification:

- The single-frequency method from firmware version v.2.4, which requires double differencing of the signal with respect to time over at least four epochs of data ($i \ldots i+3$), but only on a single frequency.

$$\frac{\delta^2 \phi_k^{Tx}}{\delta t^2} = (\phi_{i+3}^j - \phi_{i+2}^j) - (\phi_{i+1}^j - \phi_i^j) \tag{5.5}$$

  Each signal is analysed separately, initially providing two, and later four equations (Montillet, 2008).

- The single difference of all signals in respect to time, which produces six equations (Bertsch, 2009), and can identify a single multipath/interfered signal. This method is only possible with dual frequency systems.

$$\frac{\delta \phi_k^{Tx}}{\delta t} = (\phi_{i+1}^{j+1} - \phi_{i+1}^j) - (\phi_i^{j+1} - \phi_i^j) \tag{5.6}$$

In equations 5.5 to 5.6 on this page, i$\in \mathbb{Z}$ and j$\in$A-D, ϕ_k^{Tx} is a shorthand equation describing carrier-phase measurements between the receiver and the transmitter at epoch k using the Tx frequency (see equation A.5, page 138)[22]. The single-frequency approach, from equation 5.5, removes the polynomial clock, but strongly amplifies the noise. The dual-frequency approach, implemented in LINE (see equation 5.6, page 80) removes both the clock bias and common multipath between frequencies. As discussed in section 4.4 on page 51, each differencing increases observation noise, by $\sqrt{2}$, as demonstrated

[22] In LINE settings can be fine tuned by changing *SignalQuality_MaxIcpDeltaDiff*.

in figure 5.8. Both methods can determine the presence of a single multipath signal. If more signals are affected, multipath cannot be determined, as shown in previous section, but due to antenna spacial separation this is very unlikely. The case of multiple signal cycle slips is more difficult, and additional determination methods will be required. The example from section 5.1 on page 69 shows Locata reduced capacity to detect and mitigate cycle slips in a small-sized network.

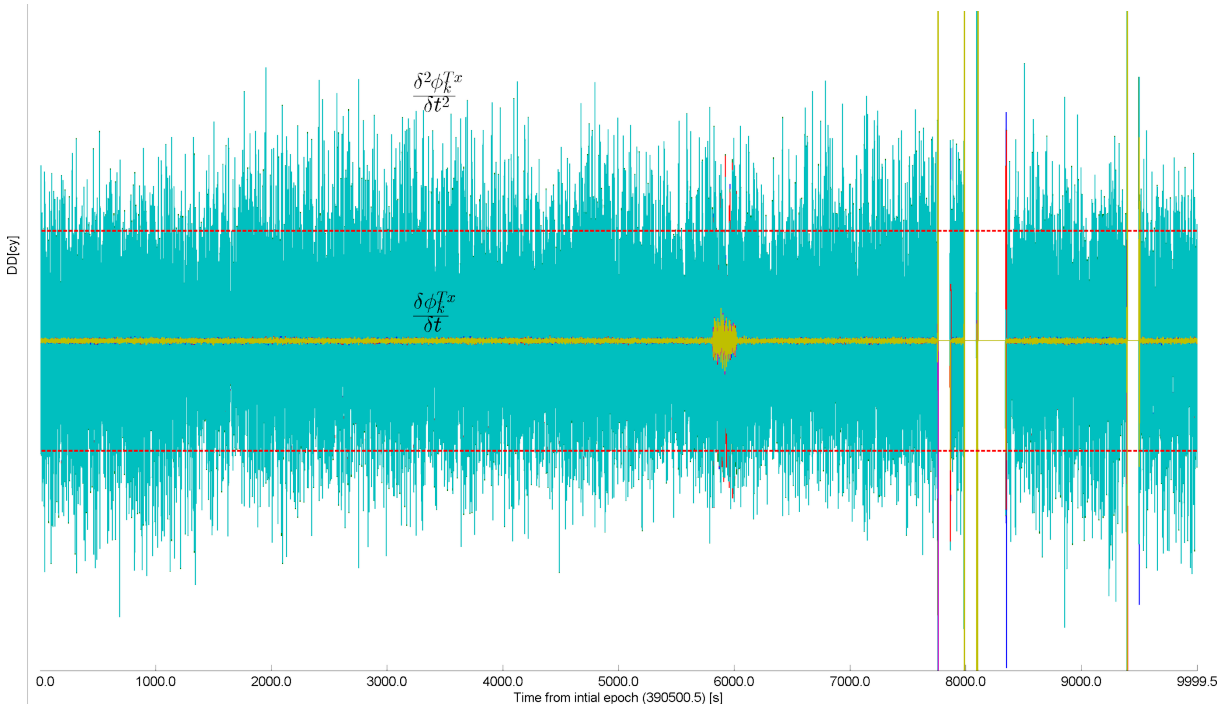

Figure 5.8 – A comparison of Locata cycle slip detection methods, based on dataset from section 7.3 on page 113

5.5 Summary

This chapter discussed known point initialisation (KPI), currently the only method of solving Locata float ambiguities. Over-optimistic static results were discussed, followed by a detailed analysis of KPI, demonstrating this method's capacity to at least partially mitigate the problems of persistent noise and multipath, as well as the biases in both the rover's initial position and the transceivers' positional biases. An improvement in kinematic fix was also presented.

Two methods of noise and interference detection were discussed towards the end of the chapter. Finally, WiFi interference and cycle-slip detection methods were described.

♣ ♢ ♣

6 Practical integration

"An expert is a man who has made all the mistakes which can be made, in a narrow field."
Niels Bohr

THIS chapter will focus on the results of integrating the two systems. Beginning with a discussion of the novelty of the solution, it will then cover algorithm and software development. This includes a detailed description of the workflow, calculation details and Ambiguity Resolution (AR). The chapter finishes with a discussion of the results and recommendations for future work.

Some of the work presented in this chapter has been previously published in Bonenberg, Roberts and Hancock (2010b, 2011); Bonenberg et al. (2012).

Contents

ENGINEERING work demands centimetre-level positioning, and both GPS and Locata can offer this, albeit with a number of limitations. Locata uses a method known as Known Point Initialisation (KPI), for mainly 2D fix (planar positioning), due to the co-planarity of transmitters. On the other hand, GPS accuracy and availability depend on satellite geometry, and open-sky visibility, with a weakened height component[1]. Section 4.2 on page 46 demonstrates that these limitations can be mitigated, if both systems are used simultaneously.

Lee et al. (2008); Meng et al. (2004); Yang et al. (2010) demonstrated the advantages for accuracy and availability, of combining pseudolite and GPS signals. Yet until now, only one loosely-coupled Locata/GPS integration system has existed - Leica Geosystems Jigsaw360[2]. Other published integration (Lee et al., 2008, 2004; Rizos, Grejner-Brzezinska et al., 2010) did not cover Locata ambiguity estimation, assuming that it would be solved outside of the extended Kalman Filter (EKF)[3]. This shows the novelty behind the closely-coupled Locata/GPS integration proposed in this thesis. The approach does not require hardware integration, but as all signals are used, it offers significant advantages over the current loosely-coupled approach as listed below:

- AR is attempted on-the-fly (OTF), on a moving platform,
- a mitigation, at least partly, of the open sky requirement for GPS,
- an improvement in geometry and overall provision of 3D fix for Locata,
- the combined ambiguity resolution (AR) of both systems,
- the utilisation of all signals[4].

Combined ambiguity resolution (AR) is essential to its OTF capacities. The novelty of the current approach lies with the utilisation of **double differencing** for GPS and **single differencing** for Locata respectively, to create a combined AR using LAMBDA. Previous research used either double differencing (Lee et al., 2005), or LAMBDA for Locata-only, using simulated data (Bertsch, 2009)[5]. The proposed approach (see section 4.2, page 46) requires a total of five signals, with a minimum of two coming from each component, to provide a 3D fix.

6.1 Algorithm development

To reduce complexity, and allow the separate assessment of each component, the integration research was conducted in stages (as shown in figure 6.1). The main difference between the stages was the use of simulated and real-time data. Consequently, only the **Final Design** implemented a fully working Locata and GPS navigation engine capable of using real life data; single differencing ($\triangle$) for Locata, and double differencing ($\triangle\nabla$) for GPS.

[1] GPS vertical accuracy is 1.2 – 2.0 times worse than the planar one.

[2] The system is actively deployed in the South Australia Boddington Gold Mine, with a Locata-only solution (after GNSS RTK initialisation), where 95% of results are within 10 centimetre horizontal and 20 centimetre vertical accuracy (Barnes, LaMance et al., 2007; Carr, 2012).

[3] Recent hardware changes (see table E.2, page 160) offer a geometry-based OTF AR, but it is not commercially available.

[4] The current loosely-coupled GPS/Locata integration can only utilise signals from one device at a time (see figure 4.1, page 46).

[5] New Locata hardware with firmware version v.7.0 is expected to solve Locata AR using EKF. This approach is similar to Bertsch, Choudhury, Rizo and Kahle (2009), as discussed in appendix C.1 on page 145.

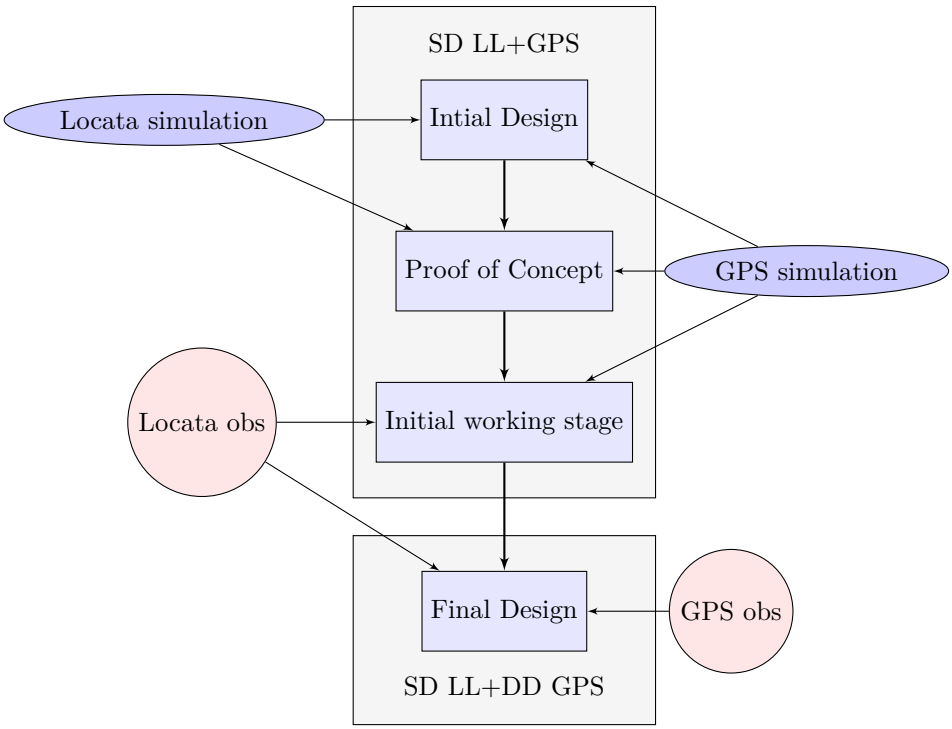

Figure 6.1 – Navigation engine software development stages

Initial design

Due to the static nature of Locata transceivers, any geometrical change has to be effected by the rover, hence any OTF AR has to be kinematic, as demonstrated by Bertsch (2009). Developing this concept, the author simulated a number of different AR scenarios. For a positional solution, both pseudo-range and integrated carrier phase (ICP) have been used, using only T_{xA} for Locata and L1 for GPS. Observations had varied levels of white noise applied, but were otherwise free of any residual biases. Phase centre offset (PCO) for both was assumed to be the same.

The navigation algorithm used a variable number of epochs for a multi-epoch solution, with all epochs re-calculated once float ambiguities had been estimated. Single differencing ($\triangle$) was used on both Locata and GPS, but this is not feasible for true GPS data. The initial design was intended to verify:

1. The most suitable method of calculating float ambiguities, using:

   a) single difference, multi-epoch results, with an initial position estimated from the pseudo-range or prior epoch results,

   b) single difference, multi-epoch results, with every position estimated from pseudo-ranges and with a 3 – 10 epoch overlap between each assignment.

2. The new quality indicator for each epoch, based on a observation matrix A

$$QI_A = \frac{1 - max(D)}{min(D)} \tag{6.1}$$

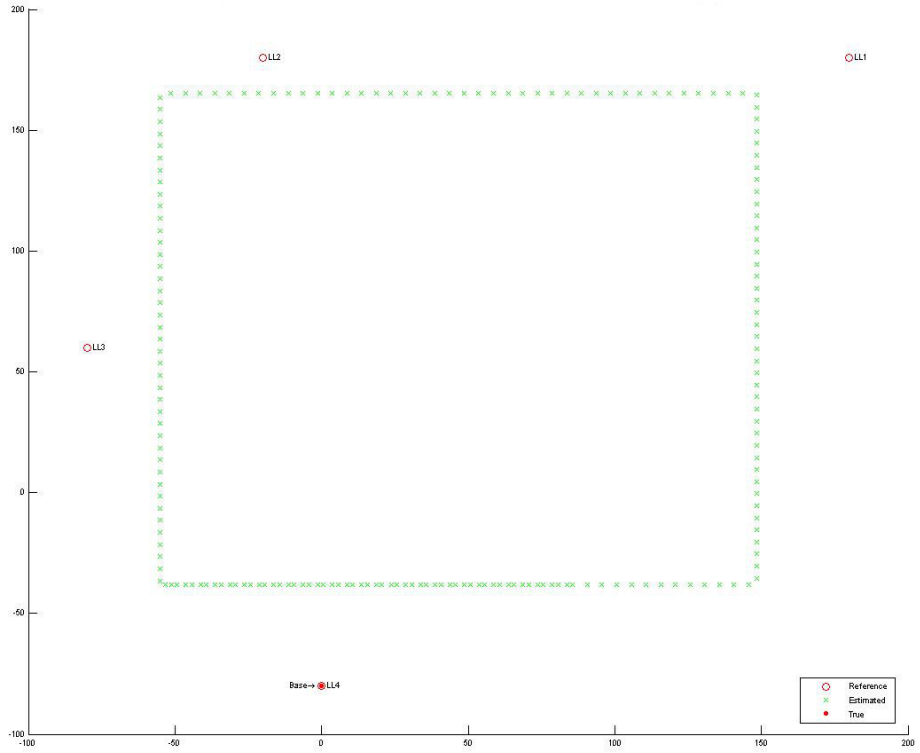

Figure 6.2 – Initial Design simulation showing rover trajectory and the location of Locata transceivers

where D is an eigenvalue of $A^T PA$. This approach would ensure that unsuitable epochs could be excluded from the calculation (see figure 6.3, page 86).

3. The most suitable selection method for the double difference base unit to be used for single differencing ($\triangle$):

   a) the differencing is always conducted against the Master unit,

   b) using the available epoch geometry indicators to select the suitable unit for every epoch.

4. Locata height fixing based on an a-priori knowledge of rover height (Amt and Raquet, 2006).

Conclusions from this pilot study demonstrated that:

1. Geometry change is vital for the AR and is directly related to the strength of matrix A. Epoch overlap limits geometry, and creates strongly correlated results, although there are higher computation costs. A much more efficient approach is to eliminate weak epochs based on the matrix A estimation.

2. There is a visible correlation between QI_A and solution strength, but direct implementation would largely reject the Locata height component, disregarding geometrical advantage. In order to implement this feature, an a-posteriori statistical model, most likely in the form of a Kalman filter is essential. As discussed below, such implementation was not feasible at this stage;

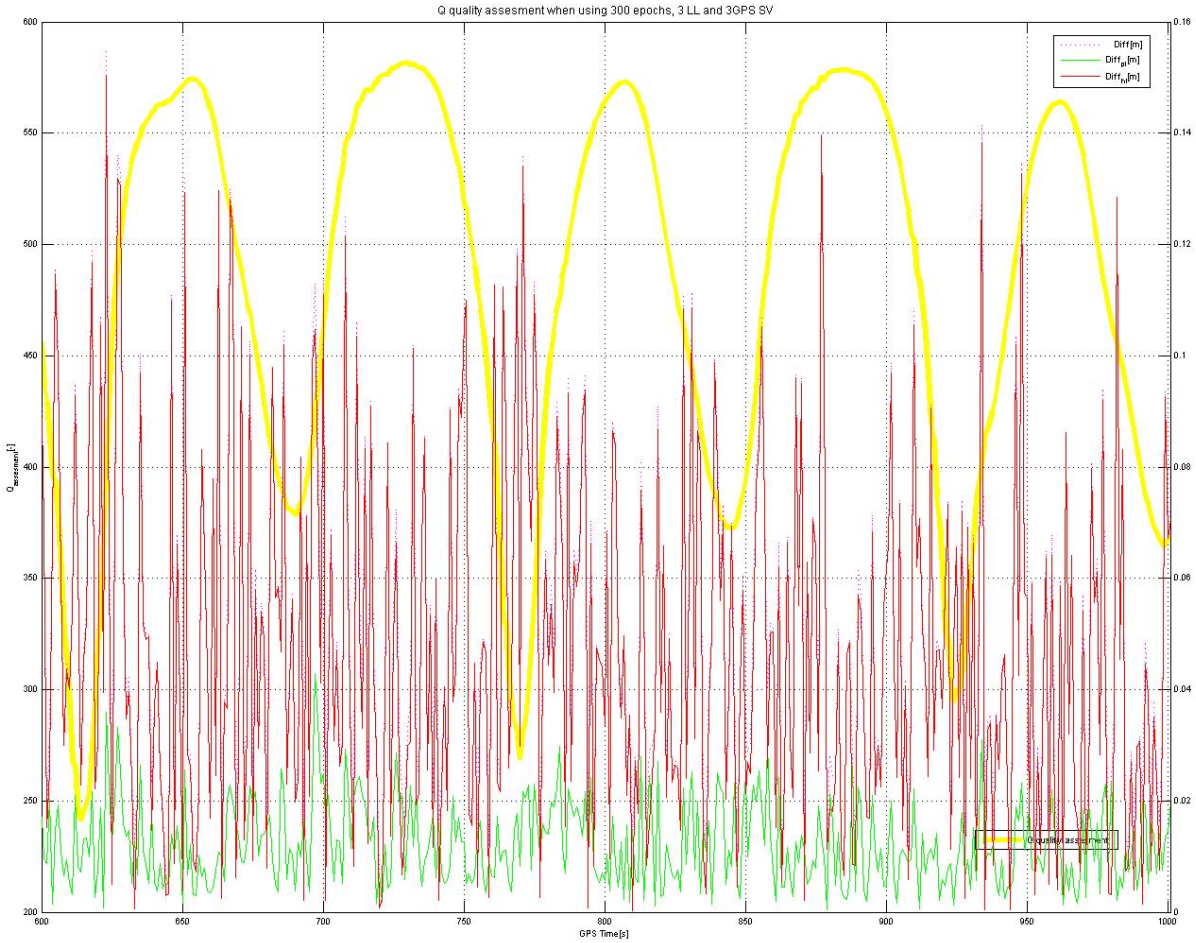

Figure 6.3 – Correlation between QI_A and fix solution accuracy

3. As TimeLoc is the largest error factor in single differencing ($\triangle$) (see section 4.4, page 50), it is advisable to calculate the difference against the Master, even if geometry would favour another unit.

4. Combined GPS/Locata geometry improves height definition; similar results were observed in previous research (Lee et al., 2008; Meng et al., 2004), therefore height fixing was not implemented.

Proof of concept

Proof of concept was conducted using the existing Locata network on the Nottingham Geospatial Institute Open Sky Roof Laboratory. The small size of the network (see figure F.2, page 162) was an advantage, as any change in geometry was exaggerated. The navigation engine, from figure 6.4, uses LSA for float estimation, and single difference was calculated against the Master. Three multi-epoch solutions, with weights based on the symmetric covariance-variance matrix Q, were used to estimate the best AR[6]. Data for both components was simulated at 1 Hz - Locata by Matlab script, and GPS by Spirent GSS8000.

[6] Detailed description can be found in section C.1 on page 145.

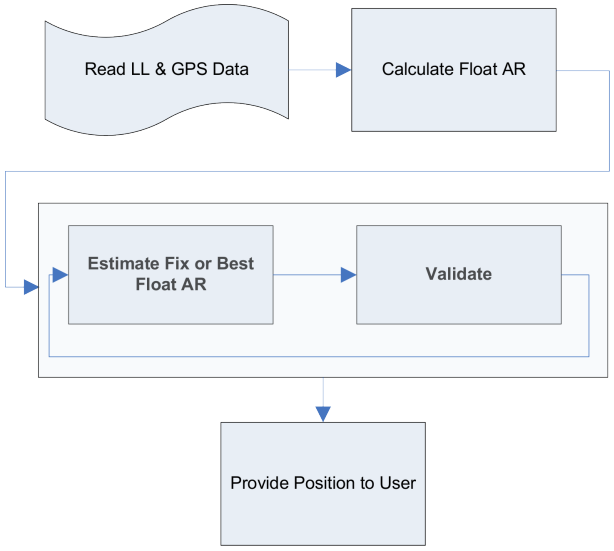

Figure 6.4 – Proof of Concept algorithm workflow

No of LL	**No of GPS**	e_n [a]	$\mathbf{d_{planar}}[\mathrm{m}]$ [b]	$\mathbf{d_{Ht}}[\mathrm{m}]$ [c]
6	6	50 [d]	0.006	0.016
2	4	50 [d]	0.056	0.188
3	3	50 [d]	0.314	3.317
6	0	100	0.251	0.054
2	4	100	0.029	0.127
3	3	100	0.071	0.467
6	6	200	0.006	0.020
3 [e]	3	200	0.013	0.061
0	9	100	0.080	0.132

Table 6.1 – Proof of Concept results for multi-epoch Locata and GPS integration using simulated data. Highlighted rows indicate a minimum signal solution.

[a] Number of the initial epoch used for each multi-epoch solution. Ambiguities were solved using three such sets.

[b] Average planar kinematic difference from 1000 epochs (seconds). Note that only $3e_n$epochs have been used to solve ambiguities.

[c] Average height kinematic difference from 1000 epochs (seconds).

[d] Only 500 epochs have been used to calculate the difference, as the solution failed.

[e] Figure 6.5 on the next page, shows graphical representation of those results.

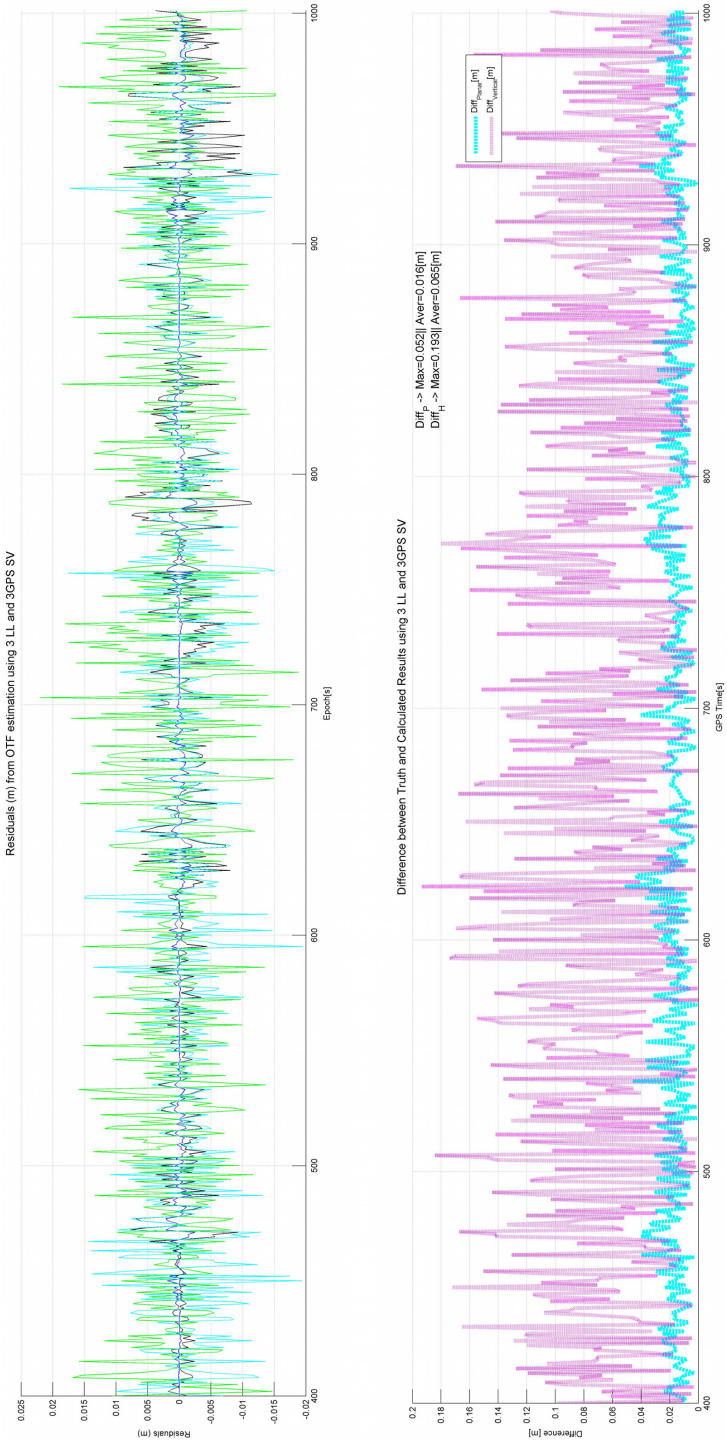

Figure 6.5 – Proof of Concept AR results – LL3+GPS3, 200 epoch solution, compare with table 6.1 on the preceding page

As more realistic geometry and environmental constraints were applied, the number of epochs required for centimetre-level solutions increased, in comparison with Initial Design results (see table 6.1, page 87). Low signal visibility scenarios (3+3) required 100 epochs[7] for the centimetre-level planar solution and 200 for the vertical solution. These kinematic results are comparable to real-world KPI Locata performance (see table 5.2, page 70), and in addition, provide a 3D fix and OTF float ambiguity estimation. The weak GPS-only solution highlights the limitations of the navigation model. This is also visible in the unnaturally weakened height solution, once number of GPS signals exceeds Locata signals. Those trials have been published in Bonenberg, Roberts and Hancock (2010b).

Initial working stage

Observations simulated for the Proof of Concept stage had white noise applied[8] but did not include the following principal sources of error (as discussed in chapter 4 (page 44)):

- orbital and clock errors,
- signal transmission errors due to atmospheric conditions,
- receiver errors,
- noise and multipath errors.

In order to obtain a centimetre-level fix, differencing is needed[9] to eliminate receiver and satellite clock biases, orbital errors and atmospheric delay[10]; this comes at the cost of an increase in observation noise, and does nothing to mitigate the receiver-specific noise and multipath (Hofmann-Wellenhof et al., 2008). The current algorithm requires co-location of Locata and GPS PCO, so the Numarela Test Facility (NTF)[11] dataset, collected using the combined Locata/GPS antenna[12] was used. This introduces a more realistic geometry change, but also made obtaining the true trajectory more difficult[13]. At this stage only real life Locata data was introduced, as the GPS component of the navigation engine was not capable of GPS double differencing.

Given the above, it is difficult to compare these results with the previous stage. Statistically, results in figures 6.6 to 6.11 on pages 90–96 are slightly more noisy and Locata only AR (see figure 6.7, page 91) shows the same accuracy oscillation as observed in Bertsch et al. (2009); J. Wang, Tsujii, Rizos, Dai and Moore (2000); J. J. Wang et al. (2004), due to a weak vertical component.

Navigation engine design

An important decision between implementing fully working navigation engine, with GPS double differencing and proper ambiguity resolution (AR) was to choose between a Least Squares Adjustment (LSA) and an Extended Kalman Filter (EKF).

---

[7] Equivalent to 100 seconds.

[8] Noise was 0.3 – 2 m for pseudo-range and 0.01 – 0.1 m for ICP.

[9] Details are discussed in section 4.4 on page 51.

[10] Baseline length should not exceed 10 km. Rover and base should have similar elevation.

[11] Collected using Locata rover firmware version v.4.0 and Leica 1200 dual-frequency GPS receiver, both as the rover and the base station, both were located within 5 km.

[12] Presented in figure 6.9 on page 93. More information can be found in section 3.1 on page 33.

[13] The truth was obtained from a combined Locata and GPS solution 4.1 on page 45. While this produces a very good approximation, it lacks the assurance of Nottingham Geospatial Institute Open Sky Roof Laboratory.

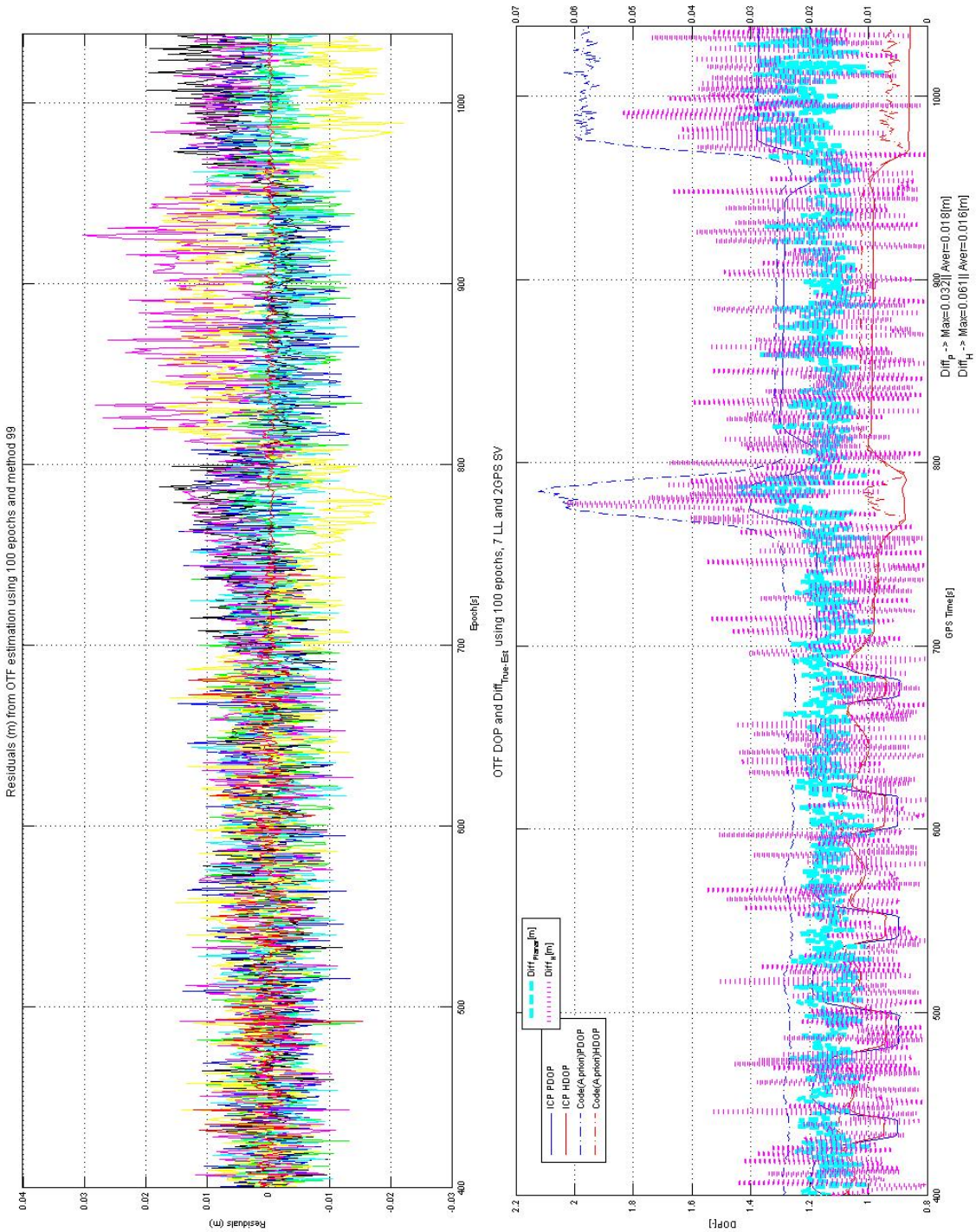

Figure 6.6 – AR using simulated GPS and real Locata data, LL7+GPS2, 100 epoch solution

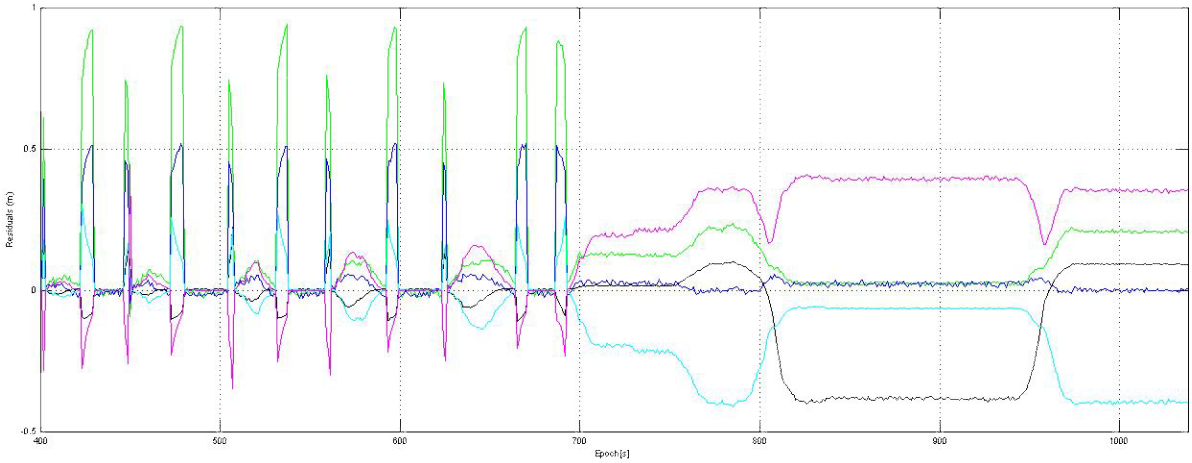

Figure 6.7 – AR using real Locata data only, LL6+GPS0, 100 epoch solution, with visible oscillation effect

While LINE, the Locata navigation engine, is still using LSA[14], Rizos, Grejner-Brzezinska et al. (2010) used an EKF, with Locata initialised via KPI. The EKF is a recursive, predictive algorithm, using a system dynamics model to compute the state estimate[15]. This can be a big advantage for multi-epoch ambiguity estimation, as long as observation noise (error) is properly modelled, and a time synchronisation maintained.

The University of Nottingham POINT Software Suite (Hide, 2009; Hide, Moore and Hill, 2007) is aimed at GNSS-based multi-sensor navigation, using an EKF. POINT uses LAMBDA and wide-line estimation fix Ambiguity Resolution (AR), with a ratio test to verify the solution (Hide, 2009; Hide et al., 2007). Its navigation engine was rewritten to handle Locata single differenced data[16].

The NTF dataset, starts with 366 840 s of static data, followed by a kinematic movement (see figure 6.13, page 99). An attempt to produce a combined Locata and GPS solution was unsuccessful – GPS and Locata observations had been forcing separate state updates due to a time issue, and the current observation model was too weak for an EKF solution.

An EKF solution can be demonstrated by setting EKF to float estimation only, without LAMBDA AR, and using the known point (initial feed). Figure 6.8 on the next page shows the results of this KPI simulation, normalised by subtracting the average value for TxA&C. The imprecision of the observation parameters model used, especially tropospheric delay, is clearly visible when a geometry change is introduced (after 366 840 s). After testing a number of models (Choudhury, 2012; Kleusberg and Teunissen, 1998; J. J. Wang et al., 2005) the conclusion was that without the ability to directly measure the atmospheric conditions, any further work will offer a very limited advantage.

This led to a decision to retain the LSA method; and unlike Bertsch (2009), to use combined ICP and pseudo-ranges in the navigation engine. This was based on Locata pseudo-range performance

[14] This refers to the current version (see section 3.1, page 36). An EKF based navigation engine is to be introduced with firmware version v.7.0 and new hardware, (see section 3.1, page 35).

[15] States are linearly related to the measurements. More details can be found in Grewal et al., 2006; Hofmann-Wellenhof et al., 2008; Kaplan and Hegarty, 2006.

[16] A dedicated C++ front end was handling Locata binary format, to avoid ASCII output restrictions, visible in prior work, and to simplify the conversion. This approach has proven problematic however, as Locata binary format (LBF) was unexpectedly significantly changed with introduction of firmware version v.4.0, v.4.2 and v.5.0.

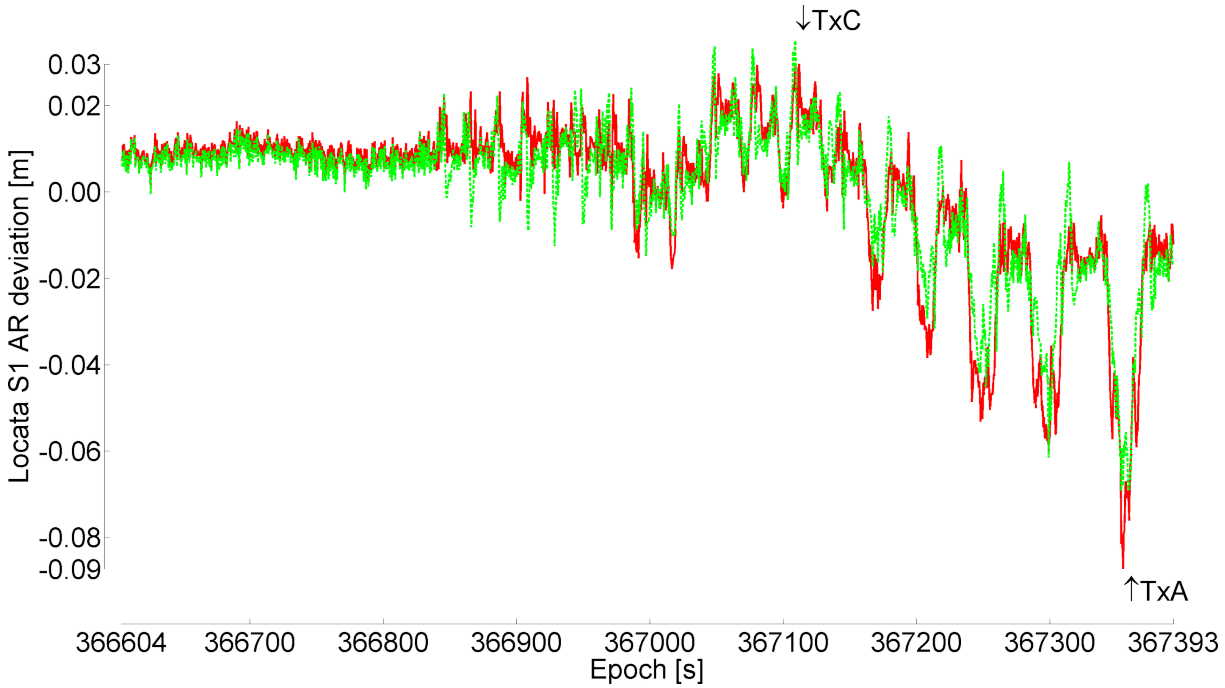

Figure 6.8 – EKF float ambiguity resolution

AR estimations are normalised by removing an average of the ambiguity value.
The first 366 840 s of observation are static.

and optimisation in ambiguity search with a small loss in accuracy as a trade-off. The new Locata hardware and firmware version v.7.0 incorporates an EKF navigation engine, and improved tropospheric modelling, which allows it to use only ICP for the float ambiguity estimates.

Ambiguity resolution

The multi-epoch AR approach estimates float ambiguity, and assuming a precise model, the resulting global minimum will mitigate biases such as: multipath, residual atmospheric effects and satellite orbit error (Kim and Langley, 2000). Estimation of fix ambiguities is a non-trivial problem, with LAMBDA being the preferred choice in previous research (Bertsch, 2009). To justify this, two other methods have been considered.

Linear frequency combination: estimates ambiguities in one step, by using a combination of signals, usually wide and narrow lane techniques, which uses the sum and difference of frequencies. This approach is frequently suggested for PPP in view of the increasing number of GNSS frequencies. Drawbacks include a loss of integer nature of ambiguity (Hofmann-Wellenhof et al., 2008). Therefore this approach is of limited use for this research, due to Locata frequency separation being smaller than GPS frequency separation, as seen in table 6.2.

Ambiguity Function Method: (AFM) reduces the computation burden and is insensitive to the presence of cycle slips in the carrier phase observations, while offering a one-stage approach (Cellmer, Wielgosz and Rzepecka, 2010; Han and Rizos, 1996). However, it does require a long initialisation time, and due to a weakened observation matrix, there is an extensive noise build up, leading to lack of fix.

[m]	**GPS**	**Locata**
$f_1 - f_2$	0.862	5.640
$f_1 + f_2$	0.107	0.061

Table 6.2 – Wide and narrow lane combinations for GPS and Locata

LAMBDA uses a mapping function $F : N \subset \mathbb{R} \rightarrow N \subset \mathbb{N}$ to find the most probable fix ambiguities. Introduction of the Z-Transformation, the separation and de-correlation of ambiguities, reduces the n-dimensional integer search space to the ambiguity search ellipsoid (de Jonge and Tiberius, 1996; P. J. G. Teunissen, 2006). This method requires three steps:

- the assessment of float ambiguities and its accuracy,
- the decorrelation of ambiguities and integer search in LAMBDA,
- the update of other unknown parameters using "fixed" ambiguities.

Based on previous results, LAMBDA offers not only the easiest implementation for the current workflow, but was also least affected by observation noise; it also allowed the most flexibility in engine development.

6.2 Final design workflow

The final implementation of the navigation engine used LSA to provide float ambiguities, and LAMBDA for AR. The workflow outlined in figure 6.10 on the following page, and the calculation details can be found in appendix C on page 145.

Figure 6.9 – Combined Locata and GPS antenna used in NTF trials

Reading GPS and Locata observables

The algorithm requires GPS C/A and ICP from L1 and L2[17] and, for Locata, the C/A-like pseudo-range,[18] and ICP on Tx_{A-D}. The GPS observables and navigation message are read from the RINEX file, while Locata data is read from Locata Binary Format (LBF) using a dedicated C++ converter[19]. Currently Locata antenna positions are imported separately, but starting from firmware version v.5.0 they will be read directly from a Locata Binary File (LBF). Locata observables can be used in three ways:

- The creation of a single code and phase observation, from the weighted average of all four signals; leading to a loss of integer nature of ambiguity, but strengthening the observation matrix A.
- The importation and use of all signals, minus those identified as faulty, either due to multipath or noise. A limitation here is currently unresolved in-frequency bias between Rx_A and Rx_{B-D}.
- To use only the Rx_A signal, identified as the most precise one. This method will prevent cycle-slip and multipath detection[20].

To simplify the working integrated solution the third solution was used, which avoids both the loss of the ambiguity integer nature as well as the inter frequency bias. Further exploitation of all signals should improve the performance of the navigation engine.

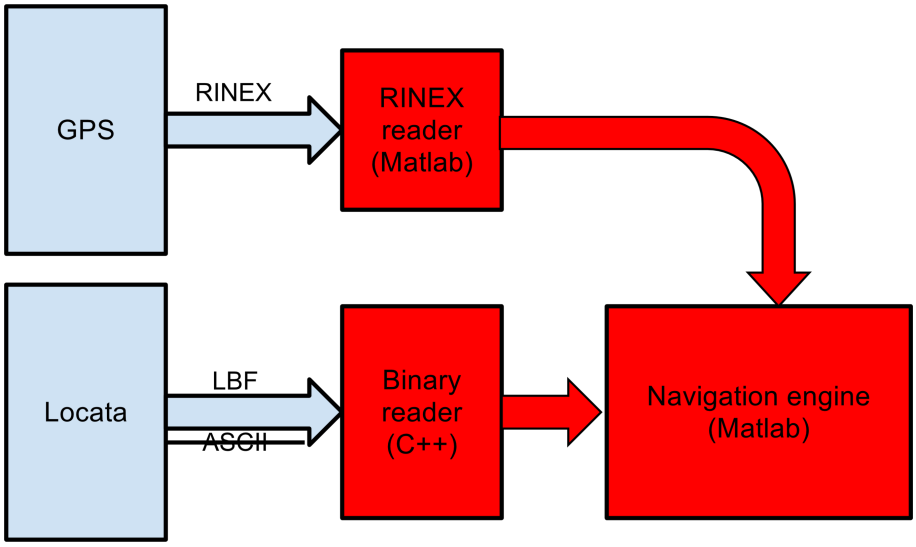

Figure 6.10 – Navigation software details

The Matlab GPS front end uses RINEX to decode GPS observables and to calculate satellite orbits[21]. Apart from orbital errors, due to modelling, the largest errors arise from the clock offset, Earth

[17] For the peculiarities of decoding P(Y) see section 3.2 on page 36.

[18] For a detailed description of Locata C/A implementation see section 3.1 on page 27 and in (Cheong, 2012; Locata Corporation Pty Ltd, 2011a).

[19] If present MET data is also read.

[20] The Locata mechanism has been described in section 5.3 on page 76 and GPS equivalent can be found in Hofmann-Wellenhof et al., 2008; Kaplan and Hegarty, 2006; Leick, 2004.

[21] Using the method described in (Global Positioning System Wing, 2010).

movement and relativistic effects. A simple way to mitigate these effects, is to estimate satellite signal transmission time T^s from the rover time T_{rov} using observed code pseudo-range to this satellite (Pinchin, 2011), as per equation 6.2.

$$T^{SV} = T_{rov} - cP^{SV}_{rov} \tag{6.2}$$

Float ambiguity estimation

The initial position can be estimated from pseudo-range measurements. This can be up to a few cycles away from the true value, as both pseudo-range and ICP are combined to calculate float ambiguity. However, this is close enough to the true value that second and higher orders of the Taylor series expansion can be neglected (Cellmer et al., 2010; Hofmann-Wellenhof et al., 2008). The Locata pseudo-range solution is visibly worse then GPS solution (see figure 6.11, page 96) for the initial AR estimation or search space limitation suggested by Amt and Raquet (2007).

Ambiguity resolution

As LSA float estimate ambiguities are contaminated with noise, and other (not fully modelled) parameters, equation A.5 can be re-written as:

$$\phi^i_A(t_k) = (d\phi^i_A(t_k) + N^i_A)\lambda_i + \epsilon^i_A(t_k) \tag{6.3}$$

LAMBDA AR can be described as finding the optimal mapping function $F : N \subset \mathbb{R} \rightarrow N \subset \mathbb{N}$ in order to estimate integer (fix) ambiguities. To limit the possibility of false positives, the **ratio test** between the first two LAMBDA integer candidates is carried out, assuming a threshold ratio between 1.5 – 3.0 (Hide, 2009; Pinchin, 2011).

Estimation of fix ambiguities for Locata and GPS has proved difficult. While the quality of GPS ambiguities improved, when Locata data was used, Locata ambiguities had to be kept as a float. This led to a modification of the algorithm with only GPS ambiguities estimated in LAMBDA, which were then used to assess Locata ambiguities. This approach can produce false positives in the ratio test, therefore the LOM[22] and a Sigma test, estimating normal distribution of Q and A, $m^2 \sim F(m-n, \infty, 0)$ (P. Teunissen, 2006) were introduced, albeit with limited success. Despite that, this AR shows a visible improvement over previous estimations (see figure 6.12, page 97). The oscillation seen in the previous stage, is no longer present (see figure 6.6, page 90).

6.3 Final design results

Results shown in table 6.3 are based on the NTF dataset. Only GPS ambiguities have been estimated using LAMBDA, Locata ambiguities were estimated using the weighted average method, based on the trace of $Q_{LL,RxA}$[23]. On this occasion however, instead of using the ratio test, the most common integer values for each GPS ambiguity were chosen. Even when using the multi-epoch approach, LAMBDA results are produced epoch-by-epoch. It is worth noting, that while the method is intended for an

[22] Also known as $\sigma^2 - test$.

[23] See section C.2 on page 151 for details.

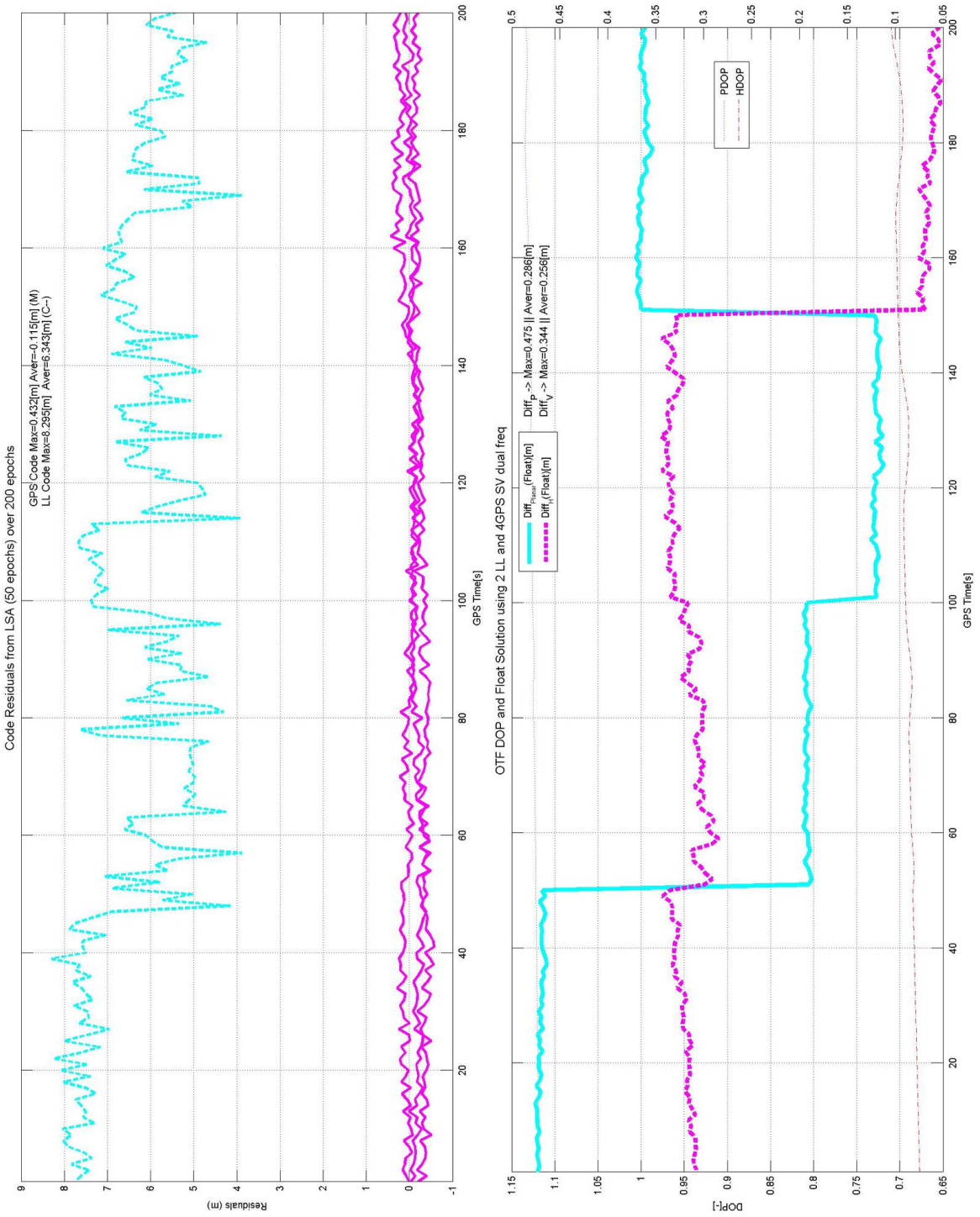

Figure 6.11 – Final Design AR results – LL2+GPS4, 50 epoch solution, float AR

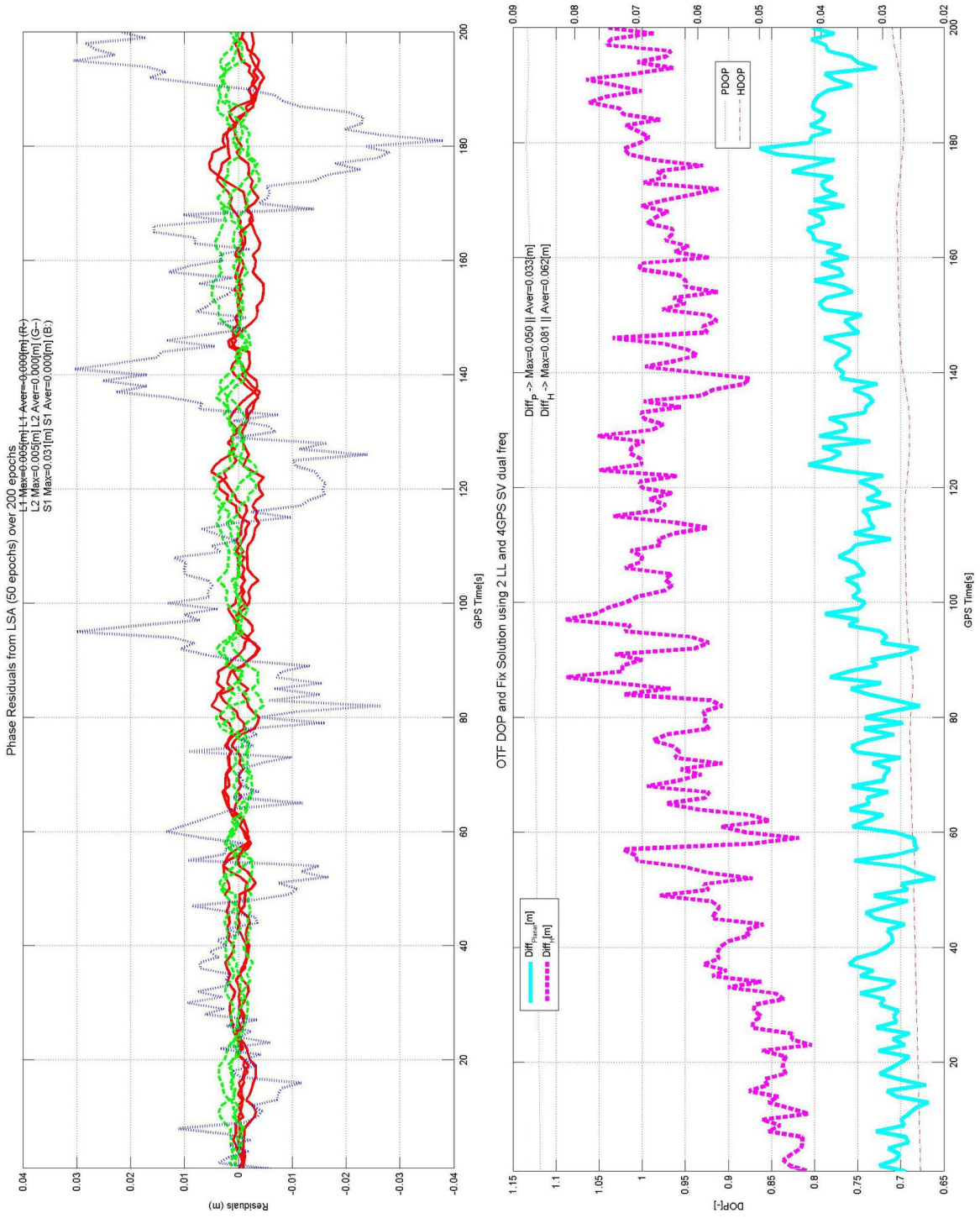

Figure 6.12 – Final Design AR results – LL2+GPS4, 50 epoch solution, AR estimated using LAMBDA

on-the-fly solution, in the same way as Amt and Raquet (2007); J. J. Wang et al. (2004), the whole dataset is used for AR then recalculated for the final solution, see figure 6.4, page 87.

The final navigation engine is capable of estimating ambiguities epoch-by-epoch or multi-epoch, in order to improve accuracy, as shown in figures 6.11 to 6.12 on pages 96–97 . The integrated solution improves the height solution. These results demonstrate the proposed combined OTF AR in practice, and are comparable with KPI kinematic Locata results (see table 5.2, page 70)[24].

No of LL	No of GPS SV	GPS Freq	$\mathbf{d}^{\mathbf{max}}_{\mathbf{planar}}$[m][a]	$\mathbf{d}^{\mathbf{average}}_{\mathbf{planar}}$[m]	$\mathbf{d}^{\mathbf{max}}_{\mathbf{Ht}}$[m]	$\mathbf{d}^{\mathbf{average}}_{\mathbf{Ht}}$[m]
3	4	L1	0.163	0.146	0.372	0.344
3	4	L1+L2	0.055	0.035	0.082	0.063
4	3	L1	0.388	0.369	0.199	0.149
4	3	L1+L2	0.171	0.156	0.448	0.401
3[b]	3[b]	L1+L2	0.142	0.127	0.383	0.338
3	3	L1	0.144	0.129	0.386	0.340
2[c]	4[c]	L1+L2	0.050[d]	0.033[d]	0.081[d]	0.062[d]
2	4	L1	0.275[d]	0.268[d]	0.068[d]	0.038[d]
0	5	L1	0.194	0.186	0.243	0.227
0[e]	5[e]	L1+L2	0.029	0.022	0.065	0.048
0	7	L1+L2	0.025	0.022	0.033	0.026

Table 6.3 – Locata and GPS integration in a limited visibility environment

[a] The kinematic difference value calculated from 250 epochs.
[b] For results before and after AR estimation, see figures 6.14 to 6.15 on pages 100–101.
[c] For results before and after AR estimation, see figures 6.11 to 6.12 on pages 96–97.
[d] Calculated using a 50 epoch solution.
[e] For results before and after AR estimation, see figures 6.16 to 6.17 on pages 102–103.

6.4 Improvements and future development

This chapter has discussed the practical implementation of a tightly-coupled Locata and GPS navigation engine. During this chapter a number of further research areas were suggested:

- tropospheric predictions using MET stations,
- investigation into the exploitation of all Locata signals - Tx_{A-D} and the new frequencies available in firmware version v.7.0,
- improved implementation of the LAMBDA method,
- a fixed baseline solution for separate Locata and GPS antennas,
- height fixing as suggested by Amt and Raquet (2006),

[24] A direct comparison is difficult, due to the different environments and the varied number of transmitters.

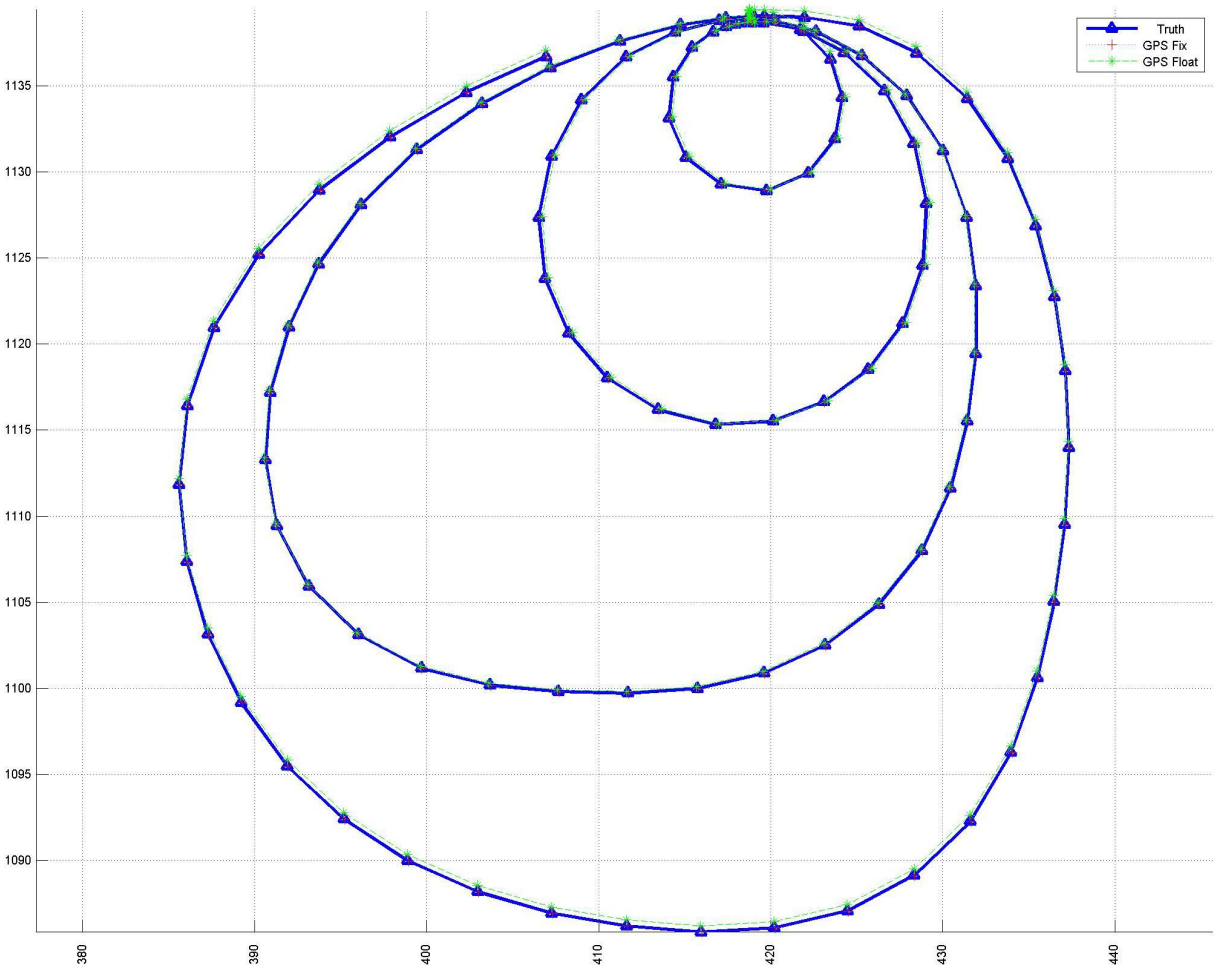

Figure 6.13 – Trajectory of the NTF dataset

The static data was collected before the movement commenced. Units are in metres.

- research into the implementation of dynamic weighting (see equation C.7, page 147),
- further research into IQ_A method feasibility.

Before such work can be conducted, a number of existing shortcomings need to be addressed:

- The implementation of a cycle slip detection method is essential for a fully operational system. Locata methods are discussed in section 5.3 on page 76 and for GPS, they can be found in (Hofmann-Wellenhof et al., 2008; Kaplan and Hegarty, 2006);
- In order to integrate all Locata signals (TxA-D), the inter-frequency bias needs to be solved. The mixing of Locata signals to produce a single, direct signal has been discussed[25] and some other suggestions, that discuss hardware implementation, can be found in Cheong (2012);
- LAMBDA is based on de-coupling of ambiguities and modelled parameters, which cannot be fully attempted until a better model has been created. Research into the use of MET-based tropospheric correction, mitigation of frequency bias, and better modelling of inter-system time offsets are essential

[25] See section 3.1 on page 36 for details.

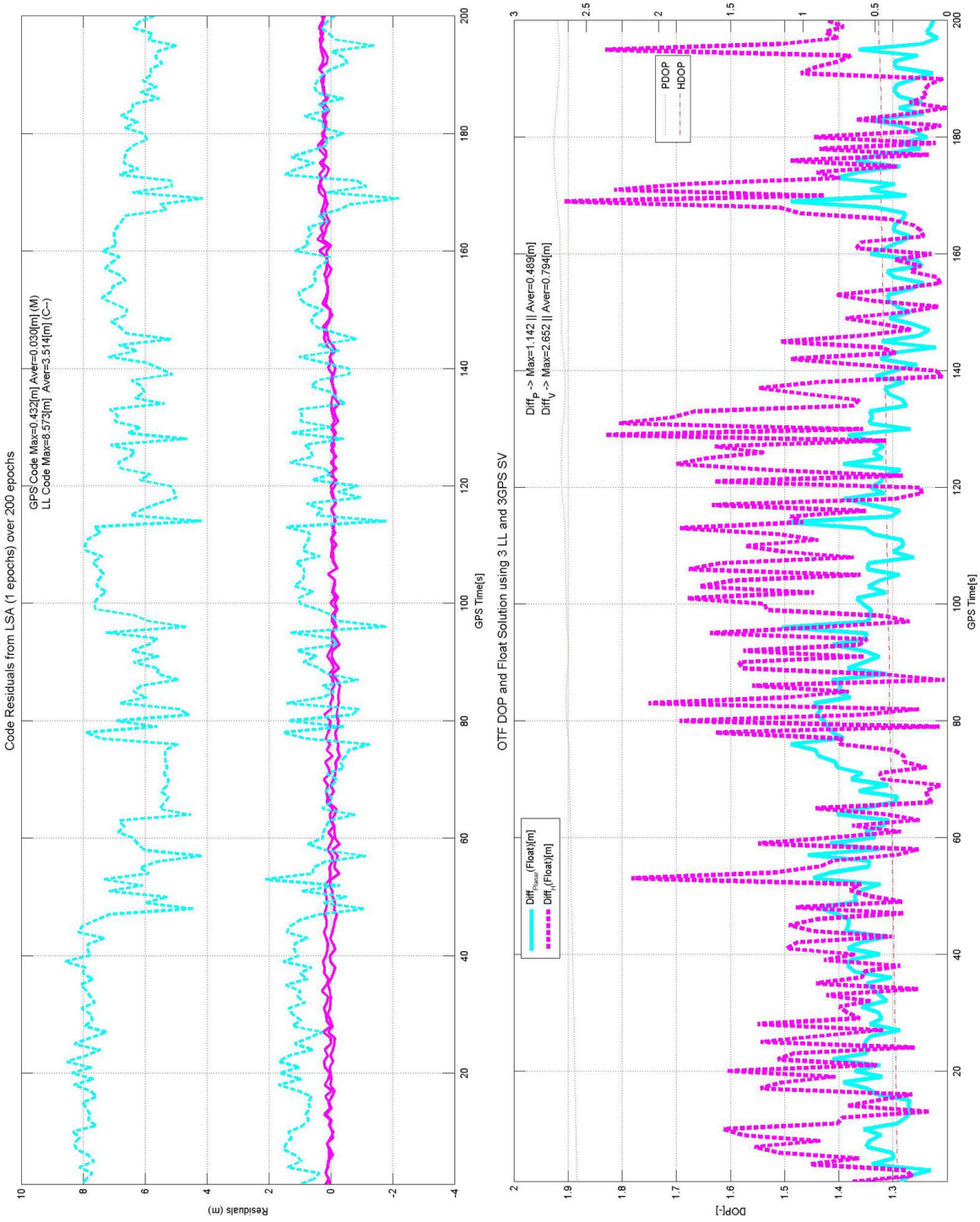

Figure 6.14 – Final Design AR results – LL3+GPS3, epoch by epoch solution, float AR

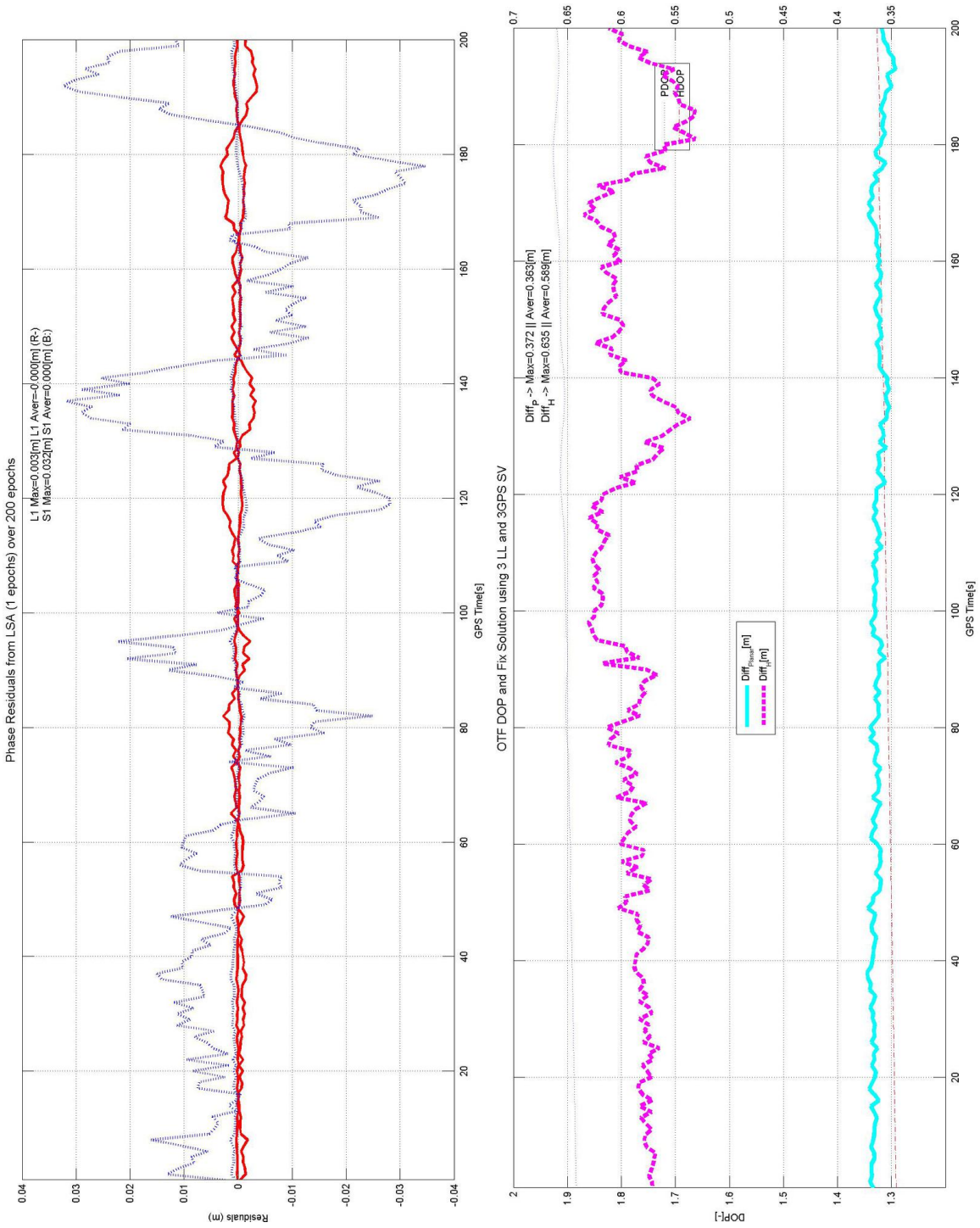

Figure 6.15 – Final Design AR results – LL3+GPS3, epoch by epoch solution, AR estimated using LAMBDA

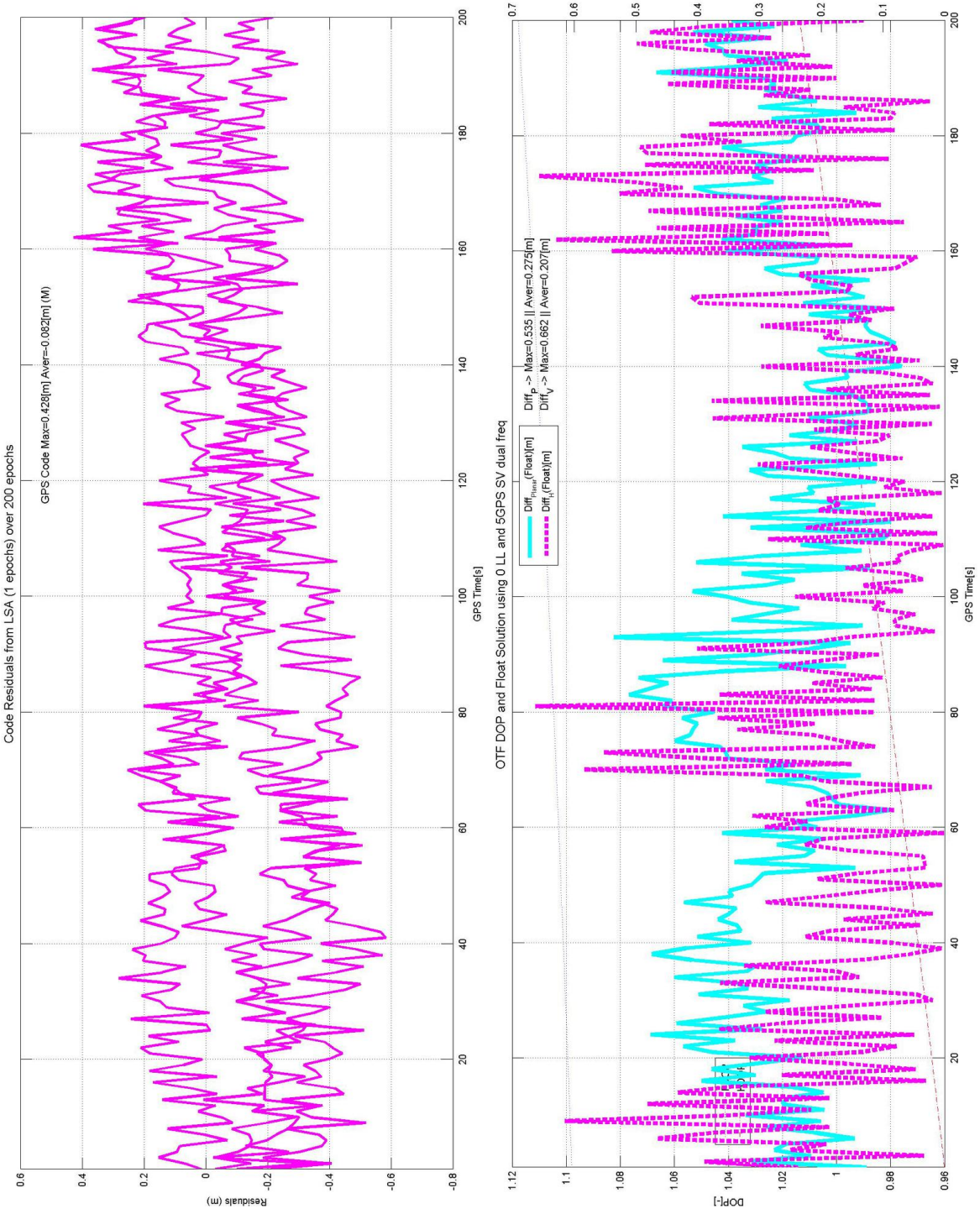

Figure 6.16 – Final Design AR results – dual-frequency GPS epoch by epoch solution, float AR

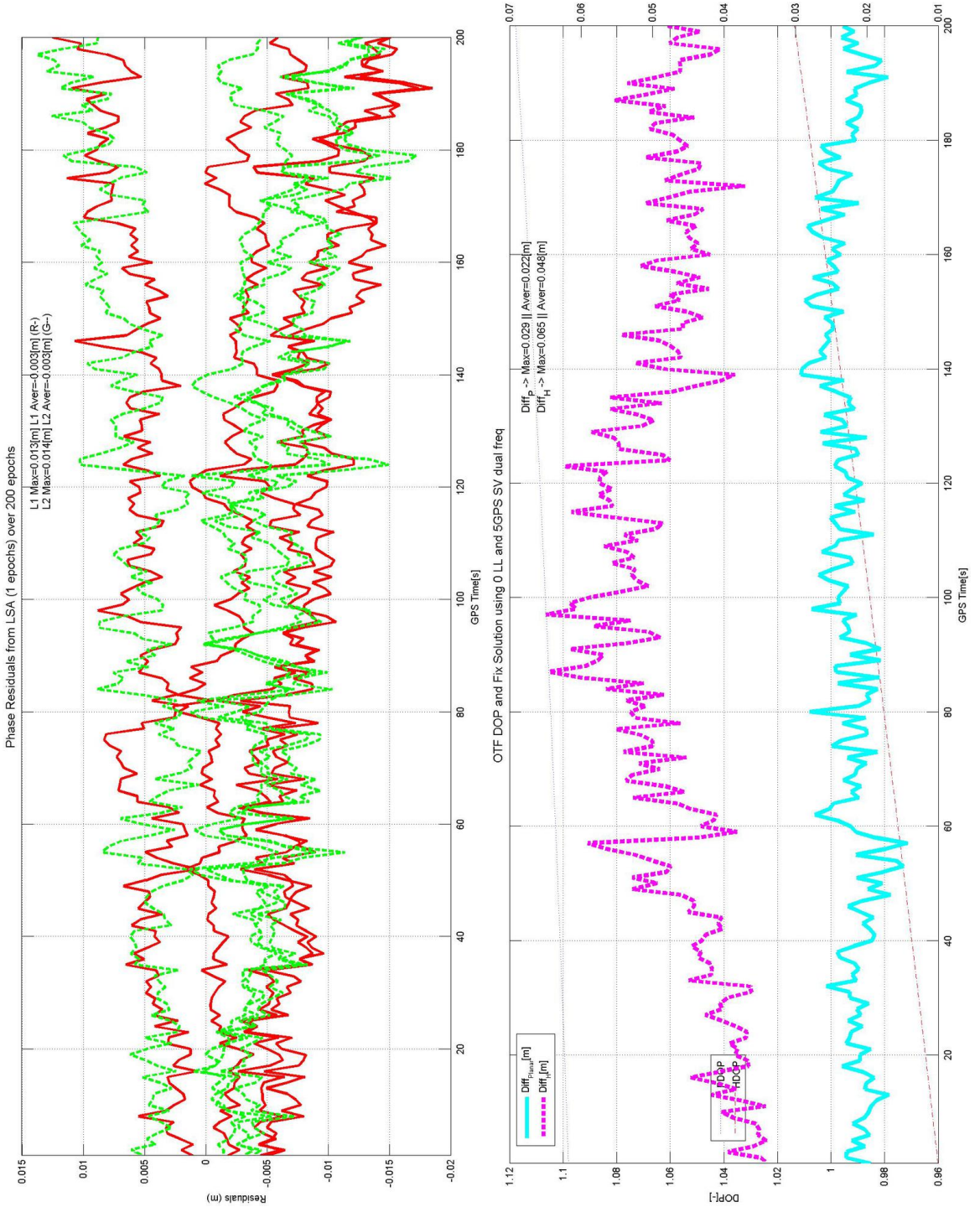

Figure 6.17 – Final Design AR results – dual-frequency GPS epoch by epoch solution, AR estimated using LAMBDA

here. A new method for obtaining initial positional estimations is fundamental to improve the Locata-only accuracy. Limiting a search space by height fixing (Abt et al., 2007; Amt and Raquet, 2006) would be a good starting point[26].

- Further research into IQ_A, as the strength of the matrix A can be optimised for the multi-epoch solution;
- A fixed baseline solution could strengthen the solutions and offer a rejection method based on the known baseline length[27]. This is especially vital as an integrated Locata and GPS antenna is not easy to produce, and common phase centre offset (PCO) will probably not be possible.

Locata technology is still subject to constant development, the implementation of new tropospheric modelling, and a solution to the phase bias represents a very important move forward (LaMance and Small, 2011; Locata Corporation Pty Ltd, 2011a; Trunzo et al., 2011). This study identified that proper separation and de-correlation of Locata and GPS ambiguities are essential for the full implementation of the LAMBDA method.

♣ ♢ ♣

[26] Timetenna is currently able to ignore those limitations by using different seeding method.

[27] During calculations baseline length is estimated, comparison of this value with known truth can be used as a rejection mechanism.

7 Applications of the Combined Systems

"I have found that all ugly things are made by those who strive to make something beautiful, and that all beautiful things are made by those who strive to make something useful." *Oscar Wide*

THIS chapter discusses the applications of the integrated system, taking into account its commercial feasibility, which must be paramount in any engineering research. Starting with a general discussion about seamless navigation in a city-wide network deployment, this chapter will then focus on practical applications in urban canyons, a long-term monitoring scenario and indoor navigation. The urban canyon application demonstrates a dedicated tool for planning deployment in these areas, while long term monitoring and indoor application demonstrate the stability, and accuracy of a Locata-only solution.

Some of the work presented in this chapter was published in Bonenberg et al. (2012).

Contents

7.1 Seamless navigation – large area deployment

An extensive number of applications, including machine control, mobile mapping, fleet management, aviation, maritime and engineering, depend on GPS for positioning fix. While accuracy requirements vary across the range of requirements, the availability, reliability and integrity of the positioning fix is vital. These requirements can only be partially met by GNSS, owning to its dependency on open sky visibility[1]. Integration with other sensors - INS, laser scanners, total stations or transport based DSRC (Alam, 2011; Toth, Grejner-Brzezinska, Wang and Sun, 2009) have been suggested, and this thesis presents a case for integration with Locata, for centimetre to decimetre level positioning fix.

Locata is currently utilised commercially to provide either independent, or augmented positioning in applications such as open-cast mines, GPS-denial zones and maritime applications in the Sydney Bay area (Barnes, LaMance et al., 2007; Barnes et al., 2003b; Craig and Locata Corporation, 2012; Harcombe, 2012). The proposed novel integration of Locata and GPS further extends the capacity of both components, leading towards seamless navigation, with position available outdoors, in areas of limited visibility, such as urban canyons, and even indoors. Seamless navigation requires system deployments over a large area, therefore dedicated planning and an understanding of the system's limitations is essential. The following sections will discuss these topics.

Coverage and range implications

The conclusions from section 4.5 listed the following range restrictions of the combined system:

- The GPS-RTK baseline should not exceed 10 km unless N-RTK is used[2];
- Locata nominal transmission power of 23 dBm offers a 10 km signal range;
- Practical geometry constraints limit the height difference between Locata transceivers.

A combined system will require the deployment of a Locata network around the area of interest, and while currently only few large area implementations exist (NTF, White Sands, Boddington Gold Mine and Sydney), it would be advisable to consider its scalability and limitations. The desk-based nature of this analysis allows us to disregard the influence of topography, and the local environment; to account for this simplification, an 80 % range utilisation has been assumed. Good visibility between transceivers is required to maintain TimeLoc (see section 3.1, page 30), hence this restriction will not apply to TimeLoc range.

To maximise system coverage, the ideal shape from a mathematical point of view, is an equally spaced grid[3], with separation equal to the mean system range[4]. This network (see figure 7.1, page 108), requires cascade TimeLoc for most of its points, and can cover an area of 400 km^2 assuming master TimeLoc range of 314 km^2.

A power upgrade to a 40 dBm for aviation trials, as described in Craig and Locata Corporation (2012), would increase the area covered to 3 600 km^2 and the Master TimeLoc range to 2 827 km^2, exceeding

[1] For details see Chapter 2 on page 8.

[2] CORS (N-RTK) can use baselines of 60 – 100 km.

[3] An octagonal network would decrease the number of TimeLoc hoops required, but would lead to a shrinkage in network size, as an inscribed circle is smaller than its square. This would also have a negative effect on the time slots assessment.

[4] In this sense, our mean range utilisation becomes a scaling factor of the network.

the current trial area of 2 000 km^2 in the White Sand area and 1 500 km^2 at Cooma airport (Gakstatter et al., 2011). This power extension is essential for any aviation applications, as commercial aircraft flying altitude exceeds 10 km.

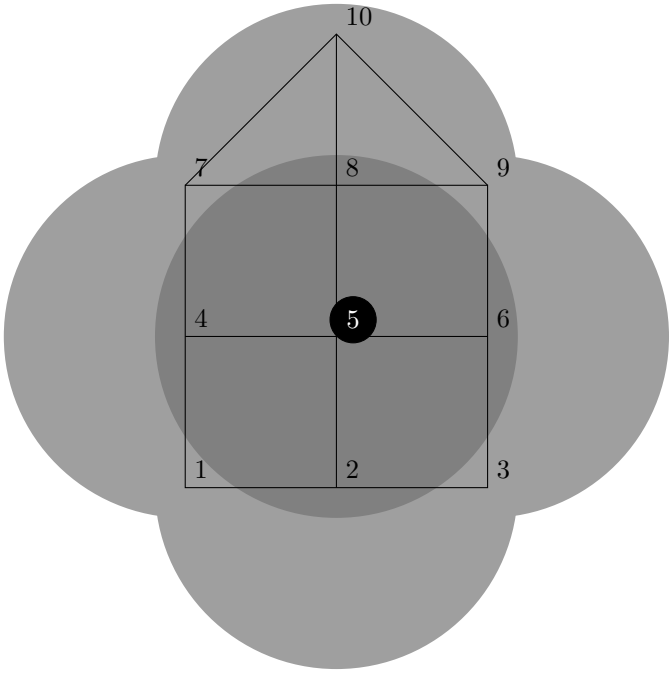

Figure 7.1 – A simplified view of a fully deployed (10 units) Locata Net

The master transmitter is marked with a black circle. TimeLoc cascade (time hopping) is shown in the background with various shades of grey.

While it is theoretically possible to implement multiple networks using the old sliding TDMA N-slot assignment sequence[5], the restriction of 10 units per sub-LocataNet, creates a non-trivial problem, as no signal overlap is possible on sub-LocataNet boundaries. Combinations are limited and one is shown figure 7.2, covering the area of 3 120 km^2 (see figure 7.3, page 110), almost twice the size of Greater London (1 570 km^2).

To address this issue, firmware version v.6.0 introduced a new TDMA scheme[5]. Up to five sub-LocataNets, each with a different sequence of N-slot assignments, can operate within a single LocataNet[6]. Each time allocation sequence repeats only once per Super Frame (see section 3.1, page 27). TimeLoc is the limiting factor here, as full coverage requires four hoops (cascaded TimeLoc) with time accuracy not lower then $1.2{\cdot}10^{-10}$ s. Certain areas of the urban environment will require a higher density of Locata transceivers, limiting the overall size of the network. However, independent networks within an urban conglomeration should not be required, unless the areas of interest are separated by more than 10 km. In this case, the use of independent networks, with separate master units and different PRN numbers to avoid any confusion, is preferred.

[5] As described in section 3.1 (page 27).

[6] Locata Corporation Pty Ltd (2011a) defines PRNs for up to 50 transmitters.

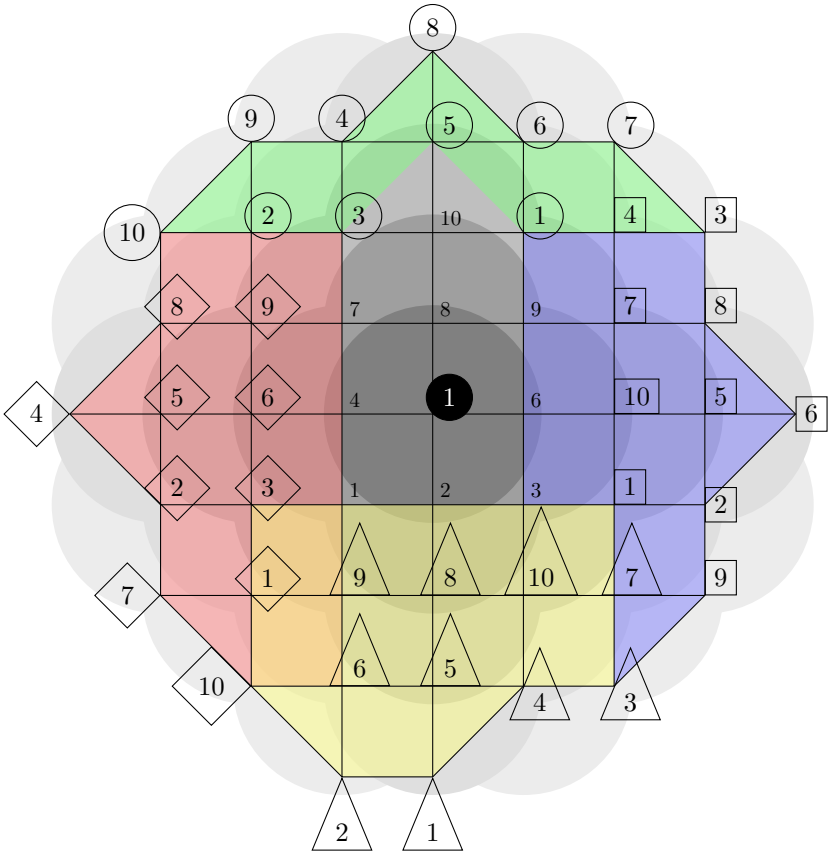

Figure 7.2 – The implementation of Locata Net with 50 transceivers, using the old TDMA scheme

The master transmitter is marked with a black circle. TimeLoc cascade (time hopping) is shown in the background with various shades of grey. Each of the five subnets is marked with a different geometrical shape.

Local transformation system implications

The previous section identified a number of possible Locata network solutions, varying in size from 400 km^2 up to 3 120 km^2. Any local transformation covering a range of 9 km or more, will affect both distance, and angle measurements (Bonenberg, 2003). For the purpose of integration, those coordinates must be coherent with the GPS coordinate frame used, for example ETRS89 within Europe. This approach makes it seamless for aviation, maritime and fleet management. A similar approach should be taken for terrestrial surveying, and engineering works, where local grid coordinates can be calculated from fix results.

Other considerations

A number of other factors, as discussed in chapter 4 (page 44), have a visible impact on any Locata placement. TimeLoc requires inter-visibility between transmitters to prevent the standing multipath phenomena, which limits placement options. Barnes et al. (2003a) demonstrated that it can occur in seemingly open areas. This is a very difficult feature to model, and while simplified models do exist[7], it

[7] As described in section 4.8 (page 62).

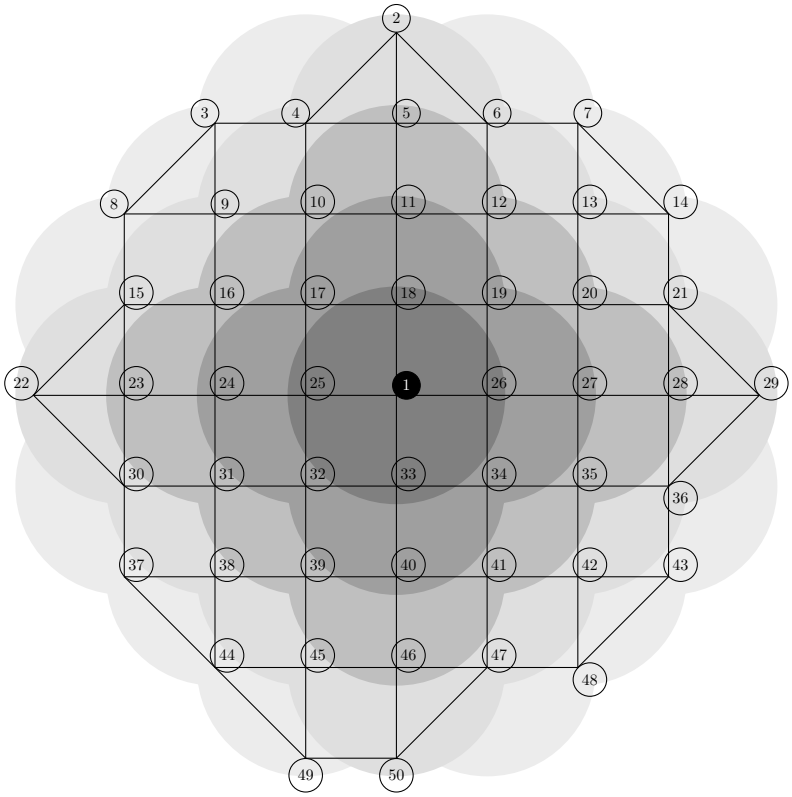

Figure 7.3 – The implementation of Locata Net with 50 transceivers using the new TDMA scheme

The master transmitter is marked with a black circle. TimeLoc cascade (time hopping) is shown in the background with various shades of grey.

is recommended that an empirical method, where master and slave observations are analysed and unit antennas are moved until no further problems are detected, is used.

7.2 Urban canyons

Urban canyons are very challenging environments for any radio based navigation system, including GNSS. Much the same can be said for natural canyons, where dense vegetation attenuates the incoming signal (Massatt et al., 2006). The overall characteristics of canyons are:

- severely limited sky visibility,
- environmentally inducted extensive noise and multipath.

GPS geometrical limitations have been studied by Hancock et al. (2009); Ji et al. (2010); G. W. Roberts et al. (2006), all of whom identified that GNSS multi-constellations will only partly alleviate the problem. On other hand, utilisation of a combined system mitigates the open sky problem. Transmitter position can be optimised to offer the best visibility and the lowest multipath, through modelling. In the urban environment, the most difficult situation arises where only non-line of sight signals are present, as any multipath mitigation technique will fail (Groves et al., 2012; L. Wang, Groves and Ziebart, 2012).

To avoid the problem of non-line of sight signals, an obstruction simulator[8] can be used, a quick tool able to estimate simplified multipath, DOP and RAIM[9], allowing feasibility and mission planning. Multipath detection methods (Andreotti, 2006; Hofmann-Wellenhof et al., 2008; Lau and Cross, 2007) are computationally heavy, so a simplified approach is used[10], with calculation based on provided ephemerides and obstruction information.

Figure 7.4 – The Urban obstruction simulator, Canary Wharf scenario

All coordinates are in the OSGB grid (ENH), with a scale factor applied. Locata transceivers are marked in green and the trajectory is in red.

Consider a scenario where a position fix is required in the Canary Wharf area of London's financial district. A large number of skyscrapers prevent sky visibility, and create severe multipath. Ground level information, footprint and height values for the nearby buildings were obtained from EDINA, University of Edinburgh (2000). Figure 7.4 demonstrates the improvement when five Locata transceivers are employed and used as combined system. Assuming a 10° GPS cut-off angle along the 0.9 km - long rover trajectory, a combined Locata/GPS system can offer:

- Almost doubling of signal availability;
- A constant number of non-line of sight (nLOS) signals, making it possible to detect and eliminate them[11], whereas utilisation of Locata or GPS on its own would lead to a serious positional biases;
- The roof placement of Locata transceivers extends its range, and limits multipath, but introduces signal gaps in the direct vicinity of the structure.

[8] Described in details in appendix D on page 155.

[9] RAIM: Receiver Autonomous Integrity Monitoring, a position quality confidence metric used in aviation.

[10] A detailed discussion about simulator limitations has been outlined in appendix D on page 155.

[11] The nLOS characteristics for each system varies, so it is possible to identify it mathematically, for more details see L. Wang et al. (2012).

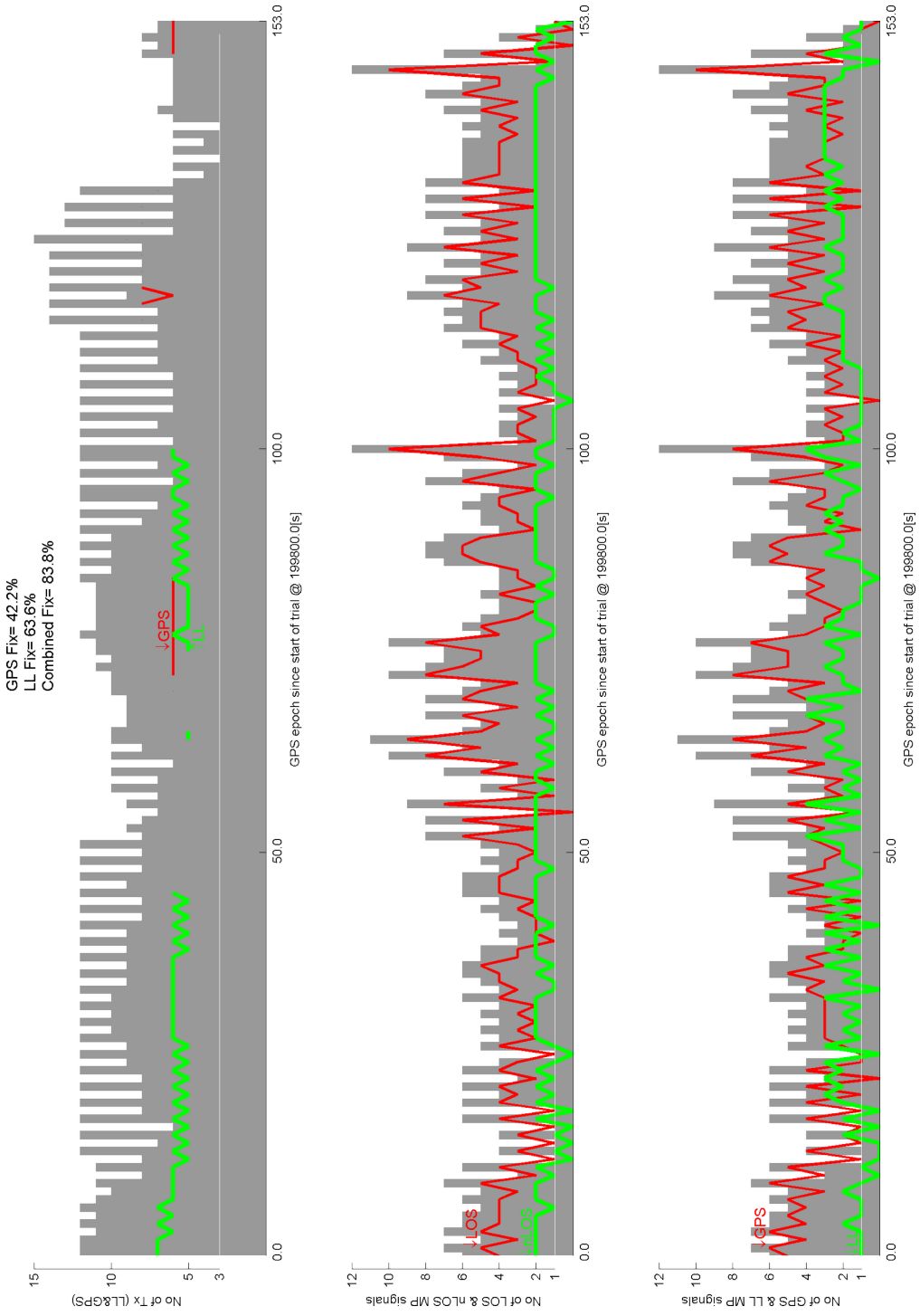

Figure 7.5 – The visibility and multipath prediction in the Canary Wharf scenario

The above factors lead to an additional integrity control mechanism, guarding against GNSS outages. Results also demonstrate that correct Locata placement is very important, in order to maximise return from the investment.

These results have been also published in Bonenberg et al. (2012).

7.3 Deformation monitoring

The demand for long-term monitoring has grown considerably over the past decades, and often monitoring schemes are often fully automated. A number of manufactures also provide online monitoring as part of their service [12]. Monitoring of rapid moving objects, such as suspension bridges, requires high frequency data, making it difficult for total stations, which would otherwise produce very predictable accuracy characteristics. This has led to the wide-spread adoption of GNSS, although its limitations due to: visibility of the sky, geometry dependant accuracy, reliability, and integrity, have not been completely solved, even with the introduction of additional constellations (Hancock et al., 2009; G. W. Roberts et al., 2006). Augmentation of GNSS with other sensors, such as total stations, accelerometers, and pseudolites, in a bid to overcome these weaknesses have been suggested (Bond, Chrzanowski and Kim, 2008; Meng, Dodson and Roberts, 2007; Meng et al., 2004; Ogundipe, Roberts and Brown, 2012; G. W. Roberts et al., 2006), as has the utilisation of other technologies, including laser scanning, remote sensing, photogrammetry, space and ground based SAR (Kocierz, Kuras, Owerko and Orty, 2011)[13].

Locata shares many characteristics with GNSS, and its deployment flexibility offers efficient geometry optimisation. This is of particular importance in areas of limited sky visibility, such as city centres (Meng et al., 2004; Saka, 2008). Trials on the Parsley Bay Suspension Footbridge, and later using an HP XY plotter table (Barnes et al., 2004; Barnes, Rizos et al., 2007), demonstrated promising accuracy, predominantly planar, with maximum planar error of 2.7 mm for Locata and 7.2 mm for GPS. However, these tests failed to show that Locata is capable of maintaining this accuracy over prolonged periods of time.

Equipment and method

The aim of the experiment was to investigate the long term capacity of Locata to detect small and unexpected movement. To simulate the behaviour of a man-made structure, this experiment consisted of long static periods with periodic random vertical movements. It is the first Locata test focusing on the vertical performance of the system.

Tests were conducted using the dedicated Locata network on the roof of the Nottingham Geospatial Building (NGB) at the University of Nottingham. The network was designed to provide 3D position (with VDOP less than 10), using a minimum of six Locata transceivers (during the actual trial an additional unit was present), see figure F.3, page 163. A Leica GS10 GNSS receiver and a Locata antenna were mounted on top of a Trimble 360° prism (see figure 7.6, page 114).

[12] For example Leica is offering support for its GNSS based deformation monitoring at `http://www.leica-geosystems.com/en/Leica-CrossCheck_75108.htm` .

[13] More details about the challenges and demands of the monitoring systems can be found in Bond, Kim, Chrzanowski and Szostak-Chrzanowski (2007); Chrzanowski, Szostak-Chrzanowski, Bond and Wilkins (2007); Kennie and Petrie (1993).

All equipment was set up on a semi-permanent monument, shown as a checked box in figure F.2 on page 162. A cranking device enabled vertical movements up to 29 cm. To avoid drag and maintain comparable results, cables were locked securely and the cranking mechanism was oiled weekly. Ideally the set-up should also provide synchronous total station measurements, but due to hardware problems, the total station was only used to measure the truth. Throughout the experiment, the Locata rover worked continuously; while the GPS was turned off during long static periods, to make data analysis more manageable. Both systems operated on the same coordinate system.

Locata deployment consisted of seven transmitters, with the master located on the central pillar, equipped with an omnidirectional LCOM HG2403MGU antenna. The remaining units were equipped with LCOM AT2400 or HG2412P antennas. Since the establishment of the network in late 2010, all antennas have been monitored at least 3 times a year, with no movement larger than 6 mm from the initial positions being detected. We observed $5-10$ GPS satellites, with an average of 7, VDOP $0.6-1.3$ and HDOP $1.1-1.7$. In comparison, Locata HDOP was 1.1.

To fully monitor the system's capacity, it was vital to maintain an extended monitoring period, to highlight any biases or drifts in the position fix. The dataset analysed, was collected between 17:58 01/08/2011 and 18:39 05/08/2011, 1 647 GPS week $151\,084-499\,124$ s, a total of just over five days of continuous data collection. By the end of the experiment, Locata transceivers operated continuously for a total of 13 days, from 1 646 GPS week 65 605 s. Locata used firmware version v.4.2.

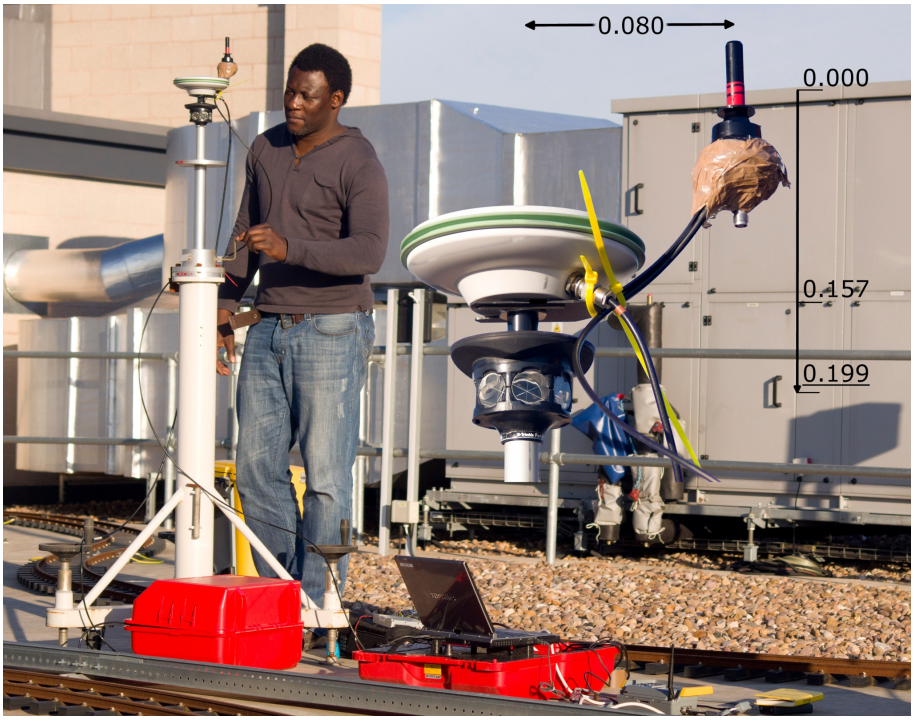

Figure 7.6 – The LTM experiment set-up with Locata HG2403U and Leica GS10 antenna on 360° prism

Results and summary

With the aim being to identify the long term capacity of each component, on-the-fly (OTF) results from each sensor were analysed separately, without use of a combined navigation engine. It was assumed

that any discrepancies during the measurements would propagate in a roughly similar manner to that experienced in distance measurements. The data was filtered using the modified Baarda method[14] (Ghilani and Wolf, 2006; Harvey, 2009).

Error ellipses were estimated using equation 5.2 on page 76, and scaled from 65% to 80% density, assuming two degrees of freedom. The shape of the ellipses strongly correlates with the network geometry, and can be used to detect periods of suboptimal performance. Due to a laptop malfunction, a part of the data towards the end of experiment was not recorded, see figure 7.7, page 116.

Results: figures 7.7 to 7.9 on pages 116–118 show absolute horizontal performance, reduced to the Locata antenna's height and to the planar spread from the truth, thus eliminating positional offset between the sensors. The truth (total station measurements of extremities of pillar arm movement) has been marked with a thick black line.

Figure 7.7 shows a comparison of overall Locata and GPS performance. Both results display visible noise and multipath due to the nature of the environment. Human interaction was needed during kinematic periods, and Locata line of sight was occasionally disrupted – again to simulate a real-world environment. The current navigation engine, firmware version v.4.2, is capable of fixing position either in planar or in the vertical. The Leica Open World Interface (OWI)[15] flag analysis shows that the rover properly detected static, or vertical only movement, by fixing in height, or in planar accordingly. During the test, this approach was very effective, significantly reducing the overall bias. The side effects can be seen with vertical and horizontal jumps, depending on which parameter had been fixed. The magnitude of the jumps, within $\lambda/4$ or 3 cm, may indicate undetected, or less than fully mitigated cycle slips.

As GPS data collection was not continuous, any overlapping data from both sensors will be referred to as a **cluster**. Comparison of initial and final clusters (figures 7.8 and 7.9), identifies a visible drift within the planar position, but height values are maintained (see figure 7.9, page 118).

Small local jumps are the clearest representation of undetected biases of the system. Those jumps (most likely to be under-corrected or over-corrected cycle slips) are repairable through a change in geometry; Though this cannot remove residual drift[16], careful design of the integrated system should mitigate this problem. This bias is more visible in cluster analysis than in the overall results. Implementation of the integrated system (Bonenberg, Roberts and Hancock, 2010b), or even a long term prediction model (Bond et al., 2007; Choudhury, 2012; Chrzanowski et al., 2007), would be beneficial here, improving the results and providing more reliable accuracy characteristics.

In summary, the experiment results show that:

- GPS and Locata accuracy are comparable, with Locata showing superior height determination;
- GPS accuracy is very dependant on geometry, especially in the determination of height;
- Locata displays a positional drift[16], visible in the cluster comparison, see figures 7.8 to 7.9 on pages 117–118;

[14] Each cluster was considered separately and overall less than 0.06 % of data was removed.

[15] Leica Open World Interface, a proprietary communication interface.

[16] Overall drift of 26 mm translates to $7.8{\cdot}10^{-5}$ mm/s, but an analysis of clusters suggests that the true value might be 30 – 50 % smaller.

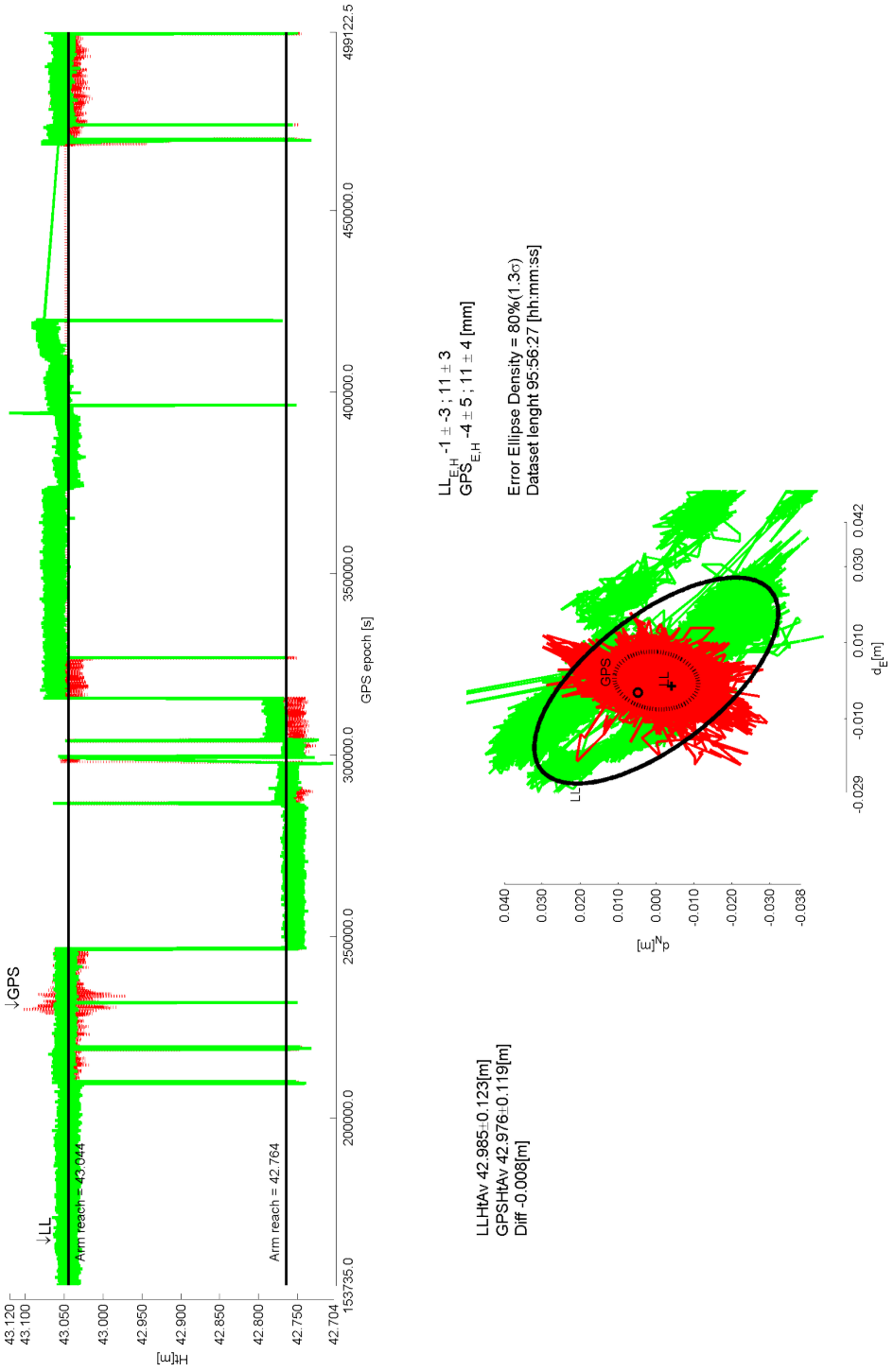

Figure 7.7 – The overall performance of integrated Locata and GPS System throughout the test

All coordinates are in the OSGB grid (ENH), with a scale factor applied. All heights are reduced to the Locata antenna height.

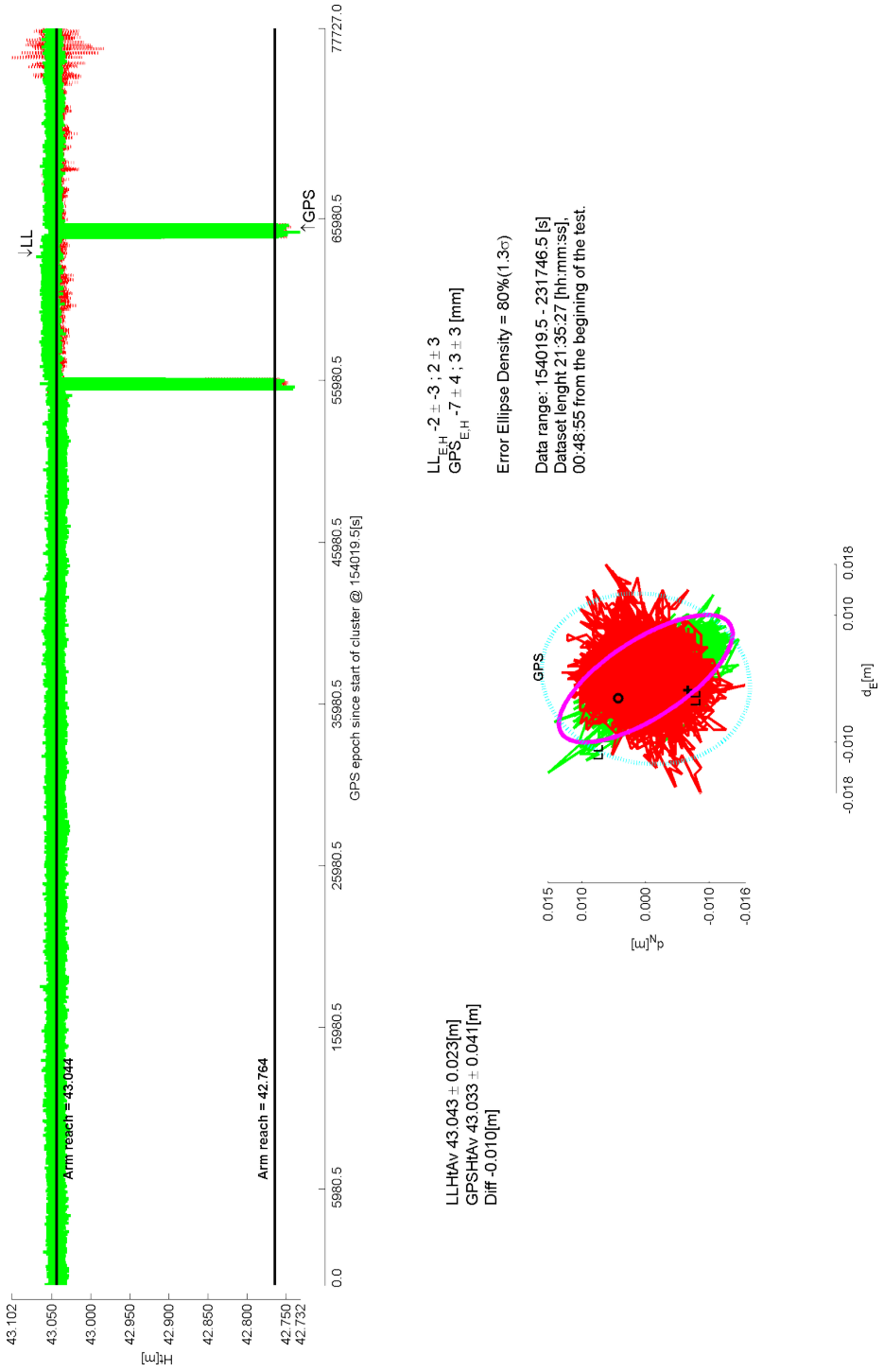

Figure 7.8 – The performance of the integrated Locata and GPS System at the beginning of the test

All coordinates are in the OSGB grid (ENH), with a scale factor applied. All heights are reduced to the Locata antenna height.

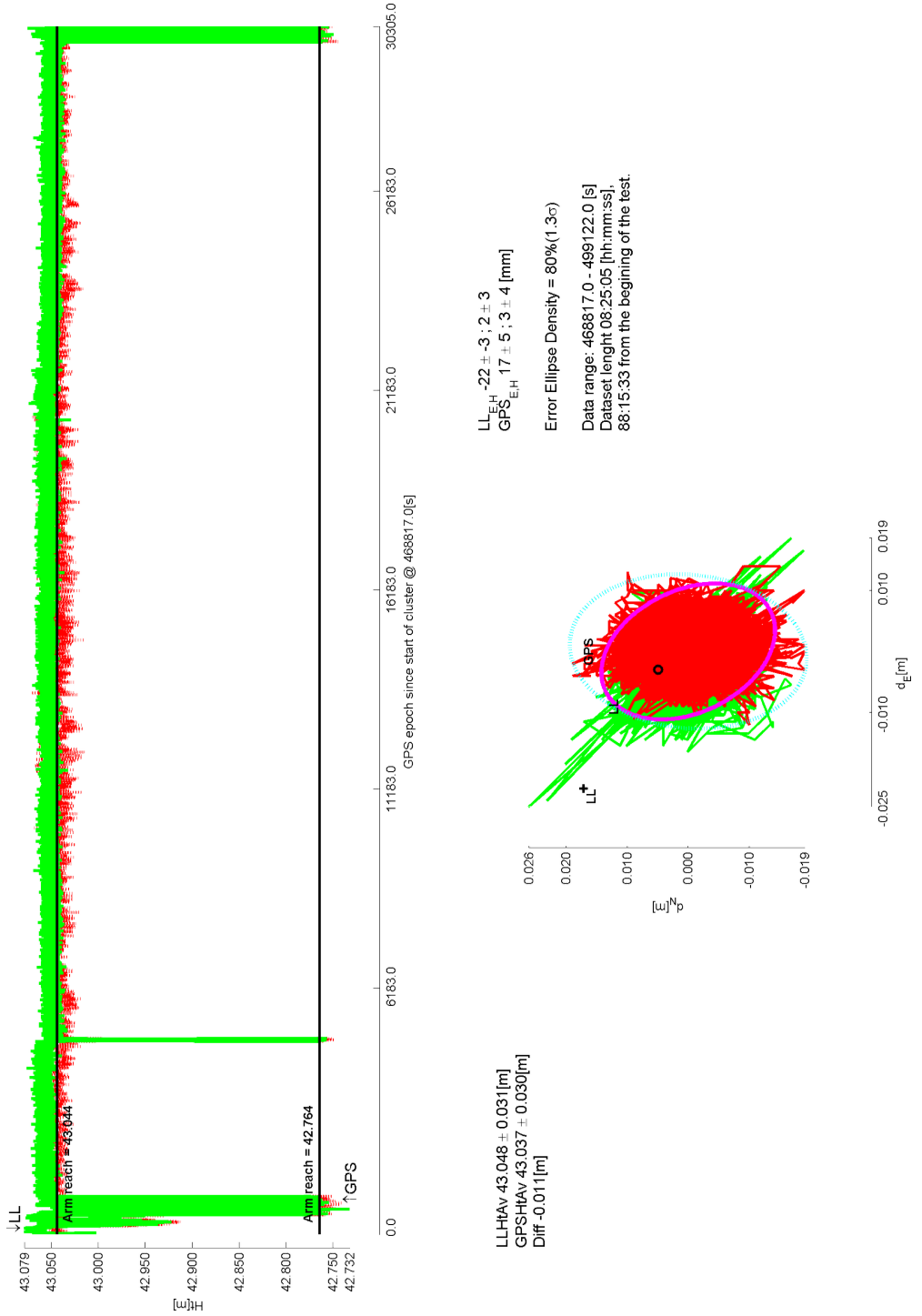

Figure 7.9 – The performance of integrated Locata and GPS System at the end of the test

All coordinates are in the OSGB grid (ENH), with a scale factor applied. All heights are reduced to the Locata antenna height.

- Small jumps such as those shown in figure 7.7, less then $\lambda/4$ or 3 cm and with visible recovery after the kinematic movement (change of geometry), may be undetected cycle slips;
- Locata results look more noisy than those of GPS.

GPS and GLONASS performance analysis of this dataset has been published in Peters (2011).

7.4 The indoor environment

Indoor environments, with no direct sky visibility, account for the majority of the GPS coverage gaps. A number of assisted technologies exist, that can offer metre level position including: INS, WiFi fingerprinting or particle filtering. Currently the only indoor system capable of centimetre-level positioning, is the Ultra-Wide Band (UWB), capable of mitigating multipath but with a limited range of up to 100 m LOS.

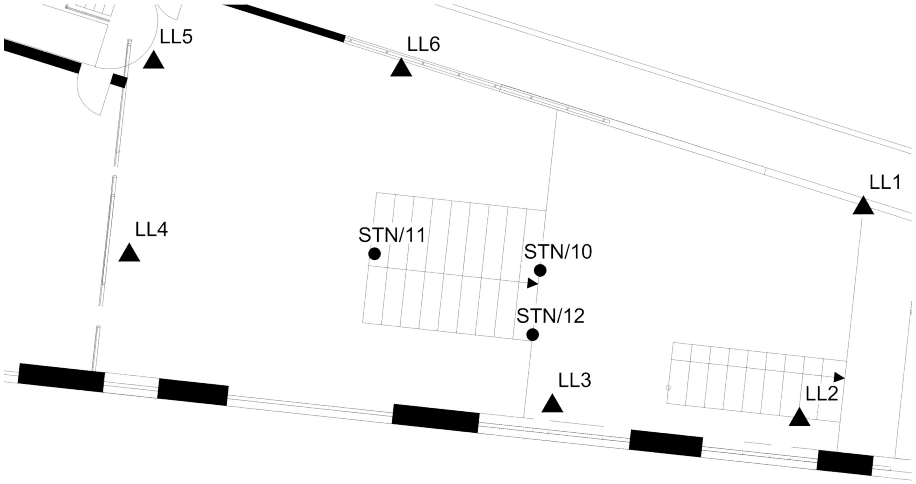

Figure 7.10 – Layout of an indoor Locata network

Locata transmitter locations and rover starting positions are marked by triangles and circles respectively.

For indoor trials, Locata transceivers used the firmware version v.3.0 and rover firmware version v.3.4. A local grid was used, roughly orientated to OSGB. Locata transceivers were distributed through all three floors to provide varied height, with rover starting locations on the first floor, approximately in the middle of the network (see figure 7.10). Over the trial period a few datasets required post-processing, as an on-the-fly solution was not obtainable. This involved removing a section of very noisy data at the start, and post-processing using LINE firmware version v.3.4 using the *h2* option, this being the most similar to receiver's real-time (on-line) solution.

The aim was to check if the indoor multipath effect could be mitigated by either changing the linear gain (LGA) for the transceiver's antenna, or by introducing a ground plane. In order to avoid any systematic errors, most notably standing multipath, three point locations were selected.

The tests lasted for a week, and a total of 32 static data sets, of varied length, were collected. Datasets suspected of severe multipath contamination, or of predominantly non-direct signal were excluded[17],

[17] Multipath is expected to be present in all observations, but it should be partly mitigated by the initialisation method

Figure 7.11 – View of the indoor network, with choke ring antenna located on STN/12

and the remaining 24 sets were analysed.

LGA[dBm][a]	**SD$_E$**[m][b]	**SD$_N$**[m]	**d$_E$**[m][c]	**d$_N$**[m]	**d$_P$**[d][m]	**%Fix**[e]
+20	0.013	0.021	0.004	-0.001	0.004	52.2
+8	0.008	0.014	-0.005	-0.005	0.007	89.9
+2	0.011	0.009	-0.001	-0.002	0.002	90.8
-4	0.004	0.009	0.000	-0.001	0.001	99.9

Table 7.1 – Effect of Linear Gain (LGA) alternation on the indoor position accuracy

[a] These results are averaged from the specific datasets.
[b] Precision.
[c] Accuracy.
[d] $\sqrt{(d_E^2 + d_N^2)}$
[e] Percentage of successfully solved epochs.

The relation between the positional results, and transmitting power, indicated by Linear Gain (LGA) is presented in table 7.1. The multipath[17] is directly related to the transmitting power and it is expected to be the largest contributor to interference and noise. Yet, if the affected signal strength falls below the noise floor, the other factors will become more prominent. KPI overcompensation was discussed in section 5.2 on page 70 and can be seen in this scenario as well, comparing accuracy (**d$_\bullet$**) and precision (**SD$_\bullet$**). A decrease in transmitting power will lead to unrealistic precision and, due to KPI, even accuracy. As discussed in section 5.2 on page 72, true accuracy can only be estimated while kinematic,

and the correlator characteristics, (see section 4.8, page 61). The datasets with positional accuracy exceeding the threshold (4 cm), have been assumed to be affected by either severe multipath or non-direct signal and were no further considered.

Type[a]	SD_E[m]	SD_N[m]	d_E[m]	d_N[m]	d_P[b][m]	%Fix
None	0.003	0.011	0.000	0.011	0.007	66.3
Plate	0.010	0.016	0.004	-0.010	0.004	78.9
Choke ring	0.007	0.005	0.003	-0.005	0.004	98.2

Table 7.2 – The effect of the ground plane on indoor position accuracy

[a] Results presented are averaged from the specific datasets.
[b] $\sqrt{(d_E^2 + d_N^2)}$

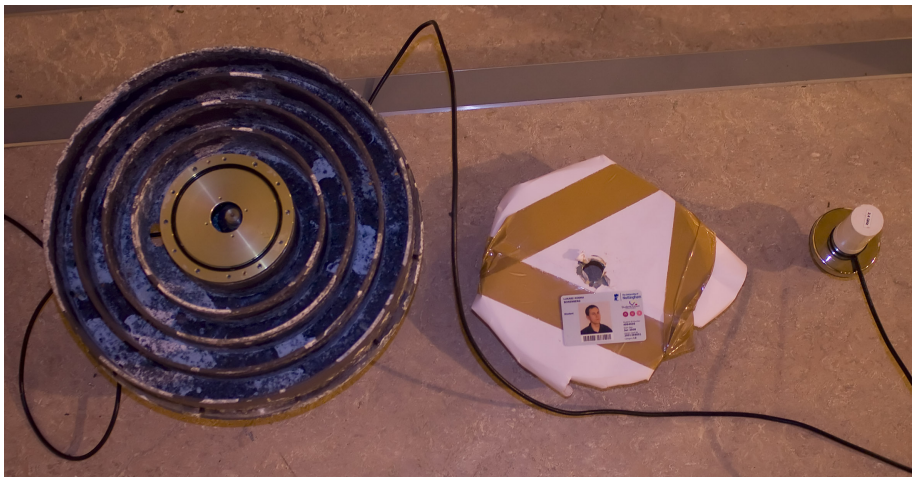

Figure 7.12 – From left to right, a modified choke ring, an iron plate shield and LCom HG2403MGURW(B) antenna

but on this occasion we can use our expectancy of centimetre-level precision and the fix percentage to deem low power solutions unreliable .

Two types of ground plane were used for the tests, A.2:

Plate shielding simply limits the antenna's negative visibility, but, due to its crude design, it was expected to suffer from the hard boundary condition[18];

Choke ring antenna is a standard GPS antenna, with Locata's phase centre raised in relation to original GPS one. Its design offers a much larger ground plate area and the provision of soft boundary conditions.

Multipath tends to be more prominent in the proximity of the antenna, and a reduction of sensitivity to negative angles of the LCom HG2403MGURW omni-directional antenna of the rover should reduce multipath as well. Table 7.2 demonstrates the difference made by the introduction of a ground plane with a choke ring. These findings can be verified by comparing two case datasets, both measured at STN/10:

[18] Soft-and-hard-surface conditions are important during antenna design, as a hard boundary will always introduce unwanted noise.

Case I a low −4 dBm power setting , without any ground plane;

Case II a medium 2 dBm power setting, with a choke ring antenna.

Case		$\mathbf{SD_E}$[m]	$\mathbf{SD_N}$[m]	$\mathbf{d_E}$[m]	$\mathbf{d_N}$[m]	$\mathbf{d_P}$[a][m]	**ff**[°]
I	OL[b]	0.001	0.003	-0.002	0.009	0.009	4.5
	h0[c]	0.002	0.003	0.028	-0.012	0.031	6.1[d]
II	OL[b]	0.009	0.006	0.002	0.000	0.002	61.3[d]
	h0[c]	0.015	0.022	0.025	-0.006	0.025	24.3
A priori error ellipse				0.023	0.013		26.7

Table 7.3 – Case study comparison

[a] $\sqrt{(d_E^2 + d_N^2)}$
[b] On-board LINE (real-time) results.
[c] LINE post processing option, see section 3.1, page 36.
[d] $\pm\pi$ as its impossible to recognise an exactly reversed ellipsoid.

In addition to the on-the-fly results (OL) the post-process option *h0* was also used[19]. While in both cases on-the-fly results are poor, case II h0 results not only match the a priori estimation, but also show a good correlation between accuracy and precision, while Case I h0 results are over estimated. A similar trend can be seen in the error ellipsoid's orientation. The use of all signals led to more realistic results with Case II h0 results only.

This report was originally published in (Bonenberg, Hancock and Roberts, 2010) coinciding with the development of Timetenna the indoor beam-steering antenna for the Locata system, which ignores (blanks) non-direct signals, provided that the antenna orientation is known and is time synchronised with the network.

7.5 Summary

There are an ever growing number of navigation and engineering applications heavily dependant on GNSS. Utilisation of the proposed integration offers a solution for current coverage gaps with improved accuracy and integrity. While, for certain applications, KPI might offer interesting new possibilities (see section 5.2, page 70), problems with absolute position need to be considered, and the proposed integrated engine presents a variable solution.

♣ ♢ ♣

[19] All signals were used, without any weighting, see section 3.1, page 36.

8 Summary and recommendations

> "He who receives an idea from me, receives instruction himself without lessening mine;
> as he who lights his taper at mine, receives light without darkening me."
> Thomas Jefferson

THERE are now four GNSS in operation (plus a number of local augmentation systems), all of which suffer from accuracy, reliability, and integrity dependency, on the number and geometric distribution of the available satellites. Space-born signals are subject to atmospheric perturbations (including scintillation), noise, and multipath. They are also easy to spoof, by hazardous misleading information (HMI); or block using freely available privacy devices.

There are number of ways to deal with these problems - for example: signal encryption and verification, or utilisation of a separate navigation system/sensor – either to augment GNSS, or to offer an independent backup. Most of the existing solutions, SBAS, GBAS, eLORAN, signals of opportunity, or devices utilising wireless communication protocol IEEE 802.11 (commonly known as WiFi), do not however provide centimetre-level accuracy, whereas inertial navigation systems (INS), offer this accuracy for limited period of time.

Locata is a novel, terrestrial-based positioning technology, using a dual-signal on the 2.4 GHz licence-free ISM band, with two spatially separated transmitting antennas, and a nanosecond synchronised network using TimeLoc. It provides centimetre-level position fix, with commercial applications including: open-cast mining (Barnes, LaMance et al., 2007; Carr, 2012), aviation (Craig and Locata Corporation, 2012), and maritime (Harcombe, 2012). Its major weakness however, is the mostly planar position and known point initialisation (KPI), which require either, a known starting position, or a GPS feed.

Previous Locata research focused on its solo performance, including indoors (Barnes, LaMance et al., 2007; Carr, 2012; Harcombe, 2012; Montillet, 2008), and on means of improving it (Bertsch, 2009; Cheong, 2012; Khan et al., 2010). A loose integration with GPS was proposed and used (Carr, 2012; Gakstatter et al., 2011; Rizos, Roberts et al., 2010), but there has not been any research on integrated ambiguity resolution (AR) before this thesis. The tightly-coupled integration addresses the shortcomings of both systems and can provide an almost instant AR producing results with improved accuracy, reliability and integrity.

8.1 Conclusions

This thesis has discussed the rationale behind the research, highlighting the shortcoming of each system. Following a detailed description of Locata technology, a feasibility study compared the advantage of a tightly-coupled integration against those offered by the loosely-integrated system (Leica Geosystems Jigsaw 360) or the Locata stand-alone solution. The issues of common time and coordinate (reference) systems, matching accuracy, range and the stability of the solution were also identified.

Discussion included Locata signal characteristics: SNR, RCRP, LCOE as a means of quantifying noise, cycle slips, and novel, geometry-based, noise and multipath detection methods. Analysis included detailed discussion of known point initialisation (KPI), the Locata ambiguity resolution method. The

effect of an erroneous initial estimation in static and kinematic scenarios demonstrated that while the absolute positions will shift, the relative (epoch by epoch) ones are less affected; and can thus be used in most of the scenarios, provided that observations are free of noise. It also highlighted a need for a proposed novel on-the-fly (OTF) tightly-coupled Locata and GPS integration System.

Practical Integration

The proposed practical integration was first demonstrated using simulated data, which combined the single differencing for Locata, and double differencing for GPS, to create a common solution and float ambiguities estimation. Conducting this process in four stages, see section 6.1, page 89, lead to the optimised design of the navigation engine. The final design used LAMBDA to provide AR fix. The algorithm is capable of providing both, epoch-by-epoch, and multi-epoch solutions.

Only one Locata signal (TxA) was used in that integration. This was expected to strengthen the solution, as the ratio of Locata and GPS observations have been found to have an important effect. These results have demonstrated the feasibility of the proposed integration, with real-life results close to those predicted. The multi-epoch solution showed an accuracy improvement, but its stability needs further research. A solution was possible with as low as three signals from a single system (Locata or GPS), which was previously impossible.

The combined solution offers a geometrical improvement, especially with respect to height determination, which again confirms previous pseudolite research. While the proposed approach failed to produce a fixed AR for the Locata component, an overall AR performance improvement was archived and a Locata AR using geometry change on-the-fly was also possible.

The final chapter presented possible applications of the combined system and the new TDMA. Standing multipath, residual noise, and range have been shown as major factors affecting accuracy.

8.2 Future recommendations

The proposed integration is capable of a combined AR for Locata and GPS. Results show an improvement in integrated positioning accuracy, which follows the trend observed in previous pseudolite trials (Cobb, 1997; Lee et al., 2008; Meng et al., 2007). Discussion in section 6.4 on page 98, highlighted opportunities for further research:

- Integration of all signals Tx_{A-B}. It is vital to address both the frequency bias and preservation of the integer nature of ambiguities. The introduction of new frequencies with firmware version v.7.0 might present future research opportunities;
- Usage of MET-based tropospheric corrections and improved modelling of observations, including frequency bias and time offset. This study identified that a proper separation and de-correlation of Locata and GPS ambiguities is essential for full implementation of the LAMBDA method. Further inclusion of Locata system characteristics – especially SNR, RCRP, LCOE into those models would also be beneficial;
- The current navigation engine is limited to integrated Locata/GPS antennas. An implementation of a fixed baseline solution capacity would improve deployability of the system, and the benefits of the proposed integration.

During the course of this research, Locata has developed new hardware, which implements an Extended Kalman Filter (EKF) and provides geometry-based initialisation. This approach is based on a new tropospheric model, which implements multiple MET stations, and should offer an improved accuracy, in a manner similar to Bertsch (2009) and unlike this thesis, only integrated carrier phase (ICP) is used in the EKF navigation engine. Craig and Locata Corporation (2012) demonstrated new tropospheric modelling, LaMance and Small (2011); Trunzo et al. (2011) have shown pseudo-range accuracy improvement.

Cheong (2012) discusses a combined Locata/GPS front end. This should provide direct time synchronisation between the two components via tight integration, see section 4.2, page 46, and improve accuracy and acquisition time. The mass market applications are very promising for any integrated navigation system. Feasibility of city-wide networks has been discussed in section 7.1 on page 107. Recent International Civil Aviation Organization (ICAO) acknowledgement shows an interest in such applications (Gakstatter et al., 2011).

Combined Locata and GPS pseudo-range observations would also benefit the mobile user, creating a more reliable and seamless navigation tool, with Barnes et al. (2003a) demonstrating good indoor penetration of the Locata signal.

Neither demand, nor the future applications, can be estimated; unless the current performance levels are improved. Meeting the challenge of improving performance levels will fuel the demand for future high-precision applications. It is the author's hope that this work will push the boundaries forward.

This is to all pioneers.

♣ ♢ ♣

References

Abello, M., Dempster, A. and Milford, G. (2007). Phase Centre Location Determination for Locatalite Antenna in the LocataNet System. In *Proceedings of the IGNSS Symposium.* Sydney, Australia.

Abello, M., Dempster, A. and Politi, A. (2007). ISM band interference and Locata. In *Proceedings of the IGNSS Symposium.* Sydney, Australia.

Abt, T. L., Soualle, F. and Martin, S. (2007). Optimal Pulsing Schemes for Galileo Pseudolite Signals. *Journal of Global Positioning Systems*, *6*(2), 133-141.

Adel, H., Thielecke, J., Grun, T. v. d. and Wansch, R. (2006). A tracking system for sports, logistics and robotics. *Fachtagung Sensoren und Messsysteme*, 425-430.

Alam, N. (2011). Three Dimensional Positioning with Two GNSS Satellites and DSRC for Vehicles in Urban Canyons. In *Proceedings of the 24th International Technical Meeting of The Satellite Division of the Institute of Navigation (ION GNSS 2011)* (p. 3975-3983). Portland, OR, USA.

Allan, D. W., Ashby, N. and Hodge, C. C. (1997). *The science of timekeeping* (No. 1289). Hewlett-Packard.

Amt, J. H. R. and Raquet, J. F. (2006). Positioning for Range-Based Land Navigation Systems Using Surface Topography. In *Proceedings of the 19th International Technical Meeting of the Satellite Division of the Institute of Navigation (ION GNSS 2006).* Fort Worth, TX, USA.

Amt, J. H. R. and Raquet, J. F. (2007). Flight Testing of a Pseudolite Navigation System on a UAV. In *Proceedings of the 20th International Technical Meeting of the Satellite Division of the Institute of Navigation (ION GNSS 2007)* (p. 1147-54). Fort Worth, TX, USA.

Andreotti, M. T. (2006). *Global Positing Systems in Urban and Indoor Environments. A new tool to Visualise, Understand and Use Multipath.* PhD thesis, University of Nottingham.

Bao-yen, T. J. (2005). *Fundamentals of Global Positioning System Receivers* (2nd ed.). Willey.

Barnes, J., LaMance, J., Lilly, B., Rogers, I., Nix, M. and Balls, A. (2007). An integrated Locata & Leica Geosystems positioning system for open-cut mining applications. In *Proceedings of the 20th International Technical Meeting of the Satellite Division of the Institute of Navigation (ION GNSS 2007).* Fort Worth, TX, USA.

Barnes, J., Rizos, C., Kanli, M. and Pahwa, A. (2006). A positioning technology for classically difficult GNSS environments from Locata. *2006 IEEE/ION Position, Location and Navigation Symposium, Vols 1-3*, 715-721.

Barnes, J., Rizos, C., Kanli, M., Small, D., Voigt, G., Gambale, N. and LaMance, J. (2004). Structural Deformation Monitoring using Locata. In *1st FIG International Symposium on Engineering Surveys for Construction Works and Structural Engineering.* Nottingham, UK.

Barnes, J., Rizos, C., Pahwa, A., Politi, N. and van Cranenbroeck, J. (2007). The Potential of Locata Technology for Structural Monitoring Applications. *Journal of Global Positioning Systems*, *6*, 166-172.

Barnes, J., Rizos, C., Wang, J., Small, D., Voigt, G. and Gambale, N. (2003a). High Precision Indoor and Outdoor Positioning using LocataNet. *Journal of Global Positioning Systems*, *2*(2).

Barnes, J., Rizos, C., Wang, J., Small, D., Voigt, G. and Gambale, N. (2003b). High Precision Indoor and Outdoor Positioning using LocataNet. , *2*(2), 73-82.

Barnes, J., Rizos, C., Wang, J., Small, D., Voigt, G. and Gambale, N. (2003c). Locata: A New

Positioning Technology for High Precision Indoor and Outdoor Positioning. In *Proceedings of the 16th International Technical Meeting of the Satellite Division of the Institute of Navigation (ION GPS/GNSS 2003)* (p. 1119-1128). Portland, OR, USA.

Barnes, J., Wang, J., Rizos, C. and Tsujii, T. (2002). The performance of a pseudolite-based positioning system for deformation monitoring. In *2nd Symp. on Geodesy for Geotechnical & Structural Applications* (p. 326-327). Berlin, Germany.

Bertsch, J. (2009). *On-the-fly Ambiguity Resolution for the Locata Positioning System.* Master thesis, The University of New South Wales.

Bertsch, J., Choudhury, M., Rizo, C. and Kahle, H.-G. (2009). On-the-fly Ambiguity Resolution for Locata. In *Proceedings of the IGNSS Symposium.*

Best-Fit Computing, I. (nd). *COLUMBUS Network Adjustment Software.* Retrieved 28 July 2012, from `http://www.bestfit.com/old/freedemo.shtml`

Bond, J., Chrzanowski, A. and Kim, D. (2008). Bringing GPS into harsh environments for fully automated deformation monitoring. *GPS Solutions*, *12*, 1-11. doi: 10.1007/s10291-007-0059-7

Bond, J., Kim, D., Chrzanowski, A. and Szostak-Chrzanowski, A. (2007). Development of a fully automated, GPS based monitoring system for disaster prevention and emergency preparedness: PPMS+RT. *Sensors*, *7*(7), 1028-1046.

Bonenberg, L. K. (2003). *Integration of RTK-GPS and TS measurements (Integracja pomiarów RTK-GPS i tachymetrycznych).* Master thesis published in Polish, University of Science and Technology, Krakow, Poland.

Bonenberg, L. K., Hancock, C. M. and Roberts, G. W. (2010). Indoor multipath effect study on the Locata system. *Journal of Applied Geodesy*, *4*(3), 137-143.

Bonenberg, L. K., Hancock, C. M., Roberts, G. W., Ogundipe, O. and Lee, J. K. (2009). Feasibility of integrated Locata and GNSS for Engineering Work Application. Jeju, South Korea.

Bonenberg, L. K., Roberts, G. W. and Hancock, C. M. (2010a). Engineering Applications of Integrated Wireless Pseudolite and GNSS System. In *Proceedings of the XXIV FIG International Congress.* Sydney, Australia. Retrieved 17 June 2012, from `http://www.fig.net/pub/fig2010/papers/fs01d%5Cfs01d_bonenberg_gethin_et_al_4250.pdf`

Bonenberg, L. K., Roberts, G. W. and Hancock, C. M. (2010b). Trial Network for Locata and GNSS Integration in an Urban Environment. In *NAV10.* London, UK: Royal Institute of Navigation.

Bonenberg, L. K., Roberts, G. W. and Hancock, C. M. (2011). Using Locata to augment GNSS. *Civil Engineering Surveyor, GIS-GPS supplement*, 19-23.

Bonenberg, L. K., Roberts, G. W. and Hancock, C. M. (2012). Using Locata To Augment GNSS In A Kinematic Urban Environment. *Archives of Photogrammetry, Cartography and Remote Sensing*, *12*, 63-74.

Brekke, D. W., Wilson, D. and Brown, A. (2008). Pseudolite Navigation for Rotorcraft and Ground-Based Vehicles. In *Proceedings of the 21st International Technical Meeting of the Satellite Division of the Institute of Navigation (ION GNSS 2008)* (p. 2583-2594). Savannah, GA, USA.

Brockmann, E. (2012). GNSS Solutions: All About Heights. *Inside GNSS*, *7*(3), 28-32.

Burnside, C. (1991). *Electromagnetic distance measurement, 3rd ed.* BSP Professional Books, Oxford.

Carr, J. (2012). *Productivity gains at Newmont Boddington using Leica JPS with Locata Technology* (Tech. Rep.). Newmont Boddington Gold Mine.

Cellmer, S., Wielgosz, P. and Rzepecka, Z. (2010). Modified ambiguity function approach for GPS

carrier phase positioning. *Journal of Geodesy*, *84*, 267-275. doi: 10.1007/s00190-009-0364-8

Cheng, X. J., Cao, K. J., Xu, J. N. and Li, B. (2009). Analysis on forgery patterns for GPS civil spoofing signals. In *ICCIT 2009 - 4th International Conference on Computer Sciences and Convergence Information Technology* (p. 353-356). Seoul, South Korea.

Cheong, J. W. (2012). *Signal Processing and Collective Detection for Locata Positioning System.* PhD thesis, University of New South Wales, School of Surveying & Spatial Information Systems.

Cheong, J. W., Dempster, A. G. and Rizos, C. (2009). Detection of Time-hopped DS-CDMA Signal for Pseuodolite-based Positioning System. In *Proceedings of the 22th International Technical Meeting of The Satellite Division of the Institute of Navigation (ION GNSS 2009).* Savannah, GA,USA.

China Satellite Navigation Office. (2011). *BeiDou Navigation Satellite System Signal In Space Interface Control Document (Test Version)* [ICD].

China Satellite Navigation Office. (2012). *BeiDou Navigation Satellite System Signal In Space Interface Control Document Open Service Signal B1I (Version 1.0)* [ICD]. Retrieved 28 June 2012, from `http://www.beidou.gov.cn/attach/2013/12/26/20131226298ff2928cc34e45b4714a6ac0e14a1c.pdf`

Choudhury, M. (2012). *Analysing Locata positioning technology for slow structural displacement monitoring application.* PhD thesis, University of New South Wales, Surveying & Spatial Information Systems.

Chrzanowski, A., Szostak-Chrzanowski, A., Bond, J. and Wilkins, R. (2007). Increasing public and environmental safety through integrated monitoring and analysis of structural and ground deformations. *Geomatics Solutions for Disaster Management*, 407-426.

Cobb, H. S. (1997). *GPS Pseudolites: Theory, Design and Application.* PhD thesis, Stanford University.

Cojocaru, S., Birsan, E., Batrinca, G. and Arsenie, P. (2009). GPS-GLONASS-GALILEO: A Dynamical Comparison. *Journal of Navigation*, *62*(01), 135-150. doi: 10.1017/S0373463308004980

Constell Inc. (2012). *Constellation Toolbox for MATLAB.* Retrieved 16-September-2012, from `http://www.constell.org/`

Craig, D. and Locata Corporation. (2012). Truth on the Range. *Inside GNSS*, *7*(3), 37-48. Retrieved 06 July 2012, from `http://www.insidegnss.com/node/3071`

Davis, L. A., Enge, P. K. and Gao, G. X. (Eds.). (2012). *Global Navigation Satellite Systems: Report of a Joint Workshop of the National Academy of Engineering and the Chinese Academy of Engineering.* The National Academies Press.

de Jonge, P. and Tiberius, C. (1996). *The LAMBDA method for integer ambiguity estimation: implementation aspects* (Tech. Rep. No. 12). Publications of the Delft Geodetic Computing Centre.

Dietz, H., Sasum, R., Meining, S., Martin, S., Voithenberg, M. v., Bestmann, U. and Becker, M. (2007). SEA GATE - The operational maritime Galileo testbed in Europe. In *Proceedings of the 20th International Technical Meeting of the Satellite Division of the Institute of Navigation (ION GNSS 2007).* Fort Worth, TX, USA.

Dixon, C. S. and Morrison, R. G. (2008). A Pseudolite-Based Maritime Navigation System: Concept through to Demonstration. *Journal of Global Positioning Systems*, *7*(1), 9-17.

DLR. (2012). *The German Galileo Test and Development Environment.* Retrieved 07 February 2012, from `http://www.gate-testbed.com/`

EDINA, University of Edinburgh. (2000). *EDINA Digimap Ordinance Survey Service.* Retrieved

19-September-2012, from http://digimap.edina.ac.uk/digimap/

Electronic Communications Committee. (2012). *ECC Report 128 Compatibility Studies Between Pseudolites And Services In The Frequency Bands 1164-1215, 1215-1300 And 1559-1610 MHz* (Tech. Rep.).

Electronic Communications Committee. (2013). *ECC Report 183 Regulatory Framework for Outdoor GNSS Pseudolites* (Tech. Rep.).

Estey, L. H. and Meertens, C. M. (1999). TEQC: The Multi-Purpose Toolkit for GPS/GLONASS Data. *GPS Solutions*, *3*(1), 42-49. doi: 10.1007/PL00012778

European Space Agency. (2011). *ESA Navipedia.* Retrieved 06 June 2013, from http://www.navipedia.net

Fried, L. (2005). *Social Defense Mechanisms: Tools for Reclaiming our Personal Space.* Master thesis, Massachusetts Institute of Technology. Retrieved 05 Oct 2012, from http://www.ladyada.net/media/pub/thesis.pdf

Fried, L. (2011). *Wave Bubble A design for a self-tuning portable RF jammer.* Retrieved 05 Oct 2012, from http://www.ladyada.net/make/wavebubble/index.html

Fugro. (nd). *Furgo Website.* Retrieved 03 July 2012, from http://www.fugro.com/

Gakstatter, E., Murfin, T. and Shears, W. (2011). Locata, A New Constellation. *GPS World*, *22*(9), 34-42. Retrieved 11 June 2012, from http://www.gpsworld.com/survey/locata-a-new-constellation-12031?page_id=1

Gao, W., Jiao, W., Xiao, Y., Wang, M. and Yuan, H. (2011). An Evaluation of the Beidou Time System (BDT). *Journal of Navigation*, *64* , 31-39. doi: 10.1017/S0373463311000452

Geospatial Research Centre. (2008). *GRC Precise Time Data Logger User Manual* [user manual].

Getreuer, P. (2009). *Writing Fast MATLAB Code.* Retrieved 25 July 2012, from http://www.mathworks.com/matlabcentral/fileexchange/5685

Ghilani, C. and Wolf, P. (2006). *Adjustment computations: spatial data analysis.* John Wiley & Sons Ltd.

Gibbons, G. and Pratt, T. (2011). *Multiple GNSS: Compatibility & Interoperability. More GNSS systems - success or excess?* Retrieved 02 July 2012, from http://www.insidegnss.com/node/3024

GIMP Development Team. (1996). *GIMP (GNU Image Manipulation Program).* Retrieved 11-July-2012, from http://www.gimp.org/

Global Positioning System Wing. (2010). *Global Positioning System Wing (GPSW) Systems Engineering & Integration Interface Specification IS-GPS-200 Revision E Navstar GPS Space Segment/Navigation User Interfaces* [ICD].

Gottifredi, F., Eleuteri, M., Morante, Q., Valle, V., Varriale, E. and Cretoni, D. (2008). Galileo Test Range Pseudolites: a Performance Augmentation System. In *Proceedings of the 2008 National Technical Meeting of the Institute of Navigation* (p. 595-602). San Diego, CA, USA.

Grewal, M. S., Weill, L. R. and Andrews, A. P. (2006). *Global Positioning Systems, Inertial Navigation, and Integration.* John Wiley & Sons Ltd.

Groves, P. D., Wang, L. and Ziembart, M. K. (2012). Shadow Matching: improved GNSS accuracy in Urban Canyons. *GPS World*, *23*(2), 14-29.

GSW, G. (2010a). *Interface Specification IS-GPS-705 Revision A - Navstar GPS Space Segment/User Segment L5 Interface* [ICD].

GSW, G. (2010b). *Interface Specification IS-GPS-800 Revision A - Navstar GPS Space Segment/User*

Segment L1C Interface [ICD].

Han, S. and Rizos, C. (1996). Improving the computational efficiency of the ambiguity function algorithm. *Journal of Geodesy*, *70*, 330-341.

Hancock, C., Roberts, G. and Taha, A. (2009). *Satellite Mapping in Cities, How good can it get?* (Vol. 162).

Harcombe, P. (2012). *NSW Sydney Satellites.*

Harvey, B. R. (2009). *Practical Least Squares and statistics for surveyors, 3rd ed* (3rd ed.). Sydney, Australia: School of Surveying and Spatial Information Systems, University of New South Wales.

Hegarty, C. and Gibbons, G. (2012). Thought Leadership Series: GNSS Modernization Challenges & Opportunities. *Inside GNSS*, *7*(2), 32-33.

Hein, G. W. (2010). QUO VADIS? Where are We Going in Satellite Navigation?. Retrieved 04 July 2012, from `http://scpnt.stanford.edu/pnt/PNT10/presentation_slides/3-PNT_Symposium_Hein.pdf` (Presentation at Stanford)

Helwig, A., Offermans, G., Stout, C. and Schue, C. (2012). Design and Performance of a Low Frequency Time and Frequency Dissemination Service. In *Proceedings of the 2012 International Technical Meeting of The Institute of Navigation (ION GNSS 2012* (p. 462-471). Newport Beach, CA, USA.

Hide, C. (2009). *Algorithm documentation for POINT software Version: 1.0* [user manual].

Hide, C., Moore, T. and Hill, C. (2007). A MultiSensor Navigation Filter for High Accuracy Positioning in all Environments. *Journal of Navigation*, *60*(03), 409-425. doi: 10.1017/S0373463307004328

Ho, D. (2003). *Notepad++.* Retrieved 11-July-2012, from `http://notepad-plus-plus.org/`

Hofmann-Wellenhof, B., Lichtenegger, H. and Wasle, E. (2008). *GNSS Global Navigation Satellite Systems GPS, GLONASS, Galileo, and more.* Springer Vienna. doi: 10.1007/978-3-211-73017-1

Holmes, J. K. (2007). *Spread Spetrum Systems for GNSS and Wireless Communications.* Artech House. doi: 978-1-159693-083-4

Huang, Y. and Boyle, K. (2008). *Antennas: from theory to practice.* John Wiley & Sons Ltd.

Humphreys, T. (2012a). Detection Strategy for Cryptographic GNSS Anti-Spoofing. *IEEE Transactions on Aerospace and Electronic Systems.*

Humphreys, T. (2012b). *Statement on the vulnerability of civil unmanned aerial vehicles and other systems to civil GPS spoofing* (Tech. Rep.). Subcommittee on Oversight, Investigations, and Management of the House Committee on Homeland Security. Retrieved 06 October 2012, from `http://homeland.house.gov/sites/homeland.house.gov/files/Testimony-Humphreys.pdf`

Inkscape Development Team. (2006). *Inkscape.* Retrieved 11-July-2012, from `http://inkscape.org/`

Insiteo. (nd). *Insiteo.* Retrieved 03 July 2012, from `http://www.insiteo.com/joomla/index.php/en/`

International Civil Aviation Organization. (1993). *Shooting Down of a Korean Air Lines Boeing 747 (Flight KE 007) on 31 August 1983.* Retrieved 14 September 2011, from `http://www.icao.int/cgi/goto_m.pl?icao/en/trivia/kal_flight_007.htm`

International Earth Rotation and Reference Systems Service. (1987). *International Earth Rotation and Reference Systems Service.* Retrieved 11 July 2012, from `http://www.iers.org`

International GNSS Service. (nd). *International GNSS Service.* Retrieved 14 July 2012, from `http://acc.igs.org/`

JabRef Development Team. (2008). *JabRef.* Retrieved 11-July-2012, from `http://jabref.sourceforge`

.net

Ji, S., Chen, W., Ding, X., Chen, Y., Zhao, C. and Hu, C. (2010). Potential Benefits of GPS/-GLONASS/GALILEO Integration in an Urban Canyon. *The Journal of Navigation*, *63*(04), 681-693.

Kale, I., Adane, Y., Ucar, A., Bardak, B. and Yavuz, I. (2012). *A Digitally Configurable Receiver for Multi-Constellation GNSS.*

Kaplan, E. A. and Hegarty, C. (2006). *Understanding GPS, 2nd ed.* Artech House.

Kendal, B. (2011). The Beginnings of Air Radio Navigation and Communication. *Journal of Navigation*, *64*, 157-167. doi: 10.1017/S0373463310000251

Kennie, T. and Petrie, G. (Eds.). (1993). *Engineering Surveying Technology.* Backie A&P. doi: 0751401935

Khan, F. A. (2011). *Locata Positioning System Performance Evaluation and Improvement in the Presence of RF Interference.* PhD thesis, University of New South Wales, School of Surveying & Spatial Information Systems.

Khan, F. A., Rizos, C. and Dempster, A. G. (2010). Locata performance evaluation in the presence of wide- and narrow-band interference. *Journal of Navigation*, *63*(3), 527-543.

Kim, D. and Langley, R. B. (2000). GPS Ambiguity Resolution and Validation: Methodologies, Trends and Issues. In *Proceedings of the 7th GNSS Workshop - International Symposium on GPS/GNSS* (p. 213-221).

Kleusberg, A. and Teunissen, P. J. G. (Eds.). (1998). *GPS for Geodesy, 2nd ed.* Springer Berlin Heidelberg.

Klobuchar, J. A. (1991). Ionospheric effects on GPS. *GPS World*, *4*(2), 48-51.

Kocierz, R., Kuras, P., Owerko, T. and Orty, L. (2011). Assessment of Usefulness of Radar Interferometer for Measuring Displacements and Deformations of Dams. In *Joint International Symposium on Deformation Monitoring.* Hong Kong, China.

Kunegin, S. V. (2000). *Global'naya navigatsionnaya sputnikovaya sistema "GLONASS".* Retrieved 29 June 2012, from `http://www.kunegin.narod.ru/ref1/glonass/index.htm`

LaMance, J. and Small, D. (2011). Locata Correlator-Based Beam Forming Antenna Technology for Precise Indoor Positioning and Attitude. In *Proceedings of the 24th International Technical Meeting of The Satellite Division of the Institute of Navigation (ION GNSS 2011).*

Langley, R. B. (1998). The GPS End-of-Week Rollover. *GPS World*, *9*, 40-47.

Lau, L. and Cross, P. (2007). Development and testing of a new ray-tracing approach to GNSS carrier-phase multipath modelling. *Journal of Geodesy*, *11*, 713-732.

Laurila, S. (1976). *Electronic surveying and navigation.* John Wiley & Sons Ltd.

Lavergnat, J. and Sylvain, M. (2000). *Radiowave propagation principles and techniques.* John Wiley & Sons Ltd.

Lee, H. K., Soon, B., Barnes, J., Wang, J. and Rizos, C. (2008). Experimental Analysis of GPS/Pseudolite/INS Integration for Aircraft Precision Approach and Landing. *The Journal of Navigation*, *61*(02), 257-270.

Lee, H. K., Wang, J. and Rizos, C. (2005). An integer ambiguity resolution procedure for GPS / pseudolite / INS integration. *Journal of Geodesy*, *79*(4-5), 242-255.

Lee, H. K., Wang, J. L., Rizos, C. and Grejner-Brzezinska, D. (2004). Analyzing the impact of integrating pseudolite observables into a GPS/INS system. *Journal of Surveying Engineering-Asce*, *130*(2),

95-103.

Leica Geosystems. (2002). *"Outside World Interface" (OWI) Interface Control Document Project GPS System 500* (4.0 ed.) [ICD].

Leick, A. (2004). *GPS Satellite Surveying.* Hoboken: John Wiley & Sons Ltd.

LeMaster, E. A., Matsuoka, M. and Rock, S. M. (2002). Field Demonstration of a Mars Navigation System Utilizing GPS Pseudolite Transceivers. In *Position, Location, and Navigation Symposium.* Palm Springs, CA, USA.

Liu, J. (2009). *The Development and Research of COMPASS/Beidou Navigation Satellite System (CNSS).* (Presentation)

Locata Corporation Pty Ltd. (2010a). *Locata v4r0 Release Notes v1.0* [user manual].

Locata Corporation Pty Ltd. (2010b). *Locata v4r2 Release Notes v1.0* [user manual].

Locata Corporation Pty Ltd. (2011a). *LocataNet Positioning Signal Interface Control Document 2011 (ICD-LOC-100A)* [user manual].

Locata Corporation Pty Ltd. (2011b). *Locata v5r0 Release Notes (BGM Deployment) v1.0* [user manual].

Massatt, P., Fritzen, F., Scuro, S. and O'Neill, K. (2006). How Constellation Design Affects GPS Users in Mountainous Terrain. In *Proceedings of the 19th International Technical Meeting of the Satellite Division of the Institute of Navigation (ION GNSS 2006)* (p. 1506-1515). Fort Worth, TX, USA.

MathWorks. (1984). *MATLAB - The Language of Technical Computing.* Retrieved 11-July-2012, from `http://www.mathworks.co.uk/products/matlab/`

Meng, X., Dodson, A. H. and Roberts, G. W. (2007). Detecting bridge dynamics with GPS and triaxial accelerometers. *Engineering Structures*, *29*(11), 3178-3184.

Meng, X., Roberts, G. W., Dodson, A. H., Cosser, E., Barnes, J. and Rizos, C. (2004). Impact of GPS satellite and pseudolite geometry on structural deformation monitoring: analytical and empirical studies. *Journal of Geodesy*, *77*(12), 809-822.

MetaGeek. (2005). *inSSIDer 2.1.* Retrieved 28-Auf-2012, from `http://www.metageek.net/products/inssider/`

Montillet, J.-P. (2008). *Precise Positioning in Urban Canyons: Applied to the Localisation of Buried Assets.* PhD thesis, University of Nottingham.

Montillet, J. P., Roberts, G. W., Hancock, C., Meng, X., Ogundipe, O. and Barnes, J. (2009). Deploying a Locata network to enable precise positioning in urban canyons. *Journal of Geodesy*, *83*(2), 91-103.

Naviva. (2012). *Naviva.* Retrieved 03 Junly 2012, from `http://naviva.fi/`

Ogundipe, O., Roberts, G. W. and Brown, C. J. (2012). GPS monitoring of a steel box girder viaduct. *Structure and Infrastructure Engineering: Maintenance, Management, Life-Cycle Design and Performance*, 1-16. Retrieved 12 September 2012, from `http://dx.doi.org/10.1080/15732479.2012.692387` doi: 10.1080/15732479.2012.692387

Parkinson, B. W., Spilker, J. J., Axelrad, P. and Enge, P. (1996). *Global positioning system : theory and applications.* Washington, DC, USA: American Institute of Aeronautics and Astronautics.

Pelgrum, W. J. (2006). *New Potential of Low-Frequency Radionavigation in the 21st Century.* PhD thesis, Delft Technical University.

Peters, G. O. (2011). *Advantages of Combining GNSS with Ground Based Pseudo-Satellites.* Master

thesis, Department of Civil Engineering, The University of Nottingham.

Pinchin, J. T. (2011). *GNSS Based Attitude Determination for Small Unmanned Aerial Vehicles.* PhD thesis, University of Canterbury, Mechanical Engineering. Retrieved 08 February 2012, from `http://hdl.handle.net/10092/5759`

Politi, N., Barnes, J., Dempster, A., Rizos, C., Tambuwala, N. and Jamal, M. (2007). Research Activities on the Locata Technology at the University of New South Wales. In *Proceedings of the 20th International Technical Meeting of the Satellite Division of the Institute of Navigation(ION GNSS 2007)* (p. 1118-1127). Fort Worth, TX, USA.

Python Software Foundation. (1991). *Python Programming Language.* Retrieved 11-July-2012, from `http://www.python.org/`

Revnivykh, S. (2012). GLONASS Status and Modernization. In *International GNSS Committee, IGC-7.* Beijing, China.

Rizos, C., Grejner-Brzezinska, D. A., Toth, C. K., Dempster, A. G., Li, Y., Politi, N., Barnes, J., Sun, H. and Li, L. (2010). Hybrid positioning a prototype system for navigation in GPS-challenged environments. *GPS World*, *21*(3), 42-47.

Rizos, C., Roberts, G., Barnes, J., and Gambale, N. (2010). Locata: A new high accuracy indoor positioning system. In *2010 International Conference on Indoor Positioning and Indoor Navigation (IPIN).* Zürich, Switzerland.

Roberts, C. (2011). How will all the new GNSS signals help RTK surveyors? In *Proceedings of the Surveying & Spatial Sciences Biennial Conference 2011.* Wellington, New Zealand.

Roberts, G. W., Meng, X., Brown, C. J. and Dallard, P. (2006). GPS measurements on the London Millennium Bridge. In *Proceedings of the Institution of Civil Engineers: Bridge Engineering* (Vol. 159, p. 153-161).

Rueger, J. M. (2002). Refractive Index Formulae for Radio Waves. In *Proceedings of the XXII FIG International Congress.* Washington, DC, USA.

Russian Institute of Space Device Engineering. (2008). *Global Navigation Satellite System Glonass Interface Control Document Navigational Radiosignal In Bands L1, L2 Edition 5.1* [ICD]. Moscow, Russia.

Saastamoinen, J. (1972). Contributions to the theory of atmospheric refraction. *Journal of Geodesy*, *105*, 279–298. doi: 10.1007/BF02521844

Saka, M. H. (2008). Optimal positioning of pseudolites augmented with GPS. *Sea Technology*, *49*(8), 39-42.

Schlötzer, S., Martin, S. and v. Voithenberg, M. (2007). Autonomous Navigation Environment with Self-Calibrating Transceivers. *Journal of Global Positioning Systems*, *6*(2), 149-157.

Schönemann, E., Becker, M. and Springer, T. (2011). A new Approach for GNSS Analysis in a Multi-GNSS and Multi-Signal Environment. *Journal of Geodetic Science*, *1*(3), 204-214. Retrieved 04 July 2012, from `http://dx.doi.org/10.2478/v10156-010-0023-2`

Scott, L. (2012). Spoofs, Proofs & Jamming. *Inside GNSS*, 7(5), 42-53.

Seeber, G. (1993). *Satellite Geodesy: Foundations, Methods & Applications.* Walter de Gruyter.

Shepard, D., Bhatti, J. and Humphreys, T. (2012). Drone Hack: Spoofing Attack Demonstration on a Civilian Unmanned Aerial Vehicle. *GPS World*, 30-33. Retrieved 05 October 2012, from `http://radionavlab.ae.utexas.edu/images/stories/files/papers/drone_hack_shepard.pdf`

SigNav. (2008). *SigNav uTevo Weak Signal Clocking Receiver Product Overview Rev 2.3.* Re-

trieved Jan 2011, from http://www.ojumpo.cn/EN/UploadFiles%5C5266ba5a-62b0-4bc8-8c38-140fbbbfb42bSigNav%20uTevo%20-%20Weak%20Signal%20Clocking%20Receiver.pdf

Soon, B., Poh, E., Barnes, J., Zhang, J., Lee, H., Lee, H. and Rizo, C. (2003). Flight Test Results of Precision Approach and Landing Augmented by Airport Pseudolites. In *Proceedings of the 16th International Technical Meeting of the Satellite Division of the Institute of Navigation (ION GPS/GNSS 2003)* (p. 2318-2325). Portland, OR, USA.

Soycan, M. and Ocalan, T. (2011). A regression study on relative GPS accuracy for different variables. *Survey Review*, *43*(320), 137-149. Retrieved 09 June 2013, from http://www.ingentaconnect.com/content/maney/sre/2011/00000043/00000320/art00004 doi: doi: 10.1179/003962611X12894696204867

Stansell, T. J. (1986). RTCM SC-104 recommended pseudolite signal specification. *Navigation*, *33*(1), 42-59.

Teunissen, P. (2006). *Testing Theory* (2nd Edition ed.). VSDD publisher, Delft.

Teunissen, P. J. G. (2006). The LAMBDA Method for the GNSS Compass. *Artificial Satellites*, *41*(3), 89-103.

The Code::Blocks Team. (2005). *Code::Blocks IDE (GNU).* Retrieved 11-July-2012, from http://www.codeblocks.org/

The LyX Team. (2009). *LyX - The Document Processor.* Retrieved 11-July-2012, from http://www.lyx.org/

The Royal Academy of Engineering. (2011). *Global Navigation Space Systems: reliance and vulnerabilities* (Tech. Rep.). London, UK. Retrieved 06 November 2012, from http://www.raeng.org.uk/news/publications/list/reports/RAoE_Global_Navigation_Systems_Report.pdf

Tolman, B., Harris, R. B., Gaussiran, T., Munton, D., Little, J., Mach, R., Nelsen, S. and Renfro, B. (2004). The GPS Toolkit: Open Source GPS Software. In *Proceedings of the 16th International Technical Meeting of the Satellite Division of the Institute of Navigation (ION GPS/GNSS 2003).* Long Beach, CA, USA.

Toth, C., Grejner-Brzezinska, D. A., Wang, X. and Sun, H. (2009). Terrestrial Laser Scanning to Support Land Navigation. In *ASPRS 2009 Annual Conference.* Baltimore, MD, USA.

Trimble. (nd). *Trimble Investor Relations.* Retrieved 03 July 2012, from http://investor.trimble.com/

Trunzo, A., Benshoof, P. and Amt, J. (2011). The UHARS Non-GPS Based Positing System. In *Proceedings of the 24th International Technical Meeting of The Satellite Division of the Institute of Navigation (ION GNSS 2011).* Portland, OR, USA.

Verhagen, A. A. (2004). *The GNSS integer ambiguities: estimation and validation.* PhD thesis, Delft University of Technology.

Wang, J., Tsujii, T., Rizos, C., Dai, L. and Moore, M. (2000). Integrating GPS and Pseudolite Signals for Position and Attitude Determination: Theoretical Analysis and Experiment Results. In *Proceedings of the 13th International Technical Meeting of the Satellite Division of the Institute of Navigation (ION GPS 2000)* (p. 2252-2262). Salt Lake City, UT, USA.

Wang, J. J., Wang, J., David, S., Leo, W. and Kyu, L. H. (2004). Pseudolite Augmentation for GPS Aided Aerial Photogrammetry: An Analysis of Systematic Errors. *Geomatics Research Australasia*, *81*(81), 31-43.

Wang, J. J., Wang, J., Sinclair, D., Watts, L. and Lee, H. K. (2005). Tropospheric Delay Estimation

for Pseudolite Positioning. *Journal of Global Positioning Systems*, *4* , 106-112.

Wang, L., Groves, P. D. and Ziebart, M. K. (2012). Multi-Constellation GNSS Performance Evaluation for Urban Canyons Using Large Virtual Reality City Models. *The Journal of Navigation*, *65*(03), 459-476. Retrieved from `http://dx.doi.org/10.1017/S0373463312000082` doi: 10.1017/S0373463312000082

Wesson, K., Rothlisberger, M. and Humphreys, T. E. (2012). Practical Cryptographic Civil GPS Signal Authentication. *NAVIGATION, Journal of the Institute of Navigation*, *59*(3), 177-193.

Willigen, D. v. (2012). It cannot go on forever - we have to find a solution! *Coordinates*, *Volume VIII*(Issue 1). Retrieved 25 June 2012, from `http://mycoordinates.org/pdf/jan12.pdf`

Wübbena, G., Bagge, A. and Schmitz, M. (2001). Network-Based Techniques for RTK Applications. In *GPS Symposium, GPS JIN 2001.* Tokyo, Japan.

Yang, G., He, X. and Chen, Y. (2010). Integrated GPS and Pseudolite positioning for deformation monitoring. *Survey Review*, *42*(315), 72-81.

Zak, A. (1997). *RussianSpaceWeb.com.* Retrieved 06 June 2013, from `http://www.russianspaceweb.com`

Ziebart, M. and Bahrami, M. (2012). *GNSS geodetic reference frames: consistency, stability and the related transformation parameters.* electronic.

Zimmerman, K., Cohen, C., Lawrence, D., Montgomery, P., Cobb, H. and Melton, W. (2000). Multi-frequency pseudolites for instantaneous carrier ambiguity resolution. In *Proceedings of the 13th International Technical Meeting of the Satellite Division of the Institute of Navigation (ION GPS 2000)* (p. 1024-1033). Salt Lake City, UT, USA.

A Locata and GPS observables

A.1 Observables

Locata and GPS provide following the observables:

- Pseudo-range;
- Integrated carrier phase ranging known as ICP;
- Doppler measurement.

Locata uses a four signal cluster to detect multipath or cycle slip, it will either mix signals (by averaging or weight averaging), or reject signals flagged as faulty see section 3.1, page 36. It also uses this approach to determine cycle slip see section 7.3, page 113. While Locata and GPS ICP are of similar accuracy, Locata pseudo-range is visibly biased, on 1 – 3 m accuracy, due to the TimeLoc procedure. Locata Doppler measurements are recorded in LBF as standard.

Code (pseudo-range)

Pseudo-range is the distance between a satellite and the receiver's antenna; it is calculated by comparing the difference between the time of transmission and that of reception. The code tracking loop within the receiver finds the maximum correlation between the received Pseudo Random Noise (PRN) codes, and its internal replica. High-end geodetic receivers can also partly decode the encrypted military P(Y) code on L2 frequency (Hofmann-Wellenhof et al., 2008; Kaplan and Hegarty, 2006; Montillet, 2008). Its value contains not only range, but also other errors as per equation A.1:

$$P_A^i(t_k) = \rho_A^i(t_k) + (d_A t_k - d^i t_k)c + dI_A^i + dT_A^i + \epsilon_A^i \quad (A.1)$$

$$\rho_A^i(t_k) = (t_{kA} - t_k^i)c \quad (A.2)$$

where:

- i is the satellite (SV) transmitting signal, A is the receiver,
- c is the speed of light,
- $\rho_A^i(t_k)$ is the geometric distance between the receiver and the satellite, defined as time difference between transmitter and receiver,
- $dI_A^S$and dT_A^S are respectively the ionospheric and tropospheric delays,
- $d_A t_k$and $d^S t_k$ is the SV and receiver clock drift of the receiver at the k-th epoch,
- $\epsilon_A^S$is the signal propagation error (e.g. shadowing, multipath fading) and all unmodelled errors, such as, hardware delay (SV and receiver), random noise.

GPS satellite atomic clock drift is very stable, and can be further steered using $d^S t_k = a_0 + a_1(t_k - t) + a_2(t_k - t)^2$, where a_0, a_1, a_2 are the polynomial coefficients, broadcast with the navigation message, and t is referenced time. The residual clock error, can be incorporated into ϵ_A^S :

$$P_A^i(t_k) = \rho_A^i + d_A t_k c + dI_A^i + dT_A^i + \epsilon_A^i \tag{A.3}$$

Numerous models have been developed to mitigate dI_A^S and dT_A^S see section 4.7, page 57. In the case of Locata, it is assumed that the TimeLoc procedure will synchronise the network to $3{\cdot}10^{-11}$s see table 3.1, page 32.

Phase measurement (integrated carrier phase ranging)

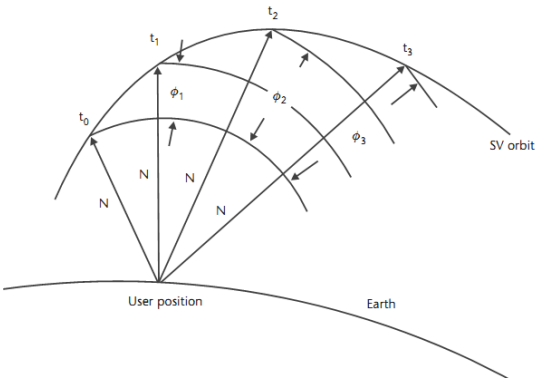

Figure A.1 – Geometric visualisation of ICP, from Kaplan and Hegarty (2006)

Once the receiver locks on to a particular satellite, it not only records code pseudo-range measurements, but also keeps a cycle count based on the Doppler frequency shift[1], by beat phase measurements (Hofmann-Wellenhof et al., 2008):

$$\begin{aligned} \phi_r^s(t) &= \frac{1}{\lambda}\varrho_r^s(t) - N_r^s + \frac{c}{\lambda}\triangle\delta_r^s(t) \\ &= \frac{1}{\lambda}\varrho_r^s(t) - N_r^s + \frac{c}{\lambda}\delta_r(t) - \frac{c}{\lambda}\delta^s(t) \end{aligned} \tag{A.4}$$

This can be decoded at $1{\cdot}10^{-3}$ cycle, but includes an unknown initial cycle count known as ambiguity (see chapter 6 and section 4.4 on page 50). Modern GPS receivers base their initial ICP count on pseudo-range, and assume their ambiguity to be within 100 cycles. The ICP between receiver A and satellite i at epoch t_k can be expressed in cycles as:

$$\phi_A^i(t_k) = (\rho_A^i(t_k) + d_A t_k + dI_A^i + dT_A^i)\lambda_i - N_A^i + \epsilon_A^i \tag{A.5}$$

where,

- λ_i is the wavelength of the carrier frequency i (for ex. L1, L2),
- N_A^i is the carrier-cycle integer ambiguity between the receiver A and the satellite SV_i
- $\epsilon_A^i$is expected to be small in comparison to other parameters, therefore the wavelength effect is not discussed. It is smaller than ϵ_A^i see equation A.3, page 138.

[1] One cycle represents an advance of 2π of the carrier phase or one wavelength.

B Detailed description of GNSS signal

	PRN Code	**Code length [chip]**	**Code rate [Mcps]**	**Modulation Type**	**Bandwidth** [MHz]	**Data rate [sps/bps]**[a]
L1	C/A	1 023	1.023	BPSK(1)	2.046	50/50
	P	~7 days	10.23	BPSK(10)	20.46	50/50
	M[b]	*not known*	*5.115*	*BOC(10,5)*	*30.69*	*not known*
	L1C$_D$[c]	*10 230*	*1.023*	*BOC(1,1)*	*4.092*	*100/50*
	L1C$_P$*c*	10 230 • 1 800	*1.023*	*BOC(1,1)*	*4.092*	-
L2	P	~7 days	10.23	BPSK(10)	20.46	50/50
	L2C[c]	*M* : 10 230	*1.023*	*BPSK(1)*[d]	*2.046*	*50/25*
		L : 767 250	*1.023*	*BPSK(1)*[d]	*2.046*	-
	M[b c]	*not known*	*5.115*	*BOC(10,5)*	*30.69*	*not known*
L5	*L5I*	10 230•10	*10.23*	*BPSK(10)*	*20.46*	*100/50*
	L5Q	10 230•20	*10.23*	*BPSK(10)*	*20.46*	_

Table B.1 – GPS Ranging signals, from Hofmann-Wellenhof et al. (2008)

[a] Symbols per second / Bits per second.
[b] Military code, only incomplete information available.
[c] Modernised signals, not yet available.
[d] Chip-by-chip time-multiplexed.

	PRN Code	**Code length [chip]**	**Code rate [Mcps]**	**Modulation Type**	**Bandwidth** [MHz]	**Data rate [bps]**
G1[a]	C/A[b]	511	0.511	BPSK(0.511)	1.022	50
	P[c]	33 554 432[d]	5.11	BPSK(5.11)	10.22	50
	C/A[e]	not known		*BOC(1,1)*[f]	not known	
	P [e]			not known		
G2[a]	C/A [b]	511	0.511	BPSK(0.511)	1.022	50
	P[c]	33 554 432	5.11	BPSK(5.11)	10.22	50
	C/A[g]			not known		
	P[g]			not known		
G3 a[h]	*C/A*$_2$[ib]	not known	*4.095*	*BPSK(4.095)*	*8.190*	not known
	P$_2$[c]	not known	*4.095*	*BPSK(4.095)*	*8.190*	not known
	C/A$_2$[e]			not known		
L5		not known		BOC(4,4)	not known	

Table B.2 – GLONASS Ranging signals, after Hofmann-Wellenhof et al. (2008)

[a] The exact transmission frequency can be calculated from equation $f = (178.0 + \frac{k}{16})Z$[MHz], where $k = \mathbb{Z} \in < -7, 6 >$ and respectively for G1–3 $Z = 9$, 7 and 6.768.

[b] Standard Precision.

[c] High Precision.

[d] The sentence is truncated so that it repeats every 1s, giving actual length of 5 110 000 chips.

[e] G1 CDMA signal to be transmitted on 1575.42 MHz.

[f] As proposed.

[g] G2 CDMA signal is transmitted on 1242.0 MHz.

[h] As frequency is not yet operational, those values are subject to change.

[i] Signal is intended to carry information and pilot channel orthogonal to each other, with equal transmitting power.

	PRN Code	**Code length**[a] **[chip]**	**Code rate [Mcps]**	**Modulation Type**[b]	**Encryption**	**Data rate [sps/bps]**
E1[c]	E1A	unavailable	2.557 5	BOCc(15,2.5)	ranging code and data[d]	50/100
	E1B	$^{4\,092}/_{1}$	1.023	MBOC(6,1,1/11)[e]	selected data fields[f]	125/250
	E1C[g]	$^{4\,092}/_{1}$	1.023	MBOC(6,1,1/11)[e]	[f]	pilot data
E6[c]	E6A		5.115	BOCc(10,5)	ranging code and data[d]	50/100
	E6B	$^{5\,115}/_{1}$	5.115	BPSK(5)	ranging code and data[h]	$^{500}/_{1\,000}$
	E6C[g]	$^{5\,115}/_{100}$	5.115	BPSK(5)	ranging code[h]	pilot data
E5[i]	E5a-I[j]	$^{10\,230}/_{20}$	10.23	BPSK(10)	selected data fields[k]	25/50
	E5a-Q[jg]	$^{10\,230}/_{100}$	10.23	BPSK(10)	selected data fields[k]	pilot data
	E5b-I[l]	$^{10\,230}/_{4}$	10.23	BPSK(10)	selected data fields[f]	125/250
	E5b-Q[lg]	$^{10\,230}/_{20}$	10.23	BPSK(10)	[f]	pilot data

Table B.3 – Galileo Ranging signals, from Hofmann-Wellenhof et al. (2008)

[a] Code length primary / secondary values.
[b] Multiplexing scheme (E1,E6): constant envelope; (E5): AltBOC(15,10).
[c] A 50% B&C 25% relative power.
[d] Public Regulated Service (PRS).
[e] Common with GPS.
[f] Open Service (OS), Commercial Service (CS), Integrity Monitoring Service (IMS).
[g] Pilot channel.
[h] Commercial Service (CS).
[i] All channels are of equal relative power (25%).
[j] Actual frequency 1 176.450 MHz.
[k] Open Service (OS), Commercial Service (CS).
[l] Actual frequency 1 207.140 MHz.

	PRN Code	**Code rate [Mcps]**	**Modulation Type**	**Bandwidth** [MHz]	**Data rate [bps]**
B1	$B1_I$ [a]	$2.046 \cdot 10^6$	QPSK	4.092	[b]
	$B1_Q$ [c]	$2.046 \cdot 10^6$	QPSK	4.092	[b]
	B1-2 [c d]	$2.046 \cdot 10^6$	QPSK	4.092	[b]
	B1-BOC[e]	$1.023 \cdot 10^6$	MBOC (6,1,1/11)	16.368	50
B2	$B2_I$ [a]	$10.23 \cdot 10^6$	QPSK	24	[b]
	$B2_Q$ [c]	$10.23 \cdot 10^6$	QPSK	24	[b]
	B2-BOC [a]	$5.115 \cdot 10^6$	BOC(10,5)	30.69	50
B3	B3 [c]	$10.23 \cdot 10^6$	QPSK	24	[b]
	B3-BOC [a]	2 557 500	BOC (15, 2.5)	35.805	50
L5	[a]	$10.23 \cdot 10^6$	QPSK	24	50

Table B.4 – Bei Dou (CNSS) Ranging signals, from China Satellite Navigation Office (2012); Liu (2009)

[a] Open Service.
[b] I: 500 (GEO), 50 (nonGEO) ; Q: 500.
[c] Authorised Service.
[d] Actual frequency 1589.742 MHz.
[e] Actual frequency 1575.42 MHz.

[a]	**PRN Code**	**Code rate [Mcps]**	**Modulation Type**	**Bandwidth**[MHz]	**Data rate [sps/bps]**
L1	C/A	1.023	BPSK(1)	4.092	50/50
	C_D	1.023	BOCs(1,1)	4.092	100/50
	C_P	1.023	BOCs(1,1)	4.092	Pilot
	L1-SAIF[b]	1.023	BPSK(1)	16.368	500/250
L2	C	1.023	BPSK(1)	24	50/25
L5	L5I	10.23	BPSK(10)	24	100/50
	L5Q	10.23	BPSK(10)	35.805	Pilot
E6	LEX[c]	5.115	BPSK(5)	24	-/2 000

Table B.5 – QZSS Ranging signals, from Hofmann-Wellenhof et al. (2008)

[a] Frequencies are the same as equivalent GNSS ones.
[b] Sub metre accuracy with integrity function signal, transmitting augmentation information.
[c] Transmits augmentation information.

	GPS	GLONASS	Galileo[a]	Bei Dou (CNSS)
First Launch	1978	1982	2005	2007
FOC[b]	1994	1996[c]	2020	2020[d]
Nominal number of SV	24	21+3	27	27
Orbital planes and inclination	6 @ 55°	3 @ 64.8°	3 @ 56°	3 @ 55°
Semi-major axis[e]	26 560km	25 480km	29 601km[f]	21 500km
Orbit plane separation	60°	120°	120°	
Phase within planes	irregular	±30°	±40°	
Ground track repeat period	~1 sidereal day[g]	~8 sidereal day[h]	~10 sidereal day	
Ground track repeat orbits	2	17	17	
Ephemerides data	Kepler elements, correction coefficients	position, velocity, acceleration vectors	Kepler elements, correction coefficients	Kepler elements, correction coefficients
Reference System	WGS-84	PE-90 (PZ-90)	GTRF	CGCS2000
Time System[i]	UTC+0 (USNO)[j]	UTC+3 (SU) [kl]	UTC+0[l]	BeiDou Time (BDT) System[m]
User time precision	$5{\cdot}10^{-8}$s of UTS[n]	$2{\cdot}10^{-8}$s of UTS[o]	$3{\cdot}10^{-8}$s of UTS	$3{\cdot}10^{-8}$s of UTS
Signal Separation	CDMA	FDMA[p] with planned CDMA	CDMA	CDMA
Carrier Frequencies [MHz]	L1 1 575.420 L2 1 227.600 L5 1 176.450	G1 1 602.000 G2 1 246.000 G3 1 202.025[q] L5 1 176.450	E1 1 575.420 E6 1 278.750 L5 1 176.450	B1 1 561.098 B2 1 207.14 B3 1 268.520 L5 1 176.450
SIS URE[r]	1.0 m	1.8 m	0.85 m[s]	unknown

Table B.6 – Comparison of four GNSS system characteristics, from China Satellite Navigation Office (2012); Davis et al. (2012); Gao, Jiao, Xiao, Wang and Yuan (2011); Hofmann-Wellenhof et al. (2008); Kaplan and Hegarty (2006); Liu (2009)

[a] The only system to be wholly civilian funded albeit with a small proportion private equity.
[b] Full Operational Capacity date (FOC).
[c] Following the disintegration of the Soviet Union, GLONASS fell into disrepair; falling below operational threshold in 2001. Subsequent renewed financial support brought it back to full capacity in 2013.
[d] Global service (Phase III).
[e] The revolution period can be calculated from Kepler's Third Law $P = 2\pi\sqrt{\frac{a^3}{\mu}}$ in IERS $\mu = GM_e = 3\,986\,004.418\,\mathrm{m}^3/\mathrm{s}^2$ with slightly different values for WGS-84(G0) and WGS-84(G873) (Hofmann-Wellenhof et al., 2008; Kaplan and Hegarty, 2006). Flight altitude is small axis minus Earth diameter a=~6 378.137km.
[f] GLOVE, Galileo test satellite, operated at the altitude of a=23 257km.
[g] Sidereal day is equivalent to 23.934 47 h as earth total rotation takes 366 days.
[h] Effectively daily repeats.
[i] Due to clock stability GNSS can only operate for 2-3 days autonomously.
[j] The GPS L5 navigation message is intended to provide the offset between the GLONASS and GPS time system.
[k] Time is not continuous - leap seconds are introduced into system.
[l] The upgraded navigation message is supposed to provide offset between GLONASS and GPS time system (GGTO).
[m] Started at 00:00 1st Jan 2006 UTC, synchronised with UTC within $100{\cdot}10^{-9}$ s.
[n] This should improve with modernised satellites.
[o] $8 \cdot 10^{-9} s$ with GLONASS-K.
[p] In FDMA exact transmission frequency can be calculated from $f = (178.0 + \frac{k}{16})Z$[MHz], where $k = \mathbb{Z} \in < -7, 6 >$and $Z = [9, 7, 6.768]$ depending on carrier frequency.
[q] G3 is to be moved to 1 207.14MHz with the upgraded GLONASS-K. L5 is unconfirmed and subject to change.
[r] Signal-in-Space User Range Error.
[s] A predicted value based on signal specifications.

C Mechanism of Integration

The proposed integrated mechanism is based on Bertsch (2009); Hofmann-Wellenhof et al. (2008); Leick (2004); Pinchin (2011). It is assumed that both Locata, and GPS observables – pseudo-range, P and ICP, ϕ , are correctly read and no cycle slips are present. The proposed solution combines single differenced ($\triangle$) Locata observations and double differenced ($\triangle\nabla$) GPS observations. Float ambiguities are estimated through a Least Squares Adjustment (LSA) process, using the LAMBDA method, to estimate the most probable Ambiguity Resolution (AR). A detailed workflow is presented in figures C.2 to C.3 on pages 152–153.

C.1 Estimation of float Ambiguities

Forming the double and single difference operator matrix

If SVn indicates a satellite n; A is the observation made at the base, and B is the observation at the rover, GPS observations can be written as:

$$\begin{aligned} ObsMat_{GPS} &= [P_{L1,A}, \phi_{L1,A}, P_{L1,B}, \phi_{L1,B}, P_{L2,A}, \phi_{L2,A}, P_{L2,B}, \phi_{L2,B}] \\ P_{L1,A} &= [P_{L1,A}^{SV1}, P_{L1,A}^{SV2}, ..., P_{L1,A}^{SVn}] \\ \phi_{L1,A} &= [\phi_{L1,A}^{SV1}, \phi_{L1,A}^{SV2}, ..., \phi_{L1,A}^{SVn}] \\ &\dots \end{aligned}$$

If LLn indicates Locata n, A an observation made, at the master LL, and B an observation made at another LL, the Locata observations can be written as:

$$\begin{aligned} ObsMat_{LL} &= [P_{RxA}, \phi_{RxA}, P_{RxB}, \phi_{RxB}, P_{RxC}, \phi_{RxC}, P_{RxD}, \phi_{RxD} \\ P_{RxA} &= [P_{RxA}^{LL1}, P_{RxA}^{LL2}, ..., P_{RxA}^{LLn}] \\ \phi_{RxA} &= [\phi_{RxA}^{SLL1}, \phi_{RxA}^{LL2}, ..., \phi_{RxA}^{LLn}] \\ &\dots \end{aligned}$$

Following (Hofmann-Wellenhof et al., 2008), single differencing $\triangle$between two receivers, GPS or Locata, can be written as:

$$D_{\triangle} = \begin{bmatrix} 1 & 0 & ... & 0 \\ 1 & -1 & .. & 0 \\ ... & ... & .. & ... \\ 1 & 0 & ... & -1 \end{bmatrix} \tag{C.1}$$

Knowing that double differencing is $D_{\triangle\nabla} = \begin{bmatrix} D_{\triangle} & -D_{\triangle} \end{bmatrix}$, we combine double differenced GPS and single differenced Locata into operator matrix D:

$$
\begin{aligned}
D &= \begin{bmatrix} D_{GPS,L1} & & & 0 \\ & D_{GPS,L2} & & \\ & & D_{LL,Rx1} & \\ 0 & & & \dots \end{bmatrix} \qquad \text{(C.2)} \\
D_{GPS,L1} &= \begin{bmatrix} D_{P,A} & 0 & -D_{P,B} & 0 \\ 0 & D_{\phi,A} & 0 & -D_{\phi,B} \end{bmatrix} \\
D_{LL,TxA} &= \begin{bmatrix} D_P & 0 \\ 0 & D_\phi \end{bmatrix}
\end{aligned}
$$

The Final observation vector O can be calculated from equation C.3:

$$O = D * ObsMat \qquad \text{(C.3)}$$

Integrating PR and ICP observations is a trade-off between accuracy and stability, mitigating the simplified tropospheric, and observation models used. In Bertsch (2009) pseudo-range P is only used for an initial estimation, with the observation matrix consisting of ICP elements only. With the release of Locata firmware version v.7.0, with EKF and precise observation modelling, this approach would be recommended.

Weighting

The weighting matrix is based on a-priori estimations using equation C.4:

$$P = (DCD^T)^{-1} \qquad \text{(C.4)}$$

$$C = \begin{bmatrix} C_{GPS,L1} & 0 & & 0 \\ 0 & C_{GPS,L2} & & \\ & & C_{LL,Rx1} & 0 \\ 0 & & 0 & \dots \end{bmatrix} \qquad \text{(C.5)}$$

$$C_\bullet = \begin{bmatrix} \sigma_\bullet^2 & 0 & 0 \\ 0 & \ddots & 0 \\ 0 & 0 & \sigma_\bullet^2 \end{bmatrix} \qquad \text{(C.6)}$$

For most applications, this can be simplified to $W = 1/diag(P)$ assuming that there is no correlation of observations. It is also possible to implement a-posteriori weighting mechanism, once our results converge closely to the estimated value. The weight matrix for next iteration W^+, can be then estimated from:

$$\begin{aligned} Q &= m_0^2(APA^T) \\ W^+ &= m_0^2 A(APA^T)A^T \end{aligned} \tag{C.7}$$

The disclosure vector L

The initial rover position A_{XYZ} can be estimated from the SPS solution (pseudo-range) for the initial epoch and using the last epoch results in the following epochs. The residual vector $L_\bullet$ (calculated - observed), incorporating GPS double difference between base and rover (A and B), can be created using the equations below :

$$\rho_{AB}^{ij}(t_k) = (\rho_B^{SVj} - \rho_B^{SVi}) - (\rho_A^{SVj} - \rho_A^{SVi}) \tag{C.8}$$

$$L_P = \rho_{AB}^{ij} - P_{AB}^{ij} \tag{C.9}$$

$$L_\Phi = \rho_{AB}^{ij} - (\Phi_{AB}^{ij} - N_{AB}^{ij})\lambda \tag{C.10}$$

For Locata, the residual vector $L_\bullet$ has to take into account the known offset between the GPS and the LL antennas d_{GPS-LL}, a single differencing between two Locata transceivers is calculated using the equations below :

$$A_{XYZ}^* = A_{XYZ} - d_{GPS-LL} \tag{C.11}$$

$$\rho_{A^*}^{ij}(t_k) = \rho_{A^*}^{LLi} - \rho_{A^*}^{LLj} \tag{C.12}$$

$$L_P = \rho_{A^*}^{ij} - P_{A^*}^{ij} \tag{C.13}$$

$$L_\Phi = \rho_{A^*}^{ij} - (\Phi_{A^*}^{ij} - N_{A^*}^{ij})\lambda \tag{C.14}$$

The final vector L, is formed from the sub-vectors for each system, see equation C.15. Vector L has to be singular, and all ICP cycles are converted to metres.

$$L = \begin{bmatrix} L_{PL1} \\ L_{\Phi L1} \\ L_{PL2} \\ L_{\Phi L2} \\ \cdots \\ L_{PTxA} \\ L_{\Phi TxA} \\ \cdots \end{bmatrix} \tag{C.15}$$

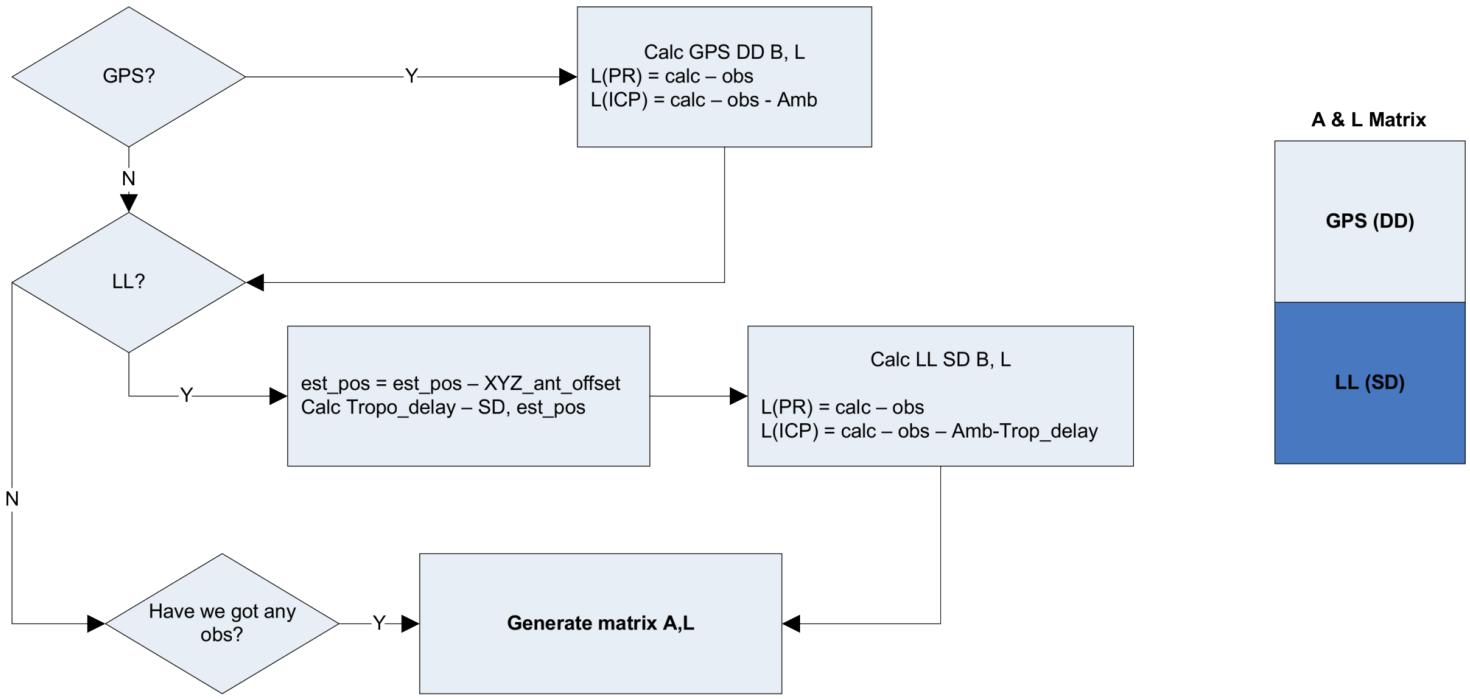

Figure C.1 – The formation of matrix A

GPS DD

```
GPS_SVj = Coords.GPS_SV_thisEpoch(j,:);
raBj = Dist(estimated_pos,GPS_SVj);
raAj = Dist(Coords.Base,GPS_SVj);

Bij = (RefSV - estimated_pos)./raBi - (GPS_SVj - estimated_pos)./raBj [1x3: X Y Z]
Lij = -((raBj-raBi-raAj+raAi))+(Obs_DDij)-estimated_amb_ij   [1x1]

A = [B Amb]
```

LL SD

```
 offset=CalcXYZOffset(Constant,Coords,estimated_pos_GPS)
estimated_pos = estimated_pos_GPS - offset';


raLLj = Dist(estimated_pos,Coords.LL(j,:));
TropoCorr = CalcTropoDelay(Base,RefLL) - CalcTropoDelay(raLLj,LLj);

Bij = -((RefLL - estimated_pos)./raBase - (Coords.LL(j,:) - estimated_pos)./raLLj) [1x3: X Y Z]
Lij = -(raBase-raLLj)+(Obs_DDij)-estimated_amb_ij - TropoCorr   [1x1]

A = [B Amb]
```

Observation matrix A

The observation matrix A is geometrically based (Ghilani and Wolf, 2006; Hofmann-Wellenhof et al., 2008; Kaplan and Hegarty, 2006). It is a combination of sub matrices $A_\bullet$ as per figure C.1 and following equations:

$$A_\bullet = \begin{bmatrix} X_{AB}^{ij} & Y_{AB}^{ij} & Z_{AB}^{ij} & 0 & \cdots & 0 \\ & \vdots & & & & \\ X_{AB}^{in} & Y_{AB}^{in} & Z_{AB}^{in} & 0 & \cdots & 0 \\ X_{AB}^{ij} & Y_{AB}^{ij} & Z_{AB}^{ij} & \lambda & \cdots & 0 \\ & \vdots & & & \ddots & \\ X_{AB}^{in} & Y_{AB}^{in} & Z_{AB}^{in} & 0 & \cdots & \lambda \end{bmatrix} \tag{C.16}$$

$$\lambda_\bullet = \begin{bmatrix} \lambda & \cdots & 0 \\ & \ddots & \\ 0 & \cdots & \lambda \end{bmatrix} \tag{C.17}$$

$$\begin{aligned} X_{AB}^{ij} &= \frac{X^i - X_B}{\rho_B^i} - \frac{X^j - X_B}{\rho_B^j} \\ Y_{AB}^{ij} &= \frac{Y^i - Y_B}{\rho_B^i} - \frac{Y^j - Y_B}{\rho_B^j} \\ Z_{AB}^{ij} &= \frac{Z^i - Z_B}{\rho_B^i} - \frac{Z^j - Z_B}{\rho_B^j} \end{aligned} \tag{C.18}$$

Matrix A is a block diagonal matrix of all GPS and LL sub matrices $A_\bullet$

$$A = \begin{bmatrix} A_{PL1} & 0 & \cdots & & & \\ A_{\Phi L1} & \lambda_{L1} & & & & \\ A_{PL2} & & 0 & & & 0 \\ A_{\Phi L2} & & & \lambda_{L2} & & \\ \vdots & & & & \ddots & \\ A_{PTxA} & & & \cdots & 0 & 0 \\ A_{\Phi TxA} & & 0 & \cdots & 0 & \lambda_{TxA} \\ \vdots & & & & & & \ddots \end{bmatrix} \tag{C.19}$$

Estimation of Float Ambiguities

Equation C.20 describe the vectors of the unknowns, consisting of rover coordinates and ambiguities N, is estimated from $L = Ax + v$, by minimising normally distributed residuals v (Ghilani and Wolf, 2006). This process is based on linearisation of the non-linear equation, by iterating solution $\hat{x}$ until $d\hat{x}$ increments are below the threshold $\sqrt{X_B^2 + Y_B^2 + Z_B^2} < threshold$. This approach requires correct initial geometric and parameter modelling so that the solution can converge to the truth (Cellmer et al., 2010). Most of the time the approach described in equation C.20 is sufficient. The float ambiguities are estimated from equation C.23:

$$x = \begin{bmatrix} X_B & Y_B & Z_B & N^{ij}_{AB,L1} & N^{in}_{AB,L1} & N^{ij}_{AB,L2} & \cdots & N^{in}_{AB,L2} & N^{ij}_{B,RxA} & \cdots & N^{in}_{B,RxA} & \cdots \end{bmatrix} \tag{C.20}$$

$$\hat{x} = (A^T P A)^{-1} A^{-1} P L \tag{C.21}$$

$$d\hat{x} = (A^T P A)^{-1} A^{-1} P L \tag{C.22}$$

$$\bar{x} = \hat{x} + \hat{dx} \tag{C.23}$$

To estimate integer ambiguities LAMBDA also requires the symmetric covariance-variance matrix Q, estimated from:

$$v = A\bar{x} + L \tag{C.24}$$

$$\bar{m}^2 = \frac{v^T P v}{n - u} \tag{C.25}$$

$$Q = \bar{m}^2 (A^T P A)^{-1} \tag{C.26}$$

Code-only (SPS) point positioning

In order to estimate initial position of the rover, GPS pseudo-ranges can be used. Equation C.21 is used with vector of unknowns x and matrix A,L defined as:

$$x = \begin{bmatrix} X_B & Y_B & Z_B & d_A t_k \end{bmatrix} \qquad A = \begin{bmatrix} A_{PL1} \\ A_{PL2} \\ \vdots \\ A_{PTxA} \\ \vdots \end{bmatrix} \qquad L = \begin{bmatrix} L_{PL1} \\ L_{PL2} \\ \dots \\ L_{PTxA} \\ \dots \end{bmatrix}$$

The initial coordinates should be close enough to truth, so the second and higher orders of the Taylor series expansion can be neglected, as they amount to no more than a few meters in practice (Cellmer et al., 2010; Hofmann-Wellenhof et al., 2008). The GPS pseudo-ranges are preferred, as those from Locata are not precise enough.

Multiple epoch solution

A multiple epoch solution can be used if the rover is kinematic, as sufficient geometry change between epochs is required Bertsch (2009). A balance between the rate of change, and the number of epochs used is required - with an increase of epochs the matrix A may be ill-conditioned. To solve this equation, C.21 is used again with the vectors of the unknowns x and matrix A,L defined as:

$$A_x = \begin{bmatrix} A_{e_1} & \cdots & 0 \\ & \ddots & \\ 0 & \cdots & A_{e_n} \end{bmatrix} \qquad L = \begin{bmatrix} L_{e1} \\ \dots \\ L_{en} \end{bmatrix}$$

$$\begin{aligned} x \;=\; \Big[\; & X_{Be1} \quad Y_{Be1} \quad Z_{Be1} \quad \cdots \quad X_{Ben} \quad Y_{Ben} \quad Z_{Ben} \quad N^{ij}_{AB,L1} \quad N^{in}_{AB,L1} \quad N^{ij}_{AB,L2} \quad \cdots \\ & \cdots \quad N^{in}_{AB,L2} \quad N^{ij}_{B,RxA} \quad \cdots \quad N^{in}_{B,RxA} \cdots \;\Big] \end{aligned}$$

C.2 Fixing integer ambiguities with LAMBDA

From de Jonge and Tiberius (1996) the linearised observation equation can be described as:

$$L = Aa + Bb + \varepsilon \tag{C.27}$$

where e and a are ambiguity related parameter vectors, and b is the vector of the remaining parameters, including that of the rover's position. The calculated covariance-variance matrix Q can therefore be written as:

$$Q \;=\; \begin{bmatrix} Q_b & Q_{ab} \\ Q_{ab} & Q_a \end{bmatrix} \tag{C.28}$$

$$Q_a \;=\; \begin{bmatrix} N_{GPS,L1} & N_{GPS,L1,L2} & & & \\ N_{GPS,L1,L2} & N_{GPS,L2} & & 0 & \\ & & \ddots & & \\ & 0 & & N_{LL,RxA} & \\ & & & & \ddots \end{bmatrix}$$

$$\begin{aligned} x \;=\; \Big[\; & X_{Be1} \quad Y_{Be1} \quad Z_{Be1} \quad \cdots \quad X_{Ben} \quad Y_{Ben} \quad Z_{Ben} \quad N^{ij}_{AB,L1} \quad N^{in}_{AB,L1} \quad N^{ij}_{AB,L2} \quad \cdots \\ & \cdots \quad N^{in}_{AB,L2} \quad N^{ij}_{B,RxA} \quad \cdots \quad N^{in}_{B,RxA} \cdots \;\Big] \end{aligned} \tag{C.29}$$

To produce independent LAMBDA results $Q_{a,GPS}$, $\bar{x}_{N,GPS}$, we need to process $Q_{a,LL}$ and $\bar{x}_{N,LL}$ via the LAMBDA routine separately. If all values are fixed, the remaining parameters b can be corrected to their final values using the equations:

$$\bar{b} \;=\; b - Q_{ba}Q_a^{-1}(a - \bar{a}) \tag{C.30}$$

$$Q_{\bar{b}} \;=\; Q_b - Q_{ba}Q_a^{-1}Q_{ab} \tag{C.31}$$

Theoretically, it is possible to solve for $Q_{a,LL}$ and $N_{LL,RxA}$ during estimation of b. Practically, for both single and multiple epochs, this approach fails if the number of Locata transceivers exceeds the number of GPS Rx, due to the ill-conditioning of the resulting matrix. Instead $Q_{a,LL}$ and $N_{LL,RxA}$ can be estimated by re-calculating equation C.21 using the estimated fix values of $Q_{a,GPS}$, $\bar{x}_{N,GPS}$ as constants.

Using this approach Locata values can be calculated using solutions from multiple epochs.

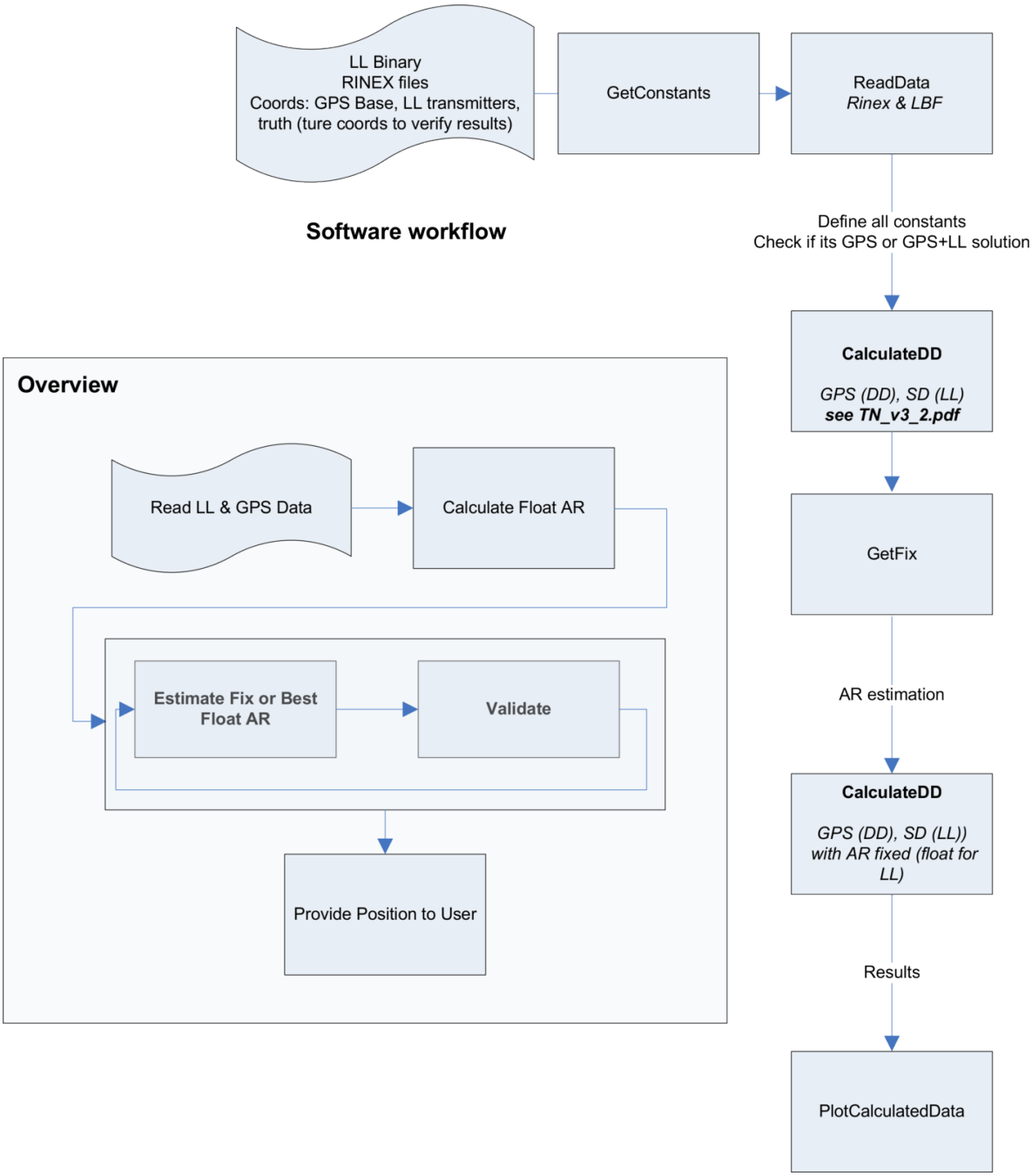

Figure C.2 – Software workflow: an overview

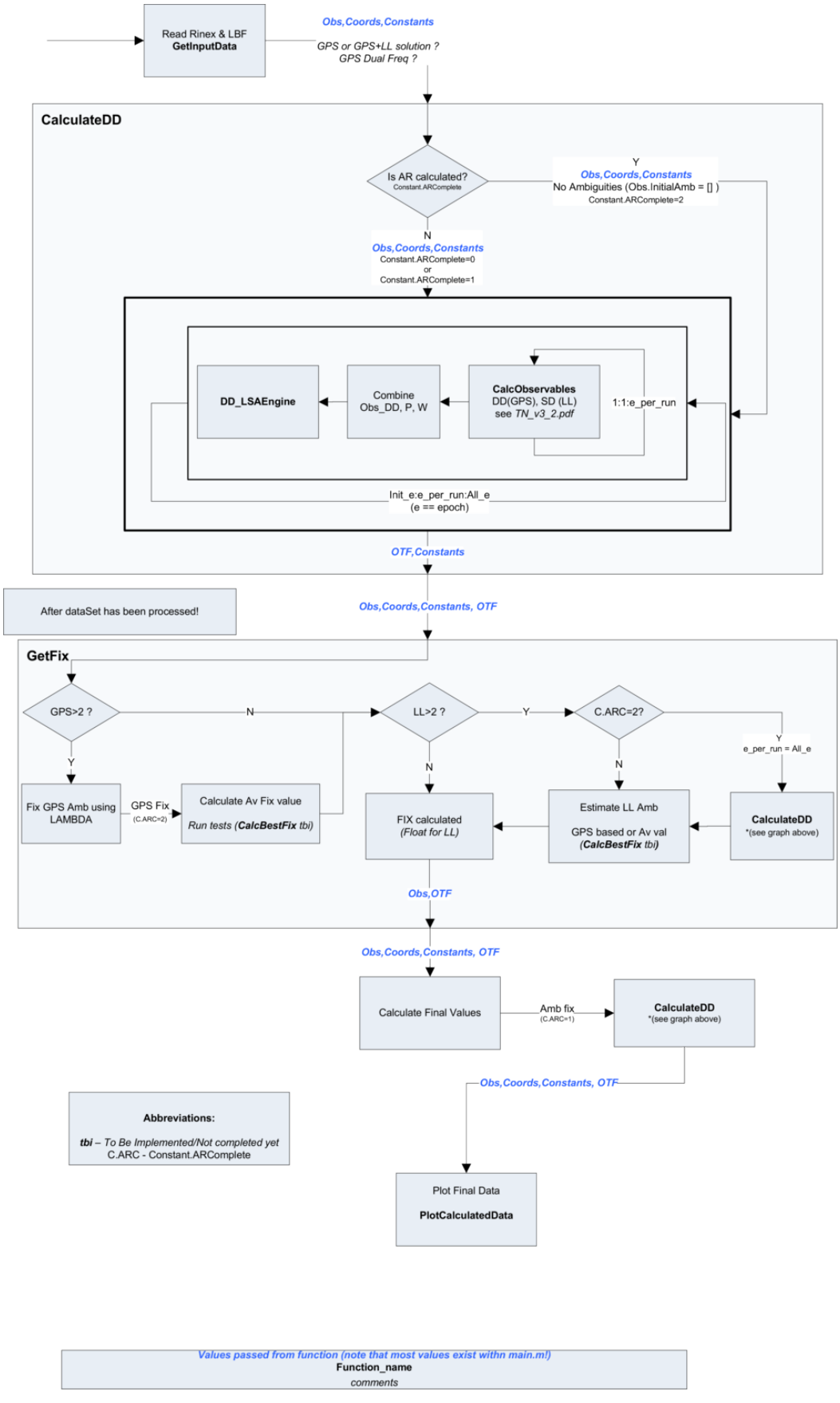

Figure C.3 – Navigation engine software overview

D The Urban obstruction simulator

This simple tool was designed to estimate visibility and multipath for Locata and GPS within an urban scenario. Positional quality estimation is not yet fully implemented. The algorithm is based on Andreotti (2006); Kaplan and Hegarty (2006); Parkinson et al. (1996). The software consists of two independent components (as per figure D.2):

CalcCoords which estimates the coordinates for all elements (SV, rover and Locata transceivers), as well as any instances of multipath.

CalcStats which calculates DOP and Minimal Detectable Bias (MDB)[1] , no noise or atmospheric effects are included in this estimation.

The inputs to the simulator model are as follows:

- parsed navigation files for Locata, with local grid coordinates, and GPS in the WGS84 coordinate system see section 3.2, page 39,
- the trajectory file, with local grid coordinates,
- the obstruction files, with local grid coordinates[2].

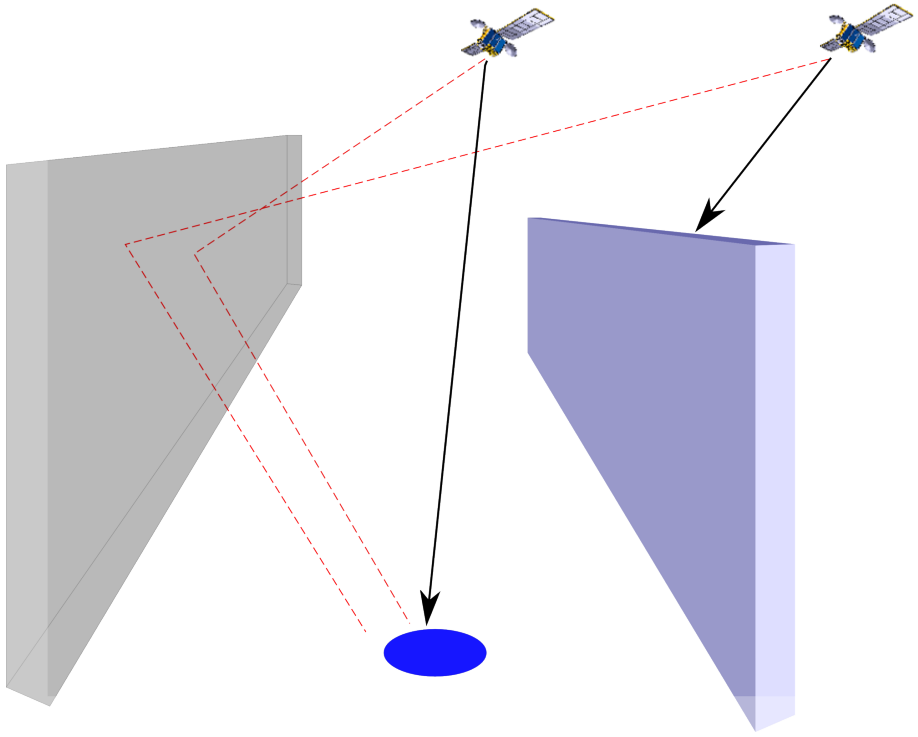

Figure D.1 – Multipath model used in simulator

[1] Also known as the internal reliability, this defines the size of the errors (biases) in the model which can be detected. In this software it also refers to the external reliability. More details can be found in Cheng, Cao, Xu and Li (2009).

[2] Each obstruction is simplified to a simple 3D face, and defined by its top edge (line).

The software is intended for an initial feasibility study, sacrificing complexity in return for a quick estimate, which leads to a number of simplifications:

- Obstructions are limited to their simple geometric facets, and are assumed to extend from a defined line to the ground thus producing only a single reflex[3];
- No material propagation is estimated, but the surface glances, using simple trigonometric rules, are included in calculations;
- Ground is defined at the antenna level, hence no ground reflections are introduced;
- Both Line Of Sight (LOS) and Non-Light Of Sight (nLOS) signals are included in the calculations (Groves et al., 2012; L. Wang et al., 2012);
- Signals are modelled with a perfect, infinitely small radius;
- The multipath (LOS and nLOS) signal needs to be reflected close to the rover to be considered, the distance is estimated from the Fresnel Zone[4];
- Multiple reflections of the same signal are considered too weak to be included in the calculations;
- It is not possible to model standing multipath ;
- The multipath effect on TimeLoc is not considered. It is assumed that all transceivers have clear visibility to the master or other units;
- All Locata transceivers are assumed to be of same accuracy;
- The simulation assumes efficient correlator mitigation, so any multipath with delay exceeding $250{\cdot}10^{-9}$ s is excluded (Kaplan and Hegarty, 2006).

This software has been used to aid research published in Bonenberg et al. (2012); Peters (2011) and its example can be found in section 7.2 on page 110.

[3] Multipath is calculated from start point of each obstruction, and line 3D azimuth is used to verify multipath signal final bearing.

[4] The Fresnel Zone is calculated using whole path length from transmitter to rover including the delayed value. The value used is the maximum spread of the zone, normally within its half length.

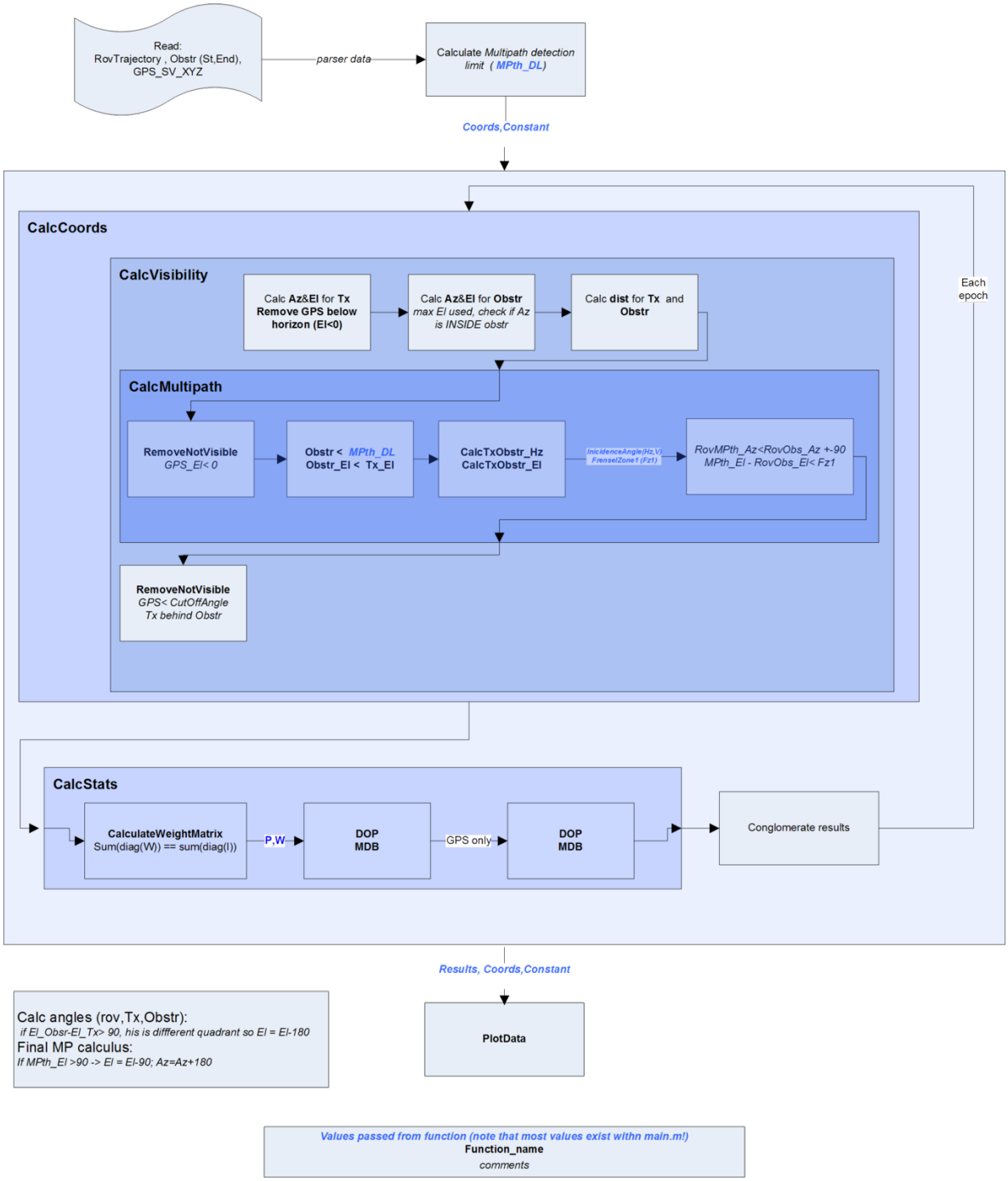

Figure D.2 – The Urban obstruction simulator, the work-flow

E Locata Hardware

	transceiver	Rover
Size [mm]	134×241×28	134×134×28
Weight	1.4 kg	0.7 kg
Input Power	9-15 VDC	
Current flow	2.1A @ 12V	0.7A @ 12V
Operational Temperature	−20 to 40 °C	
Transmission Power	$\leqslant 1W$ [a]	N/A
Communication Ports	1 x Power port (2-pin LEMO) 2 x RS-232 serial Port (5-pin LEMO) [b] 1 x Programming port (6-pin LEMO) 1 x USB port (4-pin LEMO) 2 x Auxiliary COM ports (4-pin LEMO) [c] 1 x Compact Card Flash Slot Antenna Input (SMA Female)	
	2 x Antenna Output (SMA Female) [d]	N/A

Table E.1 – Current Locata Hardware specifications, after Locata Corporation Pty Ltd (2011a)

[a] Due to compliance with FCC 15.247. With amplification, transmission power of up to 10 W was reported in the aviation trials (Craig and Locata Corporation, 2012).

[b] Only one connector is provided. The signal has to be split and users are able to define each port (2 in and 2 out). As a standard, the MET unit utilise *Port1in* and GPS Self Survey utilises *Port2in*.

[c] Aux1 serves as PPS, Aux2 seems not to be in use (Locata Corporation Pty Ltd, 2010b).

[d] Transmission is in the 2.4 GHz licence-free ISM band.

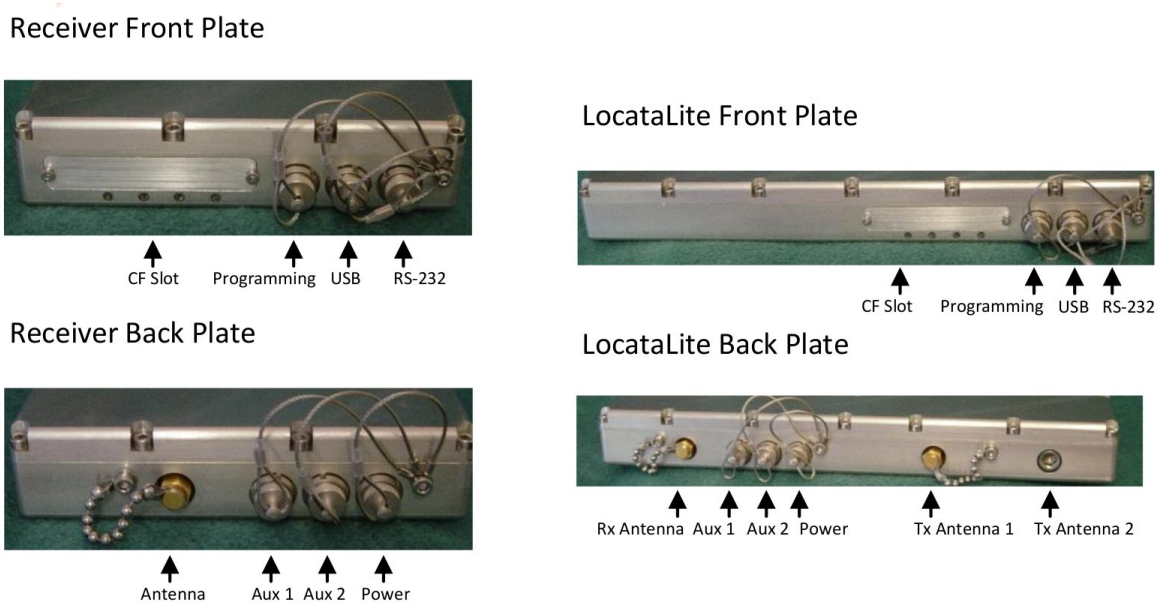

Figure E.1 – Current Locata hardware with rover on the left and transceiver on the right

	transceiver	**Rover**
Size [mm]	134×241×28	134×134×28
Weight	1.4 kg	0.7 kg
Input Power	9-15 VDC	
Current flow	2.1A @ 12V	0.7A @ 12V
Operational Temperature	−40 to 85 °C	
Transmission Power	$\leqslant 1W$	N/A
Communication Ports	1 x Power port (2-pin LEMO) 2 x RS-232 serial Port (5-pin LEMO)[a] 1 x Ethernet (6-pin LEMO) 1 x USB port (4-pin LEMO) 2 x Auxiliary COM ports (6-pin LEMO) Antenna Input (SMA Female)	
	2 x Antenna Output (SMA Female)	N/A

Table E.2 – firmware version v.7.0 hardware specifications

[a] Only one connector is provided. The signal has to be split and each port can be user defined (2 in and 2 out). As a standard, the MET unit utilises *Port1 in* and the GPS Self Survey utilises *Port2 in*.

F Nottingham Geospatial Institute Open Sky Roof Laboratory

Figure F.1 – A view of the NGB Roof

The roof of the Nottingham Geospatial Building (NGB), at the University of Nottingham, contains a dedicated testing facility; equipped with 8 observation pillars, and a purpose built 85 m long test-track, for repeatable dynamic position testing. This can be carried out by a remote controlled, multi-sensor 71 " (184 mm) gauge locomotive platform. The platform has a top speed of 7 $^{km}/_{h}$, a dedicated power supply, and five antenna mounts. The roof area is surrounded by the 1.6 m high parapet wall, and from south side, by building services, including cooling units, and 1.2 m high fence.

The Locata network on the roof was aimed at providing kinematic 3D position (VDOP of 8 or less), while using the train. For this, a Matlab simulation estimated optimal occupation of six, out of 20 predefined locations, and specific antenna height margins, as imposed by the facility and equipment used see figure F.3, page 163. Incorporated into the design, a master was located on the central pillar and equipped with an omnidirectional LCOM HG2403MGU antenna, with remaining units using LCOM AT2400 and HG2412P antennas, see figure F.2, page 162. For the experiments presented in this thesis, an additional semi-permanent location (LL7) was created. The antennas were coordinated and maintained using a network of 10 permanent directional stations and two GPS monitored pillars.

Since the establishment in late 2010, all points have been monitored with no movement larger than 6mm from the initial position being detected, which is consistent with the estimated accuracy of the measurement, given the ambiguity of antennas phase centre identification. Each monitoring campaign was carried out using a Trimble S6 total station, and consisted of two independent free-station measurements.

In early 2012, due to an ongoing work on multipath and noise, a number of the low antennas have been raised, reducing the overall VDOP.

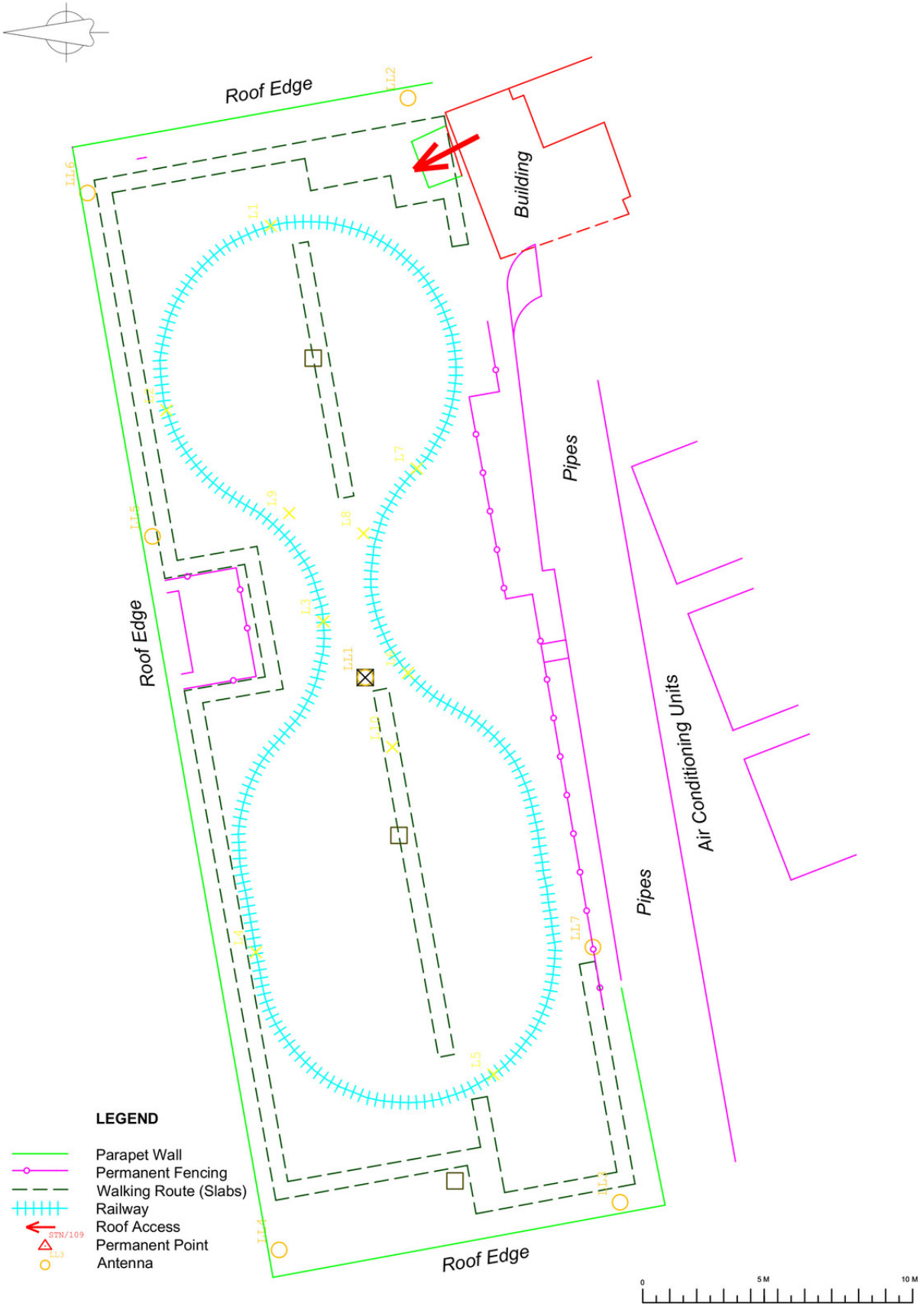

Figure F.2 – NGB Roof Layout

Only LL active during the experiments described in this work are marked. The track is measured at its centreline, as defined by the train front mount.

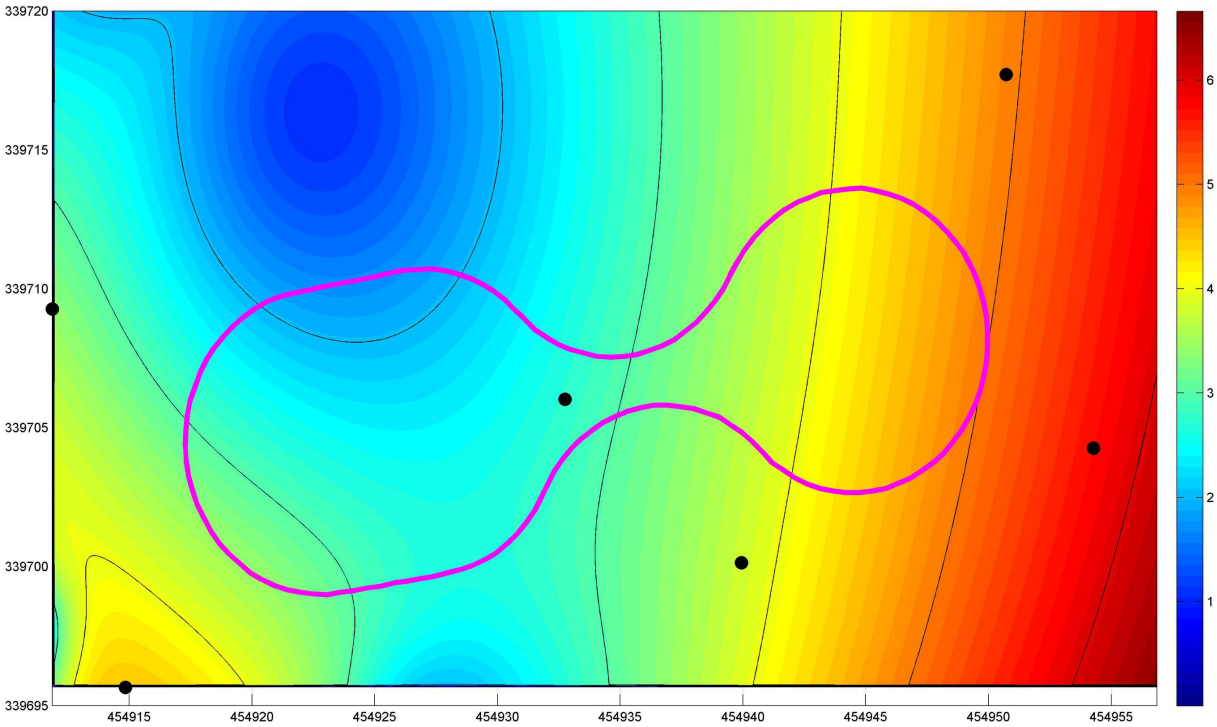

Figure F.3 – Results of Locata roof network VDOP optimisation

All coordinates are in the OSGB grid (ENH), with a scale factor applied. LL position indicated by black dots and the track outline shown in magenta.